INFORMATION TO USERS

This manuscript has been reproduced from the microfilm master. UMI films the text directly from the original or copy submitted. Thus, some thesis and dissertation copies are in typewriter face, while others may be from any type of computer printer.

The quality of this reproduction is dependent upon the quality of the copy submitted. Broken or indistinct print, colored or poor quality illustrations and photographs, print bleedthrough, substandard margins, and improper alignment can adversely affect reproduction.

In the unlikely event that the author did not send UMI a complete manuscript and there are missing pages, these will be noted. Also, if unauthorized copyright material had to be removed, a note will indicate the deletion.

Oversize materials (e.g., maps, drawings, charts) are reproduced by sectioning the original, beginning at the upper left-hand corner and continuing from left to right in equal sections with small overlaps.

Photographs included in the original manuscript have been reproduced xerographically in this copy. Higher quality 6" x 9" black and white photographic prints are available for any photographs or illustrations appearing in this copy for an additional charge. Contact UMI directly to order.

Bell & Howell Information and Learning
300 North Zeeb Road, Ann Arbor, MI 48106-1346 USA

UMI®
800-521-0600

INORGANIC CONTAMINANT TRANSPORT THROUGH UNSATURATED CLAY SOIL

Mohammad Reza Sabour

A Thesis

in

The School for Building

(Civil Engineering Program)

Presented in Partial Fulfilment of the Requirements

for the Degree of Doctor of Philosophy at

Concordia University

Montreal, Quebec, Canada

July 1997

NOTE TO USERS

Page(s) not included in the original manuscript are unavailable from the author or university. The manuscript was microfilmed as received.

ii

This reproduction is the best copy available.

UMI

ABSTRACT

"INORGANIC CONTAMINANT TRANSPORT THROUGH UNSATURATED CLAY SOIL"

Mohammad Reza Sabour, Ph.D.
Concordia University, 1997

The fate of contaminant migration through the subsurface environment as well as their potential hazard to humans , animals, and aquatic life has become one of the major current concerns of the scientific community. Accordingly, various theoretical and experimental studies have been conducted on the saturated soil by many researchers.

The literature review emphasizes that the problem of the unsaturated transport of contaminants through porous media has received little attention. Thus, the present work is carried out to contribute to the study of heavy metals migration within unsaturated clay soil through mathematical modeling of the mechanisms and parameters which influence the transport phenomenon.

For successful modeling, it is imperative that parameters which affect the transport phenomenon be investigated and determined properly. Hence, the study was conducted through two principal parts. The first part is an experimental investigation to quantify the various soil-water (solution) interactions that have an effect on the flow and contaminant transport and to derive the constitutive relationships required in mathematical modeling. The second part develops a contaminant migration mathematical model which includes unsaturated flow, hydrodynamic dispersion, and physico-chemical reaction between the solid and the liquid phase, employing the theory of mass transport.

The experimental investigation contains two main sets of laboratory tests: *i*) some independent tests in order to isolate and better understand the individual processes, and *ii*) some tests on experimental models of the real phenomena to verify the related parameters in a combined kinetic situation.

The results of all experiments are followed by discussion, in order to better understand the phenomenon behavior, and to realize the relationships among the various processes. Based on the above mechanisms, the governing equations of the problem are derived to provide a quantitative account of the behavior of the phenomenon.

Finally, a finite volume algorithm is developed, on the basis of the mathematical model, in order to solve the contaminant transport equations numerically. Using experimental results, the numerical model is then calibrated and verified. The developed computer code provides the ability to predict the contaminant migration for any depth and period of time. Based on this capability the concentration variations of the solution along the soil profile, especially for long time periods, are predicted and illustrated.

ACKNOWLEDGEMENT

This work has benefited from the support of a number of persons over the course of the past 5 years. First of all I would like to acknowledge the continuous support and encouragement of my advisor Dr. H.B. Poorooshasb, Professor of Civil Engineering, Concordia University. His confidence in my work, guidance and friendship were essential for the successful completion of this thesis.

This endeavor would not have started if it was not for the enthusiasm of my former advisor, Dr. S.H.C. Cheung, associate professor of Civil Engineering, Concordia University. His active interest in this topic and valuable directions and advice were the source of inspiration.

Grateful acknowledgment is wholeheartedly extended to Dr. M. Electorowicz, associate professor of Civil Engineering, Concordia University, for her helpful and valuable suggestions and comments in conducting this thesis.

I am deeply indebted to Dr. D. Taddeo, Dean of Faculty of Engineering and Computer Science, Concordia University, for providing financial support during the last year of my studies. I wish to thank him for his help and understanding.

I express my sincere appreciation to Mr. Ron. Parisella, Environmental Engineering Laboratory Instructor, and Mr. Rocco. Lombardo, Soil Mechanics Laboratory Technician, for their generous and valuable technical assistance and sharing of laboratory expertise.

And most of all, deepest gratitude and indebtedness are due to my parents and my family for the genuine love and support they have provided me over the years. Their understanding, patience, tireless help and unwavering encouragement throughout these years have been invaluable.

I gratefully acknowledge financial support provided by the Iranian Ministry of Culture and Higher Education, through a graduate program scholarship. The research reported here was also funded in part by grants from the Engineering and Computer Science Faculty, Concordia University.

DEDICATION

to

my wife

Afsaneh Sabouri

for all the patient support and encouragement she has given me

and to

my two lovely daughters

Ateieh and **Bahareh**

TABLE OF CONTENTS

LIST OF FIGURES

LIST OF TABLES

CHAPTER 1

INTRODUCTION

1.1 GENERAL

Nowadays, many densely populated areas rely upon groundwater for municipal water supplies. This source can be contaminated by leachate from waste disposal sites which are often located above the groundwater. This contamination is caused by the intrusion of contaminant through unsaturated soil, into the groundwater system.

Consequently, the fate of contaminant migration through the subsurface environment as well as its potential hazard to humans , animals, and aquatic life has become one of the major current concerns of the scientific community. This concern has promoted a wide range of scientists to investigate more aggressively the subject of mass transport within the vadose zone.

This investigation was manifested by the tireless drive to develop an integrated methodology for monitoring, analyzing, and predicting the contaminants migration through the soil-water system. The major tools of this methodology are mathematical models which are developed to simulate the transport of contaminants within the medium. However, for successful modeling, it is imperative that parameters which influence the transport be investigated and determined properly.

Mathematical models describing the concurrent flow of fluids in a porous medium generally consist of continuity equations, physical constraints and a set of constitutive equations required to solve the system. The complexity of balance equations and the number of constitutive relationships required for the model depend upon the complexity of the system and the completeness with which the modeler attempts to capture the behavior of the phenomenon.

Even for the simplest case, the model requires a set of equations giving the hysteretic relationships between soil water potentials, volumetric water contents, and relative hydraulic conductivities. Since they depend on both fluid and solid phase compositions and on the microscopic structure of the solid matrix, these relationships must be determined individually for each system.

The present study attempts to offer a contribution in this area through modeling, the mechanisms and the parameters which influence the transport phenomenon.

1.2 OBJECTIVES OF THE STUDY

Landfills are considered the most economical and practical means for disposal of municipal and industrial solid wastes, and as a means for containment of sludge and liquid concentrates of pollutants. The infiltration of water from rainfall, snowmelt, and surface runoff into the area produces a leachate, which contains several contaminants originating from the disposal wastes.

As the leachate moves downward, various contaminants interact with the soil components, thereby resulting in such processes as physisorption, chemisorption, precipitation, and complexation. Accordingly, soil has been reported to have a capacity to retain heavy metals (Korte et al., 1976; Harter, 1979; Elliott et al., 1981; Yong et al., 1986).

Studies have shown that the capacity of soil to retain heavy metals could be influenced by several factors depending on soil constituents, leachate, and waste characteristics. The displacement and diffusion of pollutants depend on the transport properties of the water, air, and porous medium system (Yong et al., 1992). However,

among different kinds of soil, clay soil barrier is considered a desirable feature in the siting of a land disposal site (Yong and Warkentin, 1987). Accordingly, to decrease the level of contamination of the soil, this study has been focused on the clay soil media.

The leachate from waste disposal sites usually contains various kinds of contaminant. Heavy metals as a group of contaminants that are highly toxic to human, animal, and aquatic life are commonly found in several kinds of waste, including sludge and landfill leachate (Stewart and Weber, 1976). Insufficient knowledge and improper management of waste disposal could lead to groundwater contamination by heavy metals. Thus, this study is related to soil contamination by heavy metals.

Various theoretical and experimental studies have been conducted on saturated clay soil by many researchers (Yong and Samani, 1987; Yong et al., 1992;Barry, 1993; Cooke, 1993; Schakelford, 1994; Rowe et al., 1994; Yong et al., 1995). Nevertheless, the literature review cited in this study emphasizes that the problem of the unsaturated transport of contaminants through porous media has received little attention.

The present study addresses some of the questions left unresolved in the literature. In addition, it attempts to tackle some of the shortcomings alluded to in the literature review. The major objectives of this study are:

1) To investigate the hydraulic characteristics of the soil-water system that strongly affect the transport of materials within partially saturated porous media and to evaluate their impact experimentally.
2) To investigate various contaminant transport processes and their effects on the contaminant migration within unsaturated media.
3) To develop a mathematical model that is capable of simulating the mass transport phenomenon. This model can be used to tackle practical problems and situations when either fully or partially saturated flows are encountered.
4) To predict the concentration of contaminant along the soil profile at any time. This prediction will be done by means of a computer code provided on the basis of a suitable numerical method.

The study is divided into two principal parts. The first part is an experimental investigation, where the findings of unsaturated flow and contaminant transport

experiments are reported. The purpose of the experimental work is to investigate and quantify the various soil-water (solution) interactions that influence the flow and contaminant transport in the partially saturated regime. The experimental results are used to derive the parametric relationships needed in the mathematical model as well as for calibration and verification of the model.

The second part employs the theory of mass transport within the variably saturated porous media to develop a mathematical model. The processes considered in the analysis include unsaturated flow, hydrodynamic dispersion, and physico-chemical reaction between the solid and the liquid phases. This model is achieved by employing the principles of mass balance and the continuity equations.

1.3 THESIS ORGANIZATION

In order to achieve the objective of this study, the thesis is organized into seven chapters including the introductory chapter and 6 appendices. The outline of the remainder of the thesis is presented through the following paragraphs.

Chapter 2 incorporates a literature survey of available studies on the unsaturated flow and contaminant transport phenomena. This review introduces the experimental, theoretical, and numerical investigations that have been performed by various researchers in the past, as well as containing a brief discussion about their research results.

The third chapter presents the mathematical model of the phenomenon. It deals theoretically with main mechanisms and parameters affecting the unsaturated flow and contaminant transport phenomenon, such as relative hydraulic conductivity, contaminants species dispersivity, and sorption process.

In order to achieve clear functions for the parameters of contaminant transport through unsaturated soil, a number of laboratory experiments have been performed. Chapter 3 explains the detail of equipment used and the tests conducted.

The results of all experiments described in chapter 4 are presented in chapter 5. These results are followed by discussion, in order to better understand the phenomenon

behavior, and also to better determine the relationships among related processes. Based on the above mechanisms, the governing equations of the problem are derived, in order to generalize and formulate the overall behavior of the phenomenon.

The objective of chapter 6 is to develop a finite volume algorithm for the numerical solution of the contaminant transport equations. The details about finite volume method, space and time discretization, linearization method, and programming components are presented in this chapter. In addition, verification and implementation of the numerical model is discussed in this chapter.

Finally, chapter 7 concludes the thesis, summarizing the major findings and contributions of this work. It also includes some suggested research areas for the future concerning contaminant transport within unsaturated porous media.

CHAPTER 2

LITERATURE REVIEW

2.1 INTRODUCTION

The increasing awareness and concern about the fate of contaminants' migration through the subsurface environment and their potential hazard to human health, has resulted in a great deal of effort to advance the understanding of the mechanisms responsible for the transport of such contaminants. Accordingly, a methodology for monitoring, analyzing and predicting the movement of contaminants through the soil-water environment is to be developed. Major tools of this methodology are mathematical models, which are designed to simulate the transport of chemicals within the soil system.

In the past few decades, considerable efforts have been directed towards mathematical and numerical modeling of solutes transport through saturated and unsaturated soils (Bear and Bachmat 1990, Alloway 1990, Cooley 1971, Grossl et al. 1994, Huyakorn et al. 1986, Klute 1952, Lapidus and Pinder 1982, Quigly 1993, Sykes et al. 1982, Van der zee 1993, Walter and Weber 1993).

Various theoretical models describing contaminant movement in the soil based on a saturated system have been reviewed by such researchers as Yong and Samani (1987), Gillham and Cherry (1982), Rowe (1993 and 1994), Anderson (1979), and Yong et al.

(1992). The majority of theses models are either advective (neglecting dispersion) or advective-dispersive.

Different test methods of one dimensional diffusive transport in saturated clayey soil have been reviewed and studied theoretically and experimentally: Khan et al. (1994), Barry (1993), Best et al. (1993), Streck and Richter (1997), Aiery (1993), Schakelford (1988), Yong et al. (1985-1995), Cheung (1989), Cook (1993), Barone et al. (1993), and Yin et al. (1997).

Contaminant transport through unsaturated soil has been investigated by Brusseau (1992), Lehmann and Ackerer (1997), Bouma et al. (1996), Fried (1975), Zhang et al. (1996), Freeze and Cherry (1979), Cherry et.al. (1983), Crooks and Guigley (1984), Hitchon (1985), Johnson et. al. (1989), and M.Th. Van Genuchten (1991).

The effect of the saturation degree on adsorption characteristics of unsaturated soil has been studied in the laboratory (Lim, Barbour and Fredlund, 1995), and on the diffusion coefficient by Porter et al., 1960, Barraclough and Tinker, 1982. Silvestri et al. (1995) observed and modeled the variation of water content in clay deposits. Mohammed and Yong et al. (1995) developed a transport model to predict coupled heat and moisture flow in unsaturated clay-based materials. Zhang et al. (1996) conducted a field study and stochastic analysis on solute transport through the vadose zone, and Lehmann and Ackerer (1997) determined soil hydraulic properties by inverse method in one-dimensional unsaturated flow.

Although many advances in this area have been made, there remains much to discover and understand, especially concerning unsaturated soil media. Furthermore, the literature reveals that the migration of heavy metals through unsaturated clay barriers has received little attention. Yong et al. (1994) studied the effect of soil composition on the migration of heavy metals, and Chen et al. (1997) investigated the effect of pH on heavy metals' sorption on the mineral apatite. Lee et al. (1996) predicted soil-water partition coefficients for cadmium, and Coughlin et al. (1995) studied the non-reversible adsorption of divalent metal ions onto geothite.

The methods describing the movements of contaminants in unsaturated soil are very few although clay liner systems should be constructed in unsaturated soil, and analysis

and prediction of coupled solute and moisture flow through unsaturated clay barriers over long periods are necessary for the design of new disposal facilities. Hence, in order to predict the rate of transport of pollutants through an unsaturated clay soil, a method that describes the full coupling effects on transport coefficients based on experimental work is needed to be applied to the unsaturated flow and contaminant transport theory.

This chapter reviews the most important literature dealing with unsaturated transport models. Since water is the primary carrier of contaminants towards the groundwater, unsaturated flow investigation is first reviewed.

2.2 GENERAL GOVERNING EQUATION

The study of contaminant transport through unsaturated soil is limited to the recent decades. Even though numerous investigations have been conducted on contaminant transport in the unsaturated zone, unfortunately it appears that the ability to fully characterize the transport phenomenon has not kept pace with the modeling expertise. The general governing equation which describes the transport phenomena was developed and is expressed for discussion.

The law governing the contaminant transport through unsaturated soil was obtained through a balanced equation to reflect the mass conservation of both water and contaminant. The following equation,

$$\theta\frac{\partial c}{\partial t}=\frac{\partial}{\partial z}[\theta D\frac{\partial c}{\partial z}]-q\frac{\partial c}{\partial z} \tag{2.1}$$

is a one-dimensional transport of non-reactive solute through a porous medium in the absence of sources and sinks (Bresler and Dagan, 1983).In this equation, c is solute concentration, θ is volumetric water content and q is water flux. D, z and t are the coefficients of hydrodynamic dispersion, vertical distance, and time, respectively. The term hydrodynamic dispersion denotes the spreading (at the macroscopic level) resulting from both mechanical dispersion and molecular diffusion.

Following numerous investigations conducted on contaminant transport, in 1991, Van Genuchten, presented his description for one-dimensional solute movement in the unsaturated zone, in the most complete form as:

$$\frac{\partial}{\partial t}(\theta c) = \frac{\partial}{\partial z}[\theta D \frac{\partial c}{\partial z} - qc] + s \qquad (2.2)$$

where D and s are solute dispersion coefficient and source/sink term, respectively. The source/sink term in the above equation may account for a variety of physical, chemical and biological interactions.

In order to derive this equation the following assumptions are made;

1) The equation is derived for sand soil,
2) Soil is a homogeneous material and its properties are constant with time,
3) Air is in a stationary condition, i.e. there is no flow for air within porous media,
4) There is no variation for temperature, i.e. isothermal condition,
5) Any long or short term interactions between soil and water is neglected,
6) Darcy's law is valid,
7) The osmotic and electro-chemical potentials of the pore water are negligible.

Needless to say that, these assumptions are not valid for most field situations.

Viscosity, pressure, density, soil properties (such as tortuosity, void ratio, soil-water potential, pore size distribution, fabric, mineralogy composition, and soil structure) and soil-water interactions (heat, wetting, ionic concentration, thickness of layers of water held to soil particles) are all factors associated with the forces holding water to soil and with clay-water interaction (Yong et al., 1992).

Water carrying pollutants and soil particles interact with each other. These interactions may be expected to influence the physical and physico-chemical behavior of the material while moving through an unsaturated zone. The interaction between water-contaminated water and the soil system is described in terms of ion exchange, adsorption and precipitation mechanisms. Displacement and diffusion of pollutants

depend on the transport properties of water, air, and the porous medium system (Yong et al., 1992).

The most important factor limiting the successful application of the contaminant transport equation to the actual field problem is the lack of information regarding the parameters entering the governing transport equation. Proposing general equations that can be adopted for this study, requires a comprehensive understanding of the major factors affecting the governing equations' parameters. This requirement cannot be satisfied unless the processes related to these parameters are considered properly, i.e. taking into account the essential factors affecting each process as much as possible.

2.3 THE GOVERNING EQUATION PARAMETERS

Equation (2.2) contains four general components: ***i***) unsteady, ***ii***) advective, ***iii***) hydrodynamic dispersive, and ***iv***) source/sink terms. Excluding the first term (on the right hand side), all the other terms are presented on the basis of some unknown parameters, i.e. q, D and s. In order to solve Eq. (2.2) these parameters should be determined. The following paragraphs review the history of investigations related to these parameters. The unsaturated flow parameters are first considered.

2.3.1 Unsaturated Flow Parameters

The above proposed contaminant transport equation contains the unsaturated flow parameter (q), which is an unknown variable. In order to obtain q (water flux), the unsaturated flow should be taken into consideration.

The study on unsaturated flow was started in 1907 by Buckingham. The mechanism which he introduced was based on the capillary potential concept. Israelson connected Buckingham's mechanism to Darcy's law in 1927, which states that water flows towards the direction which decreases its total potential (Bruin and Luyben, 1980),

$$q = -K_r \frac{\partial H}{\partial z} \tag{2.3}$$

where K_r, H and z are the relative hydraulic conductivity, capillary potential, and depth, respectively. In this equation K_r is a function of volumetric water content θ and/or soil water potential H. In 1931, L.A. Richards introduced capillary conduction of liquids through porous media, in order to obtain relative hydraulic conductivity K_r.

Significant advances have been made since 1950 in the mathematical description of water in medium and coarse grained soils. In 1956, Bruce and Klute explained the water adsorption with the soil horizontal column through diffusion concept,

$$\frac{\partial \theta}{\partial t} = \frac{\partial}{\partial x}[D(\theta)\frac{\partial \theta}{\partial x}] \tag{2.4}$$

where $D(\theta)$ is the water diffusivity. The diffusivity coefficient is defined as the ratio of relative hydraulic conductivity K_r to the differential water capacity of the soil $C(H)$. The latter parameter is the slope of the retention curve, i.e. $C(H)=\frac{d\theta}{dH}$.

Philip (1969) formulated the process of infiltration as

$$\frac{\partial \theta}{\partial t} = \frac{\partial}{\partial z}[K_r(\frac{\partial H}{\partial z} - 1)] \tag{2.5}$$

In addition, Yong and Warkentin (1975) considered the unsaturated flow mechanism in more detail to obtain the general governing equation. These authors also considered the effect of gravitational potential on the movement of water through unsaturated soil. Bear (1977) studied unsaturated flow based on some assumptions. He concluded up with the Richards equation, which is widely used as a model for the flow of water in unsaturated soils.

Since 1975, most studies focused on determining the coefficients governing the process of flow. In 1976, Mualem derived the following equation for predicting the relative hydraulic conductivity K_r from knowledge of the soil-water retention curve

$$K_r = \theta_e^{0.5}\left[\frac{\int_0^{\theta}\frac{dx}{H(x)}}{\int_0^{1}\frac{dx}{H(x)}}\right]^2 \tag{2.6}$$

where H is the soil water potential, given as a function of the dimensionless water content θ_e,

$$\theta_e = \theta_r + \frac{\theta - \theta_r}{\theta_s - \theta_r} \tag{2.7}$$

where s and r indicate saturated and residual values of the water content θ, respectively.

Van Genuchten (1980) presented the soil water retention curve through the following model:

$$\theta = \theta_r + \frac{\theta_s - \theta_r}{[1-(aH)^n]^m} \tag{2.8}$$

and relative hydraulic conductivity by using dimensionless water content θ_e, as

$$K_r = \theta_e^{0.5} K_s[1-(1-\theta_e^{\frac{1}{m}})^m]^2 \tag{2.9}$$

where n is a constant, m=1-1/n and K_s saturated hydraulic conductivity of the soil.

In 1972, Ahuja and Swartzendruber attempted to express diffusivity as an empirical function of θ:

$$D(\theta) = \frac{a\theta^n}{(\theta_s - \theta)^m} \tag{2.10}$$

where a, m, and n are constants for a particular soil. Yong and Warkentin (1975) and Brutsaert (1979) expressed the diffusion function in an exponential form:

$$D=a\exp(b\theta) \tag{2.11}$$

Clothier et al. (1983) proposed fitting a function chosen from those presented by Philip (1960) for which analytical relations between the soil water diffusivity and the soil water content can be developed. Johan and Robert (1985) proposed an empirical function to describe water distribution data from horizontal infiltration experiments.

In 1990, Meyer and Warrick derived soil water diffusivity from horizontal infiltration experiments by using a rotational function to conform to water content profiles, resulting from horizontal infiltration. They expressed diffusivity as:

$$D(\theta) = 0.5[\frac{A_3 - A_1 A_2}{(A_3 - A_2\theta)^2}]f(\theta,\theta_i) \tag{2.12}$$

where A_1, A_2 and A_3 are coefficients obtained from experimental results.

Probably the most complete theoretical formula for flow parameter K is the Kozeny-Carman relationship

$$K = \frac{n^3 C_s \gamma}{\eta T^2 S^2 (1-n)^2} \tag{2.13}$$

where η, T, γ, and C_s are viscosity, tortuosity, density and shape factor, respectively. Also, the parameter S in Eq. (2.13) is the wetted surface area and n is the soil porosity.

This relationship takes into account the fluid (water) and porous media (soil) properties. It does not, however, include the effect of soil-water interaction. In addition, among the different forces applied to the fluid molecules to move within the porous media, this relationship just considers the gravitational force.

Equation (2.13) applies only to granular soils, with relatively uniform particle size and

1) the ionic property of the clay soils' particles exert a surface force in addition to the gravity forces,
2) clay soils contain completely different mineralogical properties than sand soils, which results in some extra physico-chemical interaction with water, and
3) clay soils have an entirely different orientation of the particles compared to sand soils, and this causes particular hydraulic properties.

Because of these differences, it is necessary to consider the hydraulic parameters and flow behavior for these soils, separately.

The empirical unsaturated flow formula presented by previous investigators, are mostly based on θ. These formulas cannot describe the real behavior of the phenomenon as precise as those based on soil water potential H. Although very few of researchers took into account the latter variable (H), however, they either considered some certain components of H, or did not pay attention to the hysteresis effect.

2.3.2 Hydrodynamic Dispersion

The third component of the general governing equation for contaminant transport through unsaturated soil is related to the hydrodynamic dispersion parameter. One of the earliest observations of dispersion phenomena is reported by Slichter (1905), who used an electrolyte as a tracer to study the movement of groundwater. Between 1950 and 1975, a large number of articles were published, where theories on dispersion have been developed. This includes investigators such as de Josselin de Jong (1958), Saffman (1959, 1960), Bear (1969,1972) Wilson and Gelhar (1974), and Fried (1975).

Bear's (1978) main effort was to express hydrodynamic dispersion macroscopically through a partial differential equation, and to determine the nature of the coefficients. His special interest was the relationship between these coefficients, soil matrix and flow parameters. He defined the hydrodynamic dispersion coefficient D, as the summation of

the mechanical dispersion coefficient D_h, and the molecular diffusion coefficient D_m, i.e. for a porous medium

$$D = D_h + D_m \tag{2.14}$$

where both of the latter coefficients are functions of matrix and flow parameters.

But, the diffusion/dispersion coefficient of the various contaminant ions cannot be assumed as being constant. This is because the driving force for ionic movement is not only affected by the concentration gradient, but also by:

1) the electrostatic potential gradient resulting from different mobilities of ions,
2) the charged surfaces of clay minerals, and
3) the viscosity of the pore fluid solution.

These factors are to a very large extent functions of the solute components' concentration. It is, therefore, appropriate to assume that the diffusion/dispersion coefficient of every component is a function of its concentration in the pore fluid (Yong and Samani,1987). The fact that the diffusion/ dispersion coefficient in clay soils is not constant was previously observed by many researchers, including: Letey and Klute (1960), Yong and Warkentin (1975), and Crooks and Quigley (1984).

At first, the coefficient of hydrodynamic dispersion was assumed to be of the form

$$D(\theta,q) = W(q/\theta)^n \tag{2.15}$$

where W, n represent the parameters to be estimated by optimization. Beliuk and Wheatear (1990) introduced a three parameter model for the coefficient of hydrodynamic dispersion in the form

$$D(\theta,q) = W(q/\theta)^n + Y \tag{2.16}$$

in which Y is the coefficient of molecular diffusion.

It should be mentioned that some researchers (Philip 1968, Rowe et al. 1980) paid attention to the stagnant pores. As a result (Rowe et al. 1980), suggested to add the effect of this phenomenon to the diffusion coefficient

$$D=D_m+D_h+D_s \tag{2.17}$$

where D_s is the dispersion coefficient due to the effects caused by the diffusion of solutes from stagnant regions to the mobile ones. They gave the expression for D_s as below (for the case of spherical aggregates with radius r)

$$D_s = \frac{v^2 r^2 (1-\Phi)}{15 D_{es}} \tag{2.18}$$

where Φ, v and D_{es} are the pore-water fraction in the conducting region, the pore water velocity, and the effective diffusion coefficient in the stagnant region, respectively.

Additional theoretical investigations on molecular diffusion coefficient have been done. This coefficient is introduced as $D_m=D_oT$, where D_o and T are infinite solution diffusion coefficient and physico-chemical tortuosity factor, respectively. The physico-chemical tortuosity factor T, is introduced to modify the infinite solution diffusion coefficient D_o.

The treatment of molecular diffusion given by both Nernst (1888) and Einstein (1905) shows the complex interdependencies which govern the coefficient. The studies on the subject initially dealt with the movement of suspended particles controlled by the osmotic forces in the solution. The three expressions most often cited (by Nernst-Einstein, Nernst, Einstein-Stokes, (1905), respectively), are:

$$D_o=uRT/N=uK'T \tag{2.19}$$

$$D_o=RT\lambda/\xi|z|=8.928\times10^{-10}\lambda/|z| \tag{2.20}$$

$$D_o=RT/6\pi N\eta r=7.166\times10^{-21}T/\eta r \quad (2.21)$$

where u = absolute mobility of the solute, R = universal gas constant, T = absolute temperature, N = Avogadro's number, K' = Boltzmann's constant, λ = conductivity of the ion or solute, r = radius of the hydrated ion or solute, η = absolute viscosity of the fluid, z = valence of the ion, and ξ = Faraday's constant. Regardless of which D_o model one chooses, it is evident that the infinite solution diffusion coefficient is dependent on several (above) factors.

In the molecular diffusion coefficient, T is indicated by relationship $(L/L_e)^2$, where L_e and L refer to actual and straight line path lengths, respectively. Tortosity factors cited have ranged from 0.05 to about 0.9, for different types of clays.

An alternate view on the tortuosity factor T, considers this to be more than a geometric factor, dependent only on the variability of the pore sizes and connections. Wagenet (1981) contends that other soil physico-chemical factors will also participate in reducing the value of D_o as follows:

$$T=\theta L^2 wx/L_e^2 \quad (2.22)$$

where w and x are coefficients, accounting for charged soil matrix on water viscosity and anion exclusion, respectively. Another format for D_m has been suggested by Kemper and Van Schaik (1966) as follows:

$$D_m=D_m(\theta)=D_o a \exp b\theta$$

where the constants a and b are given as $0.005<a<0.01$, and $b=10$.

2.3.3 Source/Sink Term

The source/sink term is the last component of the general governing equation for contaminant transport through unsaturated soil. In addition to the dispersion phenomenon, the source/sink term attracted the investigators' attention. Since the chemical properties of both the resident pore fluid and solutes, as well as the surface-active relationships established by the clay particles, geochemical reactions will exist when the interacting solutes permeate into the clay soils (Yong and Warkentin, 1975). Geochemical reactions such as adsorption, desorption can be considered by source/sink term (such that it behaves as a sink for adsorption, and as a source for desorption due to ion exchange).

In 1915, Langmuir presented an equilibrium isothermal function for adsorbed or desorbed solute mass per unit mass of soil s, as:

$$s = \frac{ac}{1+bc} \tag{2.23}$$

and later Freundlich (1926) proposed another equilibrium isotherm function for s

$$s = K c^{n'} \tag{2.24}$$

where a, b, K and n' are isothermal coefficients.

The special case of a linear equilibrium isothermal adsorption relationship, which states that the rate of adsorption is constant, has been presented as well. Such relationships are not physically valid, since the ability of clay particles to adsorb the solute decreases as the amount of the adsorbed solute increases and hence, the rate of adsorption decreases rapidly as the concentration in the pore fluid solution increases (Yong and Warkentin,1975).

In the migration of solute leachate through soils, adsorption/desorption reactions are normally time dependent (Murali and Aylmore, 1983), because the fluid flow might be

so fast relative to adsorption reactions that equilibrium between the adsorbed solute and that solute in the pore fluid cannot be fully established. Common non-equilibrium adsorption models are given below (Murali and Aylmore, 1983):

$$\frac{\partial s}{\partial t} = K_a c - K_d s \tag{2.25}$$

$$\frac{\partial s}{\partial t} = K_a c^n - K_d s \tag{2.26}$$

$$\frac{\partial s}{\partial t} = K_a c(Q - s) - K_d s \tag{2.27}$$

$$\frac{\partial s}{\partial t} = K_a cQ - K_d s(1 + K_1 c) \tag{2.28}$$

where K_a, K_d, n, Q and K_l are empirical coefficients. These models are referred to as the non-equilibrium forms of linear, Freundlich and Langmuir adsorption models, respectively. Equations (2.27) and (2.28) are two different ways of expressing Langmuir type non-equilibrium models.

The latter investigation is limited to saturated sandy soils, i.e. it is not applicable to the unsaturated clay soils. Since the active nature of the clay minerals' surface, and the interactions established between clay particles and the surrounding pore fluid solution, cause clay soils to behave as a leaky semi-permeable membrane (Yong and Warkentin, 1975) which is very far from the sand soil behavior.

Among various models proposed for adsorption phenomena, the linear equilibrium isotherm adsorption relationship requires a constant rate of adsorption and is not valid on physical grounds. Because the ability of clay particles to adsorb solute ions decreases as the amount of adsorbed ions increases, this fact cannot conform to the limitless adsorption of the adsorbate.

An improvement over the contaminant adsorption model is the Freundlich (1926) model, $s = Kc^n$. Although this is a considerable advancement, the model still allows for unlimited adsorption. But the improved Langmuir isotherm model (Eq. 2.29)

$$\frac{c}{s} = \frac{1}{bs_{max}} + \frac{c}{s_{max}} \tag{2.29}$$

has limited the adsorption to the s_{max}, which better than others conform to the real situation.

The above isotherm models are presented for equilibrium condition. This means that the adsorption happens instantaneously, i.e. any changes in concentration of one produces an immediate change in the other. This justification is not acceptable completely, because as concentration of solute on soil surface increases, the rate of adsorption should be decreased.

Hence, non-equilibrium functions are more realistic than equilibrium ones. But in literature, very few non-equilibrium equations have been introduced. These models are presented for sand soils, and are not applicable to the clay soils.

Furthermore, these models are presented for saturated soils, and are based on the assumption that all soil particles surfaces have access to the pore solution. But these conditions do not exist for all regions, especially for unsaturated soils, in which the water does not occupy the entire pore space. Thus, none of these models could be utilized for this study.

In addition to the above weak aspects of previous sorption investigations, there are many factors missing, in the literature which some of them are

1) the nature of contaminant,
2) buffering capacity (chemical and/or physical barrier) effect,
3) temperature,
4) pH of solution,
5) osmotic effect,
6) boundary and initial conditions effects,

7) reversibility and/or irreversibility of the process,
8) shear stresses effect, in combination with the other contaminant transport processes,
9) flow (kinetic situation) effect,
10) influence of portional contact between soil particles and fluid.

Some of the latter factors effects are investigated individually, but the other effects have not received much attention in the literature. Accordingly, extra research work is required, in order to clarify the effects of various aforementioned factors, as well as, the nature of the phenomenon (contaminant transport through unsaturated clay soil).

CHAPTER 3

MATHEMATICAL MODELING

3.1 INTRODUCTION

The pollution of the environment is largely caused by mass transfer, especially in soils under the ground surface. This transformation is the final result of fluid flow, chemical reaction, mass transfer, and other related processes.

Since the processes under consideration have such an overwhelming impact on human life, one should be able to deal with them effectively. This ability can result from an understanding of the nature of the processes and from methodology with which one can predict them quantitatively.

The prediction should state how any of these quantities would change in response to the proposed changes in geometry, flow rate, fluid properties, mass species characteristics, etc. A theoretical prediction works out the consequences of a mathematical model, rather than an actual physical model, which are based on some fundamental principles. Theoretical calculation not only offers low cost and high speed over a corresponding experimental investigation, it also gives detailed and complete information.

If the methods of classical mathematics were to be used for solving these equations, there would be little hope of predicting many phenomena of practical interest. Fortunately, the development of numerical methods and the availability of large digital computers hold the promise that the implication of a mathematical model can be worked

out for almost any practical problem. The boundary and initial conditions are required to find the particular solutions of the general governing equations.

3.1.1 Continuum Fluid Field Model

The dependent variables, such as concentration (c) would, in general, be a function of three space coordinates and time. Thus, $c=c(x,y,z,t)$, where x, y, z, and t are the independent variables. In obtaining the basic equations of fluid motion, physical principles are to be applied to a suitable model of the flow. Therefore, definition of a suitable model of the flow is required. If one considers a general flow field as represented by the streamlines in Fig. (3.1), a closed volume drawn within a finite region of the flow could be imagined. This volume defines a control volume, v. A control surface, s, is denoted as the closed surface which bounds the volume.

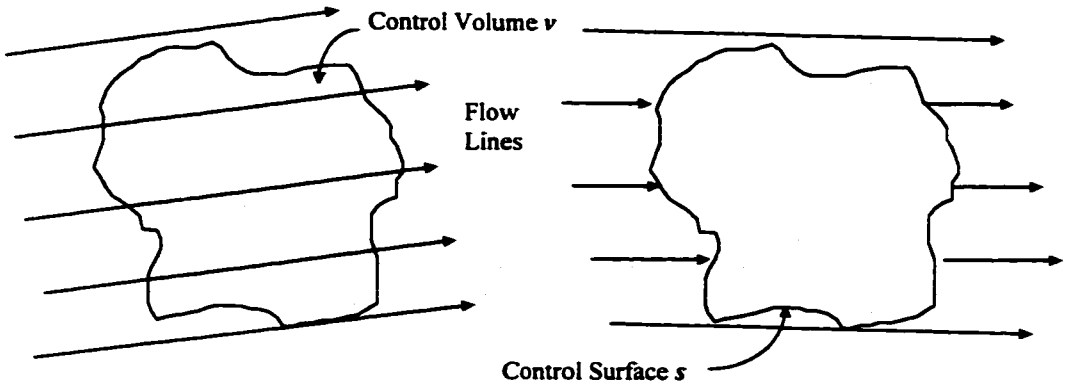

Figure 3.1 Finite Control Volume Approach

The control volume may be fixed in space with the fluid moving through it, as shown at the left of Fig. (3.1). Alternatively, a control volume may be moving with the fluid such that the same fluid particles are always inside it, as shown at the right of Fig. (3.1). In either case the control volume is a reasonably large and a finite region of the flow.

The fundamental physical principles are applied to the fluid inside the control volume, and to the fluid crossing the control surface (if the control volume is fixed in space). Thus, instead of looking at the whole flow field at once, with the control volume model the attention is limited to just the fluid in the finite region of the volume, by itself.

When one gets to numerical simulation, through the finite volume numerical method, it is necessary to cover the whole domain with a finite number of non-overlapping sub-domains (control volumes or cells) to handle the numerical method rules to those cells. As it will be noticed later, in chapter 6, the properties of the discretized domain have more applicability to that of finite control volume model.

The fluid flow equations that were directly obtained by applying the fundamental physical principles to a finite control volume are in integral form. These integral forms of the governing equations can be manipulated to indirectly obtained partial differential equations. The equations so obtained from the finite control volume fixed in space (left side of Fig. 3.1), in either integral or partial differential form, are called the conservation form of the governing equations.

Since the purpose of this study is knowing the variations of the dependent variables at a certain fixed point and time, the conservation form of the equation is preferred, i.e., the Eulerian description which is much more common for fluid motion studies is chosen.

3.1.2 Governing Differential Equations

The present study deals with contaminant (mass) transport in porous medium in which the considered mass is that of some solute moving with the solvent (water) in the interstices of a porous medium, for the unsaturated zone. The main mechanisms affecting this transport are: convection, mechanical dispersion, molecular diffusion, solid-solute interactions and various chemical reactions and decay phenomena, which may be regarded as source/sink for the solute.

Our objective in this section is to present the laws governing the movement and accumulation of pollutants in unsaturated soil flow. This will be done through a balance equation which takes the form of a partial differential equation. By subjecting this equation to specified initial and boundary conditions, future contaminant species distributions could be predicted.

Since the primary carrier for contaminant transport in soil is water, for contaminant movement prediction it becomes necessary to first consider the overall status of water within soil media. In unsaturated soils, the movement of fluid is controlled largely by internal gradients developed by forces within the soil, whereas the contaminant transport is tied closely to water movement, and the contaminants diffusion is highly dependent on the soil water content.

3.2 FLUID FLOW IN UNSATURATED CLAY SOIL

Mathematical models describing the concurrent flow of two or more fluids in a porous medium generally consist of continuity equations (one for each mobile phase), physical constraints and a set of constitutive equations required to slove the system. The complexity of balance equations and the number of constitutive relationships required for the model depend upon the complexity of the system and the completeness with which the modeler attempts to capture its physics.

The distribution and migration of water in soils are dependent on many fluxes such as those arising from the internal energy of water itself, and from external and superficial mechanisms and driving forces due to thermal, ionic, osmotic, gravitational, hydraulic and other gradients. The rate of movement or migration of water depends on the magnitude of the forces and gradients, and also on the factors determining the transmission coefficient or hydraulic conductivity of the soil.

For partly-saturated soils, the movement of water is generally considered as viscous flow and is primarily due to gradients of matric or capillary potential which arise from differences in water content. Soil water will also move under the influence of physico-chemical forces associated with the interaction of the surface active solids in the soil

and water. The potentials existing in clay soils produce gradients which will induce moisture transfer. Actually, there is a tendency for water to diffuse into regions of higher ionic concentration to attain a more uniform ionic distribution. This tendency will create a condition for osmotic flow.

Before deriving the governing equation, it is necessary to define some physical properties of the system.

3.2.1 Terminology

An unsaturated soil element consists of three phases: one solid phase (soil particles) and two fluid phases: liquid (water) and gas (air). In principle, both the water and air move simultaneously in the void space. The movement of air is ignored based on the assumption of constant pressure (atmospheric pressure) for the air all over the soil void space. Moreover, in the case of air-water systems one is normally interested in the liquid flow behavior, which plays the dominant role in the transport of non-highly-volatile chemicals (Pinder and Abriola, 1986). Therefore, attention hereafter is paid to water as the only fluid phase under consideration.

According to this assumption the definitions are as follows:

Volumetric water content θ, is defined as the volume of water per unit volume of soil. Since relative saturation s_r, is equal to the volume of water per unit volume of void space, the relationship between θ and s_r is:

$$\theta = n s_r \tag{3.1}$$

where n is the soil porosity.

Since volume of water is the product of θ and volume of soil v, then mass of water m_v, is

$$m_v = \rho^w \theta v \tag{3.2}$$

where ρ^w is fluid (water) density. On the other hand, volumetric water flux (Darcy's flux) $\vec{q}$, is the volume of water passing through the unit surface per unit time; i.e.

$$\vec{q} = \frac{\vec{\vartheta}}{At} \tag{3.3}$$

where $\vec{\vartheta}$, A and t are volume of water, surface area, and time, respectively. Discussion in more detail corresponding to $\vec{q}$ is left to the section 3.2.3. Thus q_x is the volume of water passing through unit surface perpendicular to the x axis per unit time.

Fluid velocity υ, is defined as volume of water passing through the unit surface of water per unit time. According to this definition, volumetric water flux is the product of fluid velocity and volumetric water content; i.e.,

$$\upsilon = q/\theta \tag{3.4}$$

3.2.2 Unsaturated Flow Equation

According to the first conservation law, no mass is created or destroyed. Therefore, the difference between the mass flow into the control volume and out of it must be equal to the increase or decrease in mass contained in the control volume. The mass of a moving fluid across any fixed surface is equal to the product of component of mass flux perpendicular to the surface and area of surface. Hence the elemental mass flow across the area of ds is

$$\rho q_n ds = \rho \vec{q} \cdot \vec{ds} \tag{3.5}$$

The net mass flow out of the entire control volume through the control surface s is the summation over s of the element mass flows shown in Eq. (3.5). In the limit this

becomes a surface integral, i.e., $\int_s \rho\vec{q} \cdot d\vec{s}$. The mass contained within the element volume dv is $\rho\theta dv$. The total mass inside the control volume is, therefore, $\int_v \rho\theta dv$. The time rate of decrease of mass inside v is then $-\frac{\partial}{\partial t}\int_v \rho\theta dv$.

Thus equating the net mass flow out and time rate decrease of mass gives

$$-\frac{\partial}{\partial t}\int_v \rho\theta dv + \int_s \rho\vec{q} \cdot d\vec{s} = 0 \qquad (3.6)$$

which is the integral form of the continuity equation. Applying the divergence theorem from vector calculus and doing some rearrangements, Eq. (3.6) becomes

$$\int_v [\frac{\partial(\rho\theta)}{\partial t} + \nabla \cdot (\rho\vec{q})] dv = 0 \qquad (3.7)$$

After generalization and substitution of parameters, a mass balance equation, may be written for species i in a medium consisting of an inert, immobile solid phase and n fluid phases as

$$\sum_{\alpha=1}^{n} \{\frac{\partial}{\partial t}(ns_\alpha \rho^\alpha \omega_i^\alpha) - \nabla \cdot [\rho^\alpha \omega_i^\alpha \frac{k\, k_{r\alpha}}{n\mu_\alpha}(\nabla p^\alpha + \rho^\alpha g \nabla z)] - \nabla \cdot J_i^\alpha - ns_\alpha \rho_\alpha f_i^\alpha\} = 0 \qquad (3.8)$$

(Abriola and Pinder, 1985), where ρ^α is the density of the α phase, ω_i^α is the mass fraction of species i in phase α, k is the intrinsic permeability tensor, $k_{r\alpha}$ is relative permeability to the α phase, μ_α is the kinematic viscosity of the α phase, P^α is the total potential on phase α, J_i^α is non-advective flux of species i in the α phase, f_i^α is

external supply of species i to the α phase, g is gravitational acceleration and z is elevation above some horizontal reference plane.

Eq. (3.8) is supplemented by constraints $\sum_i \omega_i^\alpha = 1$ and $\sum_\alpha s_\alpha = 1$, imposed by the physics of the system. In addition to these auxiliary conditions, Eq. (3.8) requires an extensive set of constitutive equations to solve the system. These include relationships between porosity, fluid pressure, density, relative saturation, relative permeability, chemical compositions and viscosity. In unsaturated flow models, fluid pressures are often expressed in terms of capillary pressure (matric head), which is defined as the pressure difference between non-wetting (a) and wetting (w) fluid phases; i.e., $P_{caw} = P^a - P^w$.

The aforementioned model may be used to simulate fluid flow in many geologic porous media. For the problem at hand, in the most widely used formulations, pressure gradients in the soil gas phase are assumed to be negligible. Water (w) is the wetting and air (a) the non-wetting fluid in this system. Further, it is assumed that

1) The liquid phase is incompressible and consists entirely of water (i=w; α=w; $\omega_w^w = 1$; $\nabla \cdot J_i^w = 0$);
2) Changes in water pressure in the unsaturated soil zone are insufficient to cause matrix deformation;
3) There is no external supply of water to the system ($f_i^w = 0$).

Under this set of assumptions Equation (3.8) gives

$$\frac{\partial \theta}{\partial t} - \nabla \cdot [\frac{k_r k}{\mu n}(\nabla P - \rho g \nabla z)] = 0 \qquad (3.9)$$

for the liquid phase. In Eq. (3.9) the subscripts w, are dropped since all variables refer to water.

In the nomenclature of groundwater modelers, it is customary to define saturated hydraulic conductivity (Pinder and Gray, 1977) as

$$\underset{\approx}{K_s} = \rho g \underset{\approx}{k} / \mu \tag{3.10}$$

and matric head (suction)

$$\psi = (P^w - P^a) / \rho\, g = -P_c / \rho\, g \tag{3.11}$$

where P^a and P_c are pressure in the soil gas phase and capillary pressure (P_{cnw}), respectively. If these definitions are substituted in Eq. (3.9) a form of Richards equation (Dullien, 1979) for unsaturated flow would be obtained

$$\frac{\partial \theta}{\partial t} - \nabla \cdot [k_r \underset{\approx}{K_s} \cdot (\nabla \psi - \nabla z)] = 0 \tag{3.12}$$

which is a nonlinear parabolic differential equation (Aronson, 1988).

The Richards formulation provides us with one equation in three unknowns: θ, k_r and ψ. It must be supplemented by two further equations: a relationship between relative permeability and volumetric water content $k_r = k_r(\theta)$, and a relationship between fluid pressure and volumetric water content $\psi = \psi(\theta)$. The second is often referred to as the moisture retention function. These relationships will be discussed more in section 3.2.2; however, the dependence of ψ and k_r on the volumetric water content θ, explicitly emphasizes the nonlinear nature of Richards equation.

Eq. (3.12) is known as the mixed form of Richards equation. For both analytical and numerical purposes it is sometimes advantageous to transform the mixed form to an equation with one principal unknown; i.e., θ-based or ψ-based form. The choice of the form of Richards equation becomes an issue of great importance in obtaining a numerical solution.

In order to,

1) Avoid the discontinuity of θ, caused by any kind of non-homogeneity of the soil;

2) have the sensitivity of the model to the entrance of any solute into the soil water;

the ψ-based form of Richards equation has been selected for this study. Thus, use of the chain rule for differentiation of the time term

$$\frac{\partial\theta}{\partial t}=\frac{d\theta}{d\psi}\cdot\frac{\partial\psi}{\partial t} \tag{3.13}$$

gives the ψ-based form

$$c(\psi)\frac{\partial\psi}{\partial t}-\nabla\cdot[k_r K_s\cdot(\nabla\psi-\nabla z)]=0 \tag{3.14}$$

where the specific moisture capacity is defined as

$$c(\psi)=\frac{d\theta}{d\psi} \tag{3.15}$$

Since the problem at hand is considered to be one dimensional, Eq. (3.14) is converted to

$$c(\psi)\frac{\partial\psi}{\partial t}=\frac{\partial}{\partial z}[k_r K_s(\frac{\partial\psi}{\partial z}-1)] \tag{3.16}$$

which is the ψ-based one-dimensional unsaturated flow equation along z direction, vertically positive downward.

3.2.3 Unsaturated Darcy's Flux

Many investigators conclude from experiments that when two immiscible fluids flow simultaneously through a porous medium, each fluid establishes its own tortuos path. They assume that a unique (or nearly so) set of channels corresponds to every

degree of saturation. When saturation of the wetting fluid (water) is reduced, it becomes discontinuous at the irreducible wetting fluid saturation, and therefore no flow of water can take place.

With the above idea in mind, it seems natural to apply some modification to the hydraulic conductivity, owing to the presence of the second phase which occupies part of the void space. Hence, instead of a constant value for hydraulic conductivity k, relative hydraulic conductivity K_r, as a function of volumetric water content θ may be used.

Determination of the factors affecting K_r are complicated, and these factors normally cause K_r to be defined as a non-linear function. Discussion in more details corresponding K_r function is left to the section (3.2.4.1).

The motion equation in the form of Darcy's law for three-dimensional flow of a homogeneous incompressible fluid (water) is

$$\vec{q} = -\underset{\approx}{k} o \nabla \phi \qquad (3.17)$$

where ϕ is the piezometric head. For the problem at hand, $\underset{\approx}{k}$ and ϕ should be substituted with $\underset{\approx}{K_r}$ and h_t, respectively.

Considering one-dimensional flow (vertically positive downward), h_t is the summation of three potentials: 1- kinetic, 2- pressure (capillary, ψ), and 3- gravitational potential. The first potential ($v^2/2g$), is negligible because v is very small, and the last is equal to z (elevation). Thus $h_t = \psi + z$. On the other hand, K_r could be considered as the product of relative permeability k_r, and intrinsic permeability K_s.

As a result, Eq. (3.17), after substitution reduces to

$$q = K_r(\frac{\partial \psi}{\partial z} - 1) = -k_r K_s(\frac{\partial \psi}{\partial z} - 1) \qquad (3.18)$$

3.2.4 Constitutive Relation

The solution of Equation (3.16) requires the knowledge of the relative hydraulic conductivity and moisture content relationship $K_r(\theta)$, and soil moisture retention function $\psi(\theta)$. Several investigators have proposed various parametric expressions describing $K_r(\theta)$ and $\psi(\theta)$, that these relationships are the sources of non-linearity in Richards equation. For an isothermal condition and an isotropic soil the constitutive relations are considered to depend on the volumetric water content θ, as well as the history of θ. Dependence on history produces hysteresis in these functions, which exhibit significant effect on the real value of these parameters, especially for clay soil.

The theoretical description and prediction of the $\psi(\theta)$ and $K_r(\theta)$ curves is an ongoing challenge for hydrologists and soil scientists. In modeling, except for very few theoretical models, the relationships are usually derived as a non-linear function which fits experimental data. The most frequently used expressions are outlined bellow.

3.2.4.1 Relative Hydraulic Conductivity

Relative hydraulic conductivity K_r is a variable value dependent on θ, or soil water potential, ψ. As θ decreases or ψ increases, K_r also decreases and vise versa. This relation could be affected by three major groups of factors and parameters, associated with: *i*) the permeant, *ii*) the physical and chemical properties of the soil, and *iii*) the physico-chemical interactions occurring during the permeation of the (chemical) permeant.

Among different theoretical models, the Kozeny-Carman relationship is the most complete mechanistic function for K_r which is based on the Poiseuille equation for viscous flow of fluids through narrow tubes, ($\vartheta = \frac{\pi r^2 \Delta h}{8\eta \Delta l}$). This relation expresses the relative hydraulic conductivity K_r, in terms of wetted surface area, a flow factor, and porosity, as follows:

$$K_r = \frac{c_s \gamma n^3}{\eta T S^2 (1-n)^2} \tag{3.19}$$

where c_s, T, n, S, η, and γ are shape function, tortuosity, porosity, wetted surface area per unit volume, permeant viscosity and density, respectively.

This definition, however, assumes relatively uniform particle size and absence of long and short range forces of interaction. Since none of these assumptions coincide with the clay soil characteristics, therefore, this definition cannot be utilized for this kind of soil.

Results from experimental data, have introduced some other functions, in terms of ψ or θ. Most of these formulas have neglected the hysteresis effect, which deviates from the real one. For example, Campbell (1974) suggested

$$K_r(\theta) = K_s[\frac{\theta}{\theta_s}]^m \tag{3.20}$$

and Van Genuchten (1980) proposed

$$K_r(\theta) = K_s[\frac{\theta-\theta_r}{\theta_s-\theta_r}]^\gamma \{1-(1-[\frac{\theta-\theta_r}{\theta_s-\theta_r}]^{\frac{1}{m}})^m\}^2 \tag{3.21}$$

where K_s, θ_s and θ_r are saturation and residual water content, and saturated hydraulic conductivity, respectively, while m and γ are empirical parameters. Few researchers have taken into account the hysteresis role in formulating the relative hydraulic conductivity. These formulas were discussed in preceding chapter (section 2.3.1).

3.2.4.2 Soil Moisture Retention Function

In unsaturated soil, two immiscible fluids (air and water) are in contact. When a liquid is in contact with another substance, there is free interfacial energy present between them. The interfacial energy arises from the difference between the inward attraction of molecules in the interior of each phase and those at the surface of contact, and very often this energy, appears itself as interfacial tension.

The magnitude of the pressure difference depends on the interface curvature at that point. This difference in pressure is called capillary pressure P_C (or suction as a positive value). This negative pressure head is one of the most important factors for water movement in the unsaturated zone and retaining the water within the soil pores.

The relationship between the retained water and capillary pressure (potential) is not a unique curve, even for one soil. This relationship is a function of the history of wetting and drying processes as well. This means that the retention curve (relationship between the quantity of fluid present in the void space and the prevailing capillary pressure h_c) for the drying path is different from that of the wetting one. This phenomenon of dependency upon the history of drainage and wetting of a sample, is called hysteresis.

This phenomenon is attributed to a number of causes; *i*) ink-bottle effect, which results from the shape of the pore space with interchanging narrow and wide passages, *ii*) rain drop effect, which is due to the fact that the contact angle of the advancing trace of an interface on a solid differs from that at the receding one, *iii*) the entrapment of non-wetting fluid, and *iv*) non-consolidated porous media, especially in fine soils (Bear, 1978).

In order to model the soil moisture retention function, the porous media is most widely modeled as bundle of tubes (Childs and Collis-George, 1948; and Dykstra, 1951). In the simplest version, pore space is conceptualized as a group of parallel, cylindrical tubes of constant, randomly assigned radii and having the same length. Entry pressure in the h_C-θ relationship is modeled as the pressure difference at which the wetting fluid drains from the tube with the largest radius. Successively smaller tubes are drained by successive increases in capillary pressure.

This model is widely used because of its mathematical simplicity. However, it has significant disadvantages; the inability to reproduce hysteresis and residual saturation and complete anisotropy. These disabilities arise from the disregard of the interconnected nature of pore space. Even some network models have been introduced (Larson et al., 1981; Chandler et al., 1982; Chatzis and Dullien, 1985; Celia et al., 1987; Soll et al., 1988), in which both residual saturation and hysteresis for arbitrary, two fluid porous media, have not been captured accurately.

Consequently, in order to overcome the weakness of the theoretical models some researchers have concentrated their efforts on experimental investigation. As a result of the experimental data, they have proposed some relationships between ψ and θ. For example, Clapp (1978) and Hornberger (1978) employed an exponential relation as:

$$\psi = \psi_s [\frac{\theta}{\theta_s}]^{-b} \tag{3.24}$$

and Van Genuchten (1980) derived the following empirical relationship:

$$S_e = [1 + (\alpha\psi)^n]^{-m} \tag{3.25}$$

where ψ_s, θ_s, and S_e are saturation suction head, saturation moisture content, and reduced water content, respectively. Also, parameters b, α, n are empirical constants and

$m=1-(1/n)$ and $S_e = (\theta-\theta_r)/(\theta_s-\theta_r)$.

In order to study unsaturated flow, not only the hysteresis effect, but also the total soil water potential needs to be considered. Total soil water potential as a factor which dictates the amount and direction of water movement is not limited to the capillary potential. Some other components of total water potential play significant roles in unsaturated flow, such as *i*) gravitational potential, *ii*) osmotic potential, which transfers water from a reference pool of pure water to a pool of soil solution, *iii*) pneumatic or

pressure potential (air pressure effect). Among the different models of unsaturated flow parameters, it is quite hard to find those which take into account all of the effective factors.

3.3 CONTAMINANT TRANSPORT THROUGH UNSATURATED CLAY SOIL

The study of contaminant transport through unsaturated soil has only been done in recent decades. In this period of time, investigators have tried to figure out the mechanism of this phenomenon. The objective of this section is to present the laws governing the movement and accumulation of contaminants in unsaturated flow zone. This will be done in the form of a balance equation.

A brief journey through transient mass transfer equations indicates that all the dependent variables of interest seem to obey a generalized conservation principle. If the dependent variable is denoted by ϕ the general differential equation is:

$$\frac{\partial}{\partial t}(\rho\phi) + div(\rho \upsilon \phi) = div(\Gamma grad\phi) + s \qquad (3.26)$$

where Γ is the diffusion coefficient, and s is the source term. This equation contains four major terms: *i*) unsteady, *ii*) convection, *iii*) diffusion, and *iv*) source terms. These terms, for the present problem are defined in detail, in the following sections.

3.3.1 Terminology

Definition of two parameters are presented as follows.

1) Mass fraction ω_i^{α}, is defined as the ratio of the mass of substance i within the phase α to the mass of phase α in a certain volume of soil, i.e., $\omega_i^{\alpha} = \rho_i^{\alpha}/\rho_{\alpha}$.
2) Concentration c_i^{α}, is defined as the product of the mass of substance i within the phase α and the inverse of phase α volume, in a determined volume of soil; i.e.,

$$c_i^\alpha = \rho_\alpha \omega_i^\alpha = \rho_i^\alpha \tag{3.27}$$

Note that ρ_i^α is considered here for a volume distribution of mass i equal to the phase α volume.

3.3.2 General Contaminant Migration Equation

The derivation of the governing equation for dissolved species transport follows the same procedures as that for the unsaturated flow formulation. Assuming that:

1) Soil is a homogeneous material with constant properties with respect to time,
2) Air is in stationary condition,
3) There is no variation for the temperature, i.e.: isothermal condition,
4) Darcy's law is valid,
5) Source term s_i^w, is not zero,

Solute mass flux is a product of density, mass fraction, and Darcy's flux; i.e., $\vec{m} = \rho \omega_i^w \vec{q}$, which results in a mass balance equation for the control volume as follows:

$$\frac{\partial(\rho \omega_i^w \theta)}{\partial t} + \nabla \cdot (\rho \omega_i^w \vec{q}) = s_i^w \tag{3.28}$$

Substituting Eq. (3.27) into Eq. (3.28), and dropping ρ, the superscript w, and subscript i, the mass balance equation will be in the form of:

$$\frac{\partial(c\theta)}{\partial t} + \nabla \cdot (c\vec{q}) = s \tag{3.29}$$

Since $c\vec{q}$ is the mass flux of solute $\vec{m}$, Eq. (3.29) is converted to

$$\frac{\partial(\theta c)}{\partial t} + \nabla \cdot \vec{m} = s \qquad (3.30)$$

Eq. (3.30) is the solute transport equation which contains the four general terms of transient mass transfer equation. The first term on the left hand side, and the term on the right hand side, are the unsteady and source term, respectively. The second term on the left side determines advection and dispersion (diffusion), since $\vec{m}$ is the summation of $\vec{m}_{adv}$ and $\vec{m}_{disp}$, which are mass fluxes produced through advection and diffusion processes, respectively. It is to be clarified that $\vec{m}_{disp}$ is obtained from both molecular diffusion and mechanical dispersion.

In order to solve the latter equation, the unknown parameters should be identified. This requirement cannot be satisfied unless the processes related to these parameters are considered properly; i.e., by taking into account the essential factors affecting each process as much as possible to conform to the reality.

3.3.3 Contaminant Transport Components

In Eq. (3.30), the main mechanisms that influence the solute migration in porous media are advection (convection), dispersion, and physico-chemical reactions (source/sink).

3.3.3.1 Advection

The process by which solutes are transported by the bulk motion of the flow is called advection. The rate of solute transport that occurs by advection is given by the product of the solute concentration c and the components of the apparent flow fluxes, q_x, q_y and q_z. Hence,

$$\vec{m}_{i\,adv} = c\,\vec{q}_i \qquad (3.31)$$

where i could be substituted with x, y, and z directions.

3.3.3.2 Hydrodynamic Dispersion

Hydrodynamic dispersion, is a spreading process which is induced by two mechanisms: molecular diffusion and mechanical dispersion. The driving force for ionic movement in both mechanisms is not only affected by the concentration gradient, but also by: *i*) the electrostatic potential gradient resulting from different mobility of ions, *ii*) the charged surfaces of clay minerals, and *iii*) the viscosity of the pore fluid solution.

Considering all these forces in mathematical modeling is not easy. Since these factors are to a very large extent functions of concentration of the solute components, it becomes appropriate to assume that the diffusion/dispersion coefficient of every component is a function of its concentration in the pore fluid (Yong and Samani,1987). Accordingly, the aforementioned mechanisms are defined as functions of solute concentration, as follows.

Molecular diffusion:

The random motion of solute molecules, resulting from variations in its concentration within the liquid phase, will cause a transport process which is called molecular diffusion. The rate of solute transport that occurs by diffusion is given by Fick's law. In terms of the three components of solute transport in the x, y, and z directions, the rate of solute transport by diffusion is given by:

$$\vec{m}_{i\,mol} = -D_{mol}\theta\frac{\partial c}{\partial \vec{x}_i} \tag{3.32}$$

where i takes the values *1*, *2*, and *3* which designate the x, y, and z directions, respectively. D_{mol} is the apparent diffusion coefficient.

The diffusion coefficient itself is a function of θ, which has already been introduced in some of the proposed mathematical models of the preceding chapter. Even though it is very hard to define a function which can fit the diffusion properties of all different kinds of soils and solutes, the exponential function proposed by Kemper and Van Schaik (1966) has been acceptable for most of the cases under consideration;

$$D_{mol}=D_O\, a\, exp\,(b\theta) \tag{3.33}$$

where a and b are empirical constants, and $D_O=uRT/N$. In the latter equation, u, R, T, and N are absolute mobility of the solute, universal gas constant, absolute temperature, and Avogadro's number, respectively.

Mechanical dispersion

The other process that occurs simultaneously with the molecular diffusion is mechanical dispersion. This process is essentially induced by the variations in the fluid velocity from the average, as a result of the differences in the shape and the size of the pores where the flow takes place. The velocity distribution in a pore opening is not uniform since the fluid velocity is zero on the solid phase and maximum somewhere in the center of the pore. Spatial variation in the permeability of the medium is also a major source of dispersion that is frequently overlooked when estimating the dispersion parameters.

The rate of solute transport by mechanical dispersion is given by a generalized form of Fick's law of diffusion. In terms of three components of solute transport in the x, y, and z directions, the rate of solute transport by mechanical dispersion is given by

$$\vec{m}_{i\,mech} = \sum_{j=1}^{3} -D_{ij\,mech}\,\theta \frac{\partial c}{\partial \vec{x}_j} \tag{3.34}$$

where $D_{ij\,mech}$'s are the coefficients of mechanical dispersion and functions of pore water velocity. They are members of the symmetric matrix $\boldsymbol{D}_{mech}$

$$D_{mech} = \begin{bmatrix} D_{xx} D_{xy} D_{xz} \\ D_{xy} D_{yy} D_{yz} \\ D_{xz} D_{yz} D_{zz} \end{bmatrix}$$

where i and j take the values 1, 2, and 3 which designate the x, y, and z directions, respectively.

According to the definition of hydrodynamic dispersion, the total mass flux induced by this process is the summation of Equations (3.32) and (3.34).

3.3.3.3 Source/Sink Term

According to contaminant-soil interaction, sorption phenomena is the essential process of source/sink term. Soil sorption, a term interchangeably used for both adsorption and desorption processes, is a physico-chemical process that involves the increase or the decrease of solutes at the soil-water interface. This mechanism is affected by three basic components of the region, which determine the fate of contaminants:

1) Solute: ions and molecules of contaminants in the pore fluid, as well as its concentration,
2) Solvent: aqueous phase of pore fluid, which very often is water, and the medium degree of saturation,
3) Solid phase: minerals, organic and inorganic constituents, solid surfaces and especially the part of the solid surfaces which is in contact with the aqueous phase.

The above components determine the involved chemical, electrical, and physical forces, which cause various kinds of interactions between solution and soil. Physical

adsorption occurs when the contaminants in the soil solution (aqueous phase) are attracted to the soil constituents' surfaces because of the unsatisfied charges (attractive forces) of the soil particles. This kind of adsorption is related to the valence, crystalline and hydrated radii of the solute ion. From Coulomb's law, it is expected that cations with the smaller hydrated size or higher valence be preferentially adsorbed.

Chemical adsorption refers to the covalent bonding between soil particles and the solution ions. The three principle types of chemical bonds between atoms are; *i*) ionic, *ii*) covalent, and *iii*) coordinate-covalent. In this kind of adsorption, the first layer is chemically bonded to the surface and additional layers are held by Van der Waals forces.

When the sorption on the solid includes the diffusion of the constituent into the solid matrix, the phenomenon exhibits a time-dependent behavior. Models that address this phenomenon are referred to as kinetic or non-equilibrium models (Uchrin, 1986; Di Toro and Horzempa, 1982; Ahlert et.al., 1987). If it is a surface effect phenomenon, then the process is rapid and near equilibrium, and can be modeled by linear, Freundlich, or Langmuir isotherms models (Lindstorm and Boersma, 1970; Davison and McDogal, 1973; Van Genuchten, 1974).

Linear Equilibrium Isotherm

The change in sorbed concentration in this model is instantaneous and linearly proportional to the change in solute concentration, thus

$$s(x,y,z,t)=k_d c \qquad (3.35)$$

where $c = c\ (x,y,z,t)$ and k_d is distribution coefficient which is determined experimentally.

Freundlich Equilibrium Isotherm

This model accounts for non-linearity in the partitioning of the solute between the liquid and the solid phases. The classical form is (Gupta, 1972; Grove and Stollenwerk,1984)

$$s(x,y,z,t)=k_d c^n \tag{3.36}$$

where n is introduced as Freundlich isotherm exponent.

Langmuir Equilibrium Isotherm

This model also assumes a non-linear function between the sorbed concentration and the solute concentration; moreover, it considers the saturation of sites on the solid phase. It is based on the assumption that there exists a finite number of ionic sites on the solid, and the sites are of equal free energy and have equal probability of occupancy. The adsorption in this case is described as (Gupta, 1972; Rai et al., 1984)

$$s(x,y,z,t)=Bk_d c/(1+Bc) \tag{3.37}$$

where B is an empirical constant.

Non-Equilibrium Sorption Models

These models generally describe the diffusion controlled or the chemically controlled kinetic rate reactions. Similarly, the sorption rate in these models are given by either a linear or non-linear and -reversible first order equation of the equilibrium forms. Equations

$$\frac{\partial s}{\partial t}=\alpha(k_d c-s) \tag{3.38}$$

$$\frac{\partial s}{\partial t} = \alpha(k_d c^n - s) \tag{3.39}$$

$$\frac{\partial s}{\partial t} = \alpha(\frac{Bk_d c}{1+Bc} - s) \tag{3.40}$$

are linear , Freundlich, and Langmuir non-equilibrium models, respectively. In the above

equations, α is a first-order rate coefficient which is determined experimentally.

Although, the sorption models have resulted in some improvements in predictive capabilities, success has generally been limited to specific cases. This has been attributed to various reasons, but mainly to the difficulties associated with determining the parameters corresponding to each model, and also because of the inherent assumption that the sorption process can be described either by the equilibrium or by kinetic models.

However, no matter which kind of source term models fits the problem at hand, the net rate of solute production due to sorption process between a solute and the porous medium within the control volume equals $-\frac{\partial}{\partial t}(\rho_b s)$, where s and ρ_b are sorbed species concentration and porous medium bulk mass, respectively. Since this study assumes ρ_b to be constant, this rate is defined as $-\rho_b \frac{\partial}{\partial t} s$.

From previous sections, a one-dimensional contaminant transport through a porous medium is obtained by substitution in Eq. (3.30) and arrangement as:

$$\rho_b \frac{\partial s}{\partial t} + \frac{\partial(\theta c)}{\partial t} = \frac{\partial}{\partial z}(D\theta \frac{\partial c}{\partial z} - cq) \tag{3.41}$$

where D is the hydrodynamic dispersion function. Mechanical dispersion is significant if the soil is saturated and also the pore water velocity is considerable. For this study

none of these conditions exist, therefore this component is assumed to be negligible. Thus in Eq. (3.41), D is assumed to be equal to the molecular diffusion, D_{mol}.

3.4 INITIAL AND BOUNDARY CONDITIONS

Unsaturated flow and contaminant transport equations are non-linear partial differential equations. Therefore, their solutions depend on the physical conditions existing at the boundaries of the medium and, since the equation is time dependent, on conditions existing in the medium at some initial time.

The initial condition can take one of the two forms: *i*) constant value for entire domain, or *ii*) function of space. On the other hand, boundary conditions must also be prescribed at all times. These conditions may either be steady state or transient, based upon the physical nature of the problem considered. For either case, it can be specified in one of the three general types: *i*) Dirichlet or first type, *ii*) Neumann or second type, and *iii*) Cauchy or third type.

Since both unsaturated flow and contaminant transport equations are partial differential equations, second order in space and first order in time; consequently, one initial and two boundary conditions (one at every point on the spatial boundary) are required. For the present study, according to the nature of the problem at hand, all conditions are defined on the basis of either soil suction (for unsaturated flow equation), or contaminant species concentration (for contaminant transport equation). These conditions are described in a complete detail in section (6.2).

CHAPTER 4

EXPERIMENTAL INVESTIGATIONS

4.1 GENERAL REMARKS

In order to obtain distinct functions for contaminant transport through unsaturated soil, a number of experiments was performed. This part of the study is categorized by two types of tests; **1**) unsaturated flow, and **2**) contaminant transport tests. The first consists of ***i***) saturated hydraulic conductivity, ***ii***), soil-moisture retention, and ***iii***) unsaturated hydraulic conductivity tests. The second includes ***i***) kinetic batch test, followed by ***ii***) sequential extraction, and, ***iii***) unsaturated soil column leaching tests.

chapter 4 constitutes a comprehensive presentation of experimental approach for the aforementioned tests. The results of these experiments are introduced and analyzed in chapter 5.

4.2 MATERIALS

The materials used in this study are clay soil and some chemical materials such as solutions and reagents. The following sub-sections contain more detail concerning the properties of the two essential materials; soil and solutions.

4.2.1 Soil

The soil used in these experiments was kaolinite, a clay soil. Clays comprise it major mineral components of soil, and their unique physical and chemical properties are quite essential to the distinctive properties of soil. The unique properties of clays arise from their comparatively large surface area and permanent (as well as pH-dependent) surface negative charge. Soil-solute interactions at clay particle surfaces are complex and naturally important phenomena. In addition, the value of clay soil as a physical and chemical barrier against the migration of leachate from disposal sites has been recognized due to its low hydraulic conductivity and its high adsorption capacity.

Kaolinite, is one of the most common types of clay minerals. It consists of one silica sheet and one gibbsite sheet with a Si:Al ratio of 1:1. Furthermore, it has very low swelling properties. The kaolinite under consideration (hydrate PX), is relatively chemically inert and reacts with acids and bases only under extreme conditions. Also, it is water processed, which reduces soluble salt contents to extremely low level.

The reasons for this selection are; *i*) homogeneity and isotropic property of the soil medium for better idealization, *ii*) reduction or elimination of unnecessary properties; e.g. swelling, and *iii*) elimination of organic constituents of the soil to remove microorganisms and humic substances from the medium.

In order to determine the soil mineralogy, X-ray diffraction analysis was performed on an oriented sample mount. Accordingly, the minerals present in the soil are kaolinite and mica, in the order of decreasing abundance. The X-ray diffractogram and some other physical and chemical properties of the soil are presented in Appendix (1).

4.2.2 Solutions

Solutions of selected heavy metals were used for kinetic batch tests, sequential extraction studies, and soil column leaching experiments. However, hydraulic conductivity tests were performed with distilled water as well as heavy metals solutions.

Heavy metal contamination of the earth's soils is a significant environmental problem which because of that reaching human health and ecological implications fails. In order to keep the environment far from danger of this contamination, heavy metals solutions contamination and behavior are to be investigated more thoroughly.

The contamination of soils by heavy metals is due to a number of human activities such as smelting, vehicle emissions, industrial waste, fertilizers, and pesticides, mining, and the like. Reported ranges of heavy metals concentration from various soils differ in range. In many waste disposal sites contamination levels are high, occasionally exceeding acceptable standard levels (Appendix 2). Three metals which are very common in leachate from these sites, have been selected: lead, copper, and zinc. The solutions were prepared from the metal chlorides.

Adsorption is strongly pH dependent and is related to the hydrolysis of the heavy metal ions. The pH of a soil applies to the H^+ ion concentration in the pore solution, which is in dynamic equilibrium with the predominantly negatively charged surfaces of the soil particles. Hydrogen ions are strongly attracted to the negative surface charges, and they have the power to replace most other cations. In general, heavy metal cations are most mobile under acid conditions (Alloway, 1990). When soil solution pH is greater than 5, the amount of heavy metals retained in the soil is considerable.

Moreover, adsorption of metals by the soil particles comprises three different steps: surface adsorption, diffusion into geothite particles, and adsorption and fixation at positions within the mineral lattice. The relative rate of diffusion of the metal ions into minerals increases with pH increase up to the maximum level. In order to study the adsorption process conservatively, with reference to the soil profile and groundwater contamination, a low pH for solutions was chosen.

Accordingly, hydrochloric acid was used to adjust the pH of each solution to 4.0. The concentration of metal solutions in soil column leaching tests was 2000 ppm, in order to elute measurable quantities of metal in a reasonable time period.

4.3 UNSATURATED FLOW EXPERIMENTS

In order to analyze the unsaturated flow within a clay soil media, it is vital to know the saturated hydraulic conductivity (K_s), the relationship between volumetric water content and soil water potential (Θ~H), and the unsaturated (relative) hydraulic conductivity $K_r(H)$. The main objective of this section is to explain how one can obtain these characteristics and parameters.

4.3.1 Saturated Hydraulic Conductivity Tests

The relative hydraulic conductivity $K_r(H)$ is related to saturated hydraulic conductivity K_s, as well as soil water potential H, and/or volumetric water content Θ. This test determines the value of K_s, through implementation of the constant head method (with adjustable hydraulic head). Since the soil under consideration is very fine, this method was used to facilitate flow thus shortening each experiment run.

The experimental setup for this test is shown in Fig. (4.1), illustrating double acting volume change indicator (DR), reservoir, pressure transducer, soil sample and outflow graduator container. Three calibrated pressure transducers were used in this study. Details of soil sample preparation, experimental setup and test procedure are presented in the following sub-section (4.3.1.1).

Due to the loading history, the substrate soil layers have different density. In addition, the saturation degrees of the soils are not only different for various locations, but they vary during the year, because of evaporation, plant root uptake, and other environmental phenomena.

Hence, in order to study the effect of dry density, three various dry densities of the soil (100, 85, and 55 percent of $\gamma_{d\ max}$) are chosen for the saturated permeability tests. The soil utilized for the soil column leaching had 80% of maximum dry density, however, which represents an average values of soil density in the field.

As the main goal of the study to investigate is unsaturated media, the water content of the soil columns was initially prepared at a very low level (5%), in order to have a vast range of water content variations. To obtain a uniform and constant moisture distribution and density within the specimen the wet soil was kept in a humid chamber (with a 25% humidity) for at least 24 hours prior to experiment run.

This experiment was initially run with distilled water on 3 soil samples having the same dry density ($\gamma_{d\,max}$), but with three different volumetric water contents. Moreover,

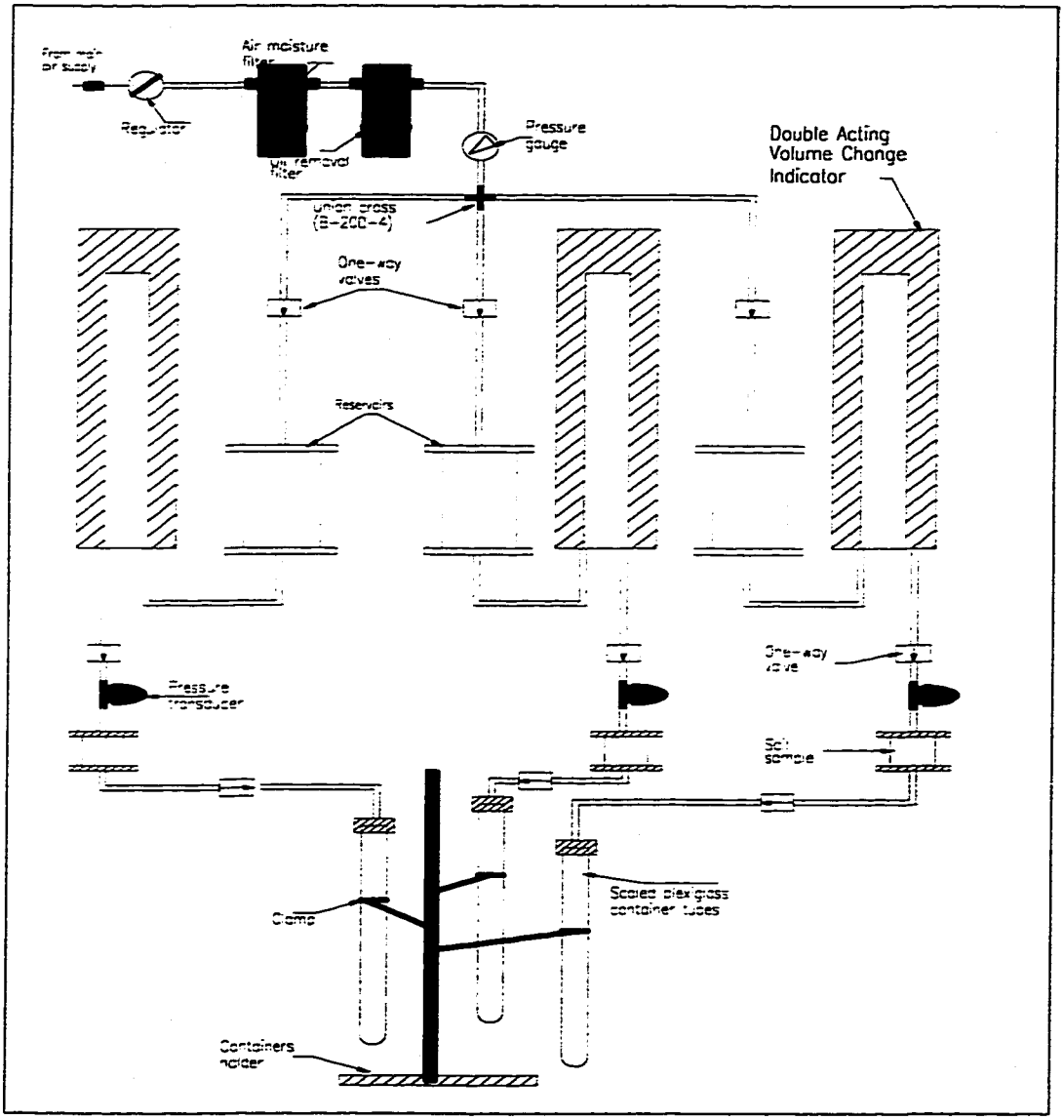

Figure 4.1 Experimental Setup for Measuring Saturated Hydraulic Conductivity

three soils of different dry densities were examined at the same water content (ω=5%), to verify the variation of K_s. Eventually, the test was done on the soil with a density of $0.80\gamma_{d\,max}$, with distilled water and three different heavy metal (lead, copper, and zinc) solutions with concentrations of 2000 ppm, in order to determine whether there is any difference in their saturated hydraulic conductivity values. In total 10 cases were investigated for this part of the study. Each process ran about 5 days to ensure that flow was in a steady state condition.

The soil sample cell and the double acting volume change indicator are illustrated in Figures (4.2) and (4.3), respectively.

4.3.1.1 Experimental Setup and Procedure

Soil samples were prepared in an aluminum cylindrical mold; one inch high and four inches in diameter (Fig. 4.2). The soil compaction was performed statically by means of a hydraulic compression apparatus. Leaking of water was prevented by using rubber O-rings between the caps and the wall of the apparatus. The effluent was collected in a Plexiglas scaled tube, to measure the discharge of water from the soil sample. Two filters (air moisture removal and oil filters) were used to purify the air entering the system.

The experimental setup for this test is shown in Fig. (4.1), depicting the double acting volume change indicator (DR), reservoir, pressure transducer, soil sample and outflow graduated container. By means of a double acting volume change indicator variations of inlet water flow to the soil sample were measured (Fig. 4.3). This device measures the inlet water flow volume twice, therefore, it enhances flow measurement accuracy and reduces reading error to 0.02 ml. The pressure transducer measures the exact hydraulic pressure applied to the top of the soil sample; consequently the error in actual pressure measurement is diminished.

After assembling the saturated hydraulic conductivity apparatus and filling the reservoir with distilled water, air pressure is applied. After removing the air from the

system, all fittings are checked for any leaks. The valves are then opened to introduce water into the soil sample.

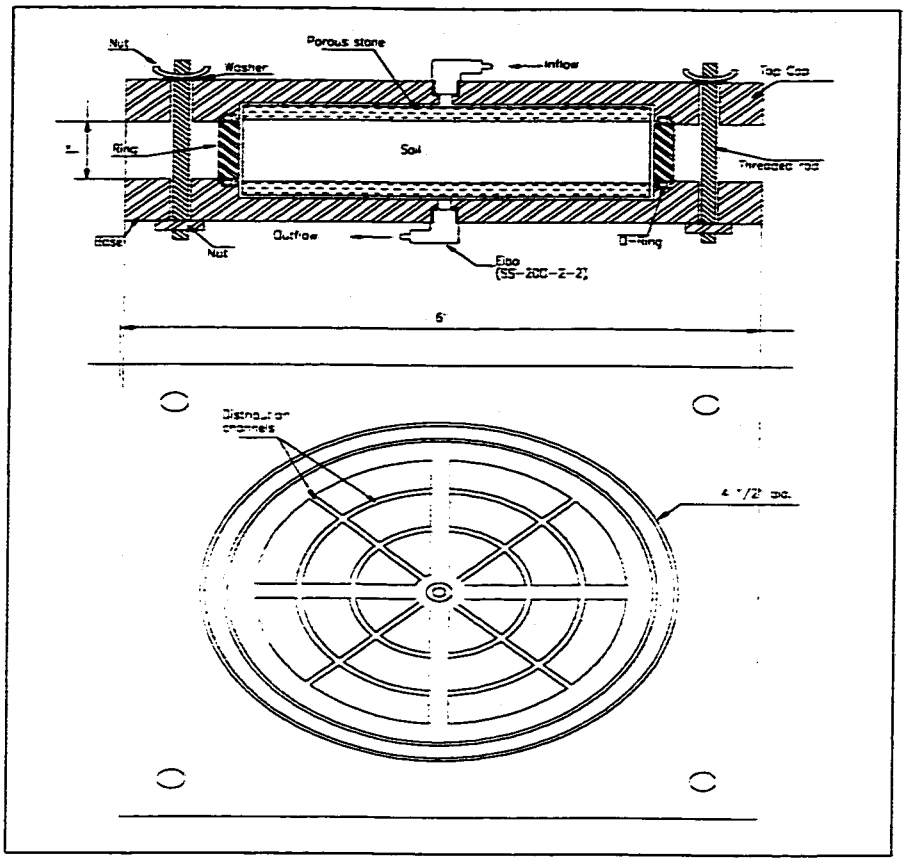

Figure 4.2 Schematic Diagram of Soil Sample Cell with Top Cap and Base Plan View

The amount of water entering the sample is then measured, and based on this measurement, the rate of water adsorption by the soil sample is determined. The amount of water exiting the sample is measured, until a constant rate of outflow is established. By using Darcy's law, the saturated hydraulic conductivity (K_s) of the soil sample is obtained.

4.3.2 Soil-Moisture Retention Test

Since the relative hydraulic conductivity is considered to be a function of soil suction, the relationship between soil suction ψ, and volumetric water content θ, is one of the most important parameters to be determined in any unsaturated flow study. This relationship becomes much more significant for clay soils because the hysteresis effect is very strong in such media.

In order to study the hysteresis mechanism and in order to establish the aforementioned relationship, soil water retention tests were conducted. The final result of this experiment is the moisture retention curve, which relates the soil suction to its corresponding moisture content. To obtain this curve, an apparatus which provides a convenient and reliable means of removing soil moisture is required. Water removal is done under controlled conditions and without any disturbance to the soil structure. In laboratory studies, the pressure membrane and pressure plate extractors have become eminently successful research tools for this purpose. The pressure membrane (plate) extractor not only extracts soil water or solutions, but also indicates the applied pressure on the soil sample (soil suction).

The soil solution may be extracted in increments of known suction values and saved for chemical analysis. The details of the pressure membrane extractor, experimental setup, and procedure for this test are explained in the following sub-section.

4.3.2.1 Experimental Setup and Procedure

Many methods, such as compaction, centrifugation, displacement, molecular adsorption, and suction have been used to investigate the physical properties of soils, as well as to remove soil solution for chemical analysis. In each of these methods the range of application is quite limited and often cumbersome. In some cases, the soil structure is destroyed in the process.

In determining the moisture characteristic of a soil, a graph of soil suction plotted against soil volumetric water content is required. Values are obtained by placing soil in

sample retaining rings, on a permeable membrane, or porous ceramic cell in an extractor. After the samples have been thoroughly wetted, the extractor is closed and air pressure applied. Fig. (4.4) shows such samples, mounted in the pressure membrane extractor; which uses a thin cellulose membrane supported on a screen drain plate.

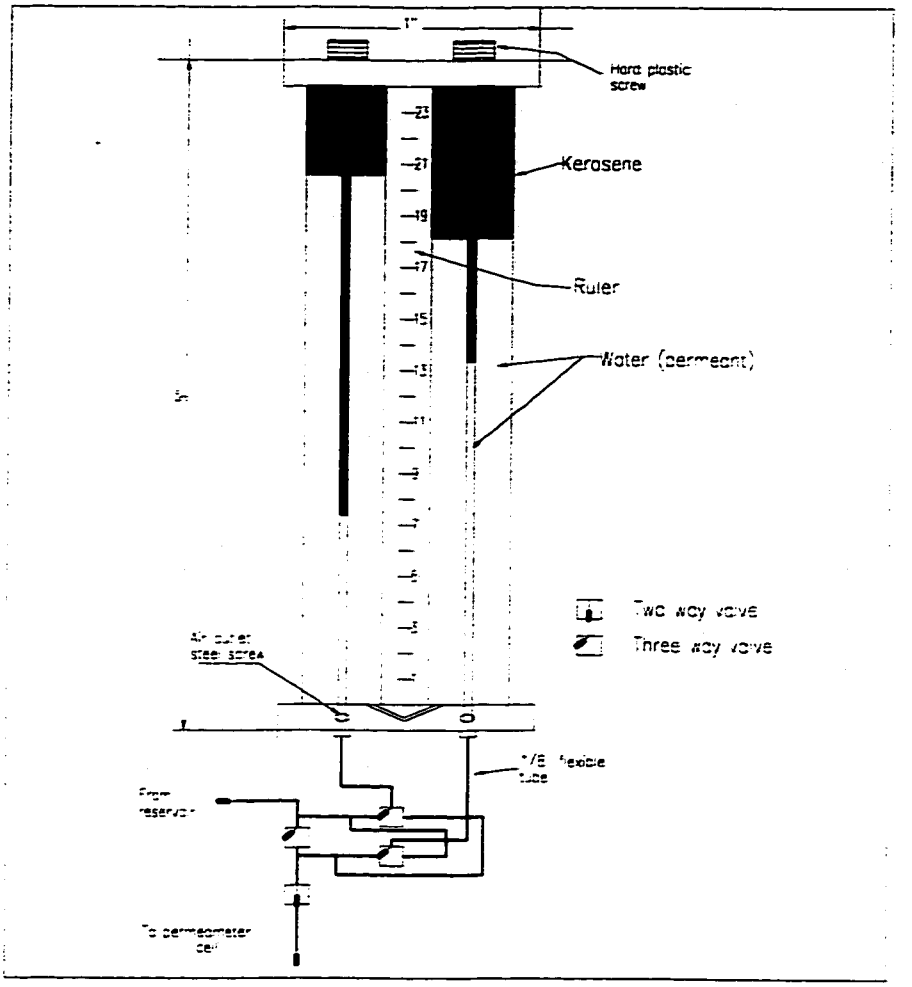

Figure 4.3 Double Acting Volume Change Indicator

While the water is removed from soil by pressure, the wetted cellulose membrane serves as a connecting link, and at the same time, as a means of maintaining a pressure difference between the liquid phase of water in the soil and the water at lower pressure on the opposite side of the wall.

As air pressure in the extractor is raised above atmospheric pressure, the higher pressure inside the chamber forces excess water through the microscopic pores in the cellulose membrane. The high pressure air will not flow through the pores, since they are filled with water, and the surface tension of the water at the gas-liquid interface at each of the pores supports the pressure much the same as a flexible rubber diaphragm.

When the air pressure is increased inside the extractor, the radius of curvature of this interface decreases. However, the water films will not break and let air pass; throughout the whole pressure range of the extractor. At any given air pressure in the chamber, soil moisture will flow around each of the soil particles and out through the cellulose membrane until the effective curvature of the water films throughout the soil are the same as that of the pores in the membrane. When this occurs, an equilibrium is reached and the flow of moisture ceases.

When the air pressure in the extractor is increased, flow of soil moisture from the samples starts again and continues until a new equilibrium is reached. At equilibrium, there is an exact relationship between the air pressure in the extractor and the soil suction ψ (and hence the moisture content Θ) in the samples. The air pressure applied determines the soil suction at equilibrium. At the end of the run, the samples are weighed and oven dried to determine soil moisture content.

Since the soil under consideration is kaolinite clay, extraction of water from the soil sample is very time consuming, and the pressure should be kept constant for a few days. Applying pressure gradually from 0 to 100 bars (10^7 Pa), to obtain the moisture retention curve, takes about 3 months to get an accurate graph of the drying curve.

The details of the experimental setup has been presented in Fig. (4.5). The mercury differential regulator measures the differential in pressure necessary to force the rubber compressing diaphragm down onto the soil samples and hold it in intimate contact with the cellulose membrane. The compressing diaphragm is used primarily with clay soils to keep them from shrinking away from the cellulose membrane as moisture is removed from the samples.

4.3.3 Unsaturated Hydraulic Conductivity Tests

In order to study unsaturated flow and its hydraulic parameters such as $K_r(H)$, a vertical soil column was prepared. This column actually simulates the infiltration of water, within unsaturated soil media. The experimental setup is the same as that of the permeability test, and the soil sample was made in a plexiglas column comprised of 14 segments with a diameter of 3.81cm and length of 2 cm. The soil within the column segments is sealed with rubber O-rings and bolted tightly in place with caps (Fig. 4.6).

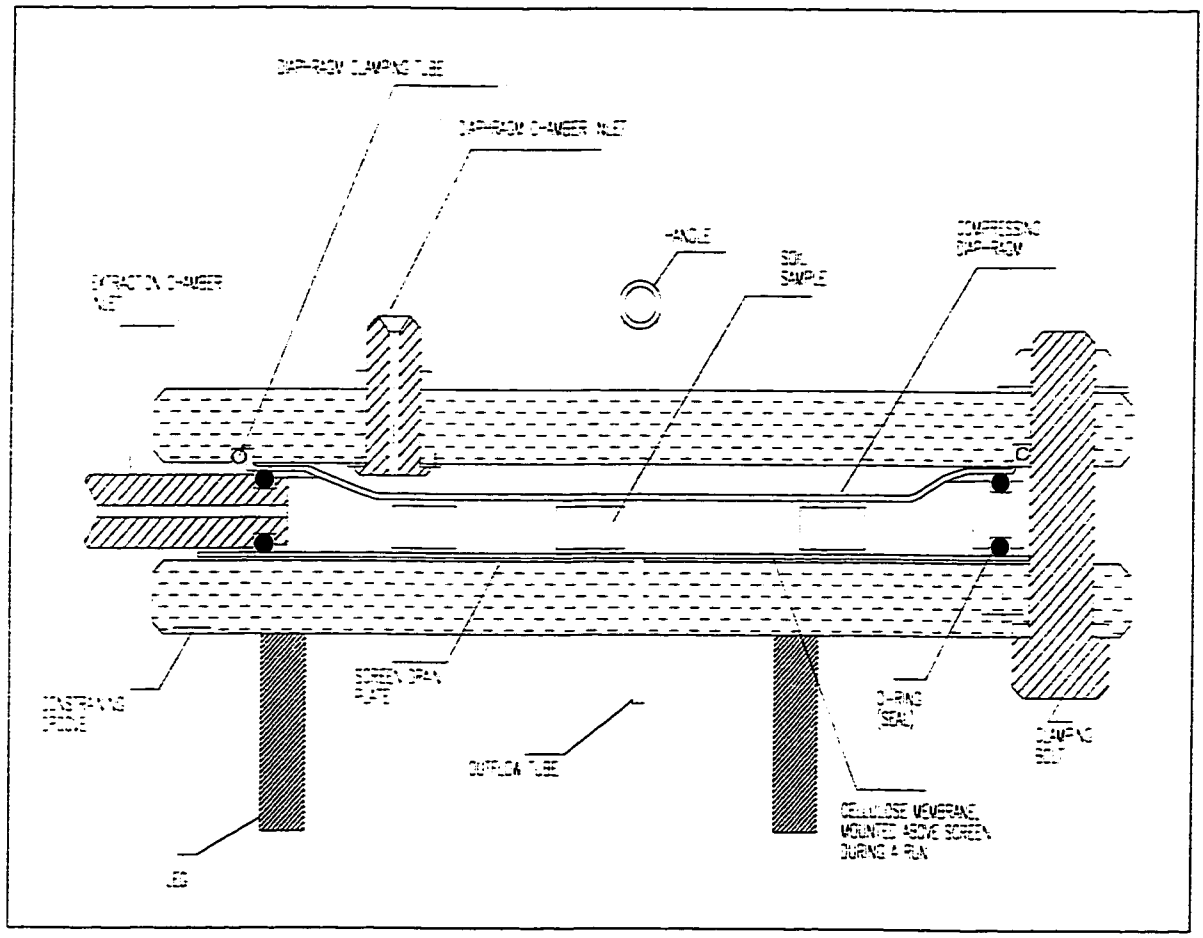

Figure 4.4 Section View of Pressure Membrane Extractor

On both upper and lower caps distribution channels are provided to uniformly distribute the inlet water beneath the top cap and to collect the effluent through the

lower cap. Uniform inlet and outlet water distribution is also induced by the porous stone and filter paper between the caps and the soil sample (Fig. 4.7).

To measure the soil water potential ***H***, a psychrometer microvoltmeter (PMV) is used (Fig. 4.6). In order to mount the thermocouple psychrometers (TS) units inside the soil column, a small hole is drilled through the wall of some segments. These drilled segments are placed strategically along the column to obtain the variation of ***H***. All the TS units are connected to different channels of the microvoltmeter (section 4.3.3.1).

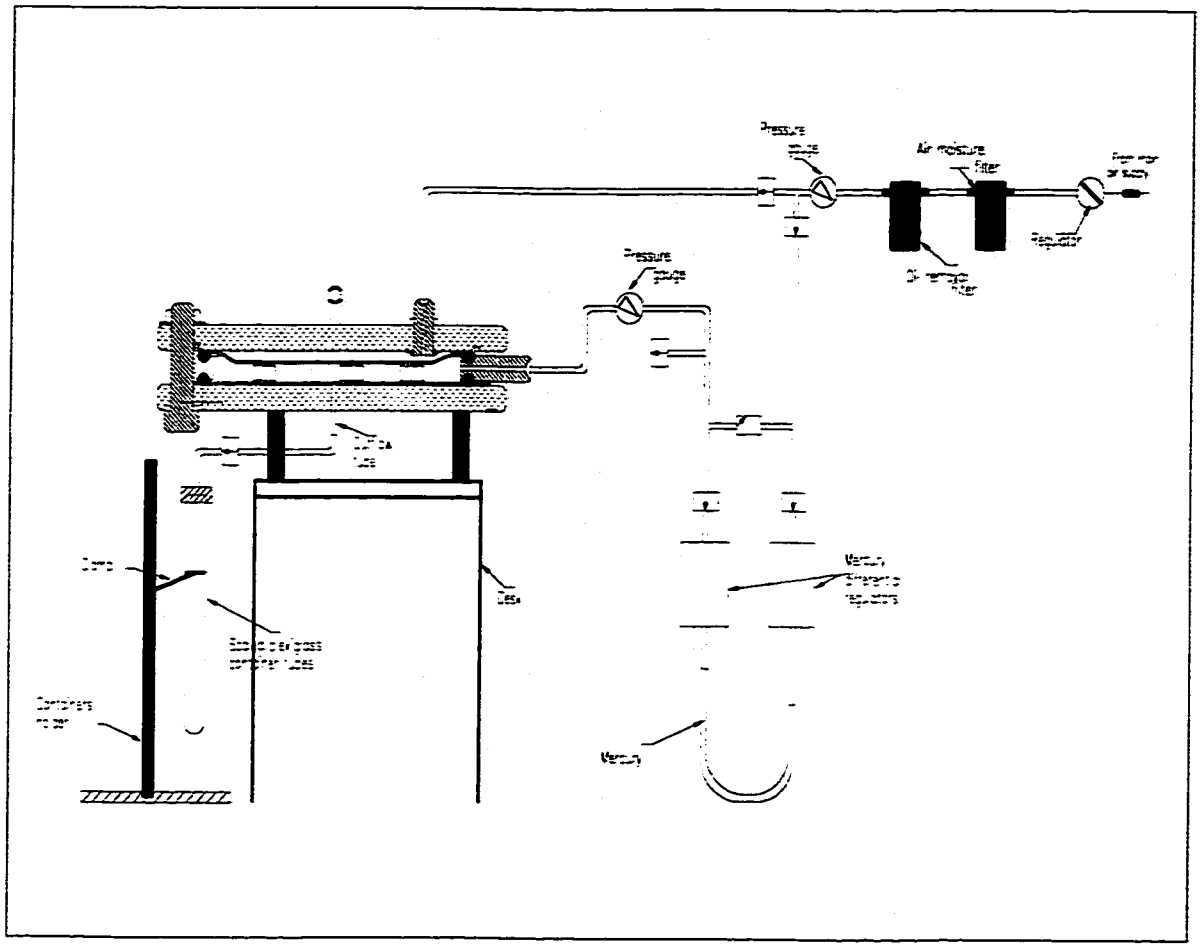

Figure 4.5 Schematic Experimental Setup for Soil Water Retention Test

The columns are prepared in segments to

1) facilitate column sectioning after each experiment,

2) minimize the disturbance of the sectioned soil samples, and

3) allow for changes in thermocouple positioning.

After column assembly, the soil is compacted in the column in 1 cm layers. The porous stones and filter papers are inserted, and the column is capped and bolted. The TS units are inserted through aluminum grooved tubes (0.30 inch diameter) into column segments holes.

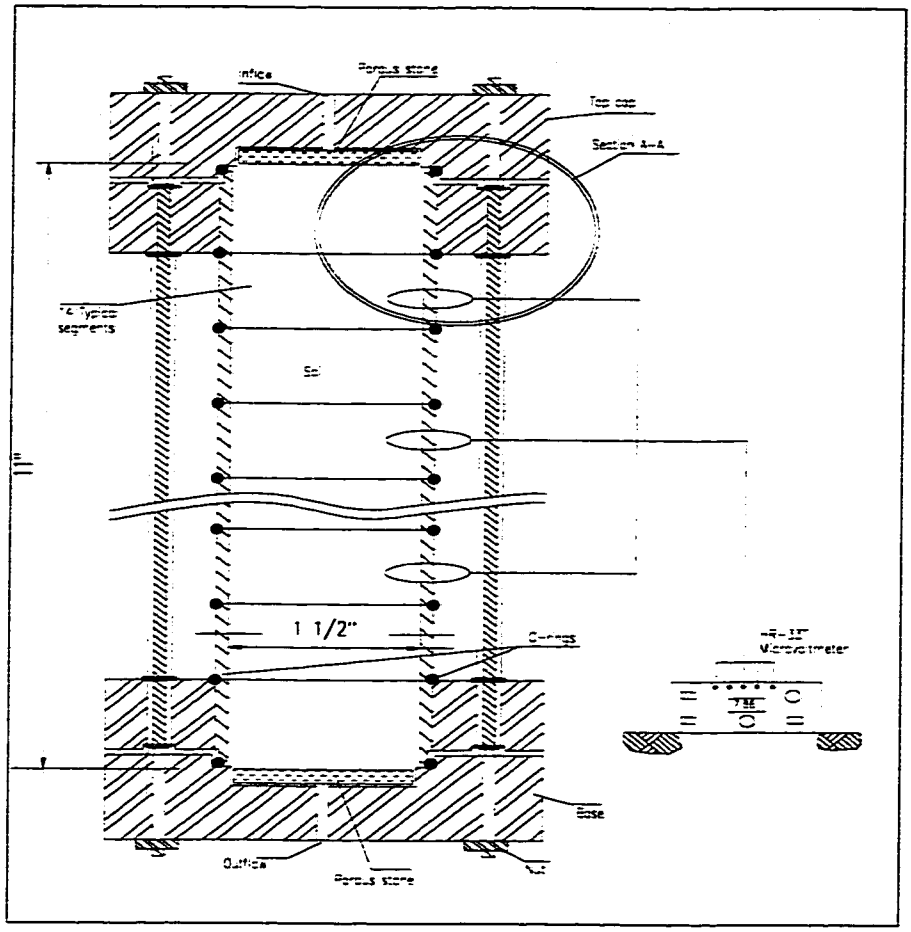

Figure 4.6 Schematic Cross Section of the Column Apparatus

This experiment is similar to the permeability test in that water is allowed to infiltrate the soil column. Infiltration is under constant hydrostatic head at ambient temperature. During infiltration, the PMV measures the electromotive force (EMF) for each TS in order to obtain the H value for each segment.

Alternatively , ***H*** values may be determined for each segment from retention curve, based on volumetric water content, after an infiltration period of one month. ***H*** values obtained in this manner were used to check the final ***H*** values from the TS readings. This test was performed on 4 columns with different solutions: distilled water, and lead, copper, and zinc chloride solutions in order to measure volumetric water content at other time intervals of less than 1 month.

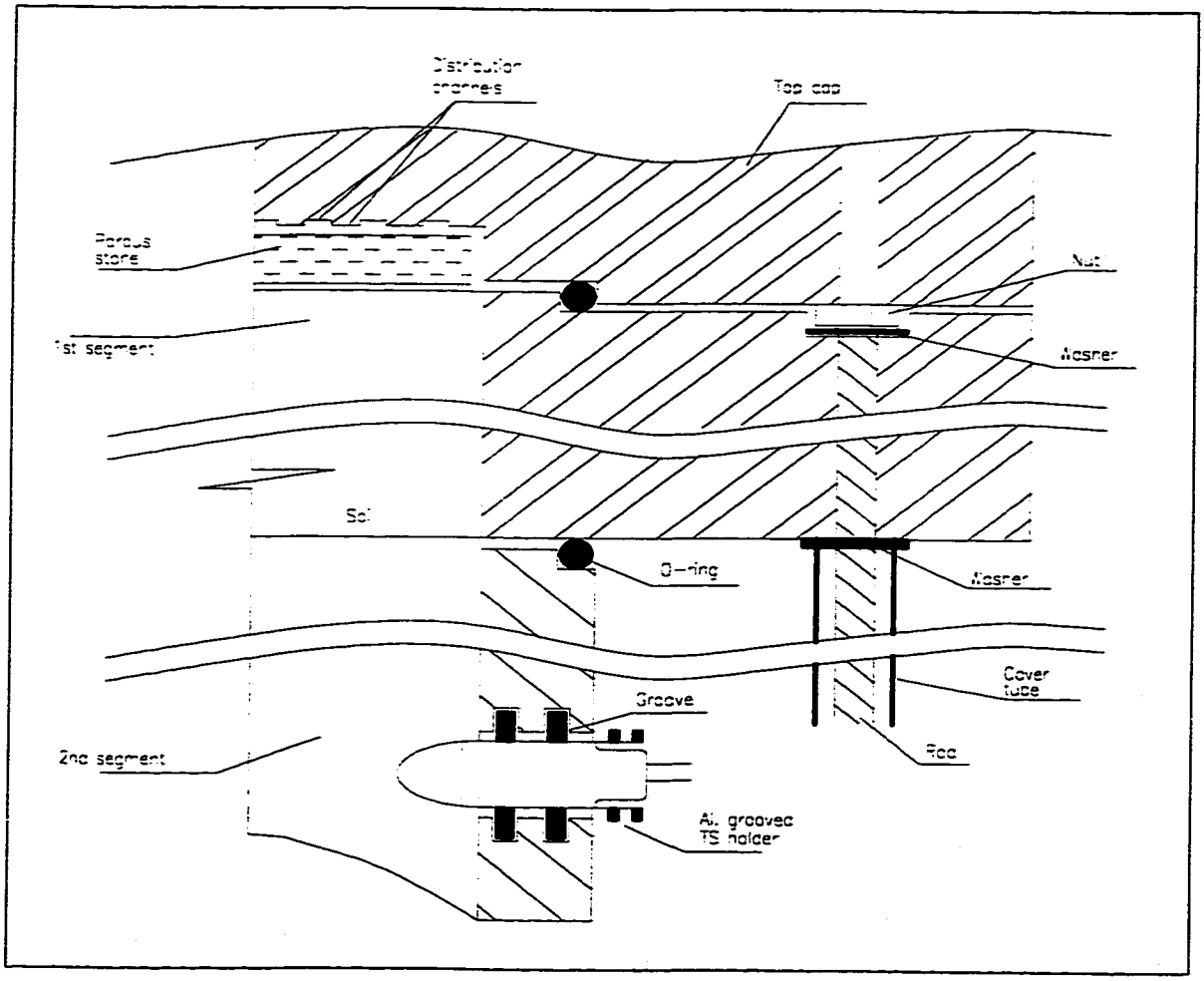

Figure 4.7 Section A-A of the Column Apparatus

4.3.3.1 Thermocouple Psychrometer and Read-Out Device

A thermocouple psychrometer TS, is a very sensitive sensor used to measure soil water potential H, or volumetric water content Θ. A schematic of a typical TS is illustrated in Fig. (4.8). The thermocouple junction, used in measurement of the equilibrium relative humidity, is formed by the chromel and constantan wires. The points of contact at the gold pins form the reference junction for this measurement. Very fine chromel and constantan wires (25 μm diameter), are used so that cooling of this junction will not significantly change the temperature of the larger reference junction.

Another thermocouple is formed by a copper and constantan junction. This junction is used to determine the temperature of the sensor. An electronic reference junction, simulating a copper-constantan junction in an ice bath, is located in the readout device. This reference enables the instrument to determine the sensor temperature accurately, regardless of changes in the ambient temperature. The water potential of a sample is calculated from the temperature difference between the two junctions, given by the thermocouple electromotive force.

Thermocouple psychrometers are inserted into soil samples and connected to the psychrometer microvoltmeter (HR-33T). The microvoltmeter is used to measure the thermocouple electromotive force, which comes from the TS. This apparatus could be operated manually or in a semi-automatic mode. The HR-33T is capable of receiving input from 10 TS units at the same time.

4.3.3.2 THERMOCOUPLE PSYCHROMETER CALIBRATION

When a TS is mounted in a column test it measures the electromotive force, which passes through the junction point. This measurement does not determine volumetric water

content Θ,or soil water potential H, for the specimen. In order to find the relationship between soil-moisture parameters and the EMF given by TS readings, the sensor must

be calibrated, i.e.: the Θ and H should be defined as functions of voltage coming out from the thermocouple psychrometer.

In order to determine volumetric water content Θ, as a function of EMF, soil samples of known Θ are utilized for the column leaching test, under identical experimental conditions. The samples are completely sealed to prevent water evaporation and air loss. Then the curve of EMF variation versus Θ is then obtained.

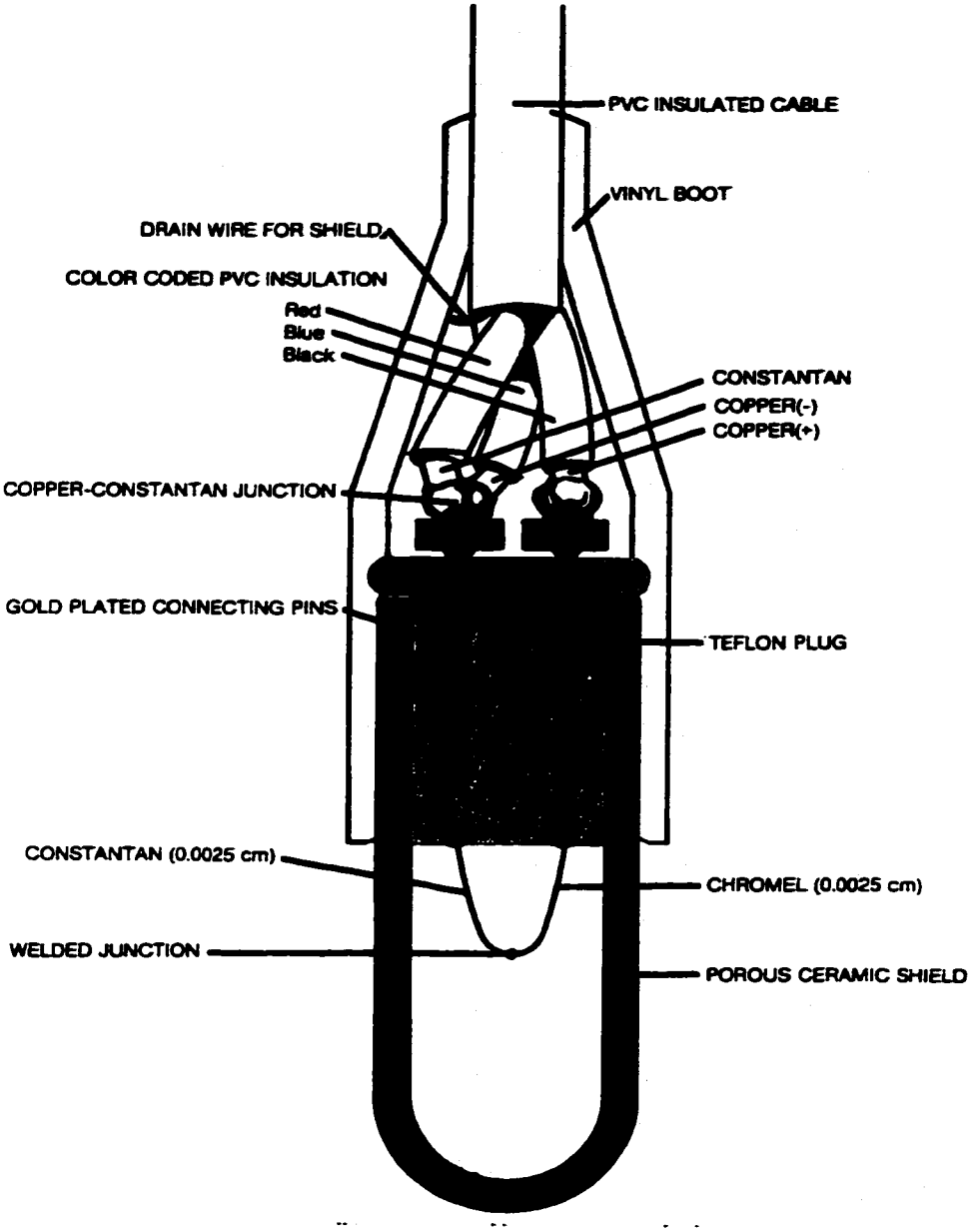

Figure 4.8 Cross Section of a Thermocouple Psychrometer

Since, the relationship between H and Θ has been found from the soil water retention test, the sensors can be calibrated for soil water potential H or soil suction ψ values as well. Calibration curves for 5 TS units, utilized in these tests are presented in Appendix (3).

4.4 CONTAMINANT TRANSPORT EXPERIMENTS

In order to understand the mechanism of contaminant transport through unsaturated clay soil, the following experiments were run: *i*) kinetic batch test, *ii*) sequential extraction, and *iii*) unsaturated soil column tests. These experiments provide adequate information regarding solution concentration within the soil profile, and particularly, comprehensive information concerning the sorption process in soil contamination.

4.4.1 Kinetic Batch Tests

The sorption process includes adsorption and desorption phenomena. Contaminant adsorption during migration in soils is particularly useful in the specification of engineered soil barriers, and contaminant desorption in the determination of techniques for removal of contaminants from soils.

Adsorption processes decrease the concentration of solute in the soil solution, and therefore reduces the probability and degree of ground water contamination. Desorption phenomena cause a remobilization which represents a preliminary step in the remediation of contaminated soils. The advantage of desorption is a considerable reduction in the cost of soil decontamination.

The interaction of soil surface properties and contaminant characteristics are complex; and as a result there is yet no clear model that would provide one with precise information on the degree or species selectivity of adsorption and desorption of contaminants by any soil, over a period of time. Thus it is necessary to obtain some physical (empirical) handle on the capability of a soil in contaminants sorption processes.

Two experimental techniques are commonly used to study the sorption characteristics of soils: 1) the batch test, and 2) the soil column leaching test. The batch test is applied to a soil suspensions, assumed to be a completely dispersed soil particle system, where all the soil particle surfaces are exposed and available for interaction with the contaminants. On the contrary, soil column leaching tests are performed on soil with a definite matrix or soil structure. The sorption characteristics obtained from the latter leaching tests are the results of contaminant interaction with a structured soil system, which resembles actual field conditions.

Both tests are required to obtain the comprehensive information about sorption processes. The batch test is used to isolate sorption process of contaminant transport and investigate partitioning phenomena of the contaminant species independently, and as a function of time (t) and concentration of contaminated solutions (c). The column leaching test is utilized to study the sorption process in a structured system, while it is simultaneously affected by the other contaminant migration processes, as occurs in nature.

In order to study contaminant retention in soil, the soil suspension batch test is utilized because of its simplicity, rapidity, and reproducibility (Maguire et al., 1981; and Harter,1983). Several soil suspension tests (22 tests) were performed on soil-heavy metal solution systems. These tests include: *i*) five adsorption and five desorption experiments on lead chloride-soil solutions (with 5 different concentrations each), *ii*) three adsorption and three desorption tests for copper chloride-soil solution, and *iii*) three adsorption and three desorption tests for zinc chloride-soil solution.

Different concentration of the heavy metals solutions are applied to the clay soil samples. Metal concentrations were selected to cover the wide range most commonly found in sewage sludge, some industrial wastes, and municipal solid wastes. Adsorption and desorption test procedures are explained in more detail in the following sections.

4.4.1.1 Adsorption Experiment Procedure

The experimental procedure followed is presented in three main stages as follows:

1) Solution Preparation

Soil suspensions are prepared with dry soil in a uniform powdery texture and mixed with various concentrations of metal solutions. The initial concentration of Pb solutions were selected as 50, 200, 500, 1000, and 2000 ppm; while 200 and 1000 ppm concentration were eliminated for Cu and Zn solutions. Metal solutions without soil were used as blank references.

Since proper dispersion of soil particles in the contaminant solution is essential, the following procedures were followed: ***a***) the solutions of heavy metals were applied to the clay soil at 1:10 soil: solution ratio (EPA, 1987); i.e., 40 g of dry soil and 400 ml of contaminated solution, ***b***) the mixed solutions are mounted on the stirrer plate during experimental period, to prevent any possible sedimentation, and to provide proper agitation. Temperature was also maintained at 20°C throughout the tests.

2) Sampling

Following agitation, 15 ml aliquots were removed to determine metal concentrations. Sampling for all these tests was done at five different time intervals (0.25, 6, 12, 48, and 120 hours; except for 2000 ppm lead concentration which was also sampled at 1, 24, and 240 hours).

Aliquots were then centrifuged (IEC HN_SII centrifuge) at 4000 rpm for 10 minutes in plastic Nalgene centrifuge tubes equipped with screw-on caps. At the end of centrifugation, the supernatant is filtered (using cellulose acetate polymers, 0.45mm mesh size and 13 mm diameter) and stored in 10 ml glass vials prior to atomic absorption (AA) spectroscopy.

3) Concentration Measurement

The total metal content in the filtered solutions was determined by AA spectroscopy (Perkin-Elmer spectrometer) in accordance with standard procedures. The amount of heavy metals adsorbed per unit weight of the soil s, (for each concentration) is determined from the difference between the initial concentration of solution applied to the soil c_o, and the final residual concentration c_f, at sampling time .

If the values of s are plotted against time, the transient function of adsorption is obtained (a kinetic case study). After an initial sharp positive slope the curve levels off (slope=0), indicating that no significant variation in contaminant solution concentration takes place. This leveling off indicates the time t at which sampling can be terminated in subsequent experiments as well. Since the test is repeated for various c_o values, the adsorption process would be a function of not only time, but also initial contaminant concentration.

At the end of an adsorption test (120 or 240 hours), the contaminated soil pellet, obtained from centrifugation is dried and subsequently used in desorption tests. The results and discussion of heavy metals retention in soil are given in section 5.3.1.

4.4.1.2 Desorption Experimental Technique

The desorption experiments are carried out as a dissolution of the adsorbed contaminant species from the soil particles. The procedure also includes the following three stages: *i*) solution preparation, *ii*) sampling, and *iii*) concentration measurement (as in the adsorption test), and follows exactly those procedures described for the adsorption test with the following two exceptions:

1) In the solution preparation stage, the solvent used is distilled water and the soil utilized is the one obtained at the end of the adsorption test. However, the soil: solution ratio is still prepared as 1:10; i.e., 20 g dry soil and 200 ml distilled water.

2) In order to obtain the desorbed contaminant concentration c_d, it should be noted that a certain amount of the measured contaminant species is a residual carry over of unbound contaminant from the wet pellet obtained during the adsorption test. This residual component is subtracted from the total desolved species according to the water content of the wet pellet.

Sequential extraction was then carried out for dried and weighed soil pellet, obtained after centrifugation, of desorption.

4.4.2 Sequential Extraction Experiments

The procedure of sequential extraction for the study of heavy metal retention in soils and sediments has been developed by Chester and Hughes (1967), Gupta and Chen (1975), Tessier *et al.* (1979), and Yanful *et al.* (1988).

This procedure allows us to obtain information on the amount and forms of heavy metals retained in the soil under different conditions of pH. The results from sequential extraction were used to elucidate the retention mechanisms of heavy metals at different soil buffering conditions.

The chemical forms of heavy metals retained in soil at various pH conditions are different (Yong *et al.*, 1986). For example, heavy metals may be retained in soils in the forms of *i*) oxides and hydroxides, *ii*) carbonates, *iii*) exchangeable cations, and *iv*) bound to organic matter, depending on the soil constituents and conditions (Yanful *et al.*, 1988). These forms of heavy metals can be extracted selectively by using appropriate reagents (Tessier *et al.*, 1979).

The soil under consideration has neither carbonate, nor organic matter, but it contains considerable amount of oxides and hydroxides. Thus, no extraction of carbonate or organic matter was performed. Since this study is mainly concerned with soil contamination and decontamination, the amount of the exchangeable cations, which could be removed from soil particles, is of great interest. The other components are all non-exchangeable, and therefore there is no need to distinguish among them.

Accordingly, the sequential extraction in this study consists of: *i*) extraction of exchangeable cations, and *ii*) extraction of the entire residue (including oxides and hydroxides components) using acid digestion. The first part contains two stages: a) extraction of exchangeable cations without utilizing any reagent, which has been discussed as a desorption process in this study (section 4.4.1.2), and b) extraction of exchangeable cations by means of the appropriate reagent. Sequential extraction was performed on the entire sample set (54 samples) obtained from desorption tests.

4.4.2.1 Extraction of the Sorbed Exchangeable Cations

In order to release the bound or sorbed exchangeable cations from the soil particles, 1 g of dry soil is dissolved in 8 ml of saturated potassium nitrate (KNO_3) solution, at room temperature. The soil- KNO_3 solution is then agitated continuously for 1 hour. In order to maintain the same pH condition for the extraction of exchangeable heavy metal cations, the KNO_3 solution was adjusted to the same pH value as the original soil-distilled water suspension.

After agitation, the soil sample is centrifuged as described earlier. The clear supernatant was analyzed for heavy metal by atomic absorption spectroscopy. The residue was washed with distilled water centrifuged, and the supernatant discarded. The residue was then passed on to the next stage of the extraction as explained in the following section.

4.4.2.2 Extraction of the Residue

In order to extract the entire sorbed metallic species from the soil particle surfaces, the following digestion procedure was followed:

i) 1 to 2 g of dry soil sample was powdered and mixed thoroughly to achieve homogeneity, and then transferred to a conical flask (250 ml).

ii) 10 ml of a HNO_3 solution (normality 15-16) was mixed with distilled water (1:1 by volume, H_2O: HNO_3) and then the solution was added to the soil and mixed

thoroughly. The flask was covered with a watch glass, and the soil- HNO_3 solution was refluxed at 95°C for 10 to 15 minutes without boiling. The sample was allowed to cool, and 5 ml of concentrated HNO_3 (normality 15-16) was added. The watch glass was replaced and the acid-soil suspension was refluxed for 30 minutes. The last step is repeated to ensure complete digestion of the soil suspension. Using a ribbed watch glass, the suspension is allowed to evaporate to 5 ml without boiling, while maintaining a covering of solution over the bottom of the flask.

iii) After completing the second step and cooling the sample, 2 ml of ASTM type II water (ASTM D1195) and 3 ml of 30% H_2O_2 are added to the sample. The flask is covered with a watch glass and returned to the hot plate to start the peroxide reaction. Care must be taken to ensure that losses do not occur due to excessively vigorous effervescence. The heating is continued until effervescence subsides and then the beaker is cooled.

iv) Adding 30% H_2O_2 in 1 ml aliquots with warming is continued until the effervescence becomes minimal or until the general sample appearance does not change. A maximum of 10 ml 30% H_2O_2 is added.

v) 5 ml of concentrated HCl and 10 ml of type II water are added to the sample and returned to the hot plate to reflux for an additional 15 minutes without boiling. After cooling, the sample is diluted to 100 ml with type II water. Particulates in the digest that may clog the nebulizer, during AA analysis, are removed by centrifugation and filtration (through whatman No. 41 filter paper or equivalent), or by allowing the sample to settle.

vi) Eventually, the sample is diluted to 100 ml with type II water and AA analysis performed to determine the amount of retained heavy metal on the soil particle surfaces.

The summation of the residue and total exchangeable cations represents the total adsorbed species.

4.4.3 Unsaturated Soil Column Leaching Tests

The column leaching tests, described in this section, attempt to model vertical contaminant migration in a soil column. This model, simulates the flow of leachate through unsaturated soil in order to develop contaminant transport functions for unsaturated media. These functions is used in the mathematical model which is generally applied to this phenomenon.

These soil column tests study the relationship of soil buffering capacity to the movement of contaminants. The studies by O'Donnell *et al.* (1977), Fuller (1977), Fuller (1978), and Yong *et al.* (1986) indicated that the soil column technique is a simple, rapid, and reliable method for predicting pollutant attenuation and pollutant movement within soils.

In this study, soil column experiments were performed following the method of Fuller (1982) and Yong *et al.* (1986). The description and setup of this experiment is very similar to the unsaturated hydraulic conductivity test. Also, in addition to Θ and H, the solution concentrations c, and concentration of adsorbed species on soil particles s, were measured throughout the soil column and at different time intervals.

The solution with a metal concentration of 2000 ppm and pressure head of 4 psi is applied to the top, and the effluent collected at the bottom of the soil column, at the atmospheric pressure. In order to determine Θ, H, c, and s, columns with TS's as well as simple column were run:

A vertical column equipped with thermocouple psychrometers, which was run for a one month period, to obtain not only Θ and H for various time intervals and depths, but also contaminant concentration c, and concentration of adsorbed species on soil particles s, for each depth of the column z. In addition, a number of simple columns, i.e.: without TS units, were utilized to obtain the c and s values as functions of column depth z, and t (other than 1 month).

In order to obtain the c and s values at each depth, the column was sectioned and the concentration of heavy metal within the pore solution c, and on the soil particles

(adsorbed species concentration) s, was measured. This measurement was done by means of atomic absorption spectroscopy.

Measuring c and s for each segment incorporates the following steps:

1) Determination of the volumetric water content Θ,
2) Mixing 5 g of the contaminated wet soil with 50 g of distilled water thoroughly, to achieve homogeneity,
3) Centrifugation of the soil suspension sample (from step 2), to extract solution from the soil particles. After determination of the concentration of metals in the supernatant, and taking into account Θ and desorbed species, c may be calculated.
4) Determination of exchangeable cations on the soil particles(section 4.4.2.1),
5) Digestion of the residue obtained from the latter stage (4), following desorption, in order to find the amount of contaminant species on the soil particles s (section 4.4.2.2).

In order to calculate the adsorption concentration s, the results of stages 4 and 5 were summed up. All these measurements were done for 3 different contaminated solutions, after 1, 3, 7, 15, and 30 days. The sections were selected at 13 various depths of the columns (from 1 to 25 cm). For each section, 3 concentrations (c, s, and desorbed species concentration) and 2 hydraulic (H and Θ) values measurements were performed.

After running the test for all columns, the variation of values obtained (c, s, H and Θ) were plotted for various depths and time intervals. These graphs were used to analyze the contaminant transport phenomenon, and afterwards, to test the numerical model.

CHAPTER 5

EXPERIMENTAL RESULTS AND DISCUSSION

The results of all experiments described in chapter 4 are presented in this chapter. The results are followed by discussion, in order to better understand the phenomena behavior, and also to better realize the relationships among related processes. Eventually, mathematical models were provided to generalize and formulate the nature of the phenomena and accordingly make the results of many other cases predictable.

This chapter consists of 7 sections concerning the experiments in the previous chapter. The first section presents the soil properties test results, whereas the second section contains the saturated hydraulic conductivity tests results and related discussion. Sections 5.3 and 5.4 are concerned with the results and discussion of soil-moisture retention and unsaturated soil column tests, respectively.

The last three sections present the results and a discussion of these results as related to the second part of the experiments; i.e. *i*) kinetic batch tests, *ii*) sequential extraction, and *iii*) unsaturated soil column leaching tests.

5.1 SOIL PROPERTIES

Some experiments were carried out to indicate the required properties and characteristics of the soil. The results are as follows:

1) The initial water content of the soil was found through weighing some samples before and after oven drying (at 100°C) for 24 hours. The obtained value was equal to 0.3%, which is very low. Furthermore, in order to determine the consistency (Atterberg) limits of the soil, relevant tests were performed. As a result, the liquid and plastic limits of the soil were determined as 66% and 40%, respectively.
2) The standard Proctor (compaction) test was run to establish the variation of dry unit weight of the soil with respect to the moisture content, as well as the

maximum dry density of the soil and the optimum water content. Table (5.1) presents the results of these experiments.

3) In order to determine the grain-size distribution curve of the soil, a hydrometer analysis was performed. Then, this curve was used to determine some of the basic parameters of the soil, such as effective size D_{10}, uniformity coefficient cu, and coefficient of gradation cc. These values are 0.18μ , 6.11, and 0.71, respectively.

Table 5.1 **Compaction Test Results**

1.36	32%	0.47	95%	43%	1.81

5.2 SATURATED HYDRAULIC CONDUCTIVITY

This experiment was performed for the soil at maximum dry density $\gamma_{d\,max}$, with three different volumetric water contents Θ, to find how the final result might be affected by this variation of Θ. Moreover, three different dry densities of the soil are examined at the same water content (ω=5%), to verify the variation of K_s. Eventually, the test was performed on the soil with density of $0.80\gamma_{d\,max}$, for distilled water and three different heavy metals solutions, lead, copper, and zinc, at a concentration of 2000 ppm. The results of the aforementioned 10 cases are presented and discussed in this section.

The first set of experimental results, regarding the saturated hydraulic conductivity, is presented in Table (5.2). The results indicate that the variation of initial water content does not have a considerable effect on saturated hydraulic conductivity value.

Thus, the results show that as long as the dry density of the soil is kept constant, the soil structural matrix does not change remarkably. Consequently, the pore size and distribution, and therefore the overall pathway for the fluid (to move through the pore spaces) remain the same, even though the initial water content is different for each test.

Table 5.2 K_s **for 3 different Water Content**

K_s (x 10^{-7}) m/s	3.10	3.63	3.31

The second set of experiments are related to three different dry densities of the soil (100%, 85%, and 55% of $\gamma_{d\,max}$). Results of this investigation have been presented in Table (5.3).

Table 5.3 K_s for 3 Different Dry Density

K_s (x 10^{-9}) m/s	1.03	2.29	7.43

In contrast to the first set of experiments, the second one shows a significant variation for the saturated hydraulic conductivity. Any change in the density of the soil results in a considerable variation in the soil structure, and therefore in the fluid pathway within the soil medium. As it is obvious in Table (5.3), a 15% decrease in γ_d increases the K_s to more than 200%, whereas, a decrease of 45% in γ_d raises the K_s to 700%, compared to the case which γ_d is equal to $\gamma_{d\,max}$.

In order to provide the soil with dry unit weight close to the field situation in the laboratory, a dry density of 80% of $\gamma_{d\,max}$ is considered for the third set of tests while the ω is equal to 5%. The results of these tests have been presented in Table (5.4).

Table 5.4 Ks for 4 Different Solutions

Solutions	H_2O (distilled)	$PbCl_2$	$CuCl_2$	$ZnCl_2$
K_s (x 10^{-9}) m/s	10.83	9.76	9.92	10.75

The solutions of heavy metals are at 2000 ppm concentration, however, their saturated hydraulic conductivity K_s is almost the same as distilled water. According to the Kozeny-Carman equation (Eq. 3.19), the fluid properties which can affect the hydraulic conductivity are viscosity and density. None of these parameters has been changed remarkably to have serious effect on the saturated hydraulic conductivity for the soil-solution system.

It may be concluded that the mean value of the K_s (Table 5.4) can be assumed to be the representative value of K_s for any kind of the solutions in the rest of the experiments in this chapter. This value has been calculated as 10.32 x 10^{-9} m/s or 8.91 x 10^{-4} m/day .

5.3 SOIL-MOISTURE RETENTION FUNCTION

In general, the pores in a soil sample have different dimensions and , therefore will not empty at the same suction. The large pores, or those with larger channels of entry, will empty at low suctions, while those with narrow channels of entry, supporting interfaces of sharper curvature, will empty at higher suctions. In contrast, the imbibition process is the reverse; the wider the entry channel, the faster and easier the pores get wet. In soil science, this property is discussed through soil-water retention curves (drying and wetting curves), as they show how water is retained in soil by capillary forces against gravity.

In the present study, two different apparatuses are utilized to obtain the drying and wetting curves: *i*) pressure plate extractor apparatus for the drying process, and *ii*) unsaturated soil column apparatus for the wetting process. The latter curve is based on the results obtained from section (5.4), which is concerned with the soil column tests. After running each experiment, the generated data are utilized to plot the retention curves.

For the drying process, the general form of the capillary pressure (suction Ψ) versus volumetric water content (degree of saturation) is shown in Fig. (5.1.a). This relationship is a function of the kind of soil and wetting fluid.

The initial desaturation or drainage curve represents a decrease in the wetting phase saturation, from being fully saturated to the level at which further increase in Ψ does not result in an additional flow of fluid from the medium ($\Theta=\Theta_r$). At this level of saturation, the wetting fluid no longer exists as a continuous phase in contact with an external fluid supply, and Θ_r is refered to as residual or irreducible volumetric water content.

The imbibition process which follows the same function as the drying process, is also depicted in Fig. (5.1.a). No decrease in Θ is observed until Ψ reaches a critical suction (capillary head) Ψ_b, at which fluid begins to flow from the soil medium. Depending on the field of application, this suction is the bubbling pressure or air entry pressure. White et al. (1972) have shown that the inflection point of the drainage curve represents the saturation (or volumetric water content) at which the non-wetting phase ceases to be continuous. In this study, according to the experimental results , the Θ_r and Ψ_b are considered as 2.46% and 8.21 bars, respectively.

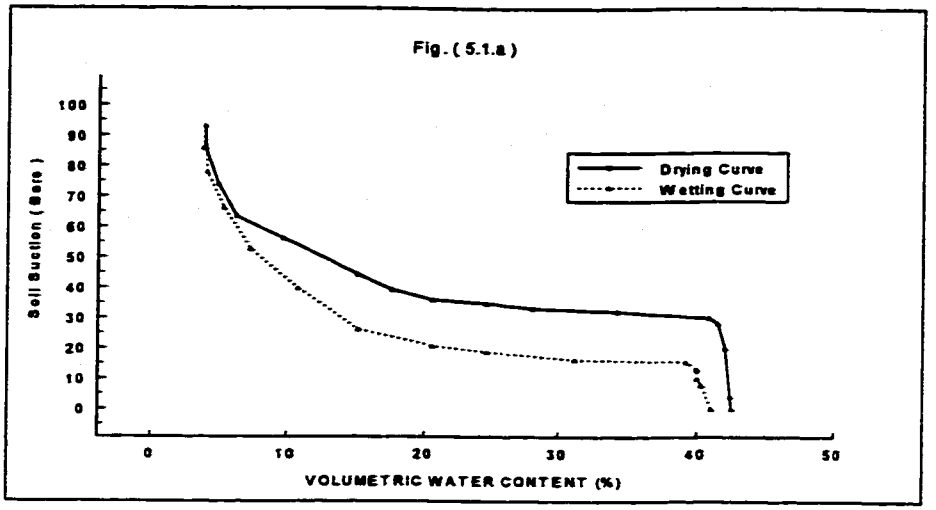

Figure 5.1.a Soil Water Retention Curve

Fig. (5.1.a) containing the above two curves presents the soil-water retention curve. Upon rewetting or imbibition, it is observed that the suction Ψ, as a function of Θ ($\Psi(\Theta)$), differs from that obtained during drainage. This difference stems from the phenomenon of hysteresis which is generally a function of other phenomena.

In this investigation, the soil-moisture retention properties exhibit strong hysteretic behavior (Fig. 5.1.a), therefore the relationship between the suction Ψ, and the moisture content Θ, is not unique. Thus, Ψ cannot be determined directly from the knowledge of Θ without investigating the past wetting-drying history of the soil under consideration.

Furthermore, the determination of Ψ is also a function of the kind of path (drying or wetting) which is selected in the investigation process. Such hysteretic behavior should be modeled by using different parametric relationships for the wetting and drying phases of the moisture transport.

5.3.1 Volumetric Water Content and Soil Suction Relationship

Once constitutive data for a given porous medium have been collected in the laboratory, they must be put in a form that is useful in the context of a simulation model. Formulations of the (Θ-Ψ) relationship which have been described by researchers range from simple tables to complex hysteretic functions.. Mathematical representations and associated parameterizations of soil suction-volumetric water

content curves are important issues, and the difficulties inherent in casting this constitutive function into numerical forms have been studied by Mercer and Faust (1976), Aziz and Setari (1979) and Abriola (1984).

The main goal in this study is the investigation of contaminant transport through unsaturated clay soil which is an imbibition phenomenon. On the other hand, in order to solve the transport equation, the volumetric water content Θ, is to be a known value. This value can be determined from the soil suction value Ψ, if the relationship between these two values is defined.

Because of a numerical requirement (see chapter 6), soil water potential (H) is utilized instead of soil suction (Ψ), wherever it is necessary. According to the definition of H and Ψ, the relationship between these two parameters is $\Psi = -H$. Obtaining the (Θ~H) relationship, Fig. (5.1.b) presents the following function as a constitutive relationship between these two values in this study

$$\frac{1}{\theta} = \frac{0.01}{a + bH^2} \tag{5.1}$$

where a and b are empirical parameters, and they are introduced separately in the figure.

On the basis of the aforementioned constitutive relationship, the specific moisture capacity $C(H)$, of the soil could be defined. By definition, the soil's specific moisture capacity is the derivative of the volumetric water content with respect to the soil water potential, i.e. $C(H)=d\Theta/dH$, thus

$$C(H) = \frac{-0.02bH}{(a + bH^2)^2} \tag{5.2}$$

5.4 UNSATURATED SOIL COLUMN TESTS RESULTS AND DISCUSSION

Understanding the mechanism of flow and retention of water in soil is of fundamental importance to hydrologists, agronomists, civil and environmental engineers. Successful development of irrigation and drainage systems, decontamination of soil, attenuation of contaminated solutions, and the like, depend on adequate prediction of water movement within the soil.

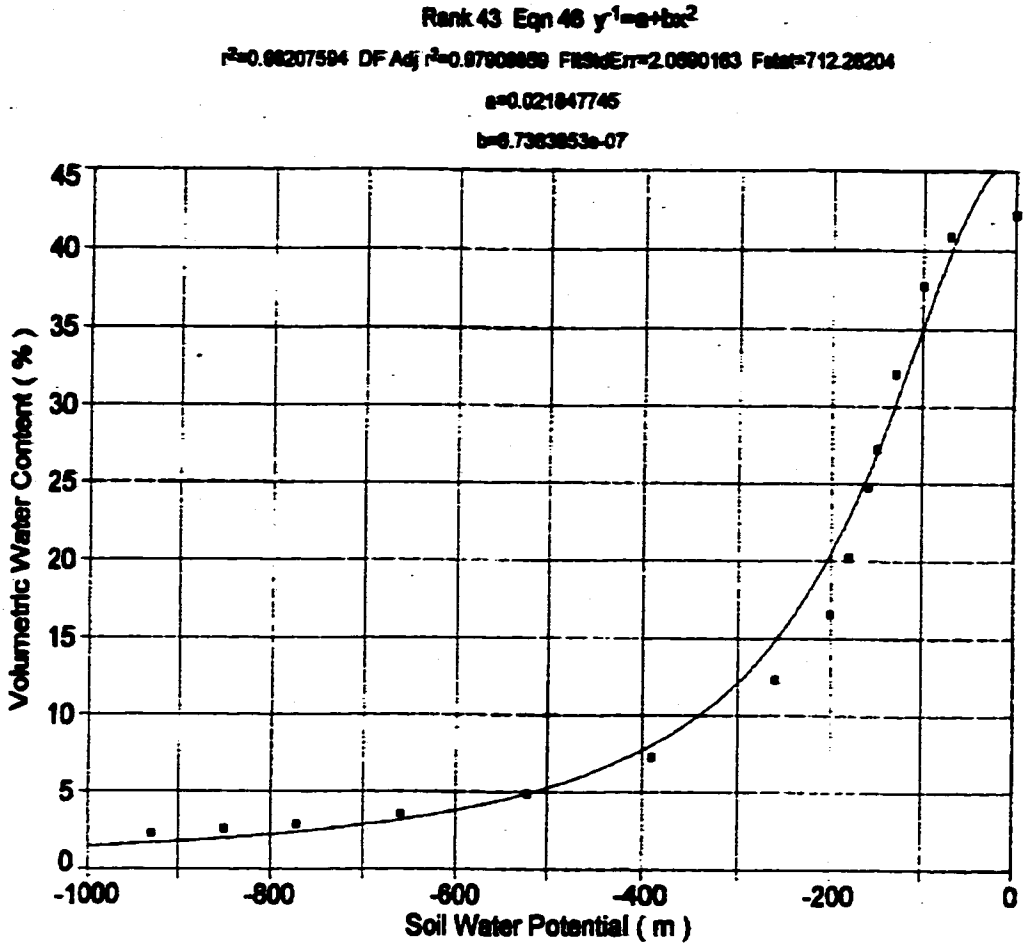

Figure 5.1.b Volumetric Water Content-Soil Water Potential Relationship

As a result, in unsaturated soil column tests, the attention has been focused on the relationship between the soil water potential and the volumetric water contents, along the soil column. This relationship and the relationship between the relative hydraulic conductivity and the soil water potential are essential in predicting the behavior of multiphase porous media systems.

The relationship between the soil water potential H, and the volumetric water contents Θ, is utilized to find the specific moisture capacity $C(H)$, and the unsaturated hydraulic conductivity $K(H)$. Afterwards, these functions are used to analyze the unsaturated flow equation (Eq. 3.16), and also simulate this equation for the numerical modeling.

Hence, this section contains two following sub-sections regarding the: *i*) variations of H and Θ at various time intervals, along the soil columns for different kinds of solutions, and *ii*) unsaturated flow parameters, namely $\Theta(H)$, $C(H)$ and $K(H)$. Having volumetric water content as a function of suction $\Theta(H)$, reduces the number of unknowns to one in the contaminant transport equation. As a result, this reduction helps the investigator to solve the contaminant transport equation, for one unknown, namely concentration c.

In porous media, suction is usually expressed by pressure units (e.g. bars). Also, there is a possibility for the suction to be expressed in terms of energy per unit weight, which has dimension of length (m).

5.4.1 Variations of H and Θ along the Soil Column

This section is concerned with the variations of soil water potential and volumetric water content along the soil column, which is 26 cm in height. The measurements were taken at 14 various depths from the top to the bottom of the column, and all the measurements were repeated at 6 different time intervals, i.e. 0.5, 1, 3, 7, 15, and 30 days.

5.4.1.1 Soil Water Potential (H)

The aforementioned measurements have been performed for soil water potential (H) where the solution was distilled water. The results of these tests have been presented in Fig. (5.2.a).

As the figure shows, the soil water potential variations range is wide at the beginning of the experiment, and becomes very narrow, when the time interval gets higher. For instance, at 0.5 day the H variations' range is about 400 m, while at 30 days this range is less than 30 m. This variation is based on the fact that the tendency of the soil particles to absorb the water decreases, as they hold more water molecules. The containing moisture in the soil, causes less soil water potential, and therefore less affinity to attract extra moisture.

Since the soil had an initial water content ($\Theta_{init.} = 6.5\%$), the soil water potential does not fall below -400 m. However, the soil column still requires more than 1 month to become fully saturated.

At the beginning most of the water molecules are absorbed by the soil particles along the soil column. However, when the soil water potential increases to a higher value, the water molecules have more freedom to move downward. Thus, the lack of freedom, delays in the saturation of the soil column, and therefore the rate of the enhancement of the soil water potential decreases remarkably with respect to time.

5.4.1.2 Volumetric Water Content (Θ)

For distilled water as a solution, variation of volumetric water content with respect to depth at various time intervals have been depicted in Fig. (5.2.b). Variations of Θ follow almost the same trend as soil water potential. The range of variation is considerably wider at the beginning of the experiment than after a 1 month, and the volumetric water content rate of variation decreases as the time progresses. The manner of both of these variations stem from the tendency variations of soil particles to absorb varying amounts of water molecules during the test run (which affects soil water potential, as well).

Fig. (5.3) compares the volumetric water content values for different solutions along the soil column. In order to find the effect of the different solutions, the experiment has been run for 3 extra solutions. The selected solutions are copper, lead, and zinc chlorides with a concentration of 2000 ppm. The tests have been run for 0.5 and 3 day time intervals.

As the figure illustrates; the variations of all 4 solutions fit within narrow envelopes, which make the difference unremarkable. Accordingly, one can suppose that the unsaturated flow variables concerned with the other 3 heavy metals solutions in the column tests, are the same as those of distilled water as long as the other experimental conditions remain unchanged.

5.4.2 Unsaturated Hydraulic Conductivity

The hysteresis effect shows that Θ cannot be considered as a suitable parameter to govern the direction of the flow. For instance, if $\Delta\Theta$ within a medium is zero, there might be some flow. The flow will occur in the direction which reduces the soil water potential, even when Θ is the same throughout the medium. On the basis of this fact, the unsaturated hydraulic conductivity is defined just as a function of soil water potential.

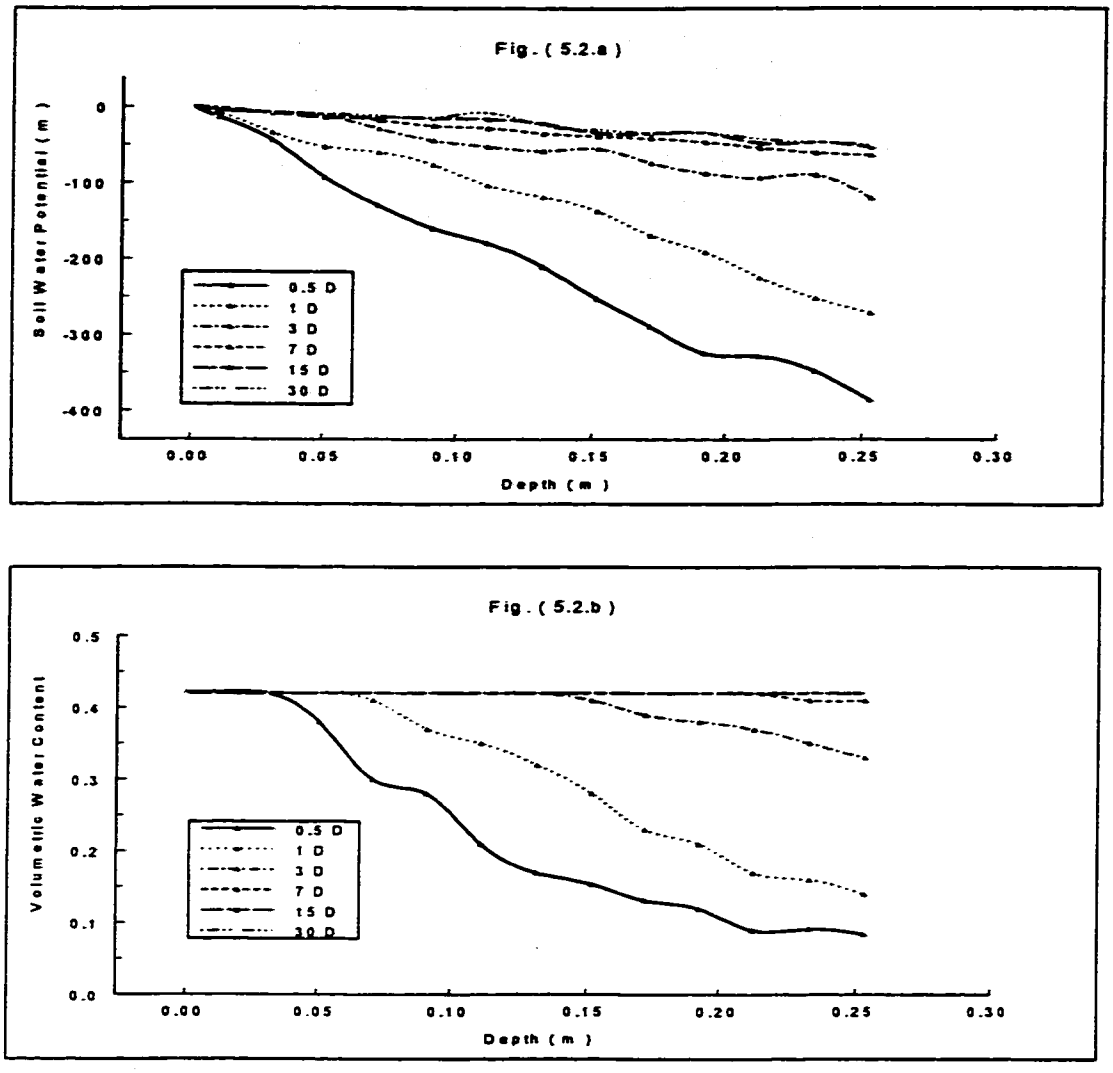

Figure 5.2 Variations of a) Soil Water Potential, and b) Volumetric Water Content at 6 Various Time Intervals along the Soil Column

In addition to the soil water potential as a variable of $K(H)$, there are some other parameters which affect the value of $K(H)$. Even though these parameters are constant values, they are related to the medium and the kind of the solution properties.

The porosity of the medium n, plays a significant role in the unsaturated flow phenomena, and the effect of irreducible water content Θ_r should be taken into account, as well. The former parameter determines the ease with which the water can move within the medium, and the latter indicates the amount of free water (solution) able to flow.

Besides these parameters, the unsaturated hydraulic conductivity function cannot be completed unless the saturated hydraulic conductivity K_s is taken into account. Since the

ideal situation for the moisture to flow within the soil medium is when the soil is fully saturated, in reality ***K(H)*** is directly proportional to the saturated hydraulic conductivity, ($K(H) \sim K_s$).

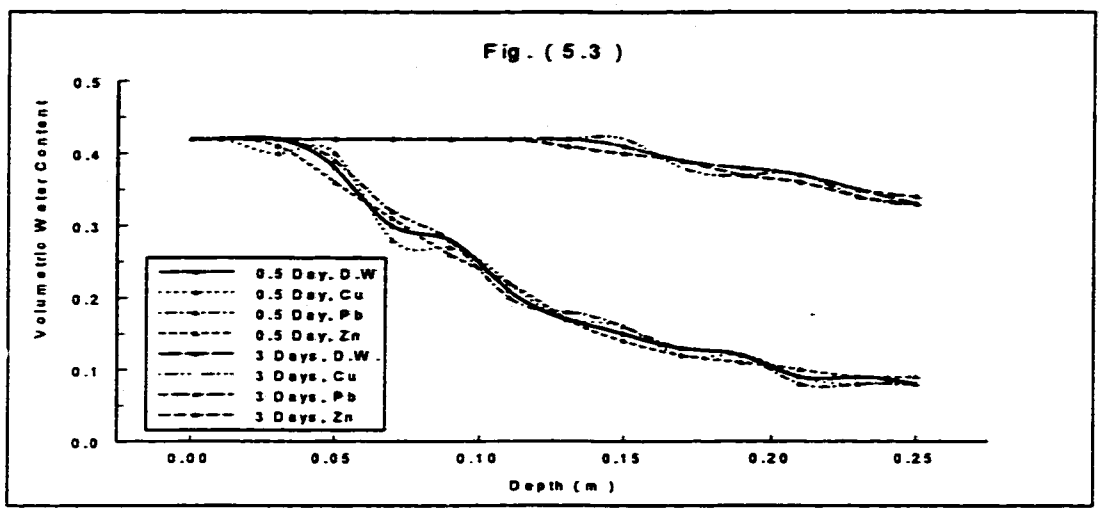

Figure 5.3 Comparison of Distilled Water and Contaminated Solutions' Volumetric Water Content Variations with Depth

Taking into account all the aforementioned parameters, the following formula is introduced for the present study:

$$K_r(H) = K_{sat}\left[\frac{0.01(a+bH^2)^{-1} - \theta_r}{n-\theta_r}\right]^d \qquad (5.3)$$

where ***a***, ***b***, and ***d*** are empirical parameters, and equal to 0.02, 6.72, and 1.51, respectively.

This formula is proposed on the basis of the proportionality between ***K(H)*** and other unsaturated flow parameters, and also takes advantage of the proposed formulas in the literature. The formula was used in the numerical modeling to obtain the unsaturated flow unknowns. Since the results of the numerical model and experiments were in a good agreement (Fig. 6.4), it shows that the proposed formula is a proper one for the problem at hand.

5.5 RESULTS OF KINETIC BATCH TESTS AND DISCUSSION

Thermodynamic data can predict only the final state of a system from an initial non-equilibrium mode. However, to rationalize chemical reaction rates, a knowledge of the involved kinetics is required. Kinetic studies provide valuable insights into the reaction pathways and the mechanisms of chemical reactions. Unfortunately, due to theoretical and experimental difficulties, it is often arduous to apply pure chemical kinetics to even simple homogeneous solutions. Moreover, when kinetic theories are applied to heterogeneous soil systems, the problems are magnified.

Thermodynamic aspects of reactions occurring in clay and soil systems have received considerable attention over the years. Yet, kinetic investigations of clay and soil systems have been sparse. While some research has been conducted on the kinetics of sorption and desorption of ions in pure clay systems, these processes are still not well understood.

The purpose of this section is to better realize the principles of chemical kinetics according to the experimental results and to show how these principles can be applied to the kinetics of adsorption and desorption of ions in soil systems. This understanding of the chemical reaction rates will help *i*) to predict how quickly a solution reaction will move to its equilibrium state, and *ii*) to reveal reaction mechanisms. A reaction mechanism can involve the break down of a chemical reaction into a sequence of elementary steps, or a knowledge of reaction mechanisms related to the detailed nature of individual steps in a reaction.

This section contains the results and discussion of several soil suspension tests (22 batch tests) which were conducted to study heavy metal retention in clay soil. Five different concentration of Pb (Pb^{2+}), (at 50, 200, 500, 1000, and 2000 ppm), and three various concentration of Cu (Cu^{2+}), and Zn (Zn^{2+}), (at 50, 500, and 2000 ppm), were applied to the kaolinite clay soil. Solution concentration measurements have been done at 0.25, 1, 6, 12, 24, 48, 120, and 240 hours after starting each batch test (total of 176 for adsorption and desorption measurements). The variations of the adsorption and desorption of these 3 heavy metals with respect to time are illustrated in Figures (5.4) through (5.6).

It can be seen from the aforementioned figures that the adsorbed and desorbed species concentrations are zero at the beginning. Within a short time period they vary considerably and then they end up with a very gradual and quite narrow variation range. Consequently, these plots could be divided into two major zones: *i*) ***sharp***, and *ii*) ***smooth*** zone. In order to highlight the sharp zone, the above figures are plotted for up to

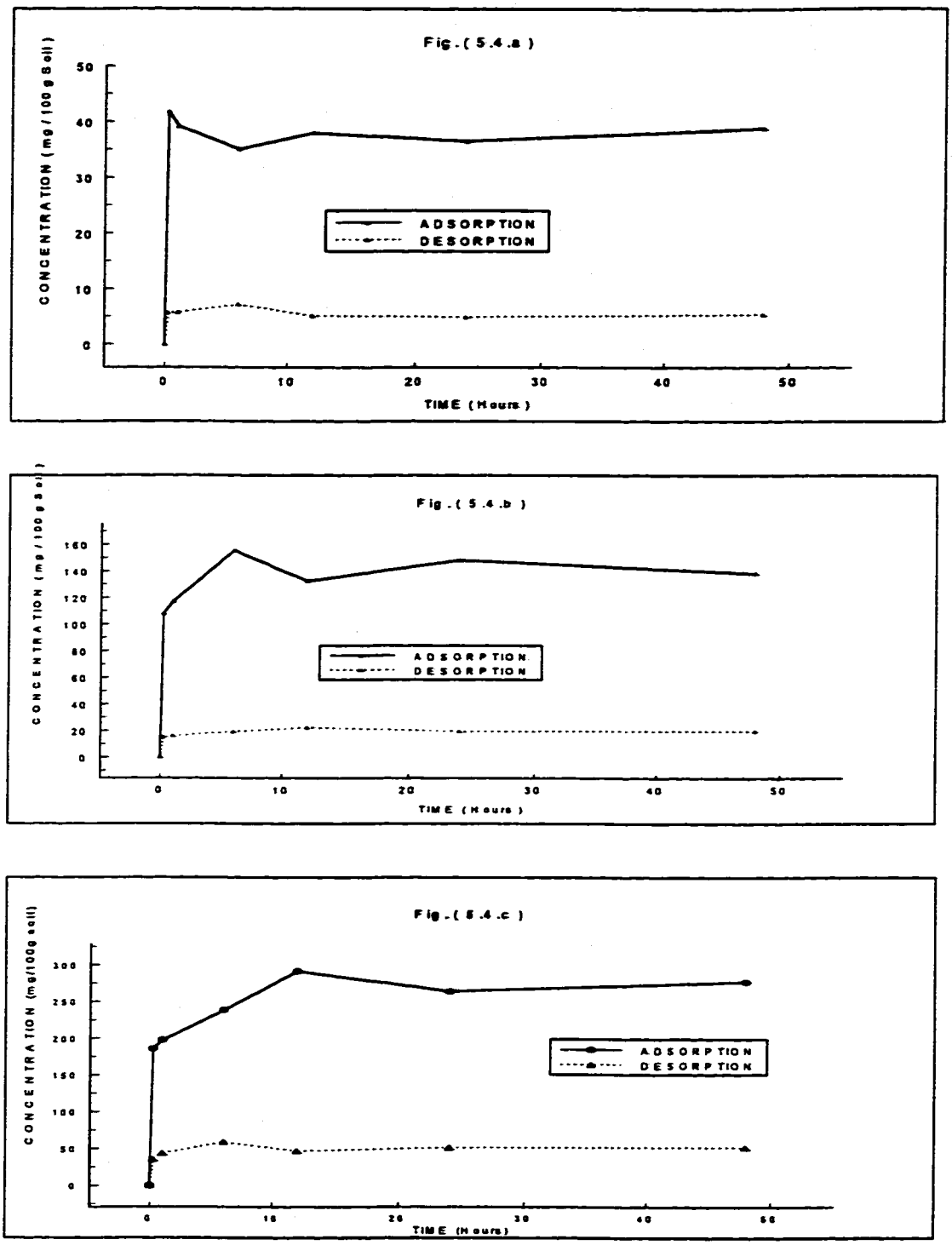

Figure 5.4 Adsorption and Desorption Concentration of $PbCl_2$ versus Time at a) 50, b) 200, and c) 500 ppm Solution initial concentration

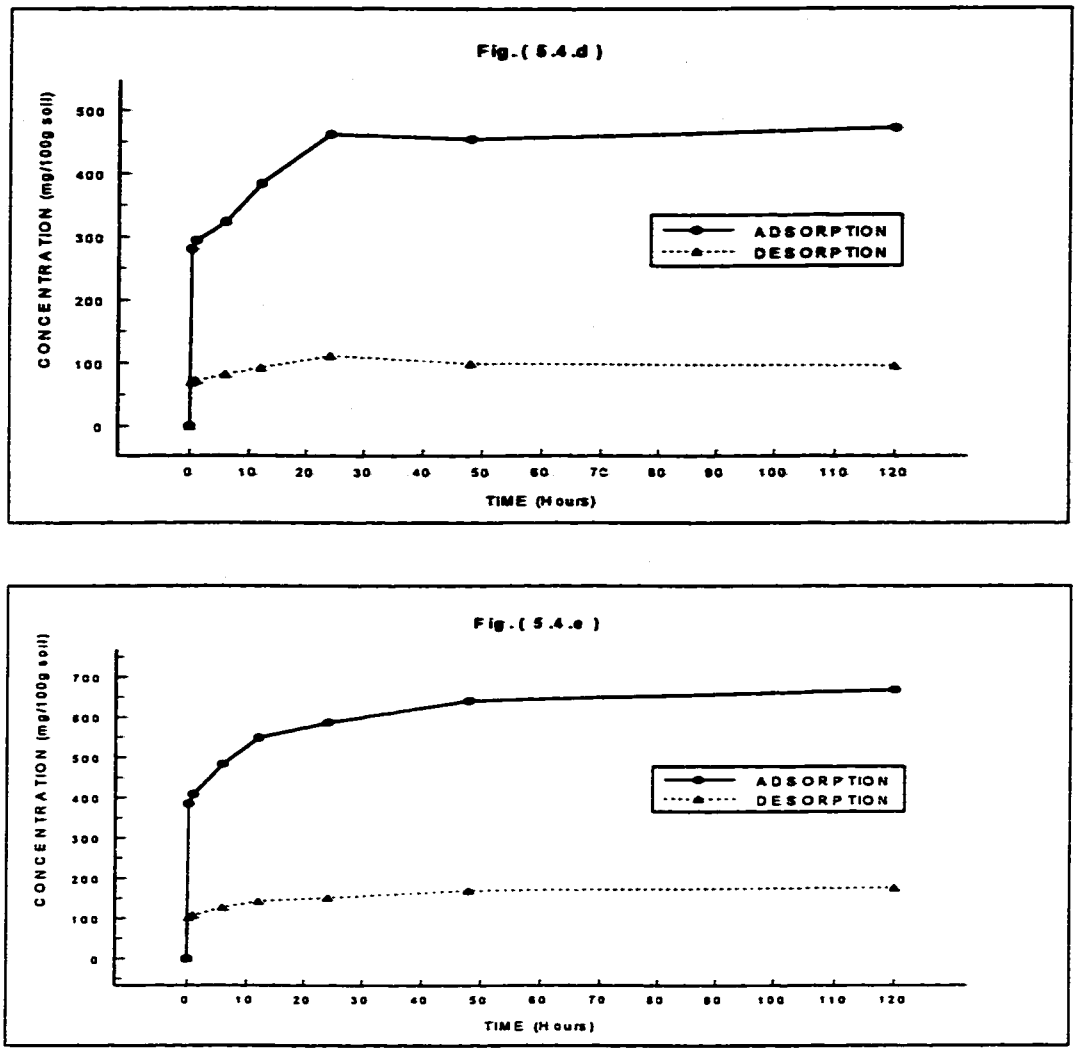

Figure 5.4 (Continued) Adsorption and Desorption Concentration of $PbCl_2$ versus Time at d) 1000, and e) 2000 ppm solution initial concentration

50 hours for concentrations less than 1000 ppm, while for concentrations equal to or over 1000 ppm the figures are plotted up to 120 hours.

Regarding to the sharp zone, it is observed that the adsorption and desorption rates are very high (more than 80% of the equilibrium concentration level) at the beginning of the experiment, whereas these rates decrease (below 20%) if the samples are taken later. Figures (5.7.a), (5.7.b), and (5.7.c) illustrate this fact clearly.

The high rate of variation in the sharp zone is expected, because the soil is completely dispersed within the solution and the soil particles surfaces are completely exposed to the solute species. As a result, the contaminant species could be adsorbed very quickly onto the soil particles' surfaces (SPS), and/or desorbed from SPS into the

distilled water. At the beginning, soil particles benefit from their highest potential to adsorb or desorb the solute species, whereas this high tendency is reduced as the adsorption or desorption process progresses.

The duration of the sharp zone depends on the initial concentration of the contaminant; i.e., the lower the initial concentration, the shorter the equilibrium time interval and therefore, the shorter the sharp zone. If the initial concentration is about 50 ppm the equilibrium duration is about 12 hours. In the case of concentrations of about 500 and 2000 ppm, this duration is about 24 and 48 hours, respectively.

Performing isothermal batch tests, very often 24 hours is considered as the adequate duration to obtain the equilibrium concentration of the adsorption process. According to the result shown in figures (5.4) through (5.6), the required time interval is more and sometimes less than 1 day. Thus, to be conservative in obtaining the equilibrium concentration of adsorbed and/or desorbed contaminant species, a minimum of 48 hours is recommended to keep the test running.

The smooth zone of the graph exhibits a very low range of fluctuation (compared to the sharp zone) within the variation bound which is limited to 20% of the equilibrium concentration. Since this variation does not diminish in the long term period, therefore it could be considered as a completely reversible process. The reversibility is induced by physical adsorption in a very weak bonding of contaminant species onto the soil particles surfaces.

When a salt dissolves in a solution (e.g.: distilled water), there would be a conversion from the inert salt state to the ionic components; for instance
$PbCl_2 \leftrightarrow Pb^{2+} + 2Cl^-$.

Thus, if any adsorption occurs, the ionic form of the heavy metal within the solution will be reduced. However, there is a limit to the amount of cations which can be adsorbed by the soil particle surfaces. At this limit, an equilibrium state between the cations inside the solution and those on the SPS is established. In the case where soil adsorption concentration goes beyond this limit, the equilibrium requirements conduct the soil-solution system towards desorption.

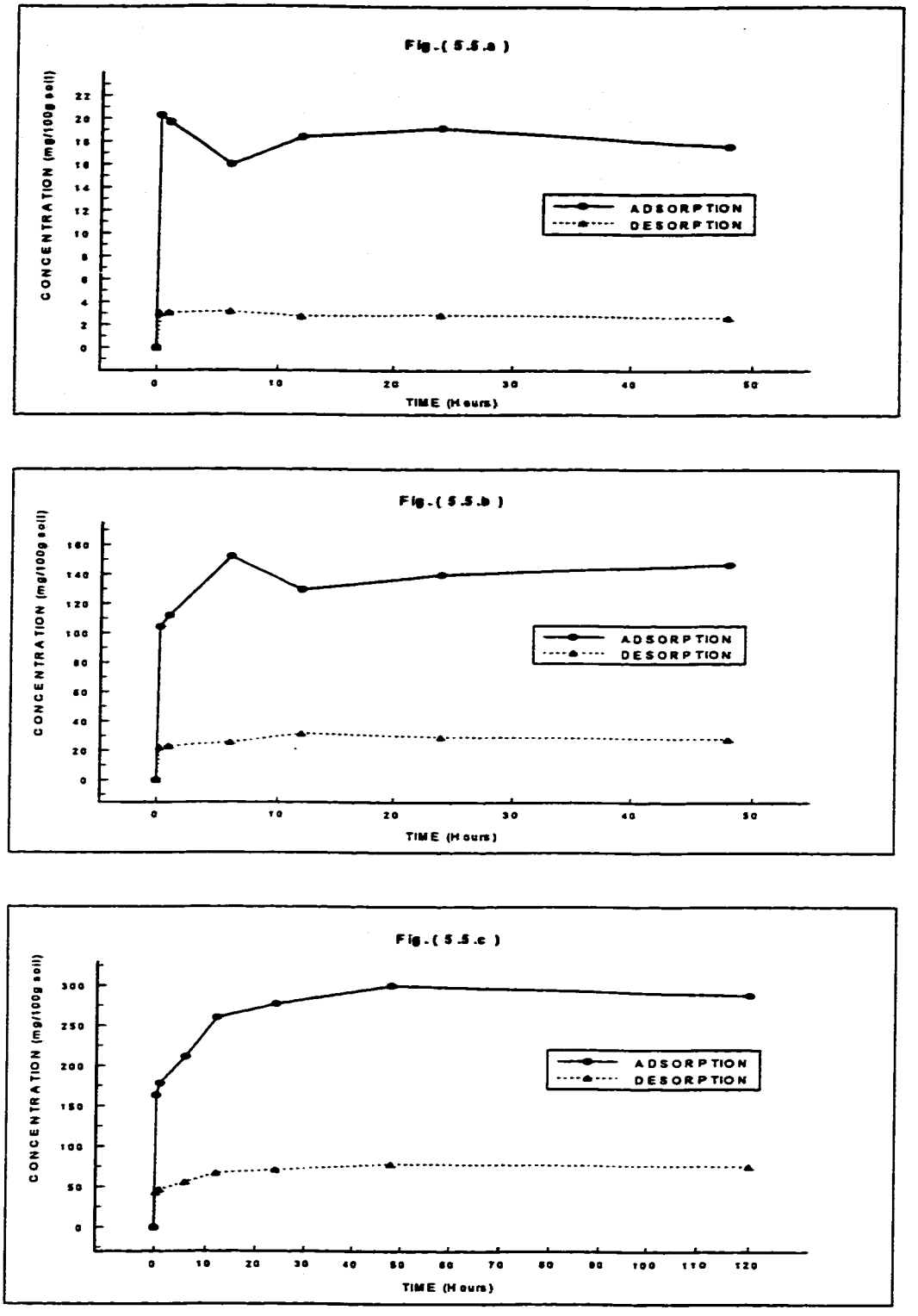

Figure 5.5 Adsorption and Desorption Concentration of $CuCl_2$ versus Time at a) 50, b) 500, and c) 2000 ppm Solution initial concentration

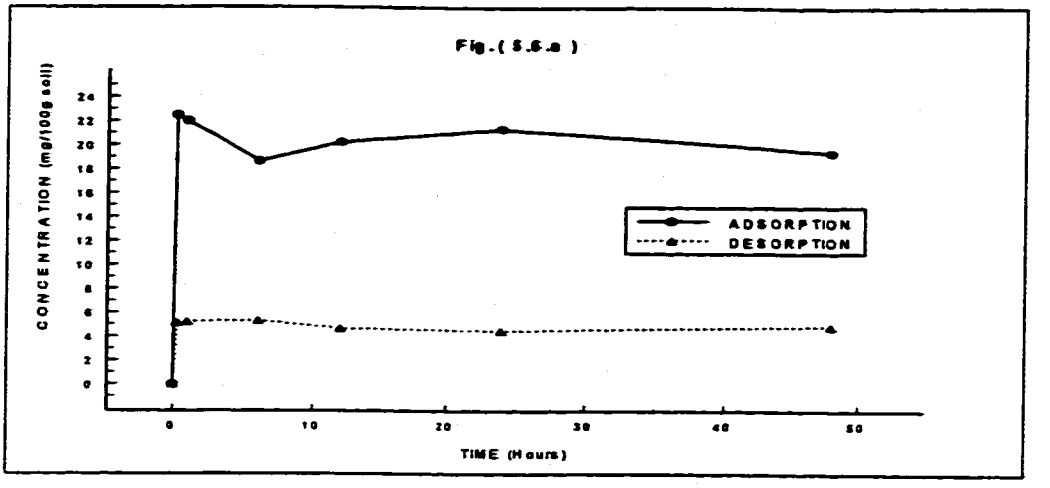

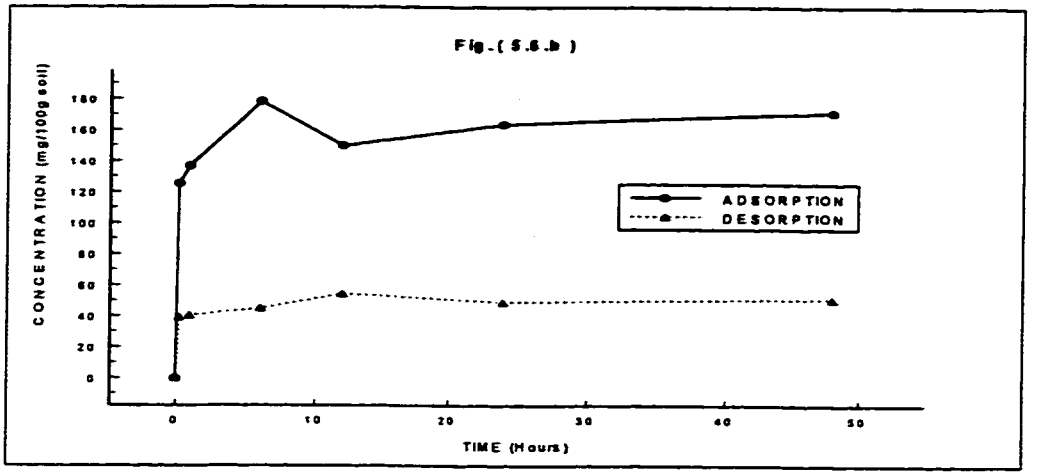

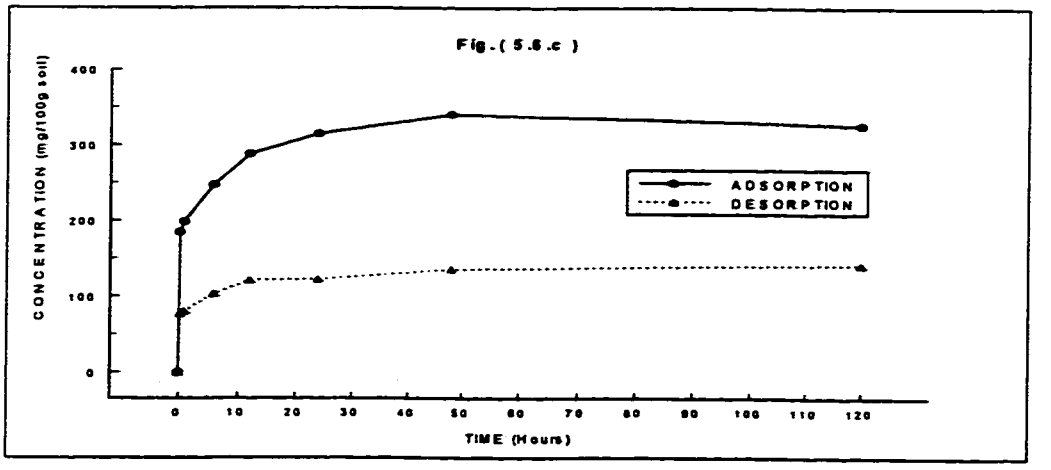

Figure 5.6 Adsorption and Desorption Concentration of $ZnCl_2$ versus Time at a) 50, b) 500, and c) 2000 ppm Solution initial concentration

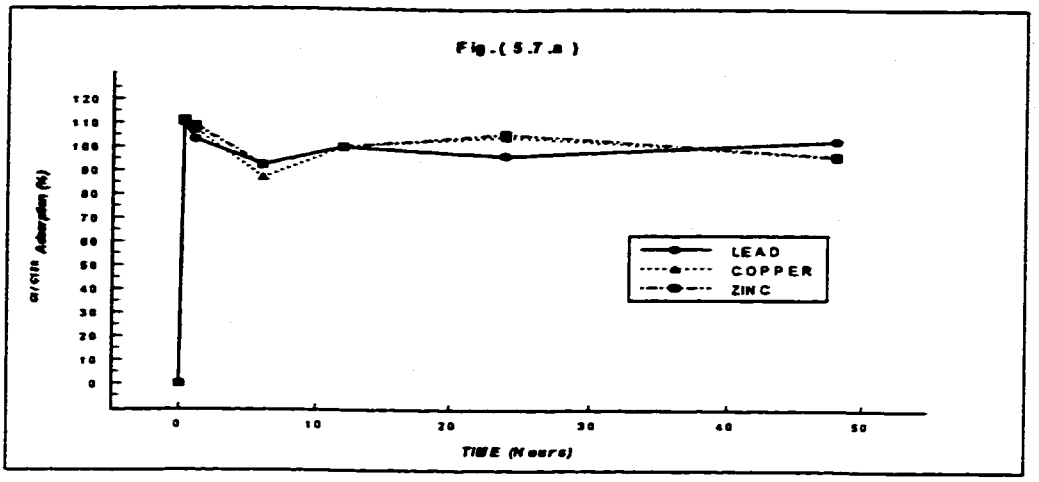

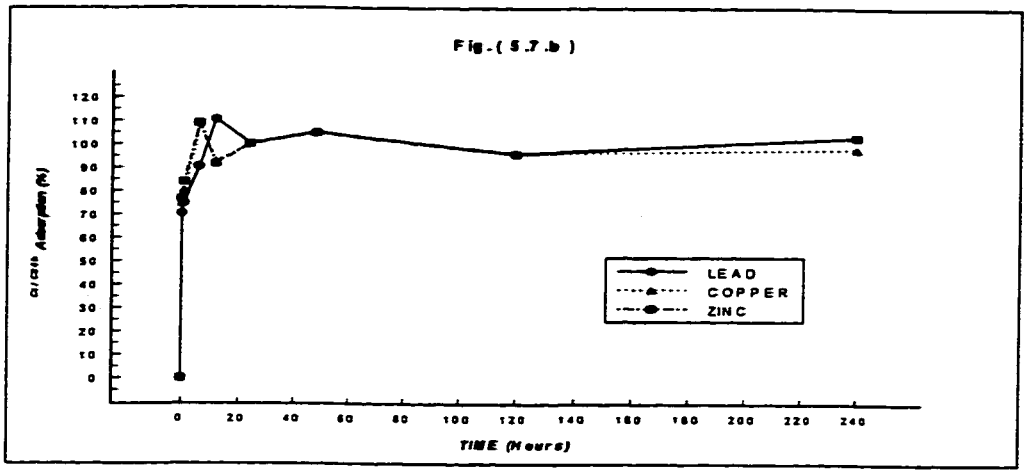

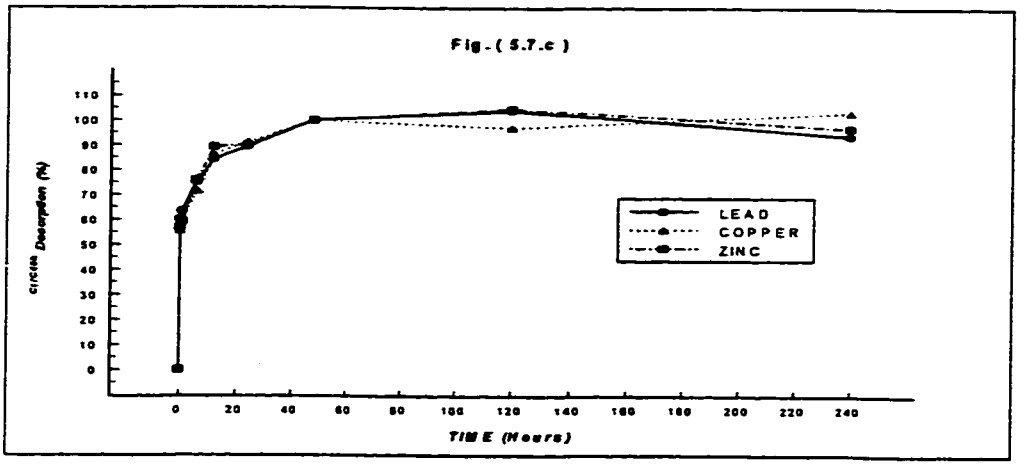

Figure 5.7 Adsorption Percentage at a) 50, b) 500, and Desorption Percentage at c) 2000 ppm Solution initial concentration versus Time for Lead, Copper, and Zinc

According to the kinetic situation of the soil-solution system, the adsorption/desorption process within the smooth zone will not cease. This oscillation is due to the highly accelerated movement of soil particles, that causes; *i*) variation of the forces exerted from the soil to the solute species, as the soil particles are not located at fixed points within the solution, *ii*) incision in the bounding of species and resulting desorption process, due to the movement of soil particles at very high acceleration along
with the adsorbed solute species which act as a volumetric block during solution stirring.

This exchange of adsorbed and desorbed species would happen as long as the kinetic situation of the soil-solution system exists. As a result, the equilibrium concentration of the soil-solution system could be proposed within the range of ±5% of the concentration at equilibrium.

In spite of the smooth zone, the sharp zone is not a completely reversible process. Part of this zone rate is contributed by chemical adsorption which is quite irreversible. However, the other part is attributed by physical adsorption, which is a partially reversible phenomenon. In order to figure out the percentage of physical or chemical adsorption, some sequential extraction tests are to be done. These tests indicate the exchangeable and unexchangeable cations which are in a direct correlation with the reversibility and irreversibility of the adsorption process. Discussion in more detail concerning the sequential extraction results is left to section (5.6).

According to the desorption experimental results, the sharp zone reversibility is not predominant, especially if the solution does not contain any particular reagent to help desorption of contaminant species (i.e., distilled water). Using some chemical reagents increases the amount of the desorbed species, and this enhancement could be extended to desorb the entire exchangeable cations from the soil particles surfaces.

Desorption of species into distilled water is due to the equilibrium requirements of the soil-solution system. As the contaminated soil particles pour into distilled water, the water molecules move immediately towards the cations bonded to the soil particle surfaces (SPS). Regarding the high concentration of the contaminant species, some of the cations are desorbed from the SPS and attracted to water molecules close to them. This desorption happens to the cations which are weakly bonded to the SPS. Based on the diffuse double layer theory, these cations which are located at the far end of the bonding zone belong to the second layer of the SPS.

On the basis of the above discussion, concentration variations with respect to time strengthen the idea of the 2 stage adsorption process. The first stage (the sharp zone) is

mostly related to the adsorption within or very close to the first layer; whereas the second stage (the smooth zone) is concerned with the species adsorbed within the second diffuse double layers (DDL) of the soil particle surface. This is the reason that, the affinity in adsorbing is very high at the beginning and therefore, the adsorption rate is also high. However, as soon as the first layer of the DDL is saturated with cations, the adsorption affinity decreases. Accordingly, the adsorption process continues slowly until this affinity reduces remarkably.

Figures (5.4) through (5.6) show the above correlation clearly, while emphasizing that the concentration variations along time variations, for the adsorption/desorption of the species onto/from SPS is neither linear, nor limitless. Thus, among 3 very common adsorption/desorption models, these figures are in agreement with the Langmuir model which accepts a limit for adsorption within a soil-solution system. Figures (5.14) and (5.15) provide more detail about governing formulae corresponding to the adsorption and desorption processes (to be discussed in the next paragraphs).

Having the same concentration, it is depicted in figures (5.8) and (5.9) that adsorption and desorption experiment results are different for various heavy metals. The first 3 figures illustrate the adsorption concentration variations with respect to time, whereas the 3 latter figures demonstrate the desorption concentrations rates.

According to the figures concerned with the adsorption process, lead shows the highest adsorbed species concentration, about 2 times those of copper and zinc. This remarkable difference is due to the considerable difference among the hydrated radii of these metals, i.e. hydrated radii of Pb^{2+}, Zn^{2+},and Cu^{2+} are about 4.5, 6.0, and 6.0 A°, respectively. The smaller the hydrated radius, the easier and faster the adsorption onto the SPS. Zinc and copper exhibit adsorption rates close to each other, however zinc has a higher adsorption rate than copper. Even though the hydrated radius of zinc is almost equal to that of copper, having a higher solubility product coefficient K_{sp}, induces a higher adsorption rate for Zn^{2+} than Cu^{2+}. Higher solubility product coefficient provides more ion availability and more of a concentration gradient, and as a result more adsorbed species.

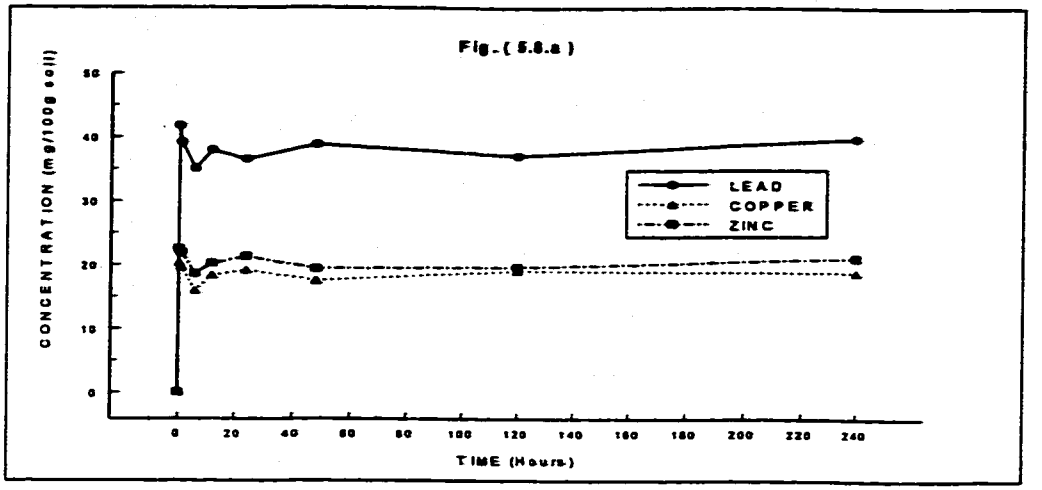

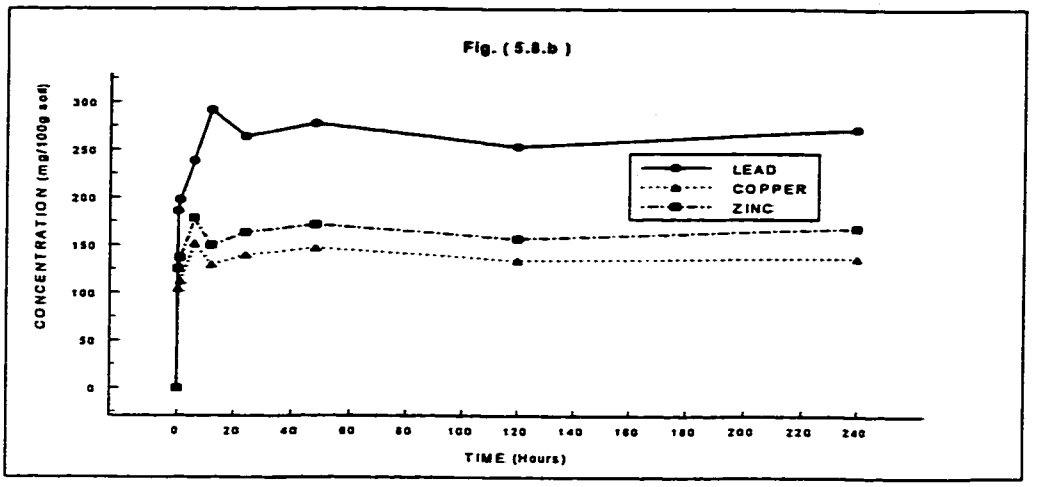

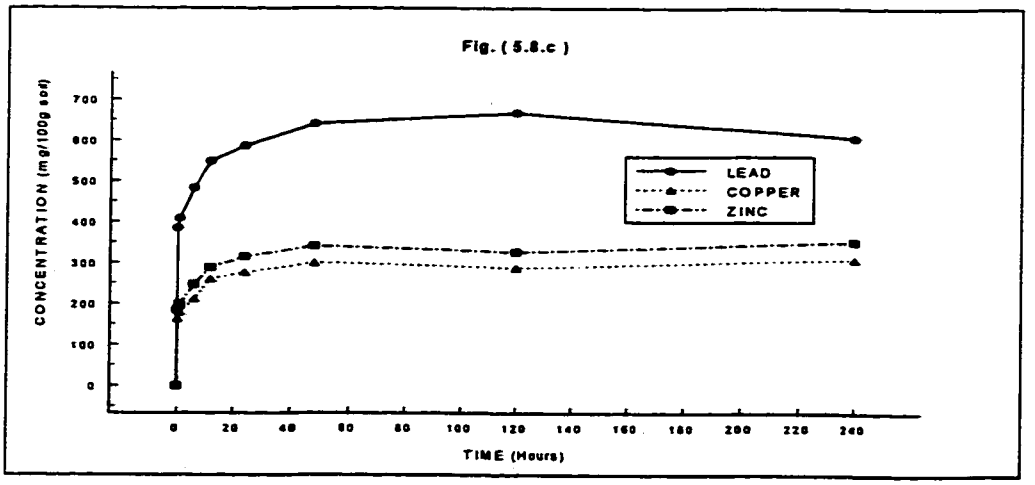

Figure 5.8 Adsorption Concentrations versus Time for Lead, Copper, and Zinc Chloride Solutions at a) 50, b) 500, and c) 2000 ppm Initial Concentrations

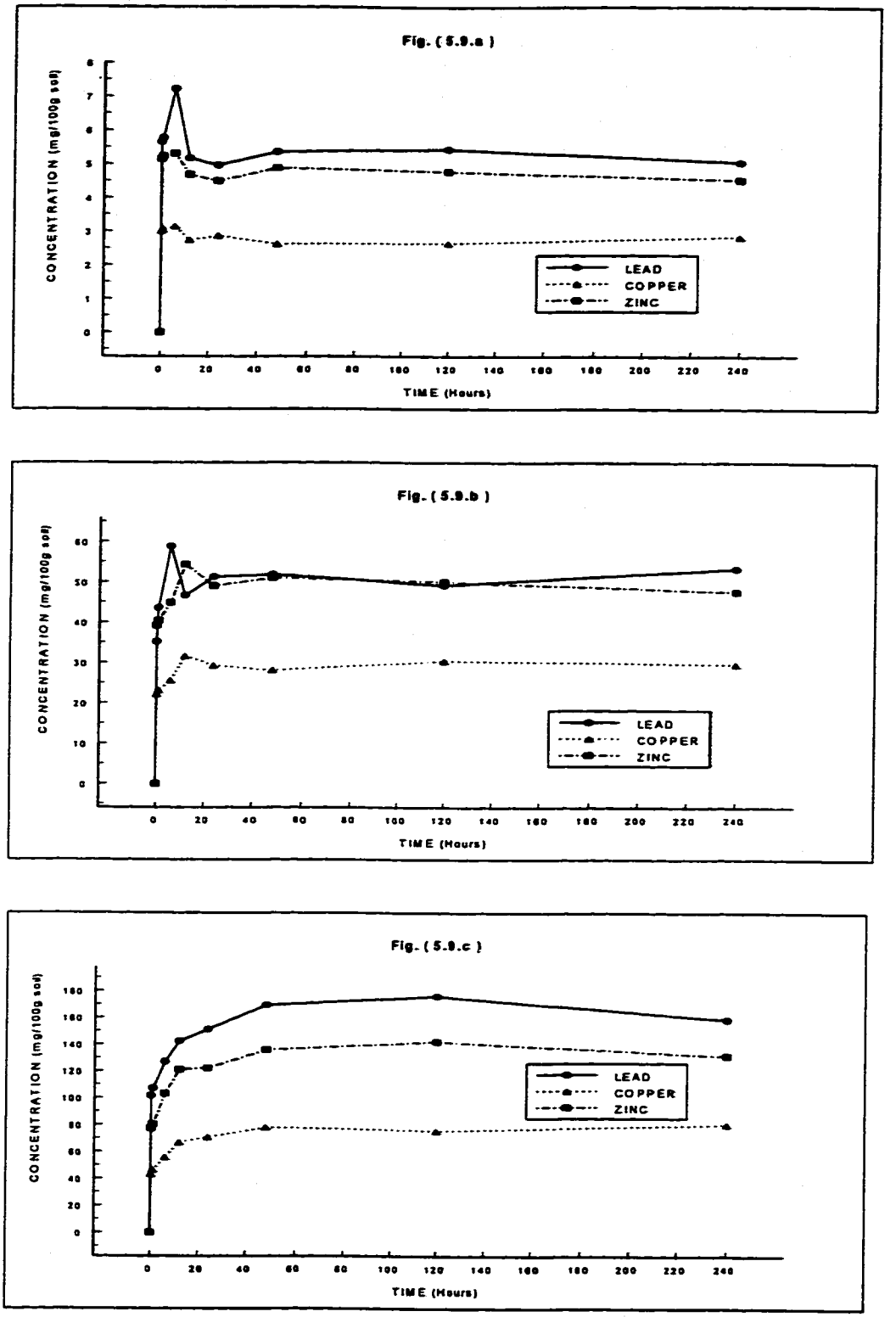

Figure 5.9 Desorption Concentrations versus Time for Lead, Copper, and Zinc Chloride Solutions at a) 50, b) 500, and c) 2000 ppm Initial Concentrations

The figures concerning desorption of the 3 heavy metals illustrate that Cu^{2+} has the lowest desorption and Pb^{2+} the highest. This is due to the fact that Cu^{2+} has the lowest ionic radius while Pb^{2+} has the highest (45% larger than Cu^{2+}). The ionic radii for Pb^{2+}, Zn^{2+}, and Cu^{2+} are about 1.19, 0.70, and 0.57 A°, respectively. If the ionic radius gets larger, the attraction force of the negative charge of SPS to the cations is reduced. Consequently, the extraction of the ion becomes easier and the desorption process is facilitated.

Adsorption and desorption variations with respect to time are depicted in figures (5.10) and (5.11), for various initial concentrations. Accordingly, as the initial concentration gets higher, the adsorbed or desorbed species concentration increases. However this relationship is not linear. The percentage of adsorbed or desorbed species decreases drastically as soon as the initial concentration of the solution gets higher. This strengthens the idea that there is a limit for adsorption or desorption capacity of the soil

Adsorption percentage rates are exhibited in Fig. (5.12) for different heavy metals. These percentages are obtained by dividing adsorption concentration by the initial concentration of the relevant solution.

On the basis of these plots, as the initial solution concentration (ISC) increases, the percentages of adsorption decreases. For instance, the adsorption percentages are about 75 and 30 for initial solution concentrations of 50 ppm and 2000 ppm, respectively (for lead chloride solution).

Even though the adsorption concentration is directly related to the ISC, the adsorption percentage has an indirect relationship with the ISC. Since adsorption capacity of soil particles are limited, the high ISC can satisfy this limit with less percentage of its initial concentration than the low ISC. However, if the ISC is very low and all contaminant species are completely available to be adsorbed, it cannot provide satisfaction of soil particles adsorption potential.

Adsorption percentages are not equal for all heavy metals. If the initial solution concentrations are between 50 ppm and 2000 ppm, adsorption percentages for copper and zinc chloride vary between 40 and 15,respectively, while these percentages are 75 to 30 for lead chloride. These results confirm that soil particles have a higher affinity to adsorb Pb^{2+} than Cu^{2+} and Zn^{2+} for reasons that have already been discussed in previous paragraphs.

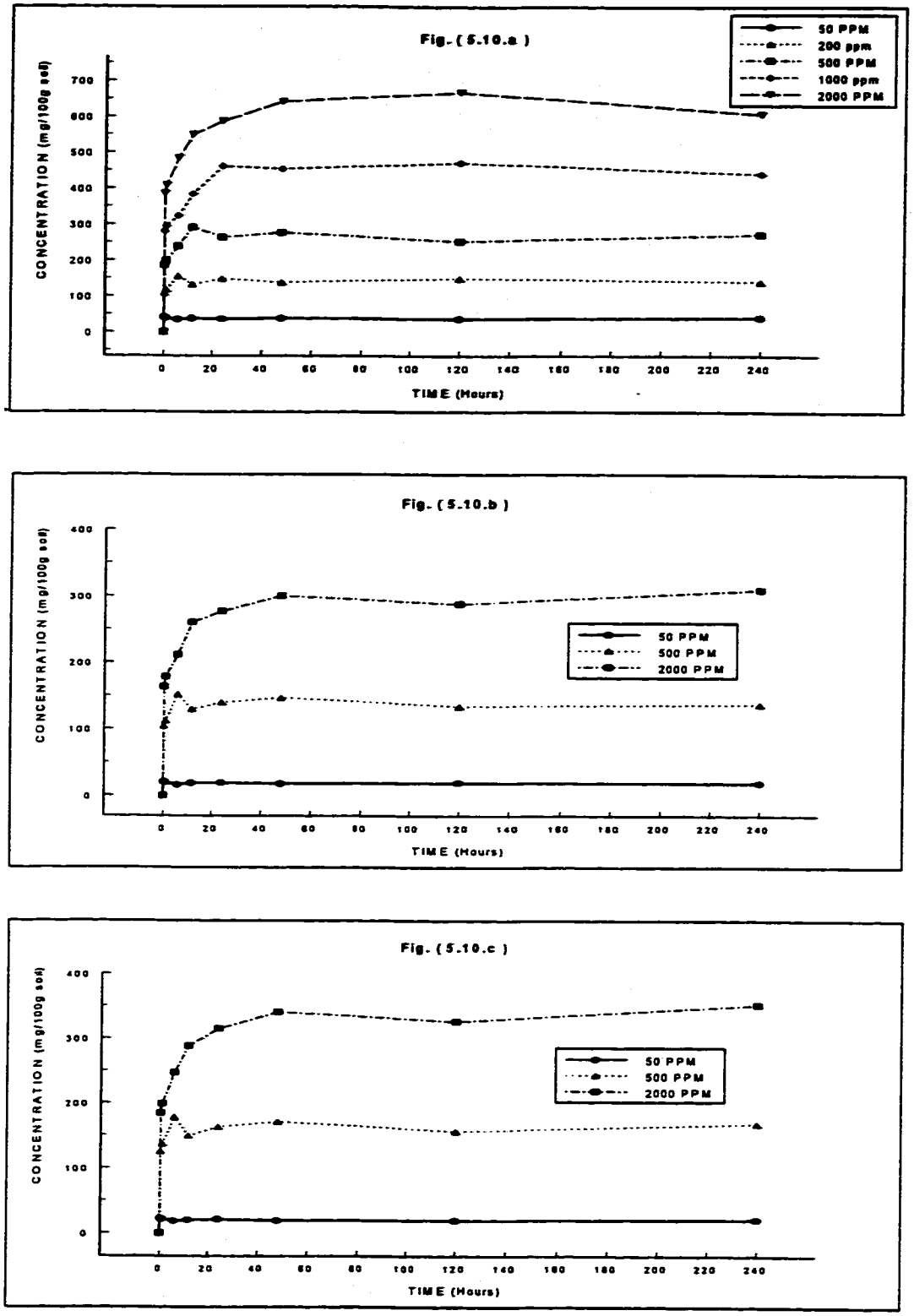

Figure 5.10 Adsorption Concentrations versus Time for a) Lead, b) Copper, and c) Zinc Chloride Solutions at 50 to 2000 ppm Initial Concentrations

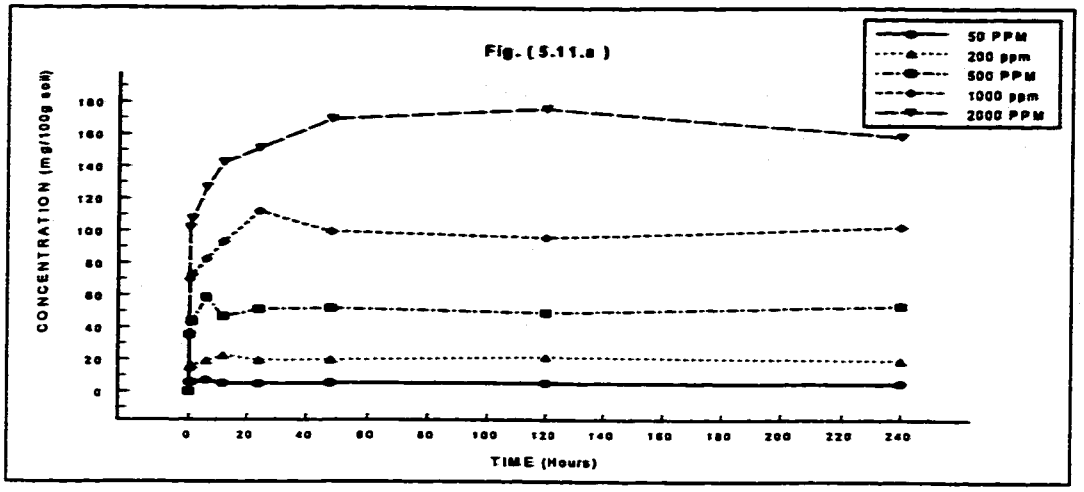

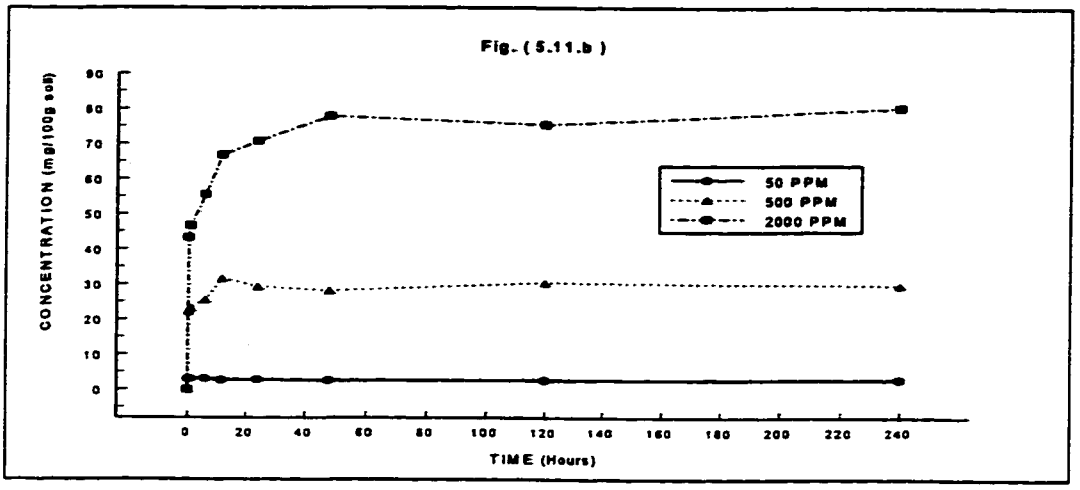

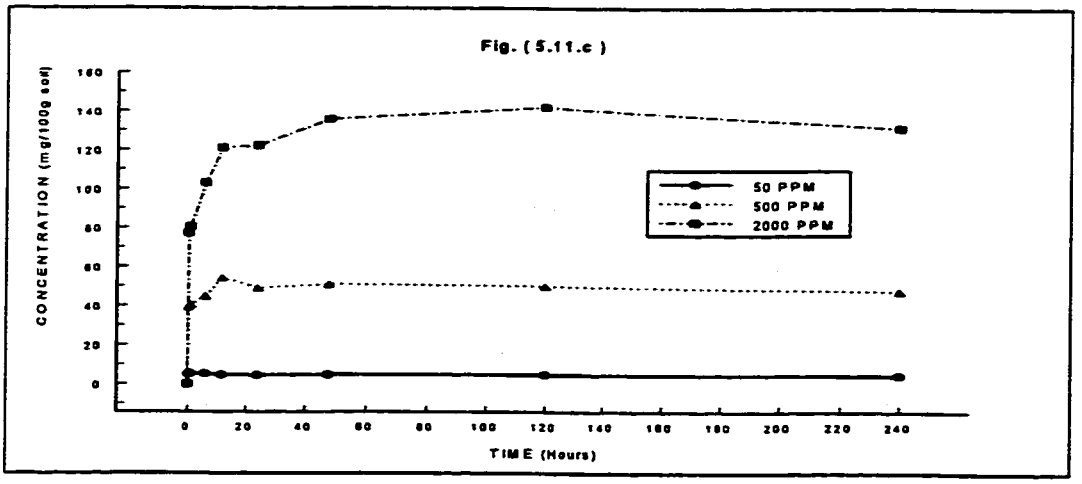

Figure 5.11 Desorption Concentrations versus Time for a) Lead, b) Copper, and c) Zinc Chloride Solutions at 50 to 2000 ppm Initial Concentrations

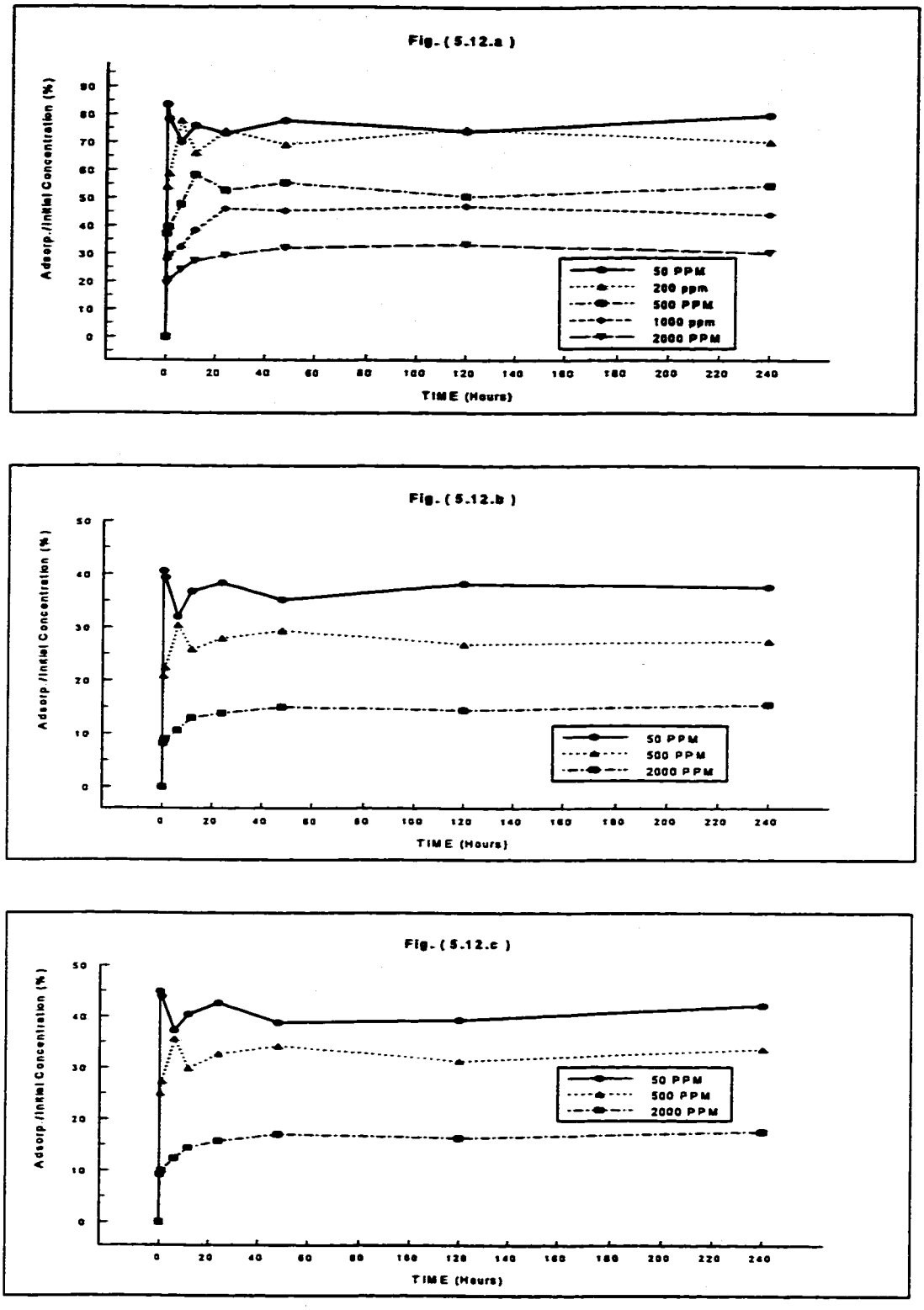

Figure 5.12 Adsorption Concentration Percentages versus Time for a) Lead, b) Copper, and c) Zinc Chloride Solutions at 50 to 2000 ppm Initial Concentrations

Contrary to the adsorption percentage rates, Fig. (5.13) shows a direct relationship between initial solution concentration ISC and desorption percentage rate. The title of the Y axis specifies that, the desorption percentages are defined as a ratio of the desorption concentration to the relevant total adsorption concentrations. The direct relationship is due to the low affinity of desorption if the adsorption concentration of soil particles are not high.

The desorption percentage varies within the range of 15 to 40 percent. These percentages are below 50% and considerably lower than (about half of) the relevant adsorption percentages. This matter stems from two facts as follows:

1) Since some contaminants species are strongly bounded to the soil particles , they are not considered exchangeable cations which could be desorbed easily. Furthermore, to desorb some parts of exchangeable cations some particular reagents are required within the soil-solution system.
2) The desorption process is conducted with distilled water (as a solution), providing a soil-solution system with pH=5.1 (greater than pH=4.0 in adsorption process). The higher pH induces higher adsorption for the soil particles, and therefore causes decrease in desorption percentages.

In order to find the rates of adsorption and desorption variations, figures (5.14) and (5.15) have been plotted. These curves in these figures may be represented by the following function:

$$C_{sorp}=a+be^{-t} \qquad (5.4)$$

where a and b are empirical parameters. The negative exponential function emphasizes the fact that the effect of time is very remarkable at the beginning of running the batch test. As time progresses, its effect becomes negligible, i.e.: the concentration of adsorption or desorption does not considerably (less than 3%) vary after a certain period of time.

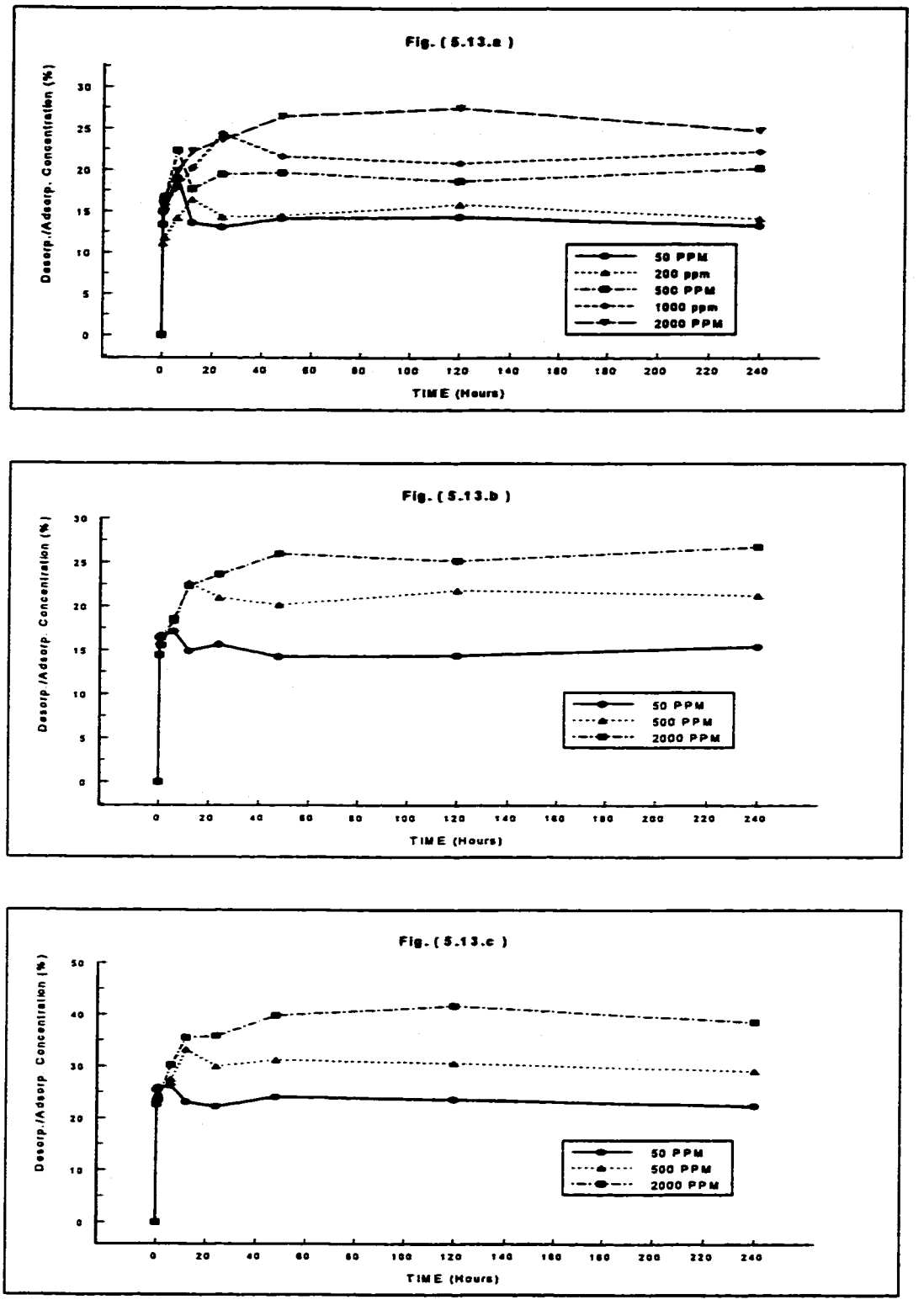

Figure 5.13 Desorption Concentration Percentages versus Time for a) Lead, b) Copper, and c) Zinc Chloride Solutions at 50 to 2000 ppm Initial Concentrations

The combined effect of time and initial solution concentration on the adsorption/desorption concentration, are shown in Fig. (5.15). The equation describing this effect is

$$s=a+be^{-t}+c\,(c_{init})^{0.5} \qquad (5.5)$$

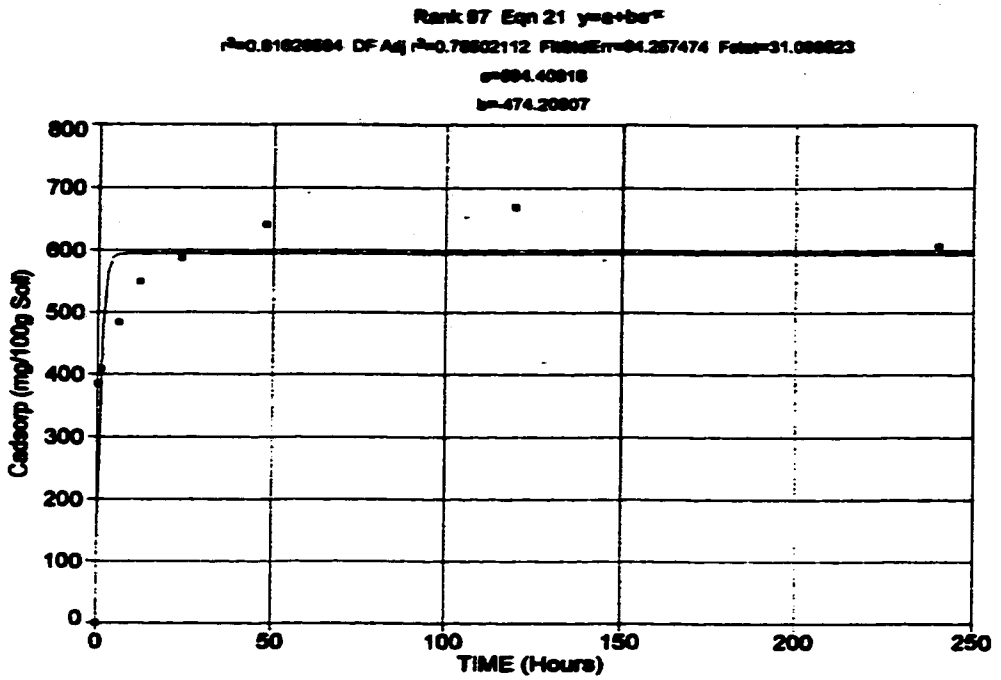

a) Adsorption

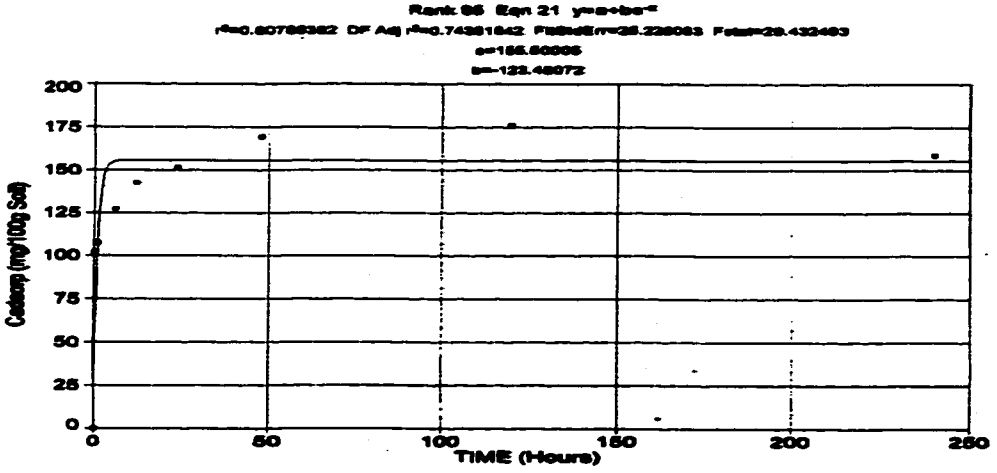

b) Desorption

Figure 5.14 The Mathematical Functions of a) Adsorption, and b) Desorption Concentrations versus Time for $PbCl_2$ Solution at 2000 ppm Initial Concentration for adsorption, and

$$s=a+be^{-t}+c(c_{init})^{0.5} \qquad (5.6)$$

for desorption processes. In these equations, t, s, and c_{init} are time, adsorption/desorption, and initial solution concentrations respectively, while a, b, and c are empirical coefficients.

The effect of time duration in Eq. (5.5) and (5.6) is diminished after a short time; therefore, adsorption/desorption concentration is predominantly governed by the initial solution concentration statement. This behavior is in complete agreement with the one understood from Fig. (5.14) and its relevant equations.

In addition, Eq. (5.5) shows the contribution of initial solution concentration ISC y, to the adsorption concentration value z, in a natural logarithmic form (ln y). Thus, the effect of ISC enhancement is reduced considerably in this equation. As a result, there would be a maximum capacity for soil particles to adsorb/desorb the contaminant species. This fact is demonstrated clearly in the Fig. (5.15.a), that over a particular ISC the curvature of the function surface will be reduced and it becomes close to a plane parallel to the initial concentration axis y.

Eq. (5.6) indicates a considerable disagreement between adsorption and desorption. Despite the adsorption process, the rate of desorption is directly related to the initial (adsorbed) concentration (IAC). The higher the IAC, the higher the desorption. This matter stems from the higher affinity of the soil particles, when the IAC is higher, especially when the IAC is close to the maximum capacity level of the soil particles.

Also, in contrast to the adsorption process, there is no limit for the desorption concentration, as far as the IAC increases. The only limitation comes from the ISC, when it does not have the capability of dissolving more contaminants species in itself. However, it should be remembered, that the IAC is not a limitless value. There is a limit for the desorption concentration, which is equal to the maximum adsorption concentration of the soil particles.

As a result, the nature of the processes are basically in good agreement with the Langmuir adsorption model, even though it does not correlate with the proposed model exactly.

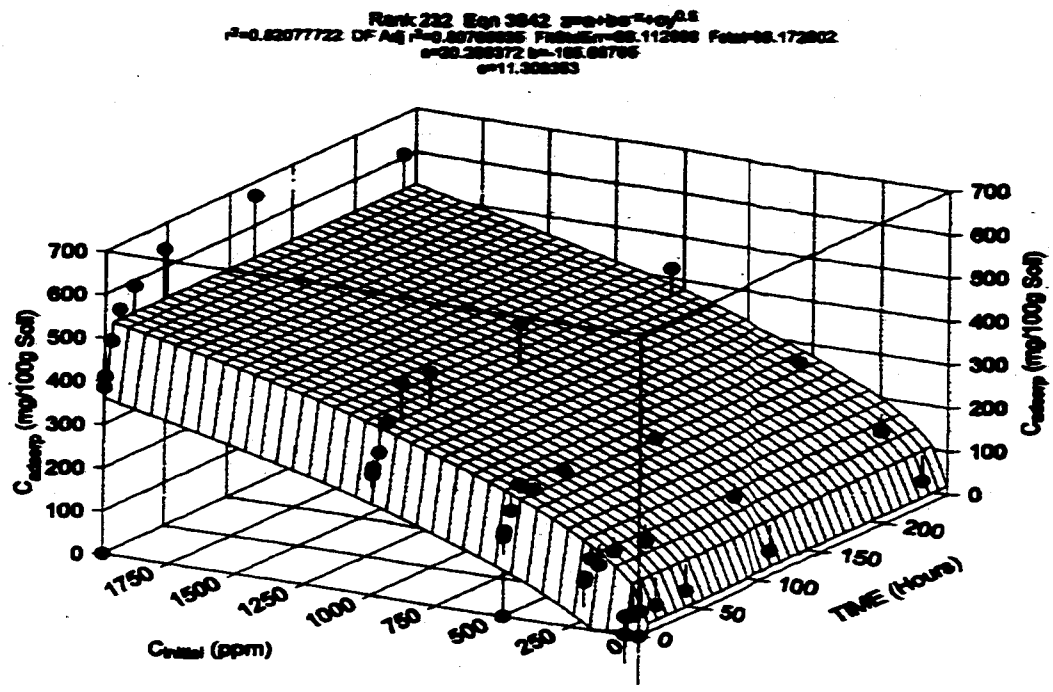

a) Adsorption

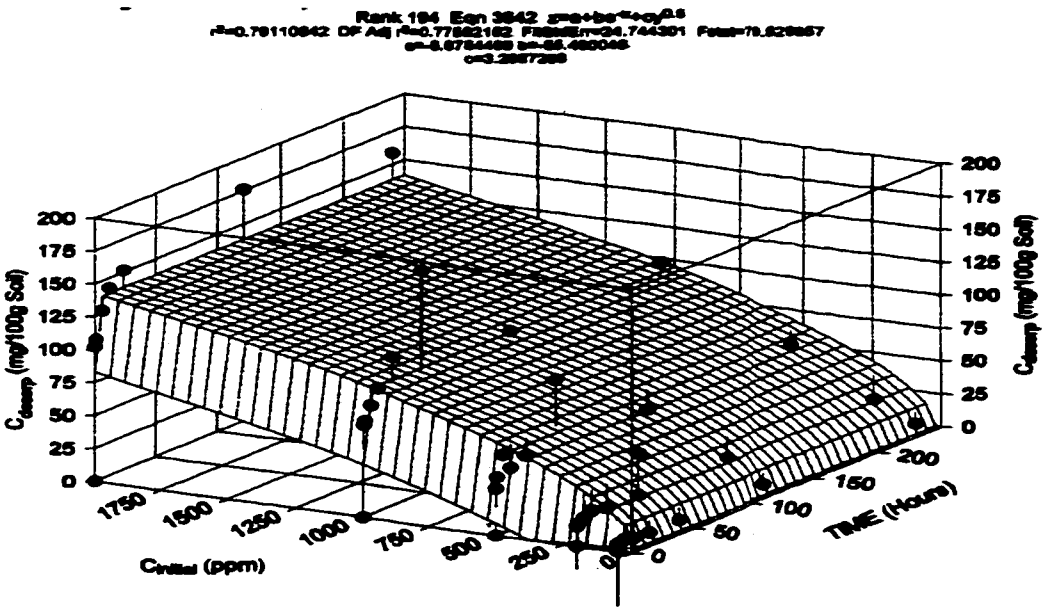

b) Desorption

Figure 5.15 The Mathematical Functions of a) Adsorption, and b) Desorption Concentrations versus Time and Initial Concentration for $PbCl_2$ Solution

5.6 SEQUENTIAL EXTRACTION RESULTS AND DISCUSSION

The procedure of selective dissolution for the study of heavy metals retention in soils has been discussed in the preceding chapter. In this experiment, the sequential extraction was used in order to obtain information on the amounts and forms of heavy metals that were retained in the soil samples. The results of the experiments will help to understand the retention mechanisms of heavy metals within the soil.

As it has been explained in section 4.4.2 of chapter 4, the forms of heavy metals retained in soils at various conditions are different. For instance, heavy metals may retain in soils in the forms of *i*) oxides and hydroxides, *ii*) carbonates, *iii*) exchangeable cations, and *iv*) bound to organic matter, depending on the soil constituents and conditions. These forms of heavy metals can be extracted selectively by using appropriate reagents.

On one hand, the soil under consideration has neither carbonate, nor organic matter, but it contains oxides and hydroxide components. Thus, there is no need to do any investigation regarding the two aforementioned components among different forms of the retained heavy metals.

On the other hand, since the study is mainly concerned with the contamination and decontamination of the soil, what really matters is the amount of the exchangeable cations which may be removed from the soil particles. The other components are all un-exchangeble; therefore there is no need to distinguish among all components of the residue.

Accordingly, the sequential extraction in this study includes two major parts: *i*) extraction of exchangeable cations, which were retained in soil by cation exchange mechanism, *ii*) extraction of the entire residue (including oxides and hydroxides components) through a digestion process. The second part includes the heavy metals that are retained by other kinds of mechanisms, such as specific adsorption in the soil mineral lattice. The first part contains two stages: *i*) extraction of exchangeable cations without utilizing any reagent, which has been discussed as a desorption process in this study (section 5.5), and *ii*)extraction of exchangeable cations by means of appropriate reagent.

The following sub-sections are concerned with part I of the second stage, paying attention to the second part of the sequential extraction. Both of these procedures have been followed for the entire samples (54 samples) obtained from the desorption process.

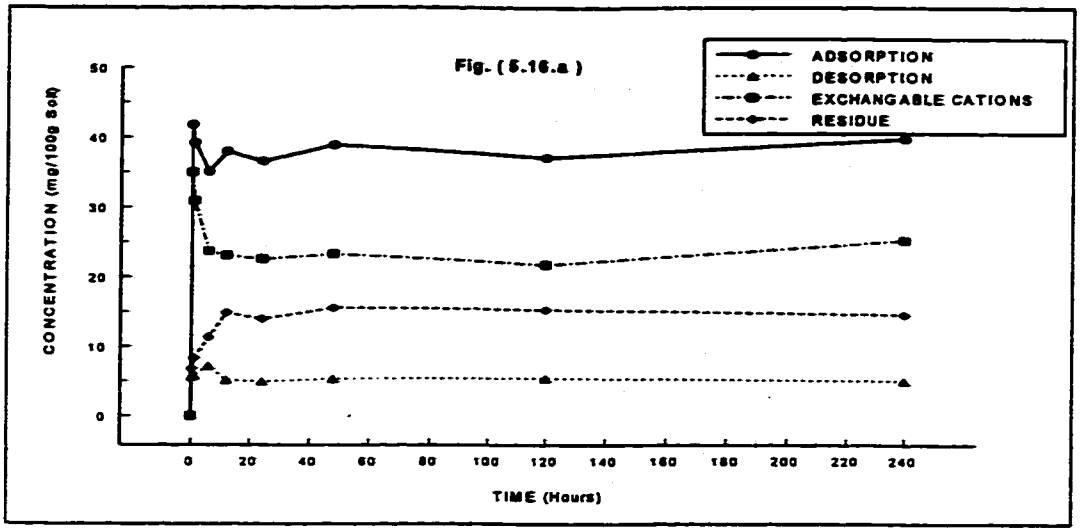

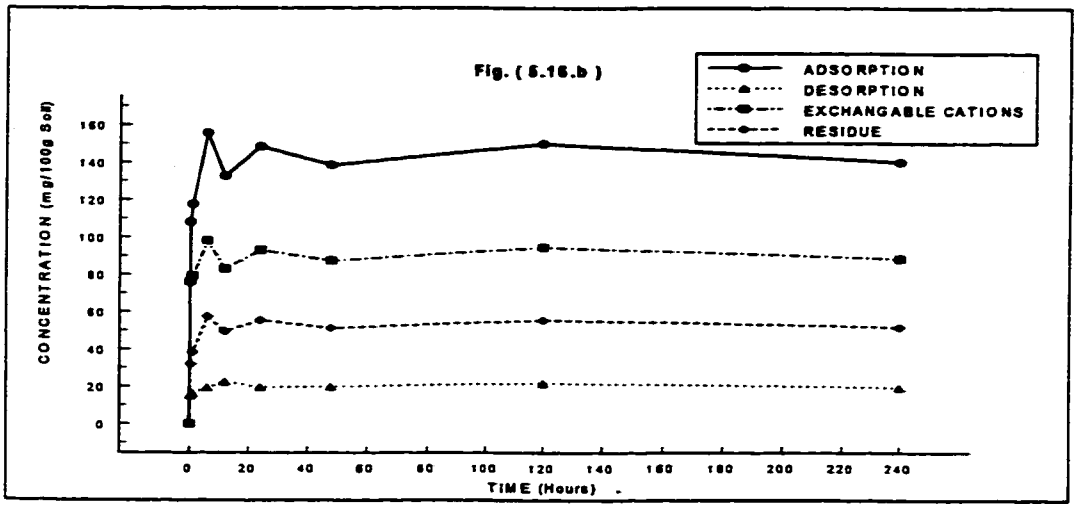

Figure 5.16 Variations of Sequential Extraction Components Rates for $PbCl_2$ Solutions at a) 50, and b) 200 ppm Initial Concentrations

5.6.1 Results of Sequential Extraction Experiments

The amount of heavy metals retained in different phases are plotted as shown in figures (5.16) to (5.18), for 3 different heavy metals (Pb, Cu, Zn). For each heavy metal, various concentrations have been selected; i.e., lead 50, 200, 500, 1000, and 2000 ppm, copper and zinc 50, 500, and 2000 ppm. Fig. (5.16) shows the amount of lead retained by different phases for various initial concentrations of the solution, whereas Fig. (5.17) presents the amount of zinc retained by different phases at various soil solution

concentrations. The variations for retention of copper on the soil particles at 3 different solution concentrations by different phases are plotted in Fig. (5.18).

5.6.2 Sequential Extraction Analysis

It can be observed from the aforementioned figures that the variations of various phases have 2 major parts, similar to the batch tests results. Since the 3 sequential extraction phases are components of the total adsorption process, it is rational to expect this similarity.

In addition, the retention of heavy metals in soils would change, according to the difference in speciation of heavy metals. As the soil solution pH is constant for the entire experiments (pH=4.0), the variations of the phases follow the same trend. According to the above figures, the exchangeable cations phase dominates the total adsorption , resulting in a low pH value ($pH \leq 4.0$). However, the amount of residue is also considerable, indicating that the amount of adsorption in forms of hydroxides and oxides are not negligible.

Paying attention to the desorption phase, the amount of this phase is very low compared to the other phases. The desorption phase determines the amount of adsorbed species which can be extracted from the soil particles surfaces without utilizing any kind of reagent. The desolution of the species regarding this phase is just exerted from the very low concentration of the solution surrounding the soil particles. This fact expresses that the adsorption of heavy metals species to the clay soil particles is attributed to strong forces, mostly exerted from chemical reactions between them.

It can be observed from Fig. (5.16) that the amount of lead retained as residue phase increases as the initial concentration of the solution increases. However, there is a limit to this enhancement, which is a function of soil capacity to combine with the heavy metals species, and the availability of the free surfaces of the soil particles. The more adsorbed species, the less power for the soil particles to attract and the less affinity of soil particles to react with the other species of heavy metals.

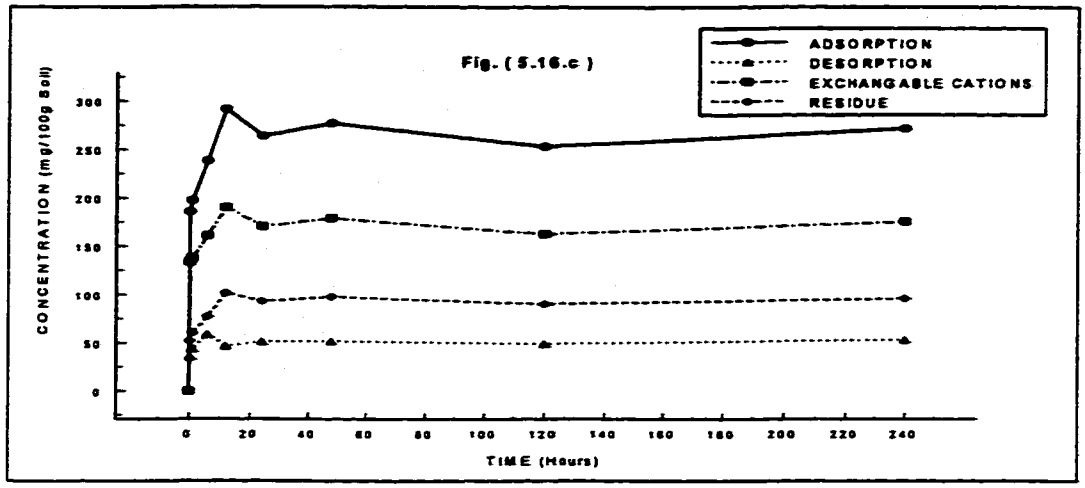

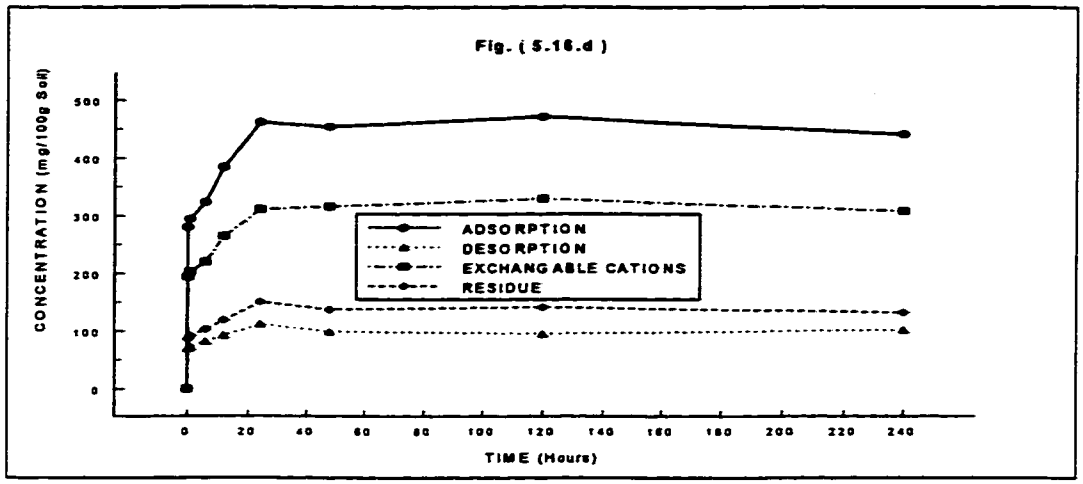

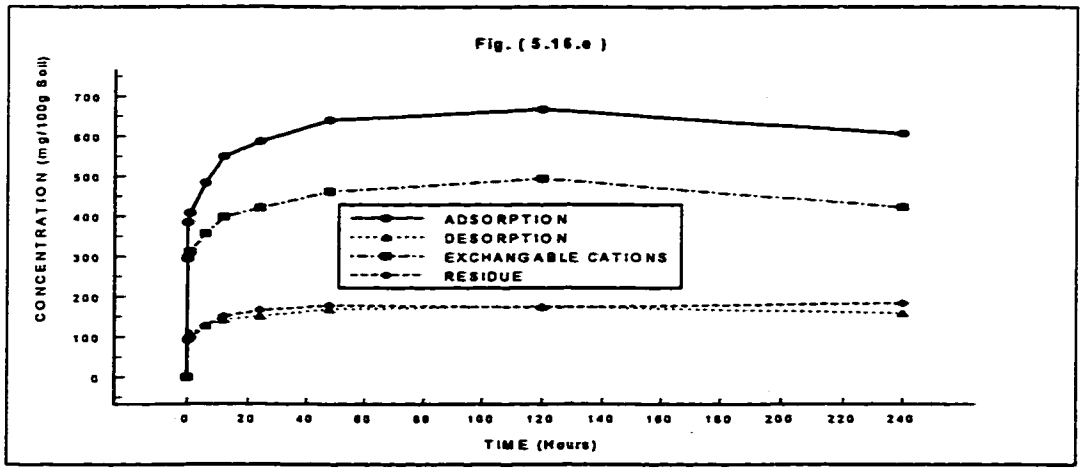

Figure 5.16 (Continued) Variations of Sequential Extraction Components Rates for $PbCl_2$ Solutions at c) 500, d) 1000, and e) 2000 ppm Initial Concentrations

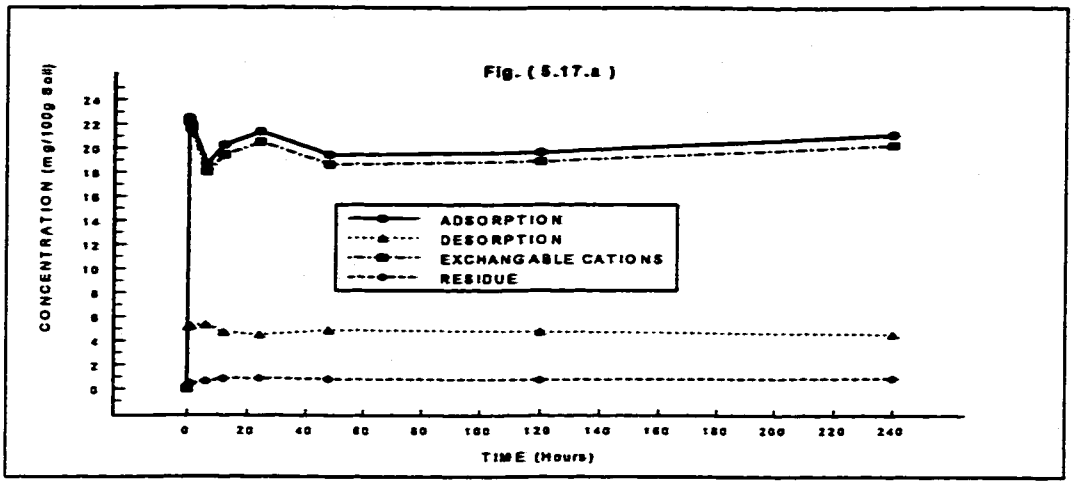

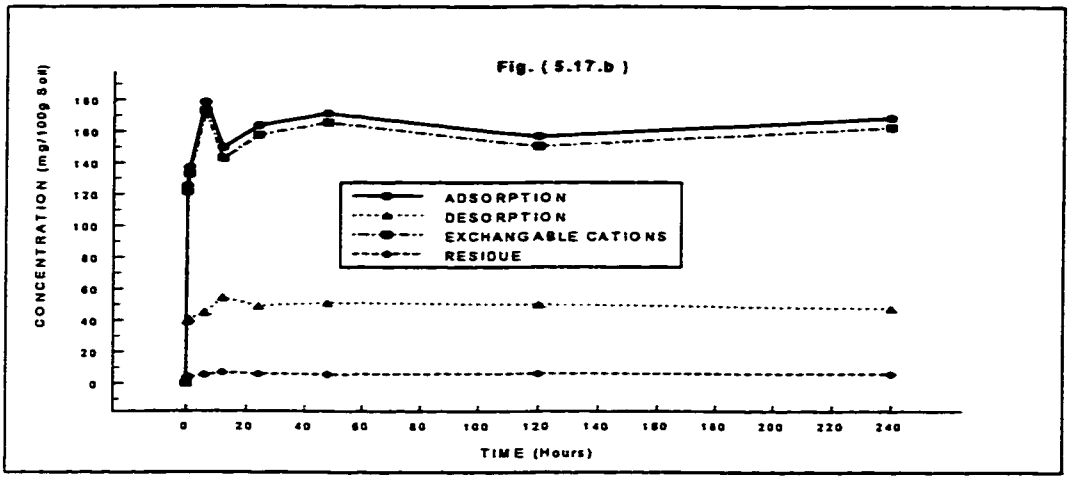

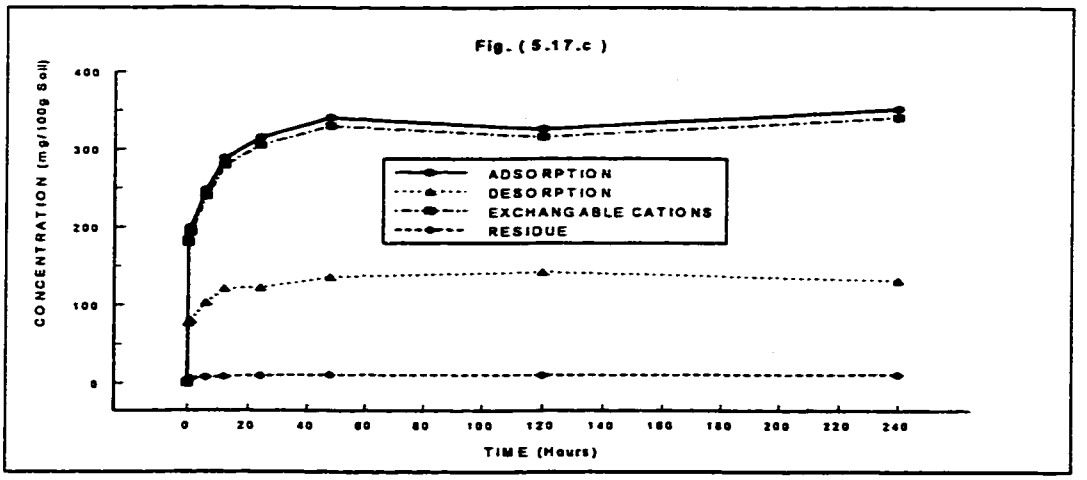

Figure 5.17 Variations of Sequential Extraction Components Rates for $ZnCl_2$ Solutions at a) 50, b) 500, c) 2000 ppm Initial Concentrations

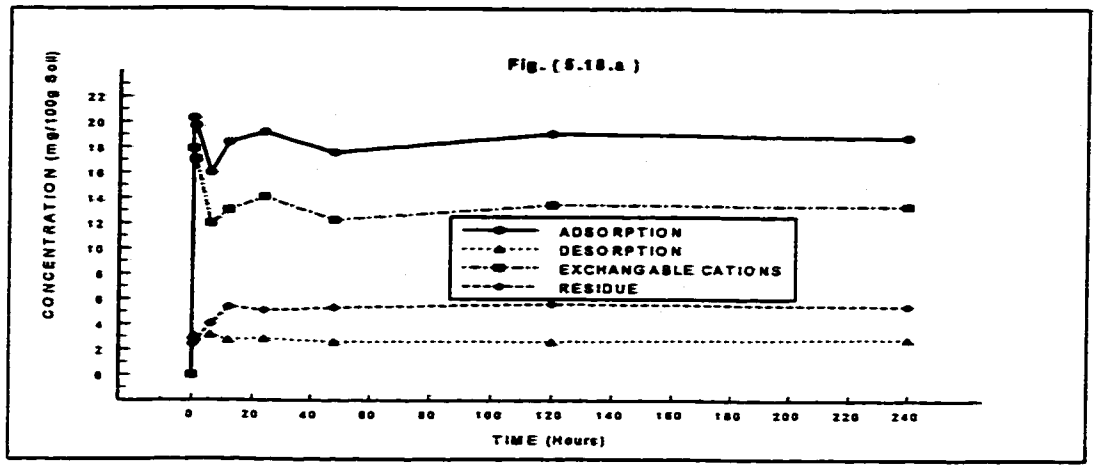

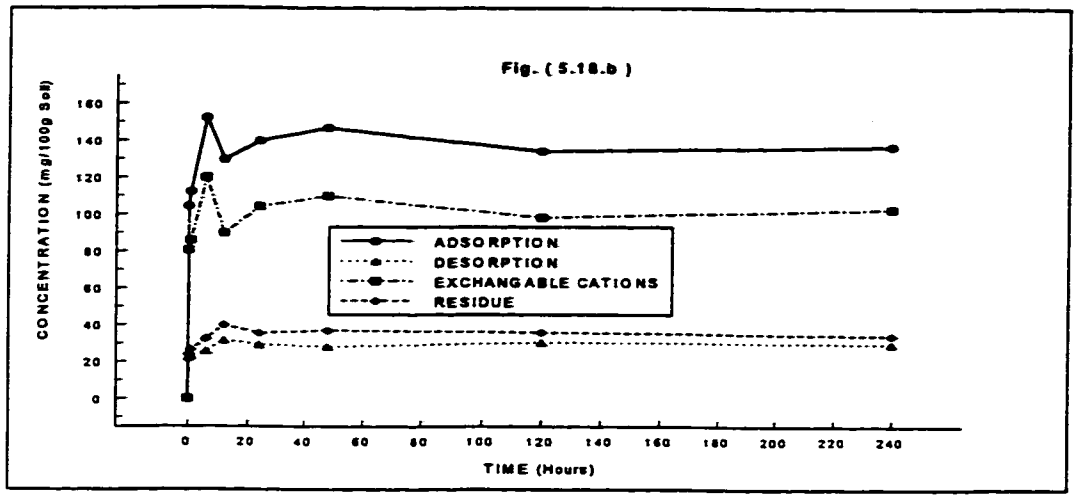

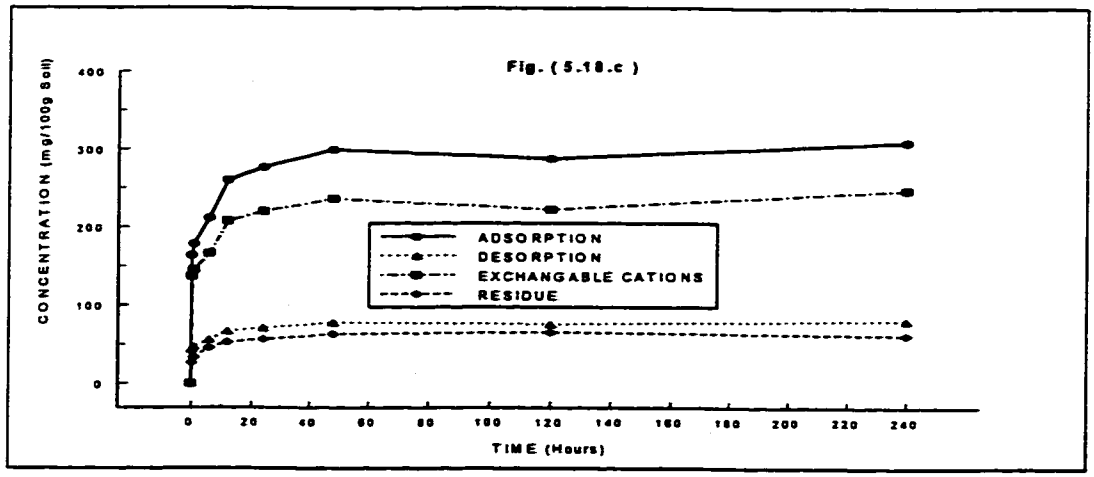

Figure 5.18 Variations of Sequential Extraction Components Rates for $CuCl_2$ Solutions at a) 50, b) 500, and c) 2000 ppm Initial Concentrations

Accordingly, the variations range of the residue phase reduces considerably with respect to the enhancement of the initial concentration of the solution (c_{init}). For instance, the amount of residue phase, varies from 15 to 150 (mg/100g soil), while c_{init} changes from 50 to 1000 ppm. Furthermore, there are no remarkable changes between the amount of residue phase for initial solution concentrations at 1000 and 2000 ppm.

The amount of residue phase on the soil particles surfaces increases as the pH of the solution reaches a high value (above 4.0). However, as the pH of the solution is low, only the exchangeable phase dominates, resulting in fewer total heavy metals being retained on the surfaces of the soil particles.

When the pH of the solution is high, a higher percentage of metals is precipitated and hydroxy species are formed, especially for lead and copper. This enhances the retention of heavy metals in the soil as hydroxide phase and therefore, the amount of residue phase increases. However, in this study, a low pH value has helped to have a low amount of the residue phase compared to the exchangeable cations phase. This is due to the change in heavy metals speciation as the soil solution pH changes. Since, at a low pH value heavy metals species are present in the solution as free cations, the retention mechanism of heavy metals in the soil is mostly by cation exchange rather than residue phase.

Comparing the amount of residue phase (RES) of 3 heavy metals at the same c_{init}, figures (5.16) to (5.18) reveal that the amount of RES for lead is about 2.6 times higher than copper. However, this amount is negligible for zinc solution. This difference stems from the difference of the affinity of various heavy metals, in combining with the oxygen of the soil particles and forming the oxides and hydroxides of the heavy metals on the soil particles surface. Among the 3 heavy metals, lead has the highest affinity for these reactions, while zinc has the lowest.

The enhancement of the exchangeable cations phase is not exactly proportional to the enhancement of the initial concentration of the solution. For example, in Figures (5.16.c) and (5.16.e) c_{init} varies from 1000 to 2000 ppm, (2 times more concentrated solution), while the amount of exchangeable cations phase (EXC) changes from 330 to 420 (mg/100g soil), (less than 30% increase).

Even though there are some heavy metals species in the medium, the amount of EXC cannot go beyond a certain limit. This is due to limited surfaces of the soil particles (SSP) which have the ability to attract the contaminant species. This tendency reduces as they attract more species to themselves. Since the EXC phase is the dominant phase in the adsorption process, this correlation strengthens the idea that there is a limit for the number of species that the soil particles surfaces can adsorb. The aforementioned correlation has been found for the other heavy metals (Cu, and Zn), as well (figures 5.17 and 5.18).

In order to understand the percentage of desorption phase with respect to the exchangeable cations phase, this value is plotted for lead , copper, and zinc in Fig. (5.19) at 50, 500, and 2000 ppm initial solution concentration. The percentage varies from 0.2 to 0.45 for the 3 heavy metals, where the range of variations for lead and copper is (0.2-0.35), and for zinc is (0.25-0.45).

Even though there is a small difference among the 3 heavy metals, the percentages of desorption are very low. Since, the heavy metals cations are exchanged with the other cations on the soil particles surfaces (SPS) and they are held strongly on the SPS, dissolution of heavy metals ions from the soil particle surfaces into the solution does not happen easily. In other words, this process needs some reagents within the solution to conduct the system towards the dissolution of heavy metals from the soil particle surfaces.

Fig. (5.20) compares the 3 heavy metals, corresponding to the percentage of the desorption phase with respect to the exchangeable cations phase at 500 ppm solution concentration. Even though the percentages for zinc is slightly higher, one can assume that the percentages are the same for lead, copper, and zinc solutions. This could be due to the fact that at a low pH, and particularly for kaolinite clay soil, the cations of the solution are very well exchanged, and they are held in a stable and strong combination within the soil particles.

Having 3 different solution concentrations (50, 500, and 2000 ppm) for the 3 heavy metals, Fig. (5.21) illustrates the variations of percentage of exchangeable cations (EXC) with respect to the total adsorption. The percentage falls within the range of

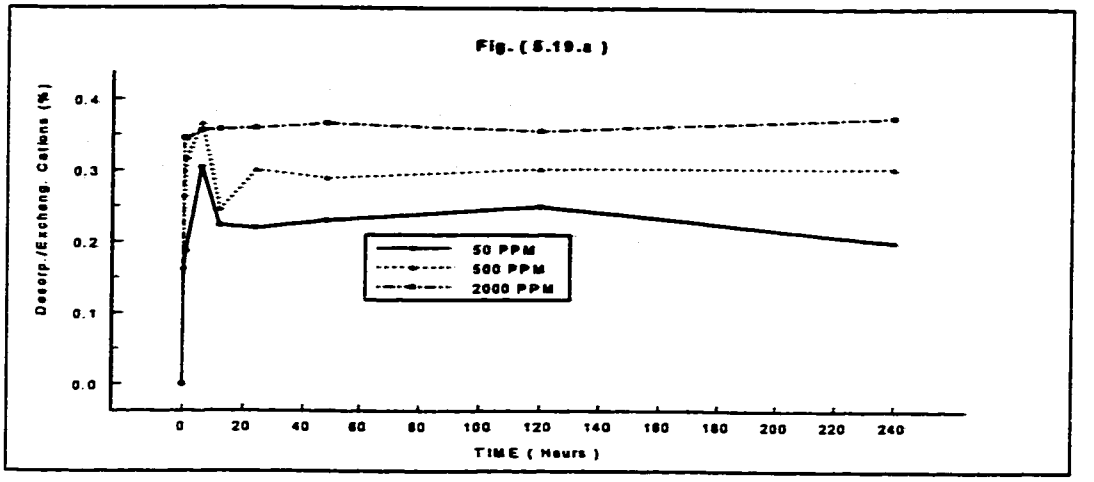

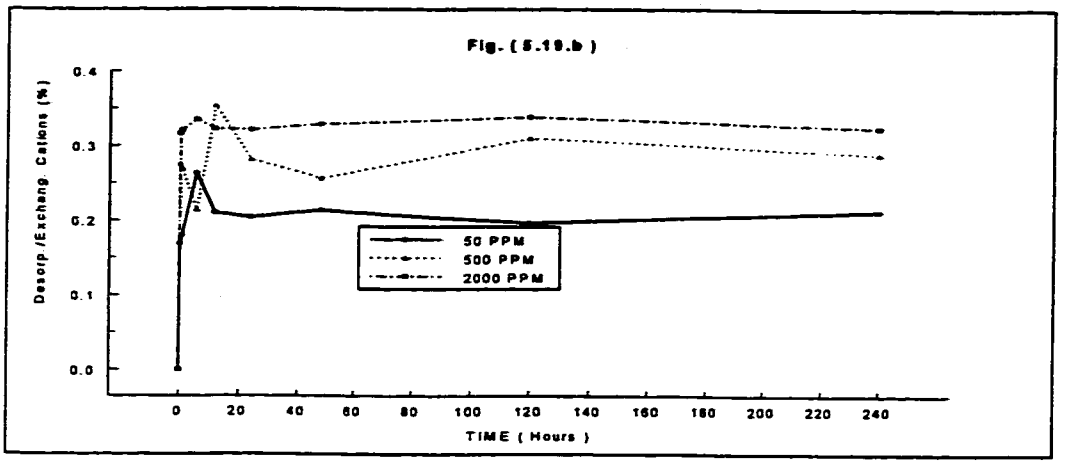

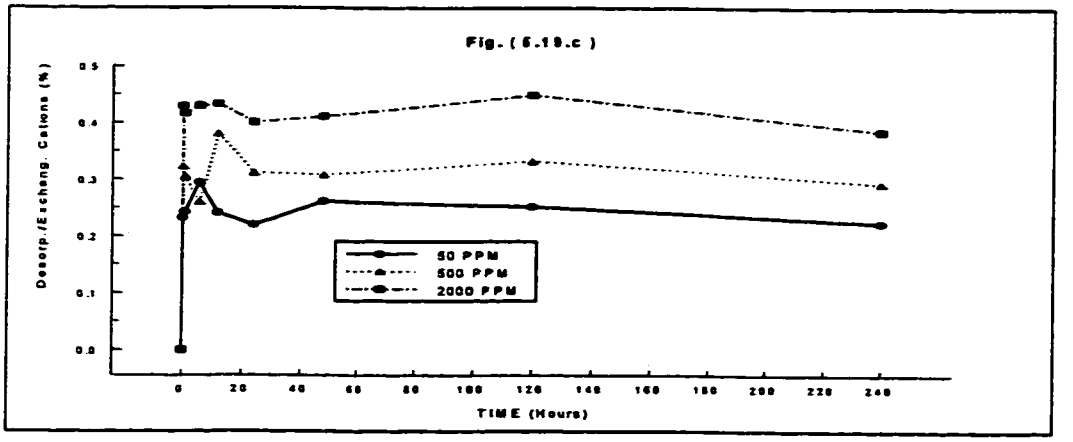

Figure 5.19 Variations of Desorption Percentage Rates for a) $PbCl_2$, b) $CuCl_2$, and c) $ZnCl_2$ Solutions at 50, 500, and 2000 ppm Initial Concentrations

(60-96)%, which is different for each heavy metal. The lead percentage varies from 60 to 75 percent which is the lowest range, whereas copper percentage variation range is from 70 to 80 percent. Zinc percentage does not change remarkably, and it is about 96% for the 3 aforementioned concentrations.

Since, the total amount of adsorption is obtained by adding the amount of the residue phase to the exchangeable cations phase. The 2 latter amounts are inversely proportional. Due to this fact, lead which has the highest amount of residue, has the least amount of exchangeable cations (EXC). Zinc has the least amount of residue and the highest amount of EXC.

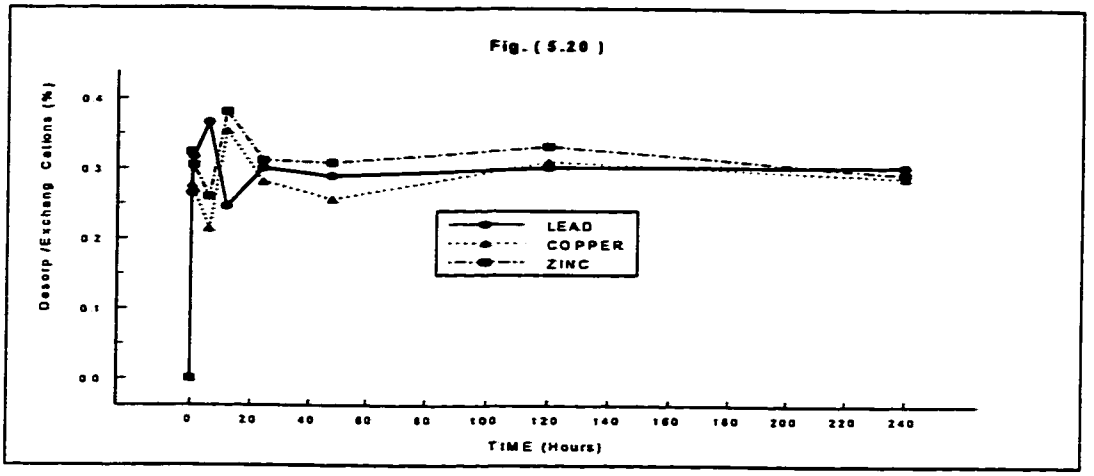

Figure 5.20 Comparison of Desorption Rates for $PbCl_2$, $CuCl_2$, and $ZnCl_2$ Solutions at 500 ppm Initial Concentration

As the initial concentration of the solution increases, the amount of exchangeable cations (EXC) increases. Likewise, when the initial solution concentration decreases, so does the amount of EXC. This could be due to the fact that higher c_{init} provides more availability of cations for the soil particles, and therefore, it provides more possibility for the soil particles to attract the cations and react chemically with them.

It can be observed from Figure (5.22) that for the solution with initial concentration of 500 ppm there is a considerable difference (about 26%) between zinc and the other 2

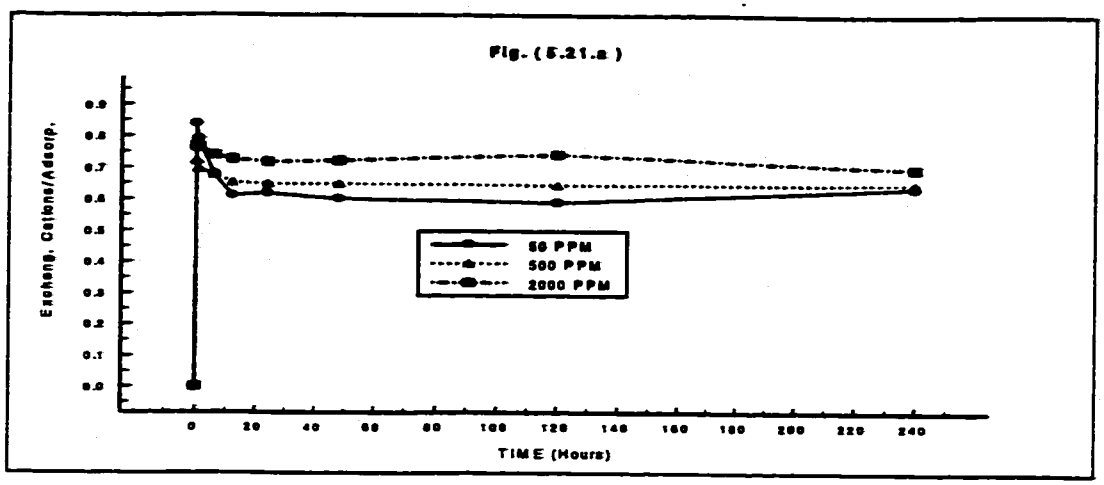

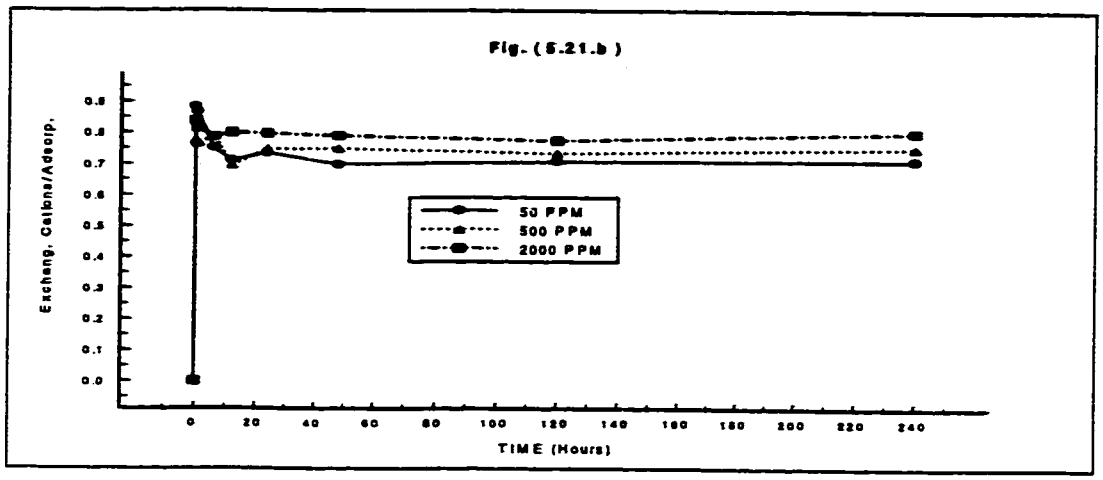

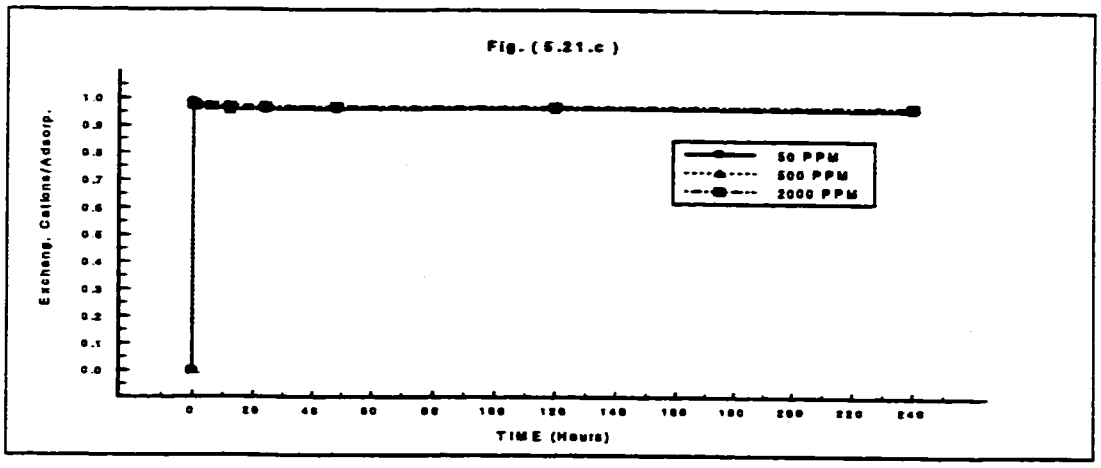

Figure 5.21 Variations of Exchangeable Cations Percentage Rates for a) $PbCl_2$, b) $CuCl_2$, and c) $ZnCl_2$ Solutions at 50, 500, and 2000 ppm Initial Concentrations

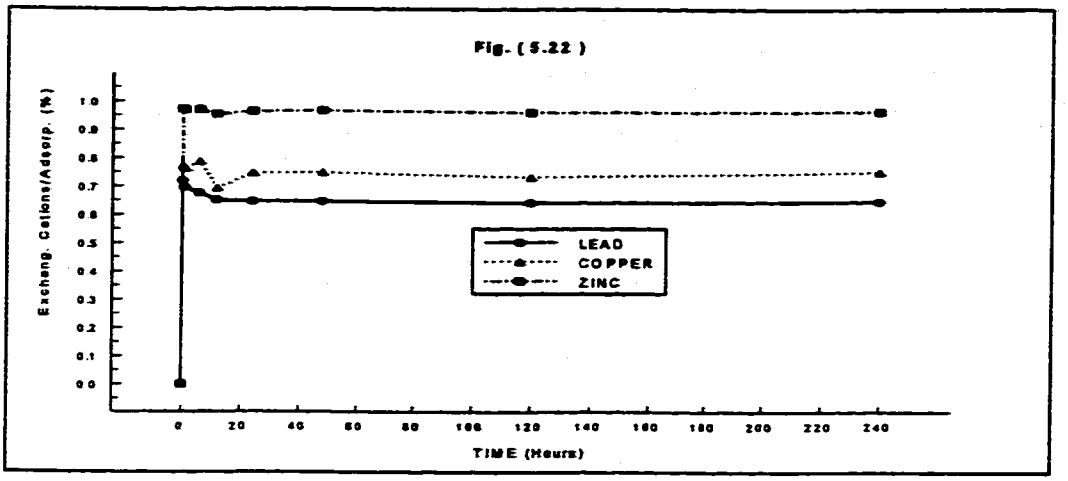

Figure 5.22 Comparison of Exchangeable Cations Percentage Rates for $PbCl_2$, $CuCl_2$, and $ZnCl_2$ Solutions at 500 ppm Initial Concentration

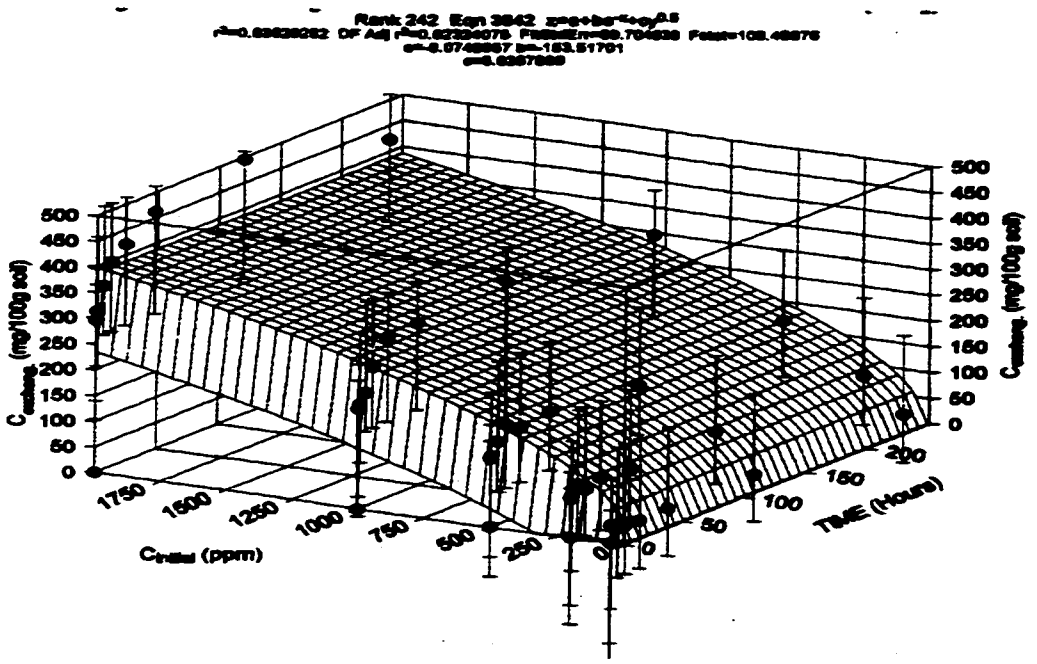

Figure 5.23 Exchangeable Cations Concentrations Variations as a Function of Time Intervals and Solution Initial Concentrations

heavy metals regarding the percentage of exchangeable cations. The percentages are 65, 75, and 96 for lead, copper, and zinc, respectively. The differences among these metals stems from the differences of their amounts of residue phase, which have reverse effects

on the amounts of exchangeable cations.

In order to have the effect of time (t) and initial concentration of the solution (c_{init}) on the EXC, a 3 dimensional plot is presented in Fig. (5.23). In this figure, the amount of exchangeable cations is introduced as a function of t and c_{init} as follows:

$$z=a+be^{-t}+cc_{init}^{0.5} \tag{5.7}$$

where z denotes the amount of exchangeable cations. This figure reveals that the effect of time interval is remarkable at the beginning of the test, and after a very short time the variation of exchangeable cations is negligible.

On the other hand, as long as the initial concentration of the solution does not reach high levels of concentration, (e.g.: less than 4000 ppm, according to the Fig. 5.23), the amount of EXC varies considerably. However, when the c_{init} exceeds 4000 ppm, the curve will be very smooth and the variation small. This is because there is a limit for the soil particles to exchange their cations with those dissolved within the solution.

The results obtained from the sequential extraction analysis can be summarized as follows:

1) The clay soils can retain heavy metals by several means, such as exchangeable cations, hydroxide, and oxide phases. However, the retention of heavy metals in any phase depends on soil constituents, soil solution pH, and heavy metals themselves. Kaolinite cannot considerably retain the metals by the hydroxide and oxide phases, because of its low initial pH.
2) The amount of zinc retained in the soils by the residue phase is less than that of lead and copper, because of differences in speciation. Furthermore, since the soil solution pH is low, retention of heavy metals by the cation exchange mechanism dominates when compared to other adsorption process mechanisms.
3) The results of the sequential extraction analysis support the idea that the soil buffer capacity in relation to heavy metals is significant. However, kaolinite could not retain high amounts of heavy metals, because the soil cannot support the retention by precipitation phases due to kaolinite low initial pH and low buffer capacity.

In conclusion, the results of the sequential extraction investigations reveal several significant points about the soil buffer capacity and its relation to the capacity of the soil to retain heavy metals.

In order to find the correlation of these findings with heavy metal migration in land disposal sites, a few soil column leaching tests were conducted. This study is presented in the next section, which provides the results of heavy metal movement along the soil column that is attributed to different forms of retention on the soil particles.

5.7 RESULTS OF UNSATURATED SOIL COLUMN LEACHING TESTS AND DISCUSSION

The soil column tests were conducted to study the relation of the soil buffer capacity to contaminant migration, when a soil column receives a leachate from any contamination source. Similar to the moisture movement, the migration of heavy metal solutions was monitored throughout the experiment's performance along the soil column.

Subsequently, the adsorption of the heavy metals species to the soil particles, along with the concentration of the solution, has been analyzed with respect to time and depth of the soil column. The results of these experiments were also used to find the adsorption function for partially saturated media and calibrate the numerical model of this phenomenon.

5.7.1 Results of the Tests

According to section 4.4.3 of the previous chapter, the soil columns were leached with 3 heavy metal solutions (lead, copper, and zinc chloride) with an initial concentration of 2000 ppm. This concentration is the same as one of the concentrations which were used for the sequential extraction tests.

In order to find the mechanism of contaminant migration within the soil medium, the concentration of the heavy metals was measured along the soil column from the top

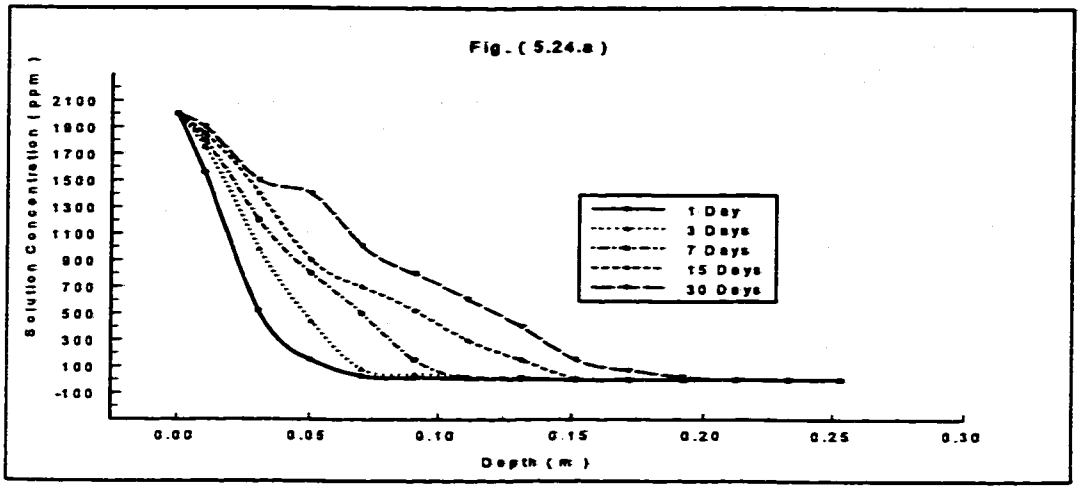

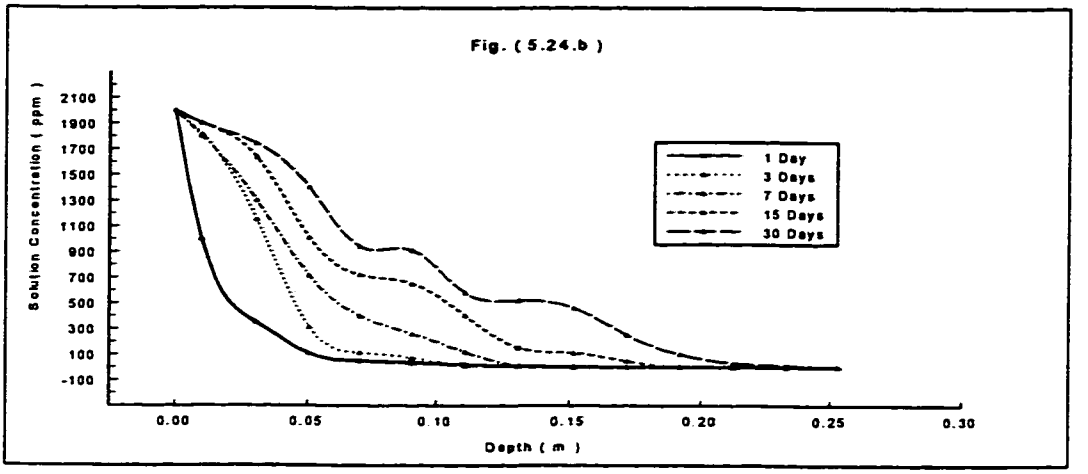

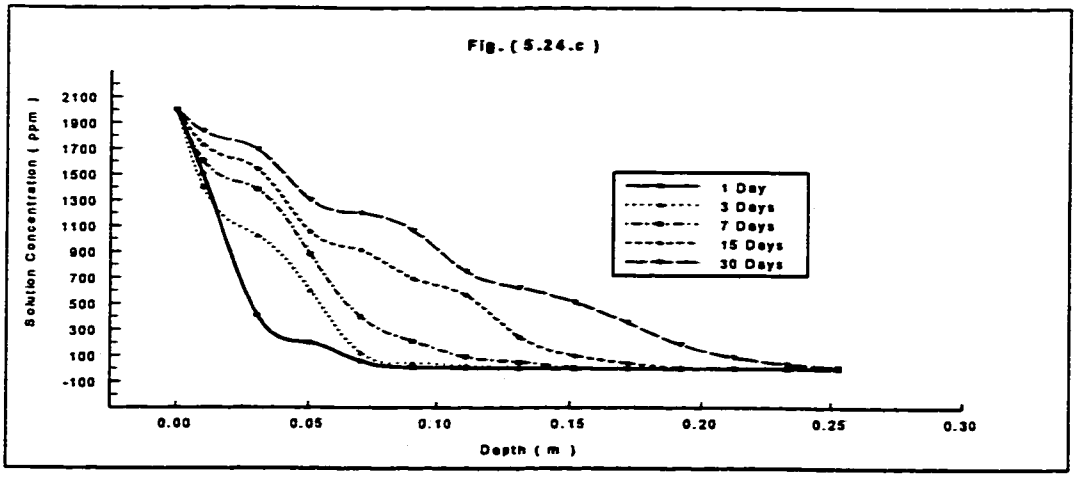

Figure 5.24 Solution Concentration-Depth Relationship for a) $PbCl_2$, b) $ZnCl_2$, and c) $CuCl_2$ Solutions along the Soil Column

to the bottom. These measurements were done at 5 different time intervals (1, 3, 7, 15, and 30 days) for the 3 heavy metals while the procedure was the same for all of them. The results are plotted in Fig. (5.24).

It can be observed from the aforementioned figures, that the concentration (*c*) varies very sharply at the beginning of the experiment along the soil column. In addition, *c* changes very slowly with time. For instance, it is very difficult to have a considerable solution concentration after 30 days at 25 cm depth of the soil column. Both of the two latter findings are due to the adsorption of heavy metals on the soil particles, which remarkably affects migration of cations within the soil column.

Since the source of contamination location is at the top of the soil column, the variations rates of c are very high at the top portion of the soil column. The bottom portion of the soil column has a very low variation rates.

In addition to the measurements of solution concentration, the adsorbed species concentration onto the soil particles were evaluated along the soil column. The measurements were done at the same points as those are for the solution concentration measurements. The measurements were repeated using the same procedure for the 3 heavy metals. Fig. (5.25) depicts the variation of the results for each heavy metal, separately.

The variation of the adsorbed species concentration (*s*) follows almost the same trend as the solution concentration (*c*). The variation rates of *s* are very high at the top portion of the soil column, and are significantly lower at the bottom portion of the soil column. Moreover, *s* changes very slowly with time. The variation of the adsorbed species is remarkably affected by the solution concentration within the soil. The higher the solution concentration, the higher the adsorption concentration.

In order to compare the variations of different phases of the adsorption process between batch test and column leaching test, the sequential extraction test was repeated for the soil samples obtained from the column test. In this test, lead chloride was the pore solution and the soil samples were obtained from different depths of the soil column.

The results of the test, where the soil column was leached by the lead chloride

solution for 7 days, are plotted in Fig. (5.26). As the figure depicts, the variation trend

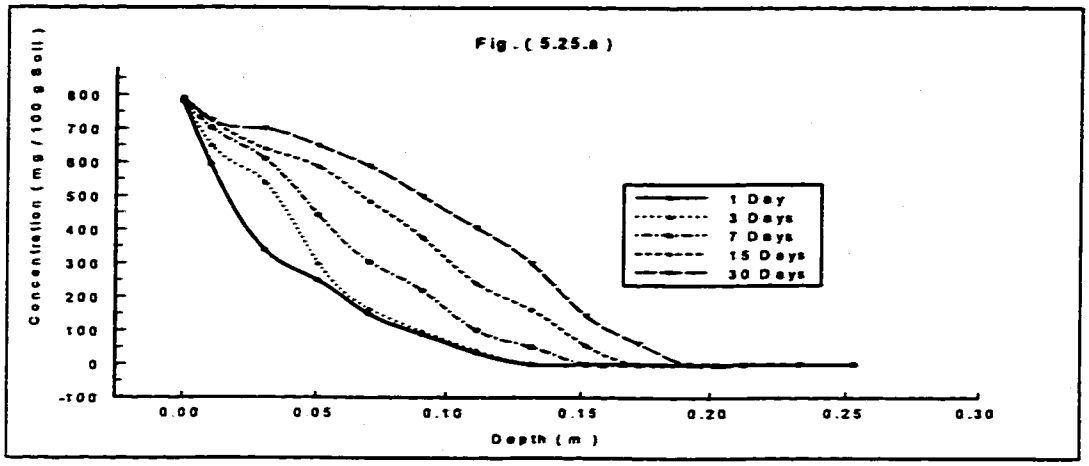

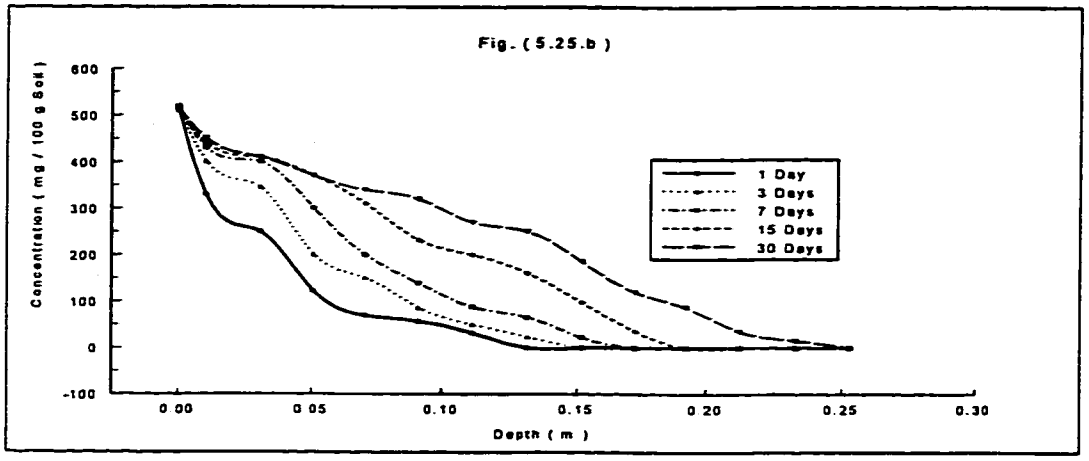

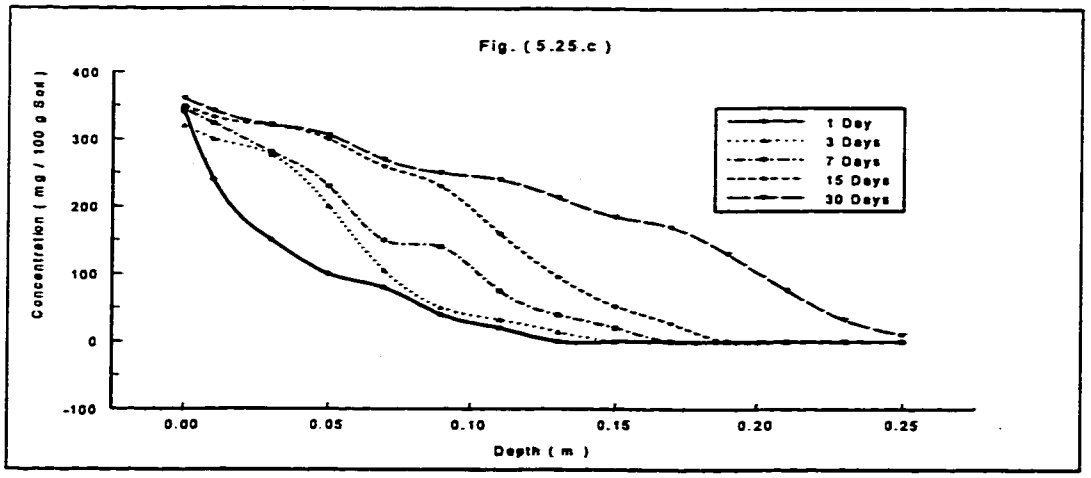

Figure 5.25 Adsorption Concentration-Depth Relationship for a) $PbCl_2$, b) $ZnCl_2$, and c) $CuCl_2$ Solutions along the Soil Column

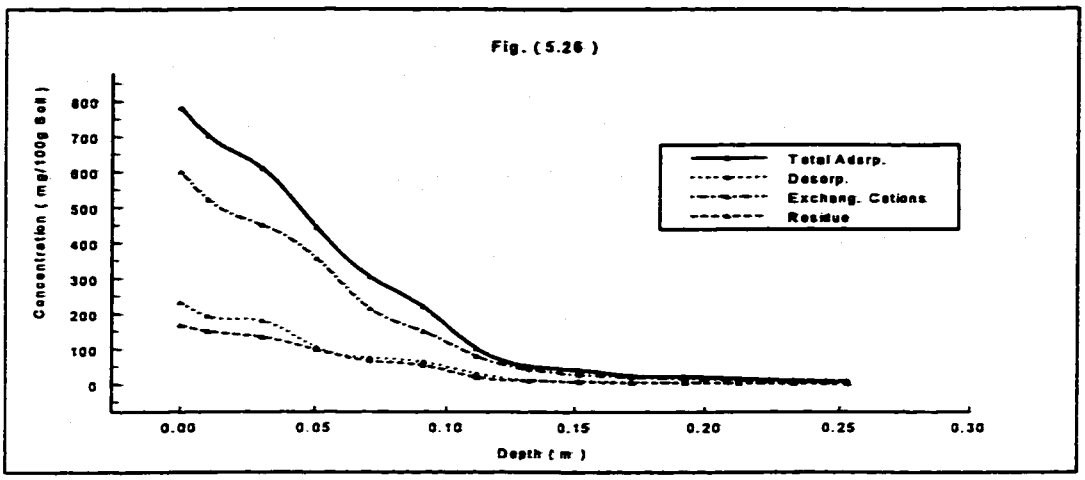

Figure 5.26 Variations of Sequential Extraction Components Concentrations for $PbCl_2$ Solution along the Soil Column

for both batch and column leaching tests is very close. This similarity determines, regardless of how the contaminant species reach and adsorb to the soil article surfaces, the percentage of the various phases of adsorption process are the same for all cases.

In addition, the experimental tests on lead indicate that sequential extraction and column leaching tests produce the same results, in terms of the percentage of various adsorption phases. Thus, there is no need to repeat the sequential extraction experiment for the other soil column specimens which are leached by zinc and copper chloride solution.

5.7.2 Analysis of the Tests Results

In order to compare the 3 heavy metals with each other, the results of the column leaching tests corresponding to lead, copper, and zinc are plotted in Fig. (5.27). This figure shows 2 sets of results: one after 3 days and one after15 days.

It can be observed that there is not much difference among the 3 heavy metals after 3 days, however, the difference is significant after 15 days. As time progresses, the volumetric water content (Θ) of the soil increases, and therefore, the solution can migrate within the soil solution (water). Due to the higher value of Θ, the soil particle

surfaces would be more available and/or involved for the adsorption of the contaminated species. Thus, adsorption of the contaminant species occurs at a considerably higher level, and this process would have a significant effect on the solution concentration along the soil column.

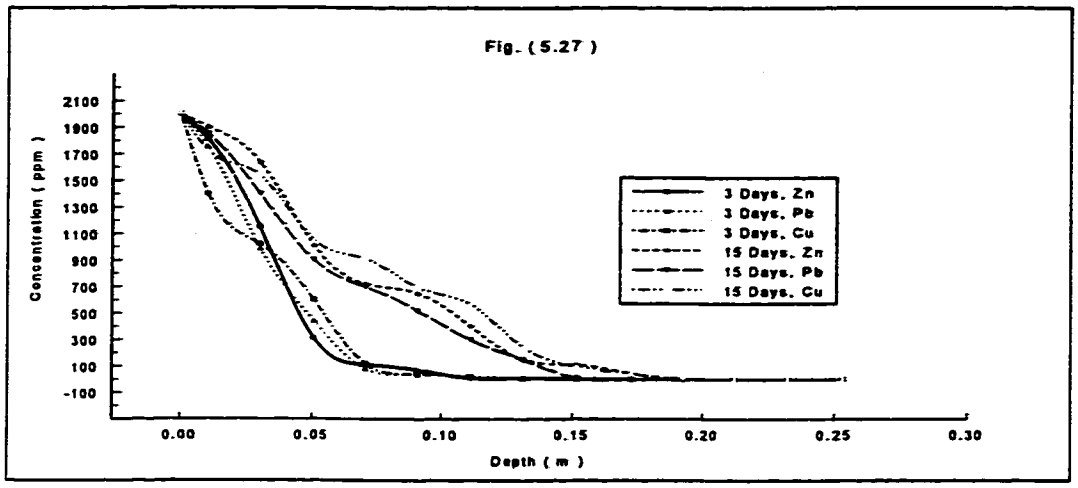

Figure 5.27 Comparison of $PbCl_2$, $ZnCl_2$, and $CuCl_2$ Solutions Concentrations along the Soil Column

Moreover, it can be seen from Fig. (5.27), that the contaminant species cannot migrate deeper than 11 cm within the soil column after 3 days. However, after 15 days Pb^{2+}, Cu^{2+}, and Zn^{2+} cations reach the soil at depths of 15, 18.5, and 19 cm of the column, respectively. The time interval increased by 5 times, whereas, the migration depth increasaed less than two times. This fact indicates that clay soils have a considerable soil buffer capacity, which results in retardation of heavy metals transport, and also retention of these contaminated species on the soil particles along the soil profile.

The relative concentration of lead was less than copper and zinc. These results indicate that the mobility order of the heavy metals in the soil column follows Pb< Zn < Cu. Elliott et al. (1986) also found the same trend of heavy metal mobility order in their study, based on the inverse proportionality to the hydrated radii. The unhydrated radii for Pb^{2+}, Zn^{2+}, and Cu^{2+} are 0.120, 0.074, and 0.072 nm, respectively.

Soil retention is not the same for different contaminant species. Fig. (5.28) shows

that kaolinite can retain less of copper than lead and zinc cations. Both figures show almost the same trend for 3 and 15 day time intervals, but the latter illustrates the difference among the 3 heavy metals more clearly than the former.

Since volumetric water content and solution concentration decrease remarkably from the top to the bottom of the column, the difference among lead, copper, and zinc cations concentrations is more considerable at the top of the column than at the bottom.

The results of the experiments have been significantly affected by the combined effect of these two factors. For instance, 200 (mg/100g soil) adsorption concentration for lead, copper, and zinc are monitored at 5.0, 5.0, and 6.75 cm depth of the soil column, respectively, after 3 days. However, after a 15 day time interval, this concentration has been found at 10, 12, and 12.5 cm from top of the soil column for lead, copper, and zinc, respectively.

On the basis of the column leaching test results, the adsorption mechanism can be simulated. This simulation is expected to take into account the factors which have significant effects on the amount of adsorption of contaminant species onto the soil particles surfaces such as solution concentration c, time interval t, and volumetric water content Θ.

Since the concentration of the solution is 2000 ppm, the results from these tests could, therefore, be readily related to the results from the batch tests. The most important differences between batch test adsorption and column leaching test adsorption correspond with: *i*) saturation degree of the soil, and *ii*) degree of soil particle dispersion within the solution.

Accordingly, in order to complete the simulation of the adsorption process within the soil column, the adsorption formula for the batch test could be considered as a base for this simulation. This formula contains the effects of soil solution concentration c, and time intervals t. The most significant parameter to be considered is volumetric water content Θ. However, some other unclear parameters might be involved in this process, regarding the two different soil-solution systems.

Accordingly, the completed form of the one dimensional formula to simulate the adsorption process within the soil medium is proposed as follows:

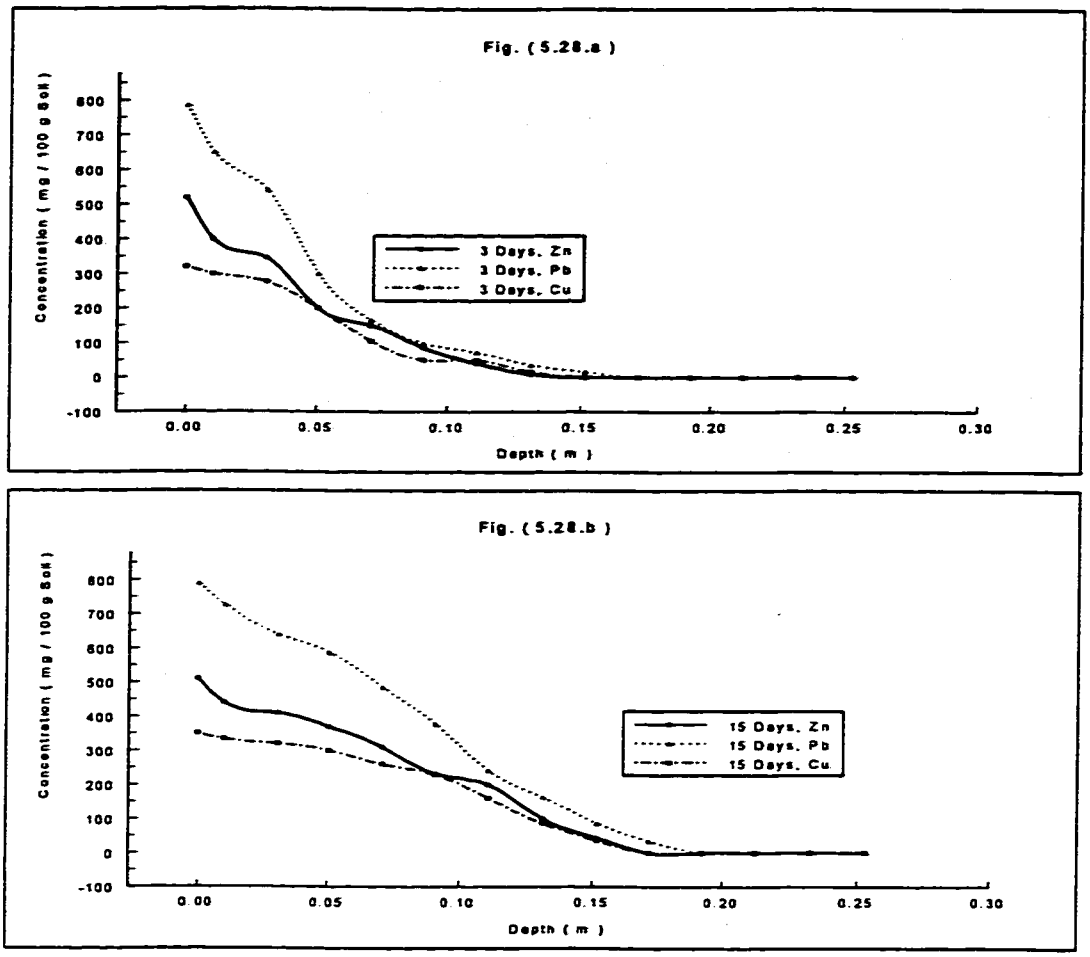

Figure 5.28 Comparison of Adsorption Concentrations for $PbCl_2$, $ZnCl_2$, and $CuCl_2$ Solutions after a) 3 and b) 15 Days along the Soil Column

$$s = f\Theta(a + be^{-t} + dc^{0.5}) \tag{5.8}$$

where a, b, d, and f are empirical parameters.

This formula has been implemented in numerical modeling to find soil solution concentration c, and adsorption concentration s, as functions of time and depth, simultaneously. The results from the numerical model have been verified with the one from experiments in figures (6.5.a) to (6.6.b), which conform to each other ($r>0.95$).

It can be concluded from the results of the sequential extraction and column leaching tests that heavy metals are considerably mobile and retain at low level in kaolinite, due to the low buffer capacity and initial pH of the soil in comparison with

the other clay soils.

Furthermore, it can be clearly seen from the above results that soil column leaching test can give an idea of how heavy metals might be retained or migrate within the soil. Also the study on heavy metal retention by sequential extraction test could be utilized to predict heavy metal movement in a soil column, to some extent.

The above results and discussion concerning the leaching column tests are summarized as follows:

1) The comparison of the results from soil column leaching tests and sequential extraction experiments indicate a very close relationship between the results. This shows that sequential extraction test results could be used to predict the heavy metal movement in soil.
2) The soil column capacity to retard or attenuate heavy metals, as it receives a continual heavy metal-leachate solution, depends on the initial concentration of the solution, solution pH, and soil buffer capacity.
3) Heavy metal mobility follows the order Pb<Zn<Cu in kaolinite clay soil, even though it does not show significant difference for these heavy metals. The order correspond to the order found in the batch test.
4) The results obtained from the determination of the soil buffer capacity, the sequential extraction analysis, and the experiment of soil column leaching tests provide a good picture of the role of the soil buffer capacity in the retention of heavy metals. This could help in the selection of a landfill site, along with other geological and physical factors to be considered in this regard.
5) If the concentration of the solution in the batch test is equal to that in the column leaching test, the results from the latter test could be readily related to the results of the batch test. The most important difference between batch test adsorption and column leaching adsorption corresponds with the degree of soil-solution saturation, and also degree of soil particle dispersion within the solution.
6) The adsorption mechanism of contaminant migration is mostly a function of soil solution concentration c, time interval t, and volumetric water content Θ. The effects of the aforementioned parameters have been taken into account by Eq. (5.8).

CHAPTER 6

NUMERICAL MODELING

6.1 GENERAL REMARKS

Many physical phenomena in nature are governed by partial differential equations, including the present problem. In general, there are two approaches for solving these equations: i.e., analytical and numerical.

The analytical solution for the unsaturated flow equations, which are nonlinear, is only available for very special cases. Hence, numerical methods such as finite element and finite difference are generally used to solve these equations. However, difficulties in obtaining the convergence of the numerical solution and serious mass balance problems have often been encountered (Celia *et al.*, 1990).

The objective of this chapter is to develop a finite volume algorithm (Patankar, 1980) to solve contaminant transport equations numerically. The method is easy to implement and provides an accurate description of physical flow features. This objective is accomplished in two main stages: first, the numerical discretization that is used to approximate the governing equations, (i.e., finite volume approach) and second, the solution of the discretized form of the governing equations through a computational algorithm.

It is to be noted, that because of the numerical requirement, soil water potential (H) is utilized instead of soil suction (Ψ), wherever necessary. According to the definition of H and Ψ, the relationship between these two parameters is $\Psi = -H$.

6.2 GOVERNING EQUATIONS

The one dimensional vertical flow of water and contaminant transport in unsaturated porous media are governed by the following non-linear set of equations.

$$c(\psi)\frac{\partial \psi}{\partial t} = \frac{\partial}{\partial z}[k_r K(\frac{\partial \psi}{\partial z} - 1)] \tag{6.1}$$

$$\rho_b \frac{\partial s}{\partial t} + \frac{\partial(\theta c)}{\partial t} = \frac{\partial}{\partial z}(D\theta \frac{\partial c}{\partial z} - cq) \tag{6.2}$$

where the soil suction ψ, and solute concentration c, are the dependent variables.

Equation (6.1) is a parabolic partial differential equation. Eq. (6.2) also becomes parabolic when the effect of convection term $\frac{\partial}{\partial z}(cq)$ becomes negligible, compared to that of diffusive term $\frac{\partial}{\partial z}(D\theta \frac{\partial c}{\partial z})$. This happens when the Peclet number approaches zero, and this is the case that usually happens for the flow through unsaturated porous media, particularly when the soil under consideration is very fine. The Peclet number represents the relative importance of convection to diffusion in the flow and it is defined as Pe=vL/D. In this formula v is the average velocity, L is the characteristic length of the pores, and D is the molecular diffusion coefficient of the solute within the liquid phase.

6.2.1 Initial and Boundary Conditions

The definition of the problem described by the equations (6.1) and (6.2) would be complete, once the proper initial and boundary conditions are specified (Fig. 6.1). For unsaturated flow the initial and boundary conditions are:

$\psi(z,0)=\psi_{zi}$ while $0 < z < L$, and

$\psi(0,t)=\psi_O$, and $\psi(L,t)=\psi_L$

where, ψ_{zi} is initial suction of the soil profile, L length of the profile and ψ_o , ψ_L are constant soil suctions at the boundaries.

The initial condition, for contaminant transport, is implemented in the form of

$c(z,0)=c_{zi}$ while $0 < z < L$

and the boundary conditions are assumed to be

$c(0,t)=c_O$ and $c(L,t)=c_L$

where, c_{zi} is initial concentration of the soil profile and c_o and c_L are boundaries' constant contaminant concentrations.

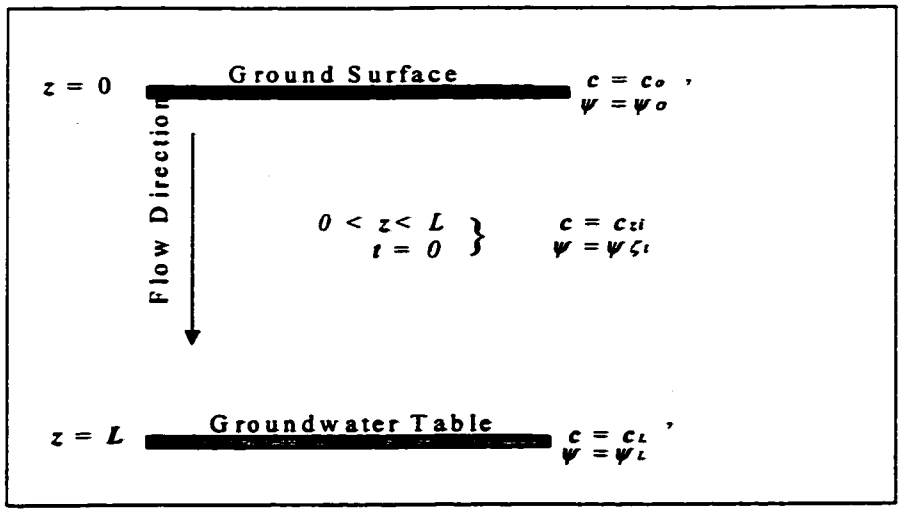

Figure 6.1 Contaminant Transport Initial and Boundary Conditions

6.3 FINITE VOLUME METHOD

The conservation laws of fluid motion (i.e., continuity, momentum and energy) may be expressed mathematically in either differential or integral form. In the finite difference method, the solution domain is divided into discrete points, upon which the differential form of the equations is solved. In the finite volume method, however, the solution domain is divided into small regions, and the integral form of the conservation law is applied in order to obtain the solution.

Before proceeding to the details of the finite volume method (FVM), it is important to state the differences between the differential and integral methods so that the advantages and disadvantages of each method can be identified.

The finite difference equations which approximate the partial differential equations are solved within a rectangular domain at equally distanced discrete points. Since the majority of physical domains are irregular in shape, a coordinate transformation from a physical space to a computational space is performed where the computational domain is rectangular. However, even with the coordinate transformation available, domains which are highly irregular would create serious difficulties in accuracy and convergence of the solution. At this point, it may be concluded that, in general, the finite difference methods possess inherited weaknesses for highly complicated domains.

On the other hand, finite volume methods (FVM), do not encounter such weaknesses. That is because the independent variables are integrated directly on the physical domain and, therefore, grid smoothness is no longer an important issue. Thus, the governing equations can be solved if only the domain can be successfully discretized into elements. Furthermore, (FVM) does not require a structured grid, as is required for the finite difference scheme; therefore, for most applications, unstructured grids are used. It is also important to emphasize that, since the integral equations are

applied directly to the physical domain, a coordinate transformation is no longer required.

In the purest form of the (FVM) method, the flow field or domain is subdivided, as in the finite element method, into a set of non-overlapping cells that cover the whole domain on which the conservation laws are applied. (In finite volume method the term cell is used instead of the term element used in finite element method). On each cell the conservation laws are applied to determine the mass flux variables in some discrete points of the cells, called nodes.

For instance, for a flow equation, the integral conservation law is written for a discrete volume as

$$\frac{\partial}{\partial t}\int_{\Omega} U d\Omega + \oint_{s} \vec{F} \circ d\vec{S} = \int_{\Omega} Q d\Omega \tag{6.3}$$

and applied to a control volume (CV) Ω_j. In this equation S, U, Q, F are the closed boundary surface, mass quantity, source value, and surface flux of the control volume, respectively. The above equation is replaced by the discrete form

$$\frac{\partial}{\partial t}(U_j \Omega_j) + \sum_{sides} (\vec{F} \circ \vec{S}) = Q_j \Omega_j \tag{6.4}$$

where the sum of the flux terms refers to all the external sides of the control cell Ω_j. The essential significance of this equation lies in the presence of the surfaces of the control volume, which accomplishes the conservation law.

Through this discrete form, the integral conservation of equations such as mass is exactly satisfied over any group of control volumes and, of course, over the whole calculation domain. This characteristic exists for any number of grid points, not just in the limiting sense when the number of grid points become large, i.e. even the coarse-grid solution exhibits exact integral balances.

The (FVM) takes the full advantage of an arbitrary mesh, where a large number of options are open for the definition of the control volumes around which the conservation laws are expected. Modifying the shape and location of the control volume (CV) associated with a given mesh point, gives considerable flexibility to the (FVM). In addition, by the direct discretization of the integral form of the conservation laws we can ensure that the basic quantities, mass, momentum and energy will also remain conserved at the discrete level. This is the most fundamental property for this numerical scheme.

Finite volume method combines the flexibility of finite element formulations for the treatment of complex geometry, with the simplicity and efficiency of traditional finite difference method.

6.4 GRID GENERATION

The dependent variables, in general, would be a function of three space coordinates and time. In general, for the numerical solution, one should choose the values of the independent variables at points at which the values of dependent variables are to be calculated. For the problem at hand, the relevant physical quantities are considered to be dependent on only one space coordinate (z). Since the phenomenon is also a function of time, the present problem is an unsteady one-dimensional problem.

The finite volume method can be generally categorized into two groups, based on where the control volume faces are to be located in relation to the grid points. The first group includes the "Cell-Centered" methods, and the second group includes the "Nodal-Point" methods.

In "Nodal-Point" methods (NP), faces are located midway between the grid points. Therefore, a typical grid point P does not lie at the geometric center of the control volume (CV) that surrounds it. However, in "Cell-Centered" methods (CC) the grid points are placed at the centers of the control volumes. In this method, one draws the control volumes first, and then places the grid points at the geometric center of each

control volume CV. In CC methods when the CV sizes are non-uniform, their faces do not lie midway between the grid points.

For the problem at hand the CC method is selected because;

1) The decisive advantage of this method is the convenience it offers. Since the control volume turns out to be the basic unit of the discretization method , it is more convenient to draw the CV first and let the grid-point locations follow as a consequence.
2) The concentration c_p (at the grid-point P inside the control volume) and other quantities can be regarded as a good representative value for the CV in calculation of source term.
3) In calculation of the fluid fluxes at CV faces, the NP method is not free from objections. The point which is located between the two grid points and on the face of the control volume is not at the center of CV face. Therefore, to assume that the fluid flux at this point prevails over the entire face entails some inaccuracy.

The design of control volumes near the boundaries of the calculation domain requires additional consideration. In NP methods the calculation domain is filled with the regular control volumes and the boundary grid points are located at the center of the boundary control volumes. As shown in Fig. (6.2), instead of a full control volume, a half CV adjacent to the boundaries is considered for the CC method.

The grid-spacing (and consequently the number of grid-points) is directly linked to the way the dependent variable c, changes. A fine grid is required where the Ψ~z or c~z variation is steep. However, according to the experimental results, suction or contaminant migration variations are almost the same for all sections along the soil profile. Thus, for the present problem a uniform grid is selected (Fig. 6.2).

6.5 DISCRETIZATION OF CALCULATION DOMAIN AND TIME

In order to solve a differential equation using numerical method applications, the continuous calculation domain is replaced with a net of non-overlapping sub-domains.

This division provides the grid points, where the attention is now focused on the values at the grid points instead of the continuous information contained in the exact solution of the differential equation. The division could be done in a same manner for the time, as well. This part of numerical solution is referred as "discretization (of space or time)." A systematic discretization of space and of the dependent variables makes it possible to replace the governing differential equations with simple algebraic equations, which can be solved with relative ease.

For a given differential equation, the required discretization equation can be derived in many ways;

1) The usual procedure for deriving finite difference equations consists of approximating the derivatives in differential equation via a truncated Taylor series. The Taylor-series formulation is relatively straightforward, but allows less flexibility and provides little insight into the physical meanings of the terms.
2) Another method of obtaining the discretization equation is based on the calculus of variations. The calculus of variation shows that solving certain differential equations is equivalent to minimizing a related quantity called the functional. The main drawback of this formulation is its limited applicability, since a variational principle does not exist for all differential equations of interest.
3) A powerful method for solving differential equations is the method of weighted residuals, which is described in detail by Finlayson (1972). The basic concept of this method is to make the error (residual) between true and approximate solution very small. This method considers the weighting function (W) for discretization.

In the numerical modeling of the problem at hand, the latter discretization method has been chosen, and the simplest weighting function is utilized, i.e. W=1. From this, a number of weighted-residual equations can be generated by dividing the calculation domain into sub-domains or control volumes, and setting the weighting function to be unity over one sub-domain at a time and zero everywhere else. This variant of the method of weighted residuals is called the sub-domain method or the control volume formulation. It implies that the integral of the residual over each control volume (CV) must become zero.

The discretization equation obtained in this manner expresses the conservation principle for the finite control volume, just as the differential equation expresses it for an infinitesimal control volume.

Since the present problem is a one-dimensional problem, a string of grid points is chosen (Fig 6.2). The 26 cm soil column is divided into very thin control volumes, whereas 2 half control volumes are located adjacent to the two boundaries. The grid points between boundaries are called the internal points, around each of which is shown a control volume.

The discretization equations can be written for each control volume, while two of them involve the boundary grid points values. It is through the treatment of these boundary values that the given boundary conditions are introduced into the numerical solution scheme.

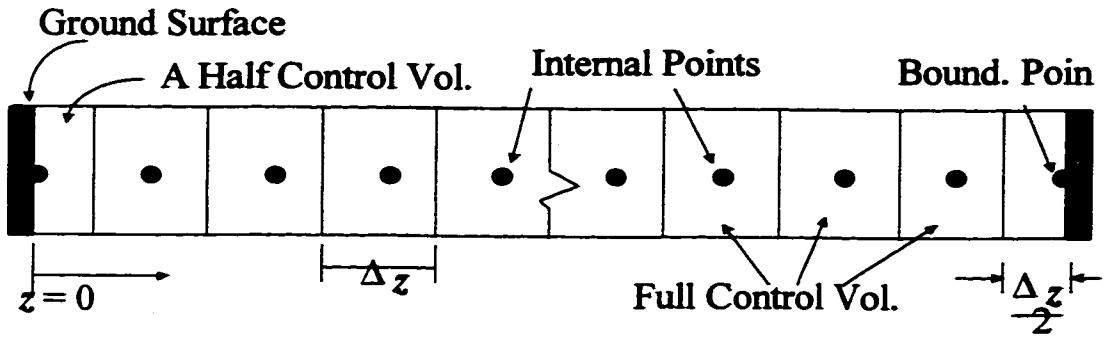

Figure 6.2 The Discretized Calculation Domain

6.5.1. The Algebraic Equations

In order to formulate the unknowns variations over the whole calculation domain, the two governing differential equations of the present problem (equations 6.1 and 6.2) are integrated over each control volume. Piecewise profiles expressing the variations of the unknown parameters between the grid points are used to evaluate the required integrals. Finally, the result is the discretization equations containing the unknown parameters for a group of grid points.

The two governing equations in this study are *i*) unsaturated flow, and *ii*) contaminant transport equations. In the former equation, the unknown is soil suction (ψ), whereas in the latter equation the unknowns are c and θ. Thus, in order to reduce the number of unknowns in the contaminant transport equation (CTE) this equation should be solved after obtaining the results of the unsaturated flow equation. Since, the unknown θ could be substituted with the known ψ, based on the relationship between these two parameters from the soil moisture retention curve, the CTE contains only one unknown (c), and therefore its solution is facilitated.

According to the experimental results, the maximum velocity of the solution within the soil column (if it is fully saturated) at room temperature (20°c) is

$v = 1.65\times10^{-9}$ m/s , therefore the Reynolds number ($Re = \rho vL/\mu$) for the present problem is

$Re = 1.85\times10^{-8} << 1.0$

and indicates that the flow is a creeping flow. On the other hand, for determining of the Peclet number, the maximum value for D (diffusion coefficient) is 4.76×10^{-8} m^2/s , and $L << 0.01$ m. Accordingly, Pe cannot exceed 3.5×10^{-4}.

Consequently, the problem is a diffusion dominated phenomenon, and each grid point value of the calculation domain is affected by the neighbors grid points values. In order to have the effects of the two immediate neighbors for each grid point in the numerical formulation, a central difference scheme is chosen for the space discretization.

Using the forward difference simulation for the time derivative results in an explicit scheme, whereas utilization of backward difference simulation leads to an implicit one. The implicit schème involves much more work in solving the set of simultaneous equations. However, this drawback is offset by the advantage that the implicit scheme is unconditionally stable, regardless of the size of the time step (Δt).

The problem at hand is to be investigated for any duration of time, and because of the nature of the phenomenon, it is mostly studied as a long term event. Hence, in order to make the program more efficient in solving the problem, it is desired that the program

have the capability of choosing (Δt) as large as required. To satisfy this property unconditionally for the numerical model, a fully implicit scheme is used for this study.

Among various implicit Schemes, the Laasonen Scheme is preferred. The Crank-Nicolson Scheme is usually described as unconditionally stable, which implies a physically realistic solution, but it encounters oscillatory solutions. The stability in a mathematical sense simply ensures that these oscillations will eventually die out, but it does not guarantee physically plausible solutions. Some examples of unrealistic solutions given by the Crank-Nicolson Scheme can be found in Patankar and Baliga (1978).

6.5.1.1 Linearization

The unsaturated flow and contaminant transport equations (Eq. 6.1 and 6.2) are both non-linear differential equations. In order to solve these equations numerically, the coefficients are to be linearized with the procedures commonly used in numerical methods.

Among different linearization methods, the iterative method is utilized to linearize the contaminant transport equation. This method is more advanced than the lagging method in providing early convergence. In this procedure the lagging value is updated until a specified convergence criterion is reached. The final unchanging state, introduces the converged solution which is actually the correct solution of the non-linear equation.

In addition, in the contaminant transport equation, the source term depends on the concentration (c);

$$S(c)=f\theta(a_2+b_2e^{-t}+c_2c^{0.5}) \qquad (6.5)$$

where a_2,b_2,c_2, and f are empirical parameters, t is a time interval, and θ is the volumetric water content of the soil.

The dependency in the aforementioned equation is not linear, and it should be linearized to be utilized for numerical modeling. It requires two values to be specified as

S_c and S_p to introduce the source term as $S=S_c+S_pc$, where S_c stands for the constant part of S and S_p is the coefficient of concentration c (the unknown value of the equation).

There are various methods to convert S to the above form. Some of them give less steep lines (compared to the S~c curve) which are undesirable, and they fail to incorporate the given rate of fall of S with c. Some others are steeper which will normally lead to slower convergence. The best choice of linearization is the one which gives a tangent line to the given curve. This line would be obtained through the following linearization:

$$S = S^* + (\frac{dS}{dc})^*(c - c^*) \tag{6.6}$$

which is tangent to the S~c curve at c^*. The symbol " * " is used to denote the guess value or the previous iteration value of c.

Utilizing the above linearization method, the source term of the contaminant transport equation would be

$$S(c)=f\theta[a_2+b_2e^{-t}+0.5c_2(c^*)^{0.5}]+0.5f\theta c_2(c^*)^{-0.5}c \tag{6.7}$$

Consequently, the final form of the contaminant transport equation is as follows:

$$\frac{\partial(\theta c)}{\partial t} = \frac{\partial}{\partial z}(D\theta\frac{\partial c}{\partial z}) - \rho_b\frac{\partial}{\partial t}\{\theta^f[a_2 + b_2e^{-t} + 0.5c_2(c^*)^{0.5}]\} - \frac{\partial}{\partial t}[0.5\rho_b\theta^f c_2(c^*)^{-0.5}]c \tag{6.8}$$

The unsaturated flow equation is a non-linear differential equation because, $c(\psi)$ (Eq. 5.3) and $K_r(\psi)$ (Eq. 5.4) are the coefficients which themselves depend on soil suction (ψ). Since both of these expressions are not simple, their derivatives would be very long and complicated equations. Thus, in order to linearize these coefficients, the soil suction ψ is substituted by the guess value or the previous iteration value of ψ. Accordingly, the unsaturated flow equation converts to the following equation:

$$C\frac{\partial \psi}{\partial t}=\frac{\partial}{\partial z}(K\frac{\partial \psi}{\partial z})-\frac{\partial K}{\partial z} \tag{6.9}$$

where C and K are the aforementioned coefficients, except that they are considered as function of z only for each time step.

6.5.2 The Discretized Forms of Equations

Referring to the general differential equation for any dependent variable (Eq. 3.26), neither the unsaturated flow nor the contaminant transport equation contain an advection term. Thus, the general form of both equations have three major terms: unsteady, diffusion and source term. In this section these two equations are discretized according to the control volume discretization method.

6.5.2.1 Unsaturated Flow Equation

The discretization equation is derived by integrating Eq. (6.1) over the control volume and over the time interval (from t to $t+\Delta t$). Since the time is one-way coordinate, the discretized form of equation is obtained by marching in time from a given initial discretization of suction (Ψ). Hence, in a typical time step the task is to find the values of Ψ at time t+Δt on the basis of the grid point given values of Ψ at time t. The new (unknown) values of Ψ at the grid points at time t+Δt are denoted by the superscript "n+1", and the given value of Ψ at time t is denoted by the superscript "n". "N" and "S" represent the space integration from the north face of the control volume to the south one. Thus,

$$\int_N^S \int_t^{t+\Delta t} C(\psi)\frac{\partial \psi}{\partial t}dtdz=\int_t^{t+\Delta t}\int_N^S \frac{\partial}{\partial z}[K_r(\psi)(\frac{\partial \psi}{\partial z}-1)]dzdt \tag{6.10}$$

where the order of integration is chosen according to the nature of the term. Since, linearization of $C(\Psi)$ and $K_r(\Psi)$ makes the equation very difficult to solve, they are converted to the constant values(section 6.5.1.1). Since they are substituted by Ψ^*, they are functions of time and depth of the soil profile, and hereafter they are replaced by C and K, respectively.

Furthermore, for the representation of the term $\frac{\partial \psi}{\partial t}$, it is assumed that the grid point value of Ψ prevails throughout the control volume. Then, the left hand side of the above equation would be

$$\int_N^S (C\psi)\Big|_t^{t+\Delta t} dz = C_i(\psi_i^{n+1} - \psi_i^n)\Delta z \tag{6.11}$$

and the other side of the equation, by utilizing the implicit method, yields to

$$\int_t^{t+\Delta t} [K(\frac{\partial \psi}{\partial z} - 1)]\Big|_N^S dt = \int_t^{t+\Delta t} [K_S(\frac{\partial \psi}{\partial z} - 1)_S - K_N(\frac{\partial \psi}{\partial z} - 1)_N]dt = [K_S^{n+1}(\frac{\psi_{i+1}^{n+1} - \psi_i^{n+1}}{\Delta z} - 1) - K_N(\frac{\psi_i^{n+1} - \psi_{i-1}^{n+1}}{\Delta z} - 1)]\Delta t \tag{6.12}$$

where i denotes the control volume number, and $K_S = \frac{2K_i^{n+1}K_{i+1}^{n+1}}{K_i^{n+1} + K_{i+1}^{n+1}}$ and $K_N = \frac{2K_{i-1}^{n+1}K_i^{n+1}}{K_{i-1}^{n+1} + K_i^{n+1}}$.

Equating both sides of the equation, the discretization form of unsaturated flow equation becomes:

$$C_i(\psi_i^{n+1} - \psi_i^n)\frac{\Delta z}{\Delta t} = K_S(\frac{\psi_{i+1}^{n+1} - \psi_i^{n+1}}{\Delta z} - 1) - K_N(\frac{\psi_i^{n+1} - \psi_{i-1}^{n+1}}{\Delta z} - 1) \quad (6.13)$$

6.5.2.2 Contaminant Transport Equation

Following the same procedure as for the development of the unsaturated flow equation, the discretized form of the contaminant transport equation is obtained by double integration of the equation over time and depth of the soil profile;

$$\int_N^S \int_t^{t+\Delta t} \frac{\partial(\theta c)}{\partial t} dt dz = \int_t^{t+\Delta t} \int_N^S \frac{\partial}{\partial z}(D\theta \frac{\partial c}{\partial z}) dz dt - \int_N^S \int_t^{t+\Delta t} \rho_b \frac{\partial s}{\partial t} dt dz \quad (6.14)$$

The left hand side and the second term of right hand side of the above integration are discretized as

$$\int_N^S (\theta c)\Big|_t^{t+\Delta t} dz = \Delta z(\theta_i^{n+1} c_i^{n+1} - \theta_i^n c_i^n) \quad \text{, and} \quad (6.15)$$

$$-\int_N^S \int_t^{t+\Delta t} \rho_b \frac{\partial s}{\partial t} dt dz = -\rho_b \Delta z(s_i^{n+1} - s_i^n) \quad (6.16)$$

The integration of the diffusion term yields

$$\int_t^{t+\Delta t} (D\theta \frac{\partial c}{\partial z})\Big|_N^S dt = \int_t^{t+\Delta t} [(D\theta \frac{\partial c}{\partial z})_S - (D\theta \frac{\partial c}{\partial z})_N] dt = [D_S \theta_{i+1}^{n+1} \frac{c_{i+1}^{n+1} - c_i^{n+1}}{\Delta z}$$
$$- D_N \theta_{i-1}^{n+1} \frac{c_i^{n+1} - c_{i-1}^{n+1}}{\Delta z}] \Delta t \quad (6.17)$$

where D_S and D_N are calculated in the same fashion as K_S and K_N.

On the other hand, since the s function is introduced as Eq. (6.5), therefore,

$$s_i^{n+1} - s_i^n = f(\theta_i^{n+1})[a_2 + b_2 e^{-t} + c_2 (c_i^{n+1})^{0.5}] - f(\theta_i^n)[a_2 + b_2 e^{-t} + c_2 (c_i^n)^{0.5}] \qquad (6.18)$$

By substituting all terms of the equation by their discretized form and rearranging, the final discretized form of contaminant transport equation yields:

$$\theta_i^{n+1} c_i^{n+1} - \theta_i^n c_i^n = [D_S \theta_{i+1}^{n+1} \frac{c_{i+1}^{n+1} - c_i^{n+1}}{\Delta z} - D_N \theta_{i-1}^{n+1} \frac{c_i^{n+1} - c_{i-1}^{n+1}}{\Delta z}]\Delta t - \rho_b \{f(\theta_i^{n+1})$$
$$[a_2 + b_2 e^{-t} + c_2 (c_i^{n+1})^{0.5}] - f(\theta_i^n)[a_2 + b_2 e^{-t} + c_2 (c_i^n)^{0.5}]\} \qquad (6.19)$$

6.6 PROGRAMMING

This study provides a general numerical model for the phenomenon under consideration. Since all the requirements for computer programming have already been provided, now it's the time to determine the algorithm and, provide the computer code to solve the problem at hand.

6.6.1 Flow Chart and Computation Sequence

The major computational sequences in the program are shown in Fig. (6.3). Before the solution starts, the model discretizes the domain and performs the related calculations, to determine locations of the grid points and control volumes' faces. These calculations are done through the subroutines **GRID** and **SETUP**. Then, the program assigns default values to control variables and other relevant variables. Initialization of all variables (including logical variables) is done at this stage.

The next step is the introduction of all problem-dependent parameters and initial (or guess) values. At this step, time is initialized, while the time increment and the maximum
desired calculation time is defined to the program.

Since volumetric water content should be obtained for the solution of the contaminant transport equation, the flow equation needs to be solved prior to the transport equation. Furthermore, in order to solve the contaminant transport equation, the variable values related to the previous time step are required (***cold***, ***thetaold***). Thus, at the beginning of each time step the calculated values of concentration and volumetric water content are defined as ***cold*** and ***thetaold***.

At the next stage, the first iteration starts, in which the subroutines DIFSOR, COEFFS, BOUNDS, RESIDUE, SOLVE, and OUTPUT are called (see next section for details regarding the performance of these subroutines). By calling these subroutines, the following are performed; ***i***) calculation of diffusion term Γ, and source term s; ***ii***) calculation of discretized form of equations coefficients ***AN***, ***AS***, and ***AP***; ***iii***) imposition of boundary conditions; ***iv***) calculation of grids average residues; ***v***) solution of the equations through utilization of three diagonal matrix analysis method, and eventually ***vi***) print of the final dependent variables values.

At the first time period, if convergence of the variable values is reached, then the time step is increased by one increment, ***DT***. The program then restarts from zero iteration, and the aforementioned procedure is followed for each time interval. This calculation cycle continues until the time equals the maximum time desired, and the program stops. It is obvious that, the variable values as a function of time and depth have already been stored in a file through subroutine output, which is accessible whenever needed.

If the convergence criterion for the solution has not been achieved, the program increases the iteration number by one and follows the calculation steps again starting from the subroutine DIFSOR until the end of the calculation cycle program. This repetition ends as soon as the iteration number reaches the maximum iteration number. At this stage, if the convergence criterion is satisfied, the program is conducted to the next time step, otherwise the program writes a message (NO CONVERGENCY), and stops.

6.6.2 Program Components

In order to solve the flow and contaminant transport equations through unsaturated soil, a one-dimensional finite volume program (CONTRANS), in the Cartesian coordinate system has been provided. The program consists of two major parts: *i*) Problem-independent, and *ii*) problem-dependent portion. The first one contains MAIN PROGRAM, SETUP, COEFFS, and SOLVE subroutines, whereas the second one consists of subroutines: GRID, DEFVAL, START, DIFSOR, BOUND, RESIDUE, and OUTPUT.

6.6.2.1 Main Program

The primary purpose of the main program is to control the overall execution of the program. At the beginning, subroutines GRID, SETUP, and DEFVAL are utilized to provide all the requirements for starting calculation of the variables values in the program, such as discretization of the domain and initialization of the variables (including the logical variables).

Afterwards, the main program leads the program to calculate and print out the variables values through iterations for each time step, and eventually for the maximum time step. The aforementioned stage is performed by calling the subroutines DIFSOR, COEFFS, BOUNDS, RESIDUE, SOLVE, and OUTPUT from the main program. The number of iteration to reach convergence for the unsaturated flow and contaminant transport processes are regulated by the main program, as well.

6.6.2.2 Subroutines

The subroutines are introduced according to the sequence of calling by the main program.

Subroutine Grid: The purpose of this subroutine is to enable the user to input the location of the grid points in Cartesian coordinates. This is done on the basis of the total height of the soil profile and the desired number of the grid points (including boundary points).

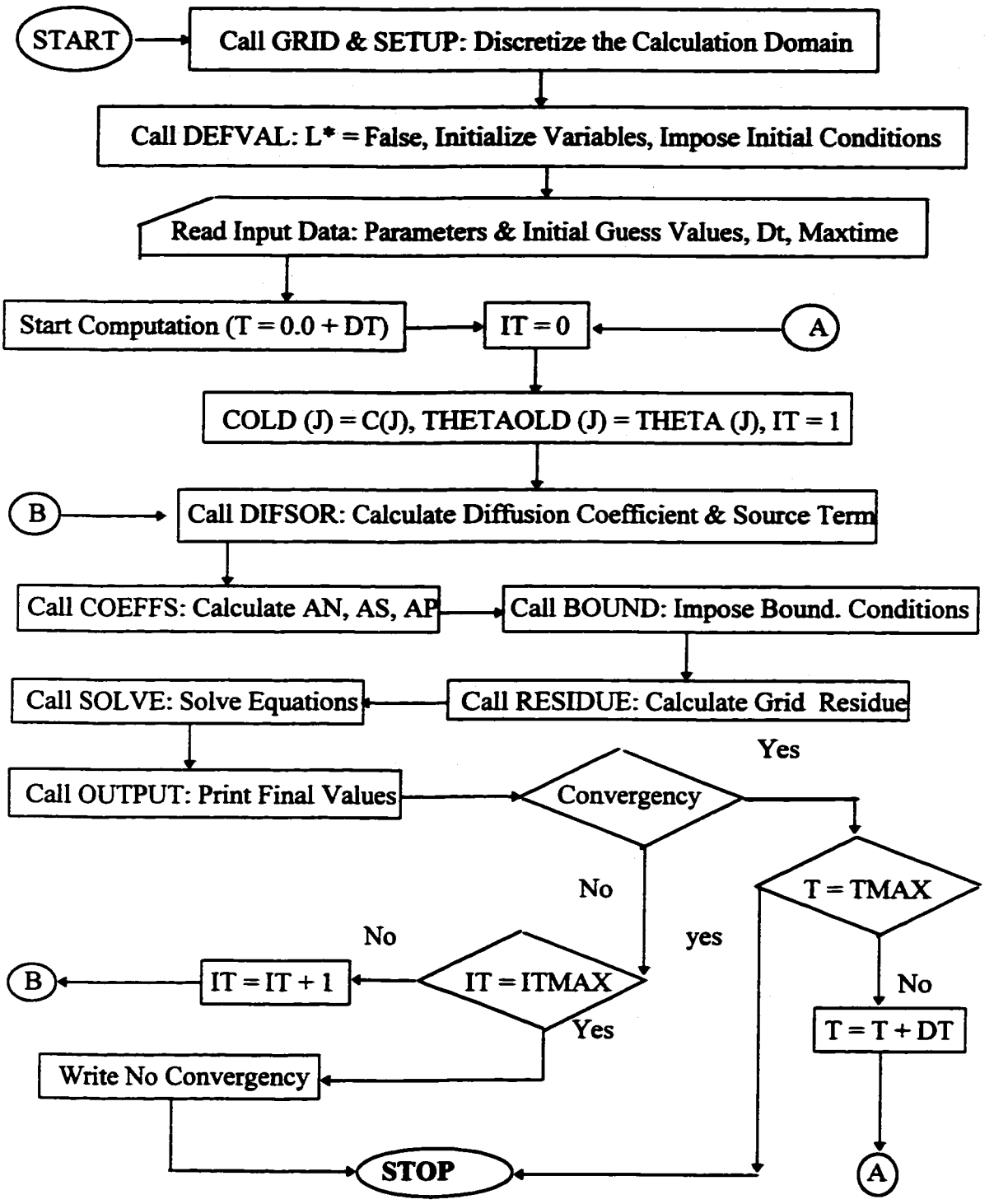

Figure 6.3 The Computer Program Flow Chart

Subroutine Setup: The function of this subroutine is to set up all the grid-related quantities, which are used in the formulation of the finite volume method. These quantities consist of: *i*) distance between adjacent main-grid control volume faces in the z direction, ***YCV(J)***, *ii*) distance between adjacent main-grid nodes (***J-1***) and ***J***, YDIF(J), and *iii*) ***J***th main-grid control volume face location, ***YV(J)***.

Subroutine Defval: In order to assign default values to control parameters and any desired variables in the program, this subroutine is utilized. All logical variables are set to false in this subroutine, and maximum desired iteration number is defined, as well.

Subroutine Start: The purpose of this subroutine is to input all problem-dependent parameters and assign proper initial or guess values for the variables of the problem. The initial conditions for the flow and contaminant transport, and also the time interval (ΔT), and maximum desired time step are imposed on the program.

Subroutine DIFSOR: The objective of this subroutine is to assign all diffusion coefficients and source terms for the flow and contaminant transport equations, separately. The volumetric water content of the soil profile Θ, (as a function of time t, and depth z), is calculated on the basis of the related suction value Ψ, in this subroutine. The unsteady coefficients for both of the equations are introduced to the program through this subroutine.

Subroutine Coeffs: The function of this subroutine is to evaluate the coefficients in the discretized equations. These coefficients are: *i*) the north neighbor coefficient for the ***J*** grid point ***AN(J)***, *ii*) coefficient for the ***J*** grid point ***AP(J)***, *iii*) the south neighbor coefficient for the ***J*** grid point ***AS(J)***, and *iv*) the constant associated with the discretized equation for the ***J*** grid point ***CON(J)***.

Subroutine Bound: This subroutine imposes boundary conditions to the program. These consist of suctions and concentrations for flow and contaminant transport equations, respectively.

Subroutine Residue: This subroutine allows the program to calculate the grid averaged residues. The residue could be calculated for any desired dependent variable, such as suction, contaminant concentration, or volumetric water content. The residue is

utilized later as the convergence criterion by the main program to control the overall execution of the program.

Subroutine Solve: This subroutine implements a tri-diagonal-matrix-algorithm for the solution of the discretized equations. This subroutine solves the matrix by Gaussian elimination through the LDU decomposition method.

Subroutine Output: This subroutine is mainly used to set up output of the desired results, but it could also be utilized to set convergence criteria, monitor convergency, and calculate auxiliary results.

6.6.3 Numerical Model Calibration

The parameters d of function $K_r(\Psi)$ in unsaturated flow and f of the source term on contaminant transport phenomena are unknown values, and they are introduced as empirical parameters. Having the values for c and Ψ from experiments based on independent variables (t and z), and utilizing proper formulas for the parameters, one can derive the values of $K_r(\Psi)$ and s.

If the measured and calculated values are designated as Φ_{exp} and Φ_{calc}, respectively, the best choice of the empirical parameters values are the ones which satisfy the following criterion:

$$\left|\Phi_{exp} - \Phi_{calc}\right| \leq \varepsilon$$

where ε is a very small number.

Thus, for the chosen t and z, Φ_{calc} can be calculated. The best way to obtain a proper value for d and f is to use the trial and error technique, by repeatedly incrementing the empirical parameter from zero, until the above criterion is satisfied. This iteration is done by means of linking the EMPRPAR (empirical parameters) subroutine, which has been added to the computer code. The main task of this subroutine is to verify that the

above convergence criterion has been satisfied. As soon as this criterion is satisfied, the program prints out the empirical parameter values (*d* or *f*).

6.7 VERIFICATION OF THE NUMERICAL MODEL

The accuracy of the computer code for simulation of contaminant transport within unsaturated soil has been tested by the experimental results. Under identical conditions, the numerical results are superimposed on the experimental results and are plotted in figures (6.4), (6.5.a), (6.5.b), (6.6.a), and (6.6.b).

In order to indicate the relationship between measured and calculated values for the variables in each plot, the correlation factor *r*, is calculated by using the following equation:

$$r = \sqrt{1 - \sum_{i=1}^{n} \frac{(\Phi_{exp,i} - \Phi_{calc,i})^2}{(\Phi_{exp,i} - \Phi_{avg,i})^2}}$$

where $\Phi_{avg,i}$ is an average value of the measured and calculated values for the variables at each point of the comparison.

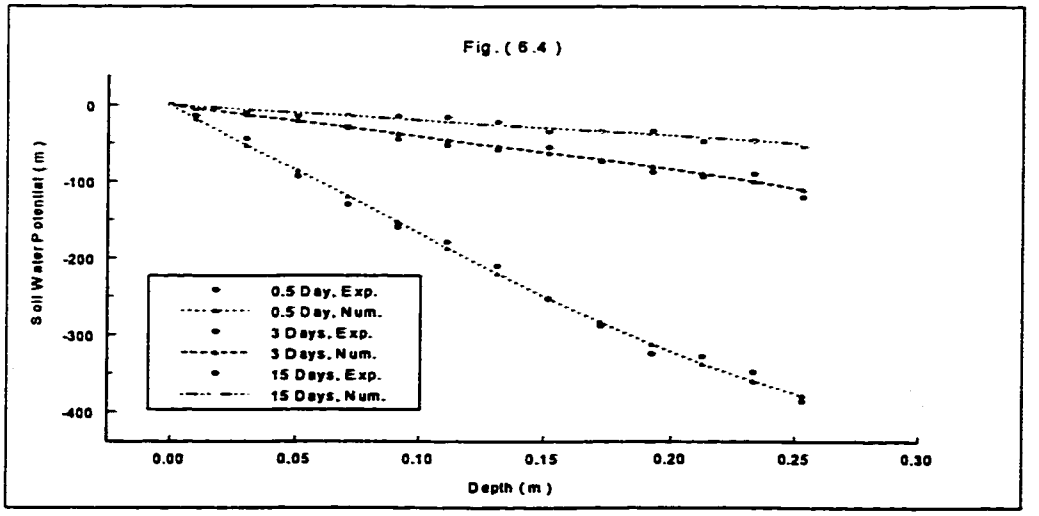

Figure 6.4 Soil Water Potential Variations with Depth (Numerical and Experimental Results Comparison)

The correlation factors in all comparisons, were above 95%. As a result, the proposed finite volume model behaves as predicted, maintaining good accuracy and non-oscillatory properties. The numerical solutions obtained for all cases, compare favorably with experimental results.

6.8 NUMERICAL MODEL IMPLEMENTATION

Although the model has the flexibility to simulate a variety of situation, its main operation describes the following scenario:

A portion of the soil profile which is partially saturated is located above the groundwater table. A contamination source of heavy metals is assumed to be located on top of the soil, which is initially assumed to be free of any contamination. The soil profile has a thickness of h , and as a porous media allows the contaminant species to move towards the groundwater table.

As time progresses, the concentration of the pore solution will increase gradually up to the concentration of the contamination source. Furthermore, the concentration of the adsorbed contaminant species onto the soil particles surfaces (SPS) will enhance, resulting in contamination of the soil particles along the soil profile.

Since, the contamination source is located on the ground surface, the concentration of the pore solution and adsorbed species onto SPS will be higher in top portion of the soil profile than in the lower portion. Thus, it takes a long time for the contaminant within the pore solution to reach the groundwater table, and cause contamination of the water resource.

However, the concentration of the pore solution at the groundwater table will reach its maximum allowable value c_{allow}, some time later at t_{max} . If t_{max} is less than the life time of the groundwater t_{life}, nothing is required to be done, otherwise, the source initial concentration c_o should be reduced to a level at which t_{max} does not exceed t_{life} , and to keep the groundwater safe from contamination. In other words, if c_o cannot be reduced, the t_{life} of the groundwater (to be utilized safely) will be limited to the t_{max} .

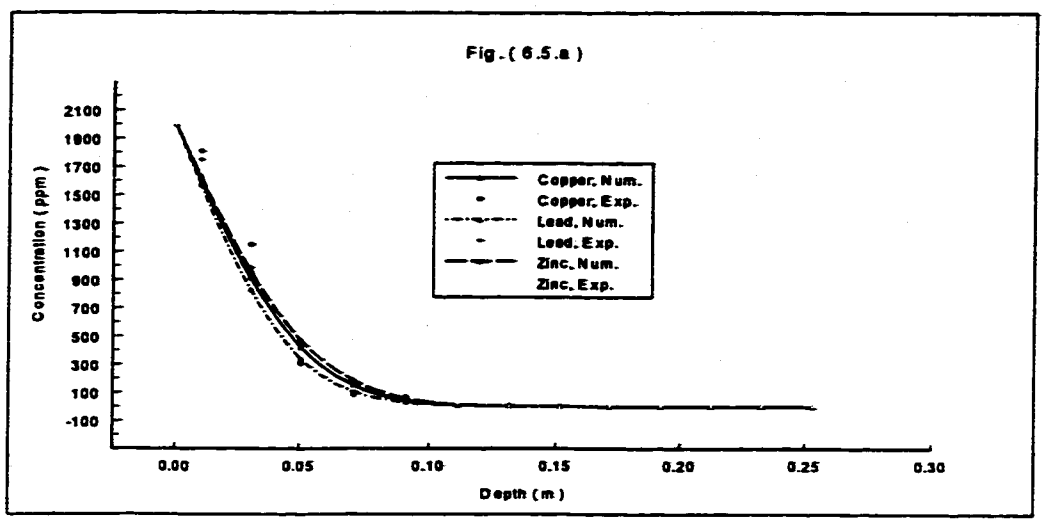

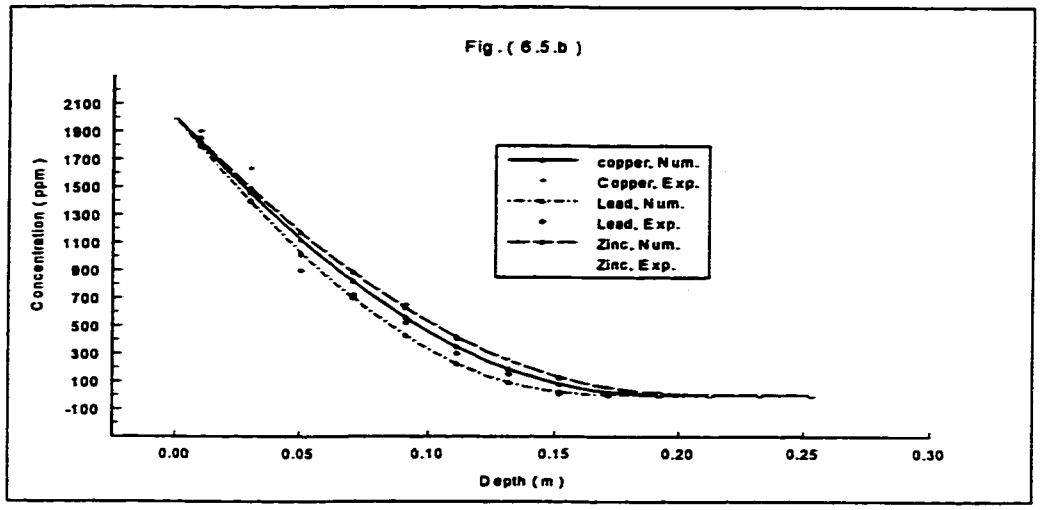

Figure 6.5 Solution Concentration-Depth Relationship for a) 3 Days, and b) 15 Days Time Intervals (Numerical and Experimental Results Comparison)

6.8.1 Running the Model

The code is written in Lahey standard FORTRAN-77, and it is executable on DOS operated personal computers as well as VAX systems. The model is equipped with the interactive data input for the following input parameters:

1) Input related to the numerical discretization and the model operation,

2) Input correspondent to the soil and hydraulic properties of the medium,

3) Input related to the contamination source,

4) Input related to the adsorption and diffusion processes within the soil medium.

Thus, the results of the numerical modeling would be affected by all of the aforementioned parameters.

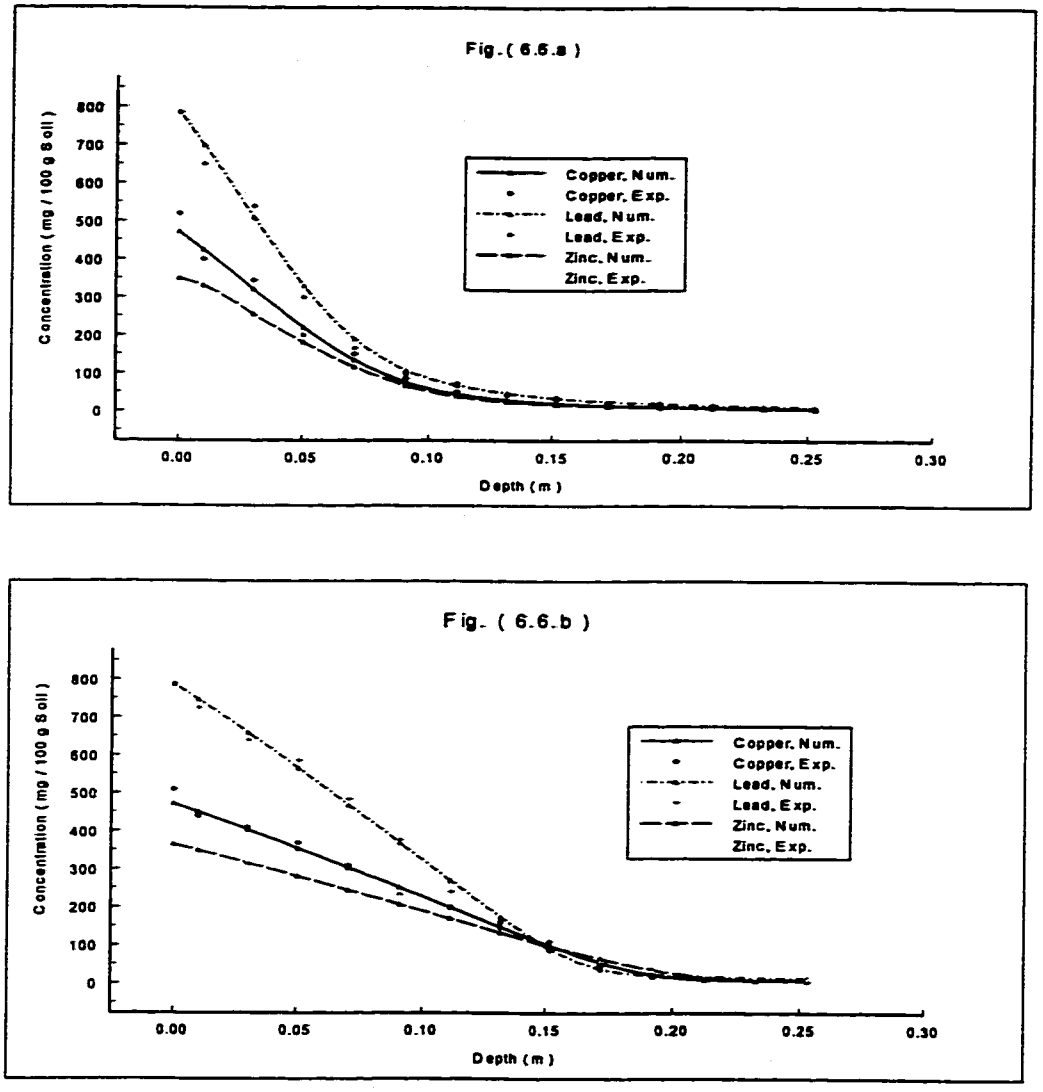

Figure 6.6 Soil Adsorption Concentration-Depth Relationship for a) 3 Days, and b) 15 Days Time Intervals (Numerical and Experimental Results Comparison)

The space and time discretization steps are to be selected somehow to obtain a stable and converged solution within a reasonable time. Having these conditions provided for in the solution, the following condition is to be satisfied for the present problem:

$$\Delta t < \frac{\rho c (\Delta z)^2}{2k}$$

where ρc and k are unsteady term and diffusion coefficients, respectively. Consequently, for the above purpose and in order to be more conservative, ρc could be substituted with its minimum value and k with its maximum value in the above equation for both flow and transport equations.

According to the flow and contaminant transport equations, ρc could be considered as $\pi/2$ and 0.065 for the flow and transport equations, respectively. Also, k could be designated as 9.34×10^{-4} m^2/day for the flow equation, and 0.41 m^2/day for the transport equation. Finally, if Δz is assumed to be 0.01 m, Δt should not exceed 7.27 and 0.68 seconds to have a stable solution for the 2 equations.

Comparing Δt for the 2 equations, the size of space discretization increment (Δz) provides a time discretization increment (Δt) for the flow equation of about 10 times that of the transport equation. This indicates that the solution of transport equation is more sensitive to the size of Δz than the one for the flow equation. Generally, it is recommended that the smallest possible value of Δz be used to obtain more accurate results. Although this recommendation may be used as a rule of thumb, however, the choice of Δz is dependent and limited by the size of Δt.

Soil type is an important factor in flow and contaminant transport phenomena. Soil not only affects the 2 phenomena by its particles properties such as density, but its hydraulic properties have significant effects on the flow and transport mechanism. Among the different parameters, unsaturated hydraulic conductivity, diffusion coefficient, and initial volumetric water content (θ_{init}) need particular attention to be evaluated precisely.

The effect of Θ_{init} is considerable in the first days of the experiment, which it is related to depth of the soil column. For instance, the effect of Θ_{init} is remarkable during first 3 days, when the soil column is 30 cm deep. Instabilities in the solution of the moisture transport equation may occur if the chosen Θ_{init} is close to the saturated moisture content or to the air-dried moisture content, due to the sharp moisture gradients that are formed close to the soil surface.

Contamination source properties play a significant role in the transport mechanism,

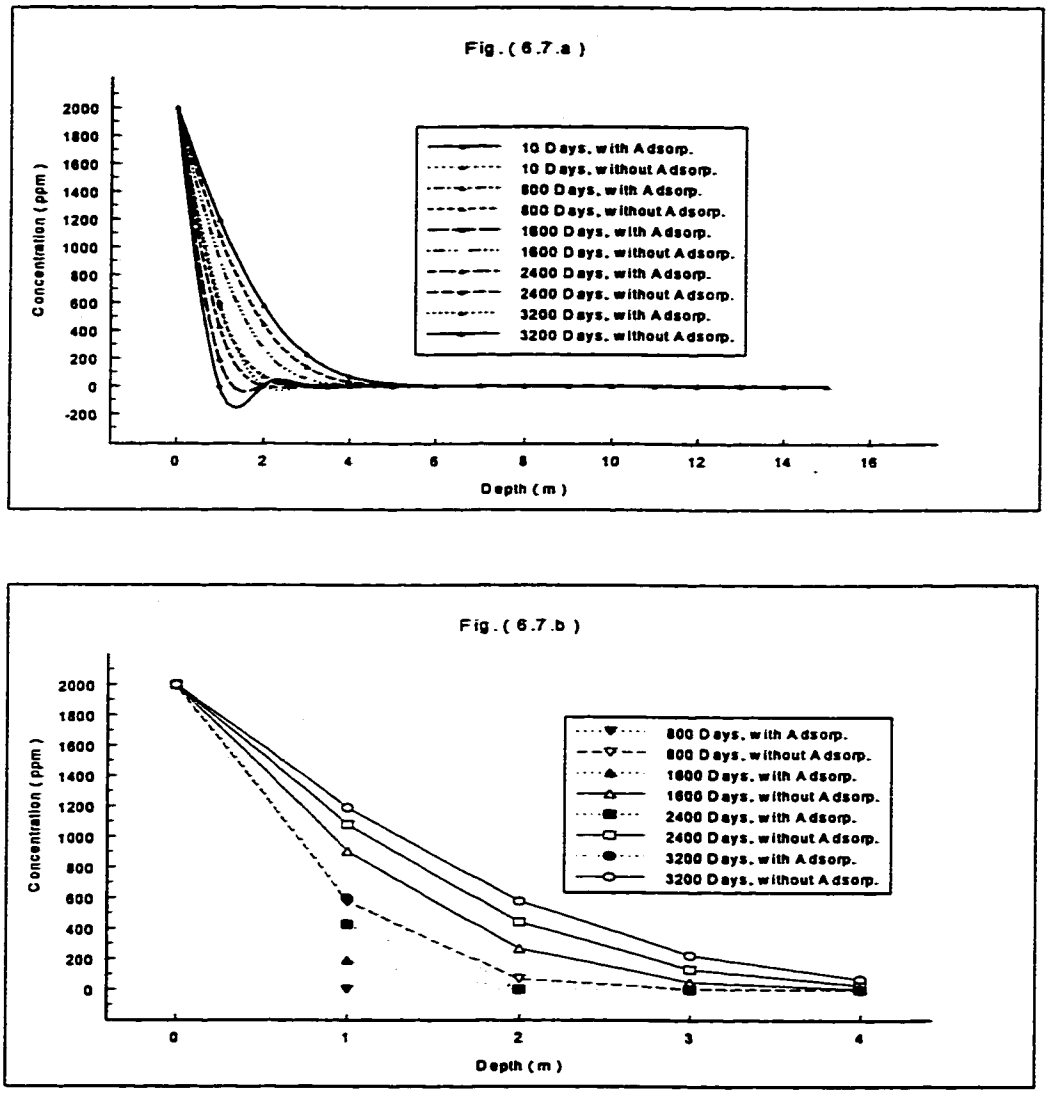

Figure 6.7 Adsorption Process Effect on Solution Concentration ($PbCl_2$, 2000 ppm)

and in concentration variations along the soil column. These parameters could be specified as initial concentration of source solution, kind of contaminant and its constituents, kind of reactions which it could have with the soil particles, and location of the source along the soil profile. If any of these parameters change, the concentration of the solution within the soil medium will change.

The effect of adsorption/desorption of the contaminant species onto/from the soil particles surfaces cannot be ignored, particularly when the medium is a kind of clay soil. This phenomenon, causes remarkable retardation/acceleration of the contaminant front within the medium.

Figures (6.7.a) and (6.7.b) illustrate the effect of the adsorption process on pore solution concentration along the soil column. The former figure is plotted for 15 m depth of the soil profile, comparing the solution concentration with and without the adsorption process effect. The program was run for 3200 days time interval, while the figure shows the concentration variation for 10, 800, 1600, 2400, and 3200 days.

Since significant variations take place within the first 4 m of the soil profile, Fig. (6.7.b) was plotted to highlight the variation and the effect of adsorption process on concentration of the solution c. As the figure shows, the effect of this process is very high at the beginning of the experiment, however, this effect reduces as time progresses and reaches long term intervals.

For example, the reductions of c for 800, 1600, 2400, and 3200 days at 1 m depth of soil profile are 95, 78, 59, and 50 percent, respectively. The results of this comparison reveals clearly the important role of the buffer capacity of the soil in retardation and prevention of groundwater from contaminated leachate.

6.8.2 Soil Profile Concentration Prediction

Numerical modeling can provide this tool to examine the effects of various soil properties and/or different chemical constituents on the model output. This examination result can be utilized to compare different scenarios, and consequently, to select the

most proper one in concern with the particular purpose. This selection would be the most efficient and the most economic one.

Furthermore, the computer code can be used to predict the short and especially long term variations of the hydraulic properties and contamination of soil along the soil profile. This prediction may help the designer of a waste disposal site to evaluate the life time of the project safely, and, accordingly, keep the groundwater contamination level below the allowable one (c_{allow}).

As an example of this prediction, the following sample run presents a contamination scenario, where the soil profile between ground surface and the groundwater table has a thickness of 15 m. The soil is initially unsaturated and free of heavy metals contamination, and the simulation is performed for 3200 days time interval. The contamination source contains lead chloride with 2000 ppm concentration, and it is located above the ground surface.

Figures (6.8) depicts the variations of soil water potential and volumetric water content, and Fig. (6.9) shows solution concentration and adsorption concentration variations. As the figures show, the variations are plotted for five different time intervals; 10, 800, 1600, 2400, and 3200 days.

All the aforementioned variations are obtained for a 15 m depth of the soil profile; however, the solution and adsorption concentration variations are plotted for the first 3 and 4 m, respectively. The depth of the soil profiles are reduced, in figure (6.9), due to zero concentration of the solution and adsorption below those levels.

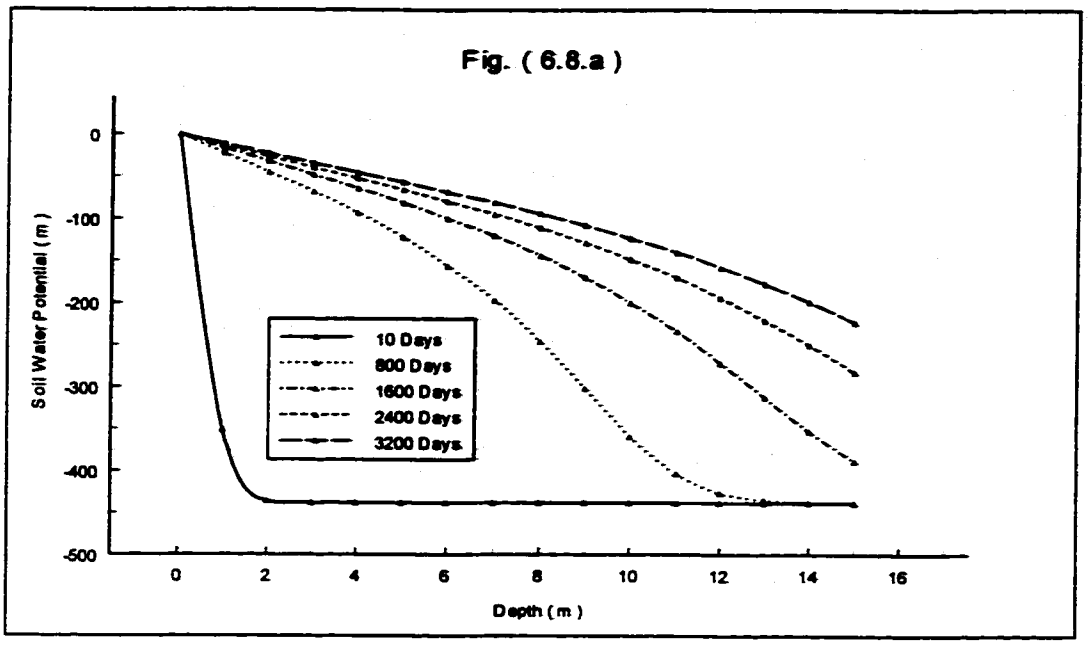

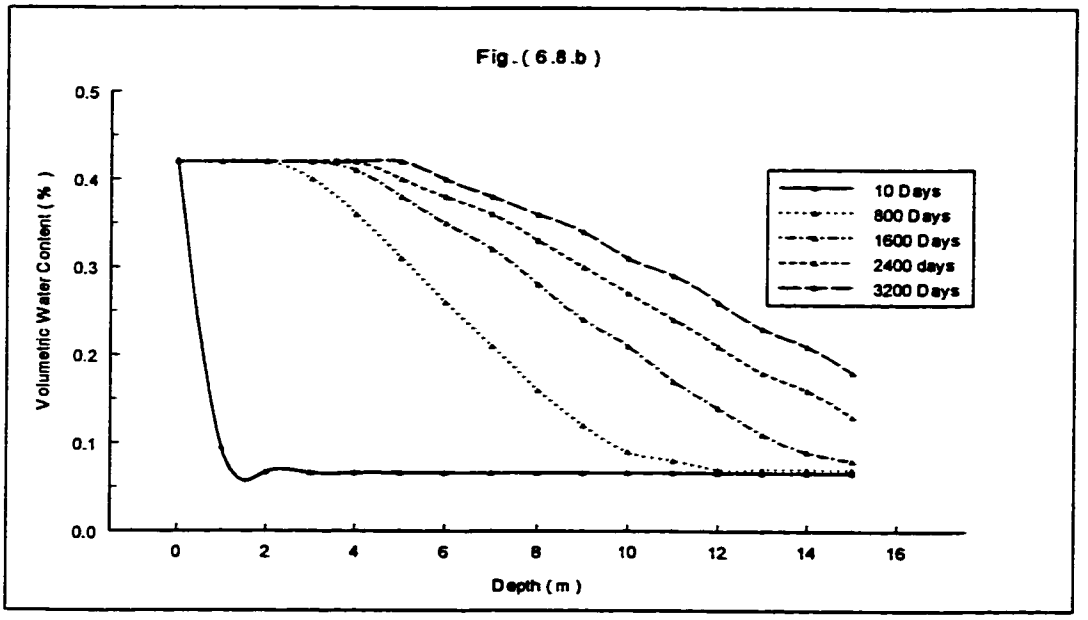

Figure 6.8 Prediction of a) Soil Water Potential and b) Volumetric Water Content

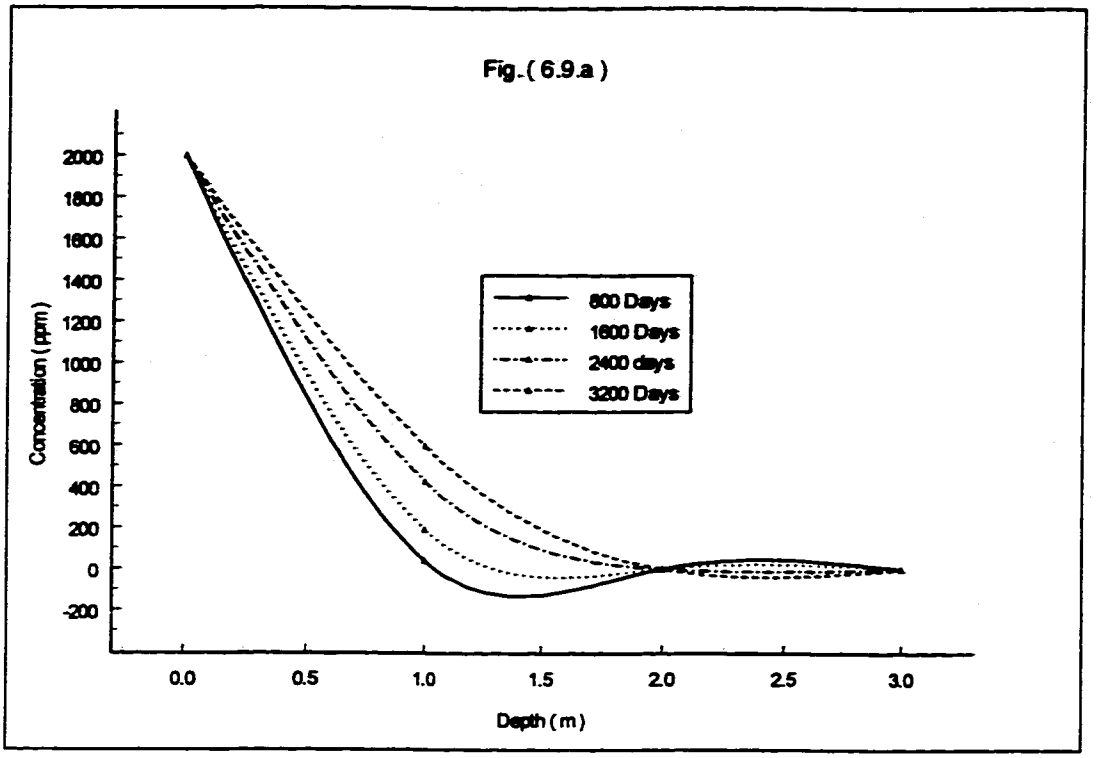

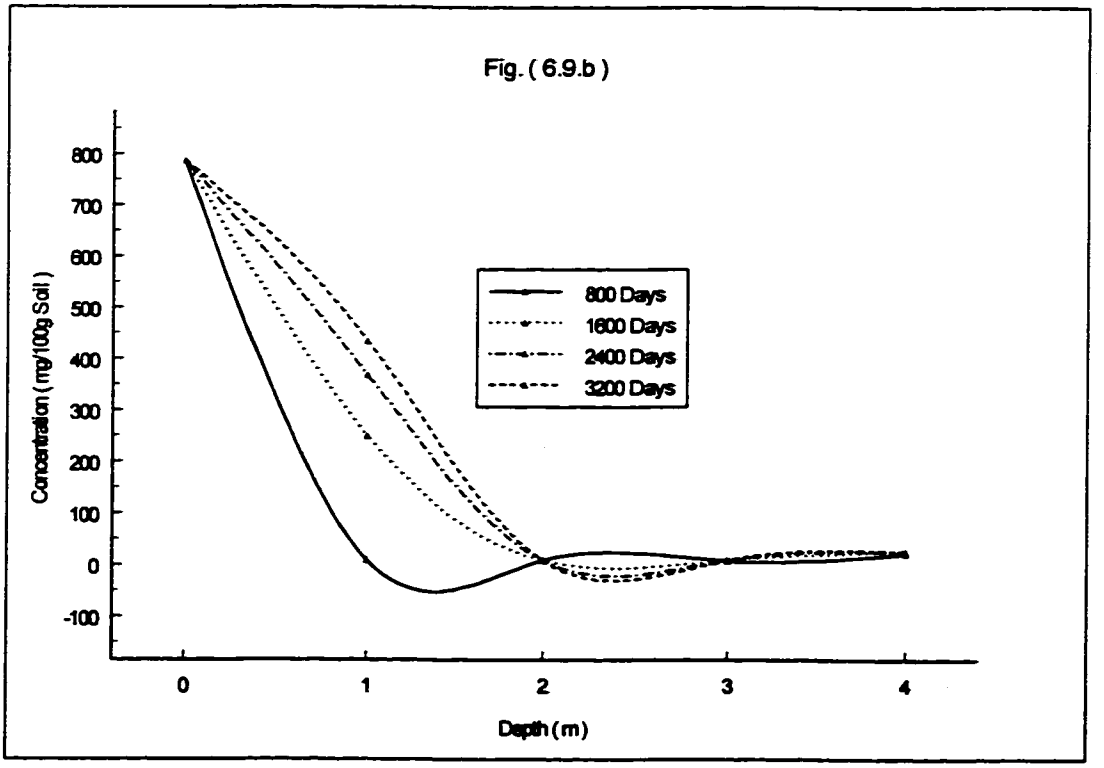

Figure 6.9 Prediction of a) Solution and b) Adsorption Concentration

CHAPTER 7

CONCLUSIONS AND RECOMMENDATIONS

The main objective of this study was to develop a mathematical model which simulates flow and transport processes within unsaturated clay soil. In this chapter the major contributions of the present work are summarized, and conclusions and recommendations for future research are presented.

7.1 SUMMARY

Intrusion of leachate from waste disposal sites through unsaturated soil to the groundwater system, contaminates the source of drinking water. Safety assessment of these sites is related to the mechanism of contaminant transport within unsaturated zone.

The main objective of this study was to develop a mathematical model which simulates flow and transport processes within unsaturated media. The work described proceeded in two stages: *i*) the first stage was an experimental investigation to quantify the various soil-water (solution) interactions that influence the flow and contaminant transport and to derive the constitutive relationships required in mathematical modeling, and *ii*) the second part employed the theory of mass transport to develop contaminant migration mathematical models which include unsaturated flow, hydrodynamic dispersion, and physico-chemical reaction between the solid and the liquid phase.

Theoretical studies were conducted on laws governing the movement of contaminants in unsaturated soil media through a balance equation which takes the form of a partial differential equation. By subjecting this equation to specified initial and boundary conditions, future contaminant species distributions could be predicted. Since the primary carrier for contaminant transport in soil is water, the overall status of water within the soil media was first considered.

The main mechanisms affecting this transport, such as mechanical dispersion, molecular diffusion, solid-solute interactions and various chemical reactions and decay phenomena, were discussed theoretically.

The experimental investigation contains two main sets of laboratory tests: *i*) some independent tests in order to isolate and better understand the individual processes, and *ii*) some tests on experimental models of the real phenomena to verify the related parameters in a combined kinetic situation.

The laboratory tests consists of *i*) saturated hydraulic conductivity, *ii*) soil-moisture retention, *iii*) unsaturated hydraulic conductivity, *iv*) kinetic batch test, followed by *v*) sequential extraction, and *vi*) unsaturated soil column leaching tests.

The experimental investigation was completed by evaluating the results and discussion, in order to better understand the phenomenon behavior, and also to better realize the relationships among related processes. Based on the above mechanisms, the governing equations of the problem is derived to generalize and formulate the behavior of the phenomenon.

Finally, a finite volume algorithm , on the basis of the developed mathematical model, was developed to solve the contaminant transport equations numerically. Details about finite volume method, space and time discretization, linearization method, and programming components are presented in chapter 6 of this dissertation.

The computer code, called CONTRANS, was written in FORTRAN-77, and made versatile by including several features which intend to make it efficient, accurate and user friendly, such as interactive input.

Using experimental results, the numerical model was then calibrated and verified. The developed computer code provides the ability to predict the contaminant migration

for any depth and any period of time. Based on this capability, the concentration variations of the solution along the soil profile, especially for long time periods, were predicted and illustrated.

7.2 CONCLUSIONS

The following comments and conclusions are based upon the results and discussion presented in the previous chapters:

1. The results of saturated hydraulic conductivity test indicate that the variation of initial water content does not have a considerable effect on saturated hydraulic conductivity value. Because, as long as the dry density of the soil is kept constant, the soil structural matrix does not change remarkably. Consequently, the pore size and distribution, and therefore the overall pathway for the fluid (to move through the pore spaces) remain the same, even though the initial water content is different for each test.
2. Using three different dry densities of the soil (100%, 85%, and 55% of $\gamma_{d\,max}$) shows a significant variation for the saturated hydraulic conductivity. Any change in the density of the soil results in a considerable variation in the soil structure, and therefore in the fluid pathway within the soil medium. A 15% decrease in γ_d increases the K_s to more than 200%, whereas, a decrease of 45% in γ_d raises the K_s to 700%, compared to the case which γ_d is equal to $\gamma_{d\,max}$.
3. The saturated hydraulic conductivity K_s, is almost the same as distilled water for solutions of heavy metals at 2000 ppm concentration. According to the Kozeny-Carman equation, fluid properties which can affect the hydraulic conductivity are viscosity and density. None of these parameters has been changed remarkably to have serious effect on the saturated hydraulic conductivity for the soil-solution system.
4. The soil-water retention curve depicts that suction variation, as a function of Θ ($\Psi(\Theta)$), is not unique for imbibition and drainage processes. This difference stems from the phenomenon of hysteresis. In this investigation, the soil-moisture retention

properties exhibit strong hysteretic behavior. Accordingly, Ψ cannot be determined directly from the knowledge of Θ without investigating the past wetting-drying history of the soil under consideration.

5. The unsaturated soil column test results illustrate that the soil water potential variations range is wide at the beginning of the experiment, and becomes very narrow, when the time progresses. This variation is based on the fact that the tendency of the soil particles to absorb water decreases, as they hold more water molecules. The containing moisture in the soil, causes less soil water potential, and therefore less affinity to attract extra moisture.
6. Taking into account significant parameters, the unsaturated hydraulic conductivity ***K(H)***, was introduced for the present study. The formula was used in the numerical modeling to obtain the unsaturated flow unknowns. Since the results of the numerical model and experiments were in agreement, it reveals that the proposed formula is rational.
7. Thermodynamic aspects of reactions occurring in clay and soil systems have received considerable attention over the years. However, kinetic investigations of clay and soil systems have been sparse. This study investigated the principles of chemical kinetics according to the experimental results and showed how these principles can be applied to the kinetics of adsorption and desorption of ions in soil systems. This understanding of the chemical reaction rates will help *i*) to predict how quickly a solution reaction will move to its equilibrium state, and *ii*) to reveal reaction mechanisms. A reaction mechanism can involve the break down of a chemical reaction into a sequence of elementary steps, or a knowledge of reaction mechanisms related to the detailed nature of individual steps in a reaction.
8. Kinetic batch test results, show two major zones for the variation of adsorption and desorption processes: *i*) ***sharp***, and *ii*) ***smooth*** zones. Regarding to the sharp zone, adsorption and desorption rates are very high (more than 80% of the equilibrium concentration level) at the beginning of the experiment, whereas these rates decrease (below 20%) if the samples are taken later. The high rate of variation in the sharp zone is expected, because at the beginning, soil particles benefit from their highest

potential to adsorb or desorb the solute species, whereas this high tendency is reduced as the adsorption or desorption process progresses.

9. Performing isothermal batch tests, very often 24 hours is considered as the adequate duration to obtain the equilibrium concentration of the adsorption process. According to the result of kinetic batch test, the required time interval is more and sometimes less than 1 day. Thus, to be conservative in obtaining the equilibrium concentration of adsorbed and/or desorbed contaminant species, a minimum of 48 hours is recommended to keep the test running.
10. The smooth zone of the graph exhibits a very low range of fluctuation (compared to the Sharp zone) within the variation bound which is limited to 20% of the equilibrium concentration. This variation does not diminish even in a long time period, therefore it could be considered as a completely reversible process. The reversibility is induced by physical adsorption in a very weak bounding of contaminant species onto the soil particles surfaces.
11. According to the desorption experiments results, the sharp zone reversibility is not considerable, especially if the solution does not contain any particular reagent to help desorption of contaminant species (i.e., distilled water). Using some chemical reagents increases the amount of the desorbed species, and this enhancement could be extended to desorb the entire exchangeable cations from the soil particles surfaces.
12. Adsorption concentration variations with respect to time strengthen the idea of the 2 stage adsorption process. The first stage (the sharp zone) is mostly related to the adsorption within or very close to the first layer; whereas the second stage (the smooth zone) is concerned with the species adsorbed within the second diffuse double layers of the soil particle surface.
13. The results of kinetic batch test reveals that the concentration variations along time variations, for the adsorption/desorption of the species onto/from soil particle surfaces is neither linear, nor limitless. Thus, among 3 very common adsorption/desorption models, these results are in agreement with the Langmuir model which accepts a limit for adsorption within a soil-solution system.

14. According to the figures concerned with the adsorption process, lead shows the highest adsorbed species concentration, about 2 times those of copper and zinc. This remarkable difference is due to the considerable difference among the hydrated radii of these metals. The smaller the hydrated radius, the easier and faster the adsorption onto the soil particle surfaces.
15. Zinc and copper exhibit adsorption rates close to each other, however zinc has a higher adsorption rate than copper. Even though the hydrated radius of zinc is almost equal to that of copper, having a higher solubility product coefficient K_{sp}, induces a higher adsorption rate for Zn^{2+} than Cu^{2+}. Higher solubility product coefficient provides more ion availability and more of a concentration gradient, and as a result more adsorbed species.
16. The figures concerning desorption of the 3 heavy metals illustrate that Cu^{2+} has the lowest desorption and Pb^{2+} the highest. This is due to the fact that Cu^{2+} has the lowest ionic radius while Pb^{2+} has the highest (45% larger than Cu^{2+}). If the ionic radius gets larger, the attraction force of the negative charge of soil particle surfaces to the cations is reduced. Consequently, the extraction of the ion becomes easier and the desorption process is facilitated.
17. The combined effect of time and initial solution concentration on the adsorption/desorption concentration, was presented in the form of a mathematical model. According to this model, the effect of time duration diminishes after a short time, therefore, adsorption/desorption concentration is predominantly governed by the initial solution concentration statement.
18. According to the sequential extraction results, the exchangeable cations phase dominates the total adsorption , resulting from low pH value ($pH \leq 4.0$). However, the amount of residue is also considerable, indicating that the amount of adsorption in forms of hydroxides and oxides are not negligible. This is due to the change in heavy metals speciation as the soil solution pH changes. Since, at a low pH value heavy metals species are present in the solution as free cations, the retention mechanism of heavy metals in the soil is mostly by cation exchange rather than residue phase.

19. Comparing the amount of residue phase of 3 heavy metals at the same c_{init} reveals that the amount of residue phase for lead is about 2.6 times higher than copper. However, this amount is negligible for zinc solution. This difference stems from the difference of the affinity of various heavy metals, in combining with the oxygen of the soil particles and forming the oxides and hydroxides of the heavy metals on the soil particles surface. Among the 3 heavy metals, lead has the highest affinity for these reactions, while zinc has the lowest.
20. The clay soils can retain heavy metals by several means, such as exchangeable cations, hydroxide, and oxide phases. However, the retention of heavy metals in any phase depends on soil constituents, soil solution pH, and heavy metals themselves. Kaolinite cannot retain considerable amount of metals by the hydroxide and oxide phases, because of its low initial pH.
21. The results of the sequential extraction analysis support the idea that the soil buffer capacity in relation to heavy metals is significant. However, kaolinite could not retain high amounts of heavy metals, because the soil cannot support the retention by precipitation phases due to kaolinite low initial pH and low buffer capacity.
22. It can be observed from the soil column leaching test result, that the concentration varies very sharply at the beginning of the experiment along the soil column. In addition, concentration changes very slowly with time. For instance, it is very difficult to have a detectable solution concentration after 30 days at 25 cm depth of the soil column. Both of the two latter findings are due to the adsorption of heavy metals on the soil particles, which remarkably affects migration of cations within the soil column.
23. In order to compare the variations of different phases of the adsorption process between batch test and column leaching test, the sequential extraction test was repeated for the soil samples obtained from the column test. It can be observed from the results that the variation trend for both tests is very close. This similarity determines, regardless of how the contaminant species reach and adsorb to the soil particle surfaces, the percentage of the various phases of adsorption process are the same for all cases.

24. The relative concentration of lead was less than copper and zinc. These results indicate that the mobility order of the heavy metals in the soil column follows Pb< Zn < Cu. Elliott et al. (1986) also found the same trend of heavy metal mobility order in their study, based on the inverse proportionality to the hydrated radii.
25. In order to complete the simulation of the adsorption process within the soil column, the adsorption formula for the batch test could be considered as a base for this simulation. The most significant additional parameter to be considered is volumetric water content. Accordingly, the completed form of the one dimensional formula to simulate the adsorption process within the soil medium was proposed and implemented in numerical modeling to find soil solution concentration, and adsorption concentration, as functions of time and depth, simultaneously. The results from the numerical model have been verified with the one from experiments which conform to each other, perfectly.
26. The soil column leaching test can give an idea of how heavy metals might be retained or migrate within the soil. Also the study on heavy metal retention by sequential extraction test could be utilized to predict heavy metal movement in a soil column to some extent.
27. The results obtained from the determination of the soil buffer capacity, the sequential extraction analysis, and the experiment of soil column leaching tests provide a good picture of the role of the soil buffer capacity in the retention of heavy metals. This could help in the selection of a landfill site, along with other geological and physical factors to be considered in this regard.
28. It was also concluded from the experimental analysis that the model is very sensitive to the sink/source parameters, such as adsorption partitioning coefficient. Most of these parameters are not readily available in the literature, therefore, their applicability is limited.
29. The correlation factors between numerical and experimental results were above 95% in all comparisons. As a result, the proposed finite volume model behaves as predicted, maintaining good accuracy and non-oscillatory properties. The numerical solutions obtained for all cases, compare favorably with experimental results. Thus,

the provided computer code can be utilized to predict the contaminant migration rate through unsaturated soil, and evaluate the safety of waste disposal sites as well.

7.3 RECOMMENDATIONS FOR FUTURE RESEARCH

Although a great deal of insight has been obtained in this study concerning the phenomenon of contaminant transport in porous media, the conclusions given in the preceding section are based on the results of analyses in which many idealizations and assumptions have been made. Prior to assuming that these conclusions can be generally acceptable for other similar cases, further research is necessary. Some of the pertinent points that need further investigation may be described as follows:

1. It seemed evident from the discussion of the experimental results that soil-matrix-soil-solution interaction has a significant impact on the transport phenomena. Therefore, the experimental investigation presented here should be extended to include different types of soils as well as different chemicals at different concentrations.
2. Although the model developed in this study takes a variety of complex physico-chemical processes into account there are nevertheless some other processes which could be considered in true modeling of the phenomenon, such as plant uptake, radioactive decay, and biodegradation. Inclusion of such factors will improve the proposed model to be more complete and realistic.
3. Several simplifying assumptions have been made to describe the transport phenomena mathematically. Some of these assumptions have been found in literature extensively. Among these assumptions, the negligence of air flow through the porous media is the one that requires further investigation. Hence, if a more complete model is to be developed, an equation describing the air flow in the unsaturated zone has to be solved simultaneously with the moisture flow equation.
4. The partitioning of the chemical into different phases has been assumed to be in equilibrium at all times, and this requires further investigation in order to determine the effect on the predicted maximum liquid phase concentration values. For this

reason, kinetic models which describe the partitioning of chemicals transiently are required to be included in the model. Coupled equations for each phase should be solved simultaneously.

5. The model input parameters require further experimental investigation and calibration, especially for the processes where field data are not readily available in the literature. Thorough experimental studies should be conducted for each of the key processes in laboratory and particularly in situ to quantitatively establish ranges for the input parameters.
6. The numerical model presented in this study could be enhanced further by including other transport mechanisms, such as biodegradation and volatilization. This can be achieved with minor programming efforts. In addition, for the purposes of calibration and verification of the model it is highly recommended that the actual field data be utilized to validate the model.
7. It is recommended further application of the proposed numerical model for the flow and transport equations, in order to gain a better understanding of the physical processes within partially saturated porous media. Accordingly, the capability of the model could be examined through application for other kinds of soils and contaminated solutions.
8. Finally, this investigation could be extended to two- and three- dimension to study the transport phenomena more accurately. Furthermore, the laboratory techniques and numerical methods utilized in this work may be extended for multi-fluid porous media studies which offers a natural avenue for further research.

BIBLIOGRAPHY

Abriola, L.M. and G.F. Pinder, "A multiphase approach to the modeling of porous media contamination by organic compounds, 1. Equation development. " Water Resour. Res., 21(1), 11-18,1985a

Aharoni c. and Sparks DL., Kinetics of soil chemical reactions, Soil Sci. Soc. Amer., Madison, WI, 1991.

Ahlert, W.K., Katz, J., and Uchrin C.G., On the validity of partition coefficients, Pollution, Risk Assessment, and Remediation in Groudwater, pp 295-320, Scientific Publications Co, Washington, D.C., 1987

Ahuja, L.R. and Swartzendruber, D., An improved form of soil-water diffusivity function, Soil Sc. Am. Proc. Vol. 36, pp.9-14, 1972.

Airey, D.W., Migration of a pollutant through a natural clay liner, Geotechnical Management of Waste and Contamination, Fells, Philips, and Gerrard, pp323-328, 1993

Allison, G. B.; Gee, G. W.; Tyler, S. W., vadose-zone techniques for estimatinggroundwater recharge in arid and semiarid regions, Soil Science Society of America Journal, v 58, p 6-14, January/February 1994

Alloway, B.J., Heavy metals in soils, John Wiley and Sons Inc., 1990.

Amoozegar, A., a compact constant-head permeameter for measuring saturated hydraulic conductivity of the vadose zone, Soil Science Society of America Journal, v 53, p 1356-61, September/October 1989

Anderson, D.A., Tannehill J.C., Pletcher R.H., Computational fluid mechanics and heat transfer, Hemisphere Publishing Corporation, 1984

Aronson, D.G., Regularity of flows in porous media, in W.M. Ni et al., (eds) Nonlinear diffusion equations and their equilibrium states I, Springer-Veriag, 1988.

Barone, F.S., Description of diffusion and adsorption coefficient used for modeling contaminant migration through clayey soil, Geotechnical News, v 11-4, pp 47-49, 1993

Bear, J. and Bachmat, Y., Introduction to modeling of transport phenomena in porous media, ISBN 0-7923-0557-4, 1990.

Bear, J., Dynamics of fluid in porous media, American Elsevier, New York, 1972

Bear, J., Hydraulics of groundwater, Mc Graw-Hill, 1978.

Bear, J., Hydrodynamic dispersion in flow through porous media (R. J. M. De Wiest, Ed.), Chap. 4, pp. 109-200, Academic Press, New York, 1969.

Bruce, R. R. and Klute A., The measurement of soil moisture diffusivity, Soil Sci. Soc. Am. J. Vol. 20, pp.458-462, 1956

Brusseau, M. L., factors influencing the transport and fate of contaminants in the subsurface, Journal of Hazardous Materials, v 32, p 137-43, December 1992

Brutsaert, W., The concise formulation of diffuse sorption of water in a dry soil, Water Resources research, v 12, no 6, pp 1118-1124, 1976

Buckingham, E., Studies on the movement of soil moisture, Bur. Soils Bull., v 38 U.S. Dep. Of Agric., Washington D.C., 1907

Campbell, G.S. " A simple method for determining unsaturated conductivity from moisture retention data," Soil Science, 117:311-314, 1974

Carnahan, B., Luther, H.A., Wilks, J.O., Applied numerical methods, John Wiley and Sons, New York, 1969

Celia M.A., Ahuja, L.R., and Pinder, G.F., Orthogonal colloction and alternating-direction procedures for unsaturated flow problems, Adv. Water Resources, v 10, pp178-187, 1987

Celia M.A., Bouloutas E.T., and Zabra, R., On mass conservation properties of numerical solutions of unsaturated flow, Submitted to Water Resources Research, 1989

Chandler, R.J., Koplic, K.L., Willemesen, J.F., Capillary displacement and percolation in porous media, J. Fluid Mech., v 119, pp 249-267, 1982

Chen, X., Wright, J. V., Conca, J. L., effects of pH on heavy metal sorption on mineral apatite, Environmental Science & Technology, v 31, p 624-31, March 1997

Childs, E.C., and Collis-george, N., The permeability of porous materials, Proc. Roy. Soc. (London) A, 201, 392-405, 1950

Clapp, R.B., Hornberger, G.M., Empirical equations for some soil hydraulic properties, Water resources Research, v 14, no 4, pp 601-604, 1978

Clemente, R. S.; De Jong, R.; Hayhoe, H. N., testing and comparison of three unsaturated soil water flow models, Agricultural Water Management, v 25, p 135-52, April 1994

Cook, A.B., Physical modeling of contaminant transport in unsaturated zone, Geotechnical Management of Waste and Contamination, Fells, Philips, and Gerrard, pp 343-348, 1993

Cooley, R.L., A finite difference method for unsteady flow in variably saturated porous media: Application to a single pumping well, Water Resources Research, v 7, no 6, pp 1607-1625, 1971

Coughlin, B. R.; Stone, A. T., nonreversible adsorption of divalent metal ions (M[supII], Co[supII], Ni[supII], Cu[supII], and Pb[supII]) onto goethite: effects of acidification, Fe[supII] addition, and picolinic acid addition, Environmental Science & Technology, v 29, p 2445-55, September 1995 ; Discussion v30, p1411-12, April 1996

Davidson, J.M., and Mcdougal, J.R., Experimental and predicted movement of three herbicides in a water saturated soil, J. Environm. Quality, v 2, pp 428-433, 1973

Dullien, F.A.L., "Porous media: Fluid transport and pore structure," Academic Press, New York, 1979

Einstein, A., Uber die von der molekular kinetischen theorie der warme geforderte bewegung von in ruhenden flussigkeiten suspendierten teilchen, Annualen der physick, 4, 17, 549-660, 1905

Freeze, R. A. and Cherry, J. A., Groundwater, Prentice-Hall Inc. London, 604 p, 1979.

Fried, J. J., Groundwater pollution, In Development in Water Science, Am. Elsvier, New York, 330 p, 1975

Gillham, R.W., and Cherry, J.A., Contaminant migration in saturated unconsolidated geologic Deposits, Recent Trends in Hydrogeology, Et. T.N. Narasimhan, geological Soc. Of America, Special Paper 189, pp 31-62, 1982

Grossl, P.R., Sparks, D.L., Ainsworth, C.C., rapid kinetics of Cu(II) adsorption/ desorption on goethite, Environmental Science & Technology, v 28, p1422-9, August 1994

Huyakorn, P.S., Jones, B.G., and Andersen, P.F., Finite element algorithms for simulating three-dimensional groundwater flow and solute transport in multilayer systems, Water Resources Research, v 22 (3), pp 361-374, 1986

Janna, W.S., Introduction to fluid mechanics, 3rd edition, PWS Publishers, 1985

Jiao, J.J., Data-analyses methods for determining two dimensional dispersive parameters, Groundwater, vol. 31, No. 1, pp. 57-62, 1993

Johnson, R.L., Cherry, J.A., and Pankow, J.F., Diffusive contaminant transport in natural clay: a field example and implications for clay-lined waste disposal sites, J. Environmental Science and Technology, v 23, no 3, pp 340-349, 1989

Khan, S. A.; Riaz-ur-R.; Khan, M. A., Sorption of cesium on bentonite, Waste Management, v14 no7, p 629-42, 1994

Klute, A. A numerical method for solving the flow equation for water in unsaturated materials, Soil Sci., pp 73: 105-116, 1952

Lapidus, L. and Pinder, G.F., Numerical solution of partial differential equations in science and engineering, John Wiley and Sons, 1982

Lee, S., Allen, H. E., Huang, C. P., predicting soil-water partition coefficients for cadmium, Environmental Science & Technology, w 30, p 3418-24, December 1996

Lehmann, F., Ackerer, P., determining soil hydraulic properties by inverse method in one-dimensional unsaturated flow, Journal of Environmental Quality, v 26, p 76-81, January/February 1997

Lehmann, F., Ackerer, P., determining soil hydraulic properties by inverse method in one-dimensional unsaturated flow, Journal of Environmental Quality, v 26, p 76-81, January/February 1997

Lerman, A., Geochemical processes: water and sediments environments, John Wiley and Sons, New York, 1979

Lim, P.C., Barbour, and Fredlund, D.G., Effect of degree of saturation on the adsorption characteristics of inorganic chemical in unsaturated soils, 2000 Geoenvironmental, v 1, Geotechnical Special Publication, no 46, pp 816-817, 1995

Lindstorm, F.T., and Boersma, L., Theory of chemical transport with simultaneous sorption in water saturated porous medium, Soil Sci. , v 110, no 1, pp 1-9, 1970

Meyer, J. J. and Warrick, A. W., Analytical expression for soil water diffusivity derived from horizontal infiltration experiments, Soil Sci. Soc. Am. J. Vol. 54, pp. 1547-1552, 1990.

Michell, J.K., Fundamentals of soil behavior, John Wiley and Sons Inc., 1976

Mohamed, A. M. O., Yong R. N. and Cheung S. C. H., Temperature dependence of soil water potential, ASTM, Geotech. Testing J., GT JODJ, Vol. 15, No. 4, pp. 330-339, 1992.

Mohamed, A. M. O., Yong, R. N. Caprouscio, F., Cheung, S. C. H., and Kjartanson, B.H., A coupled heat and water flow apparatus, Geotech. Testing J., GT JODH, Vol. 16, No. 1, pp. 85-99, 1993.

Mohammad, A.M.O., Shooshpasha, I., and Yong, R.N., Boundary layer transport of metal ions in frozen soil, Int. J. for Numerical and Analytical Methods in Geomechanics, 1995

Mualem, Y., "Anew model for predicting the hydraulic conductivity of unsaturated porous media," Water Resource Research, 12:513-522,1976

Mualem, Y., A new model for predicting the hydraulic conductivity of unsaturated porous media. Water Resource Research, 12: 513-522, 1976

Nernst, W., Zur kinetik der in losuny befinlichen korper, Zeitschrift fur physikalishe chemie, 2, 613-637, 1888

Patankar, S.V., Numerical heat transfer and fluid flow, McGraw-Hill, 1980

Petruzzelli D., and Lopez A., Solid-phase characteristics and ion-exchange phenomena in natural permeable media, NATO ASI Series, Vol. G32, 1993.

Philip, J. R. and Smiles D. E., Kinetics of sorption and volume change in three-component system, Aust. J. Soil Res., Vol. 7, pp. 1-19, 1968.

Philip, J. R., Theory of infiltration, in Advances in Hydroscience (V. T. Chow, Ed), 5, 215-296, Academic Press, New York, 1969

Pinder, G.F. and L.M. Abriola, "On the simulation of nonaqueous phase organic compounds in the subsurface, " Water Resour. Res. , 22(9), 109S-119S, 1986.

Pinder, G.F. and W.G. Gray, "Finite element simulation in surface and subsurface hydrology, " Academic Press, New York, 1977.

Porter, L.K., Kemper, W.D., Jakson, R.D., and Stewart, B.A., Chloride diffusion in soils as influenced by moisture content, Proceedings Soil Science Society of America, v 24, pp 460-463, 1960

Quigly, R.M., Clay minerals against contaminant migration, Geotechnical News, v 11-4, pp 44-47, 1993

Ragab, R., Feyen, J., and Hillel, D., Comparative study of numerical and laboratory methods for determining the hydraulic conductivity function of a sand, Soil Sci., v 131 (5), pp 375-388, 1981

Rao, P.S.C., and Davidson, J.M., Estimation of pesticide retention and transformation parameters, Environmental Impact of Nonpoint Source pollution, Ann Arbor Science Publications, Ann Arbor, MI, 1980

Richards, L.A., Capillary conduction of liquids in porous media, Physics, v 1, pp 318-333, 1931

Rowe, R.K., Contaminant migration in soils introduction, Geotechnical News, v 11-4, pp 39-40, 1993

Rowe, R.K., Diffusive transport of pollutants through clay, Landfillings of Waste Barriers, Edited by Christensen, T.H., Cossu, R., Stegmann, R., 1994

Saffman, P. G., A theory of dispersion in a porous medium, J. Fluid Mech., 6(3), 321-349, 1959.

Saffman, P. G., Dispersion due to molecular diffusion and macroscopic mixing in flow through a network of capillaries, J. Fluid Mech., 7(2), 194-208, 1960.

Samani, H.M.V., Mathematical modeling of contaminant transport through clay soils using irreversible thermodynamics, Ph.D. Thesis, department of Civil Eng. And Applied Mechanics, McGill University, Montreal, 1987

Schakelford, C.D., waste-soil interactions that alter hydraulic conductivity, Hydraulic Conductivity and Waste Contaminant Transport in Soil, ASTM STP 1142, David E. Daniel and Stephen J., Trautwein, Eds., American Society for Testing and Materials, pp 111-183, 1994

Schakelford, Diffusion as a transport process in fine grained barrier materials, Geotechnical News, v 6, no 2, pp 24-27, 1988

Silvestri, V., Tabib, C., Behidj, F., Observations and modeling of soil water content changes around trees, Canadian J. of Civil eng., v 21, n 6, pp 980-989, 1994

Silvestri, V., Tabib, C., Behidj, F., On the modeling of water content changes in clay deposits, Canadian Geotechnical Conference, pp 980-989, 1995

Soll, W.E., Ferrand, L.A., and Celia, M.A., An enhanced percolation model for capillary pressure-saturation relations, Proceedings of VII Intl. Conf. On Computational Methods in Water Resources, Southampton, UK, 1988

Streck, T., Richter, J., heavy metal displacement in a sandy soil at the field scale Measurements and parameterizations of sorption, Journal of Environmental Quality, v 26, p 49-56, January/February 1997

Sykes, J.F., Pahwa, S.B., Lantz, R.B., and Ward, D.S., Numerical simulation of flow and contaminant migration at an extensively monitored landfill, Water Resources Research, 1982

Tim, U. S.; Mostaghimi, S., modeling phosphorus movement and distribution in the vadose zone, Transactions of the ASAE, v 32, p 655-61, March/April 1989

Trescott, P.C., Documentation of finite difference model for simulation of three-dimensional groundwater flow, Technical report, U.S. Geological Survey, July 1976

Uchrin, C.G., Sorption kinetics and equilibria of organic chemicals to soils, Groundwater Hydrology, Contamination and Remediation, pp 323-338, Scientific Publications Co., Washington, D.C., 1986

Van der zee, S.E.A.T.M., and J.C.M. de Wit, Theoretical and practical aspects of soil chemical behavior of contaminants in soil, NATO ASI Series, Vol. G32, pp. 27-45, 1993.

Van Genuchten, M.Th. "A closed-form equation for predicting the hydraulic conductivity of unsaturated soils," Soil Science Society of America Journal, 44:892-898,1980

Van Genuchten, M.TH., Models for describing water and solute movement through soils with large pores. Agronomy Abstracts, Amer. soc. of Agron., 1980.

Vellidis, G.; Smith, M. C.; Thomas, D. L., detecting wetting front movement in a sandy soil with ground-penetrating radar, Transactions of the ASAE, v 33, p 1867-74, November/December 1990

Walter J. and Weber Jr., Contaminant sorption and retardation, NATO ASI Series, Vol. G32, pp. 3-26, 1993.

Warith, M.A., Migration of leachate through clay soil, Ph.D. Thesis, Dept. of Civil Eng. And Applied Mechanics, McGill University, Montreal, 1987

Weber J. Jr., Mc Ginley PM, Katzle, A distributed reactivity model for sorption by soils and sediments, Env. Sci. Tech. in Press, 1992.

Yeh, G.T., and Ward, D.S., A finite element model of waste transport through saturated-unsaturated porous media, Rep. ORNL-5601, Oak Ridge, TN., 1981

Yin, Y., Allen, H. E., Huang, C. P., kinetics of mercury(II) adsorption and desorption on soil, Environmental Science & Technology, v 31, p 496-503, February 1997

Yong, R. N. and Samani, H. M. V., Modeling of contaminant transport in clays via irreversible thermodynamics, Proceedings of Geot. Practice for Waste Disposal, 87/GT Div. ASCE, pp. 846-860, 1987.

Yong, R. N., and Warith, M., Contaminant migration effect on dispersion coefficients, ASTM, STP 1095, pp 69-80, 1990

Yong, R. N., and Warkentin, B. P., Soil properties and behavior, Elsevier, New York, 1975

Yong, R. N., Mohamed A.M.O. and Warkentin, B. P., principle of contaminant transport in soils, Elsevier Scientific-Publishers B.V. Sara Burgerhartstraat 25, 1992.

Yong, R. N., Mohamed A.M.O. and Warkentin, B. P., principle of contaminant transport in soils, Elsevier Scientific-Publishers B.V. Sara Burgerhartstraat 25, 1992.

Yong, R.N. and Cabral, A.R. , A clay-heavy metal compatibility analysis using permeability testing, 45th Canadian Geot. Confe., Canadian Geotechnical Society, Toronto, October 1992.

Yong, R.N., Mohammad, A.M.O., and Shooshpasha, I., Thermal and moisture diffusivity in buffer material due to temperature and hydraulic gradients, Report Prepared for Atomic Energy of Canada Limited, Pianawa, Manitoba, 1994

Zhang, J., Yeh, T.-C. J., an iterative geostatistical inverse method for steady flow in the vadose zone, Water Resources Research, v 33, p 63-71, January 1997

Zhang, R.; Yang, J.; Ye, Z., solute transport through the vadose zone: a field study and stochastic analyses, Soil Science, v 161, p 270-7, May 1996

Zienkiewiez, O.C., The finite element method, 3rd Edition, McGraw-Hill, New York, 1977

Zou, S. and A. Parr., Estimation of dispersion parameters for two-dimensional plums, Groundwater, Vol. 31, No. 3, pp. 389-392, 1993.

APPENDICES

APPENDIX 1. Some Properties of Kaolinite Soil (Hydrate PX)

In order to determine the soil mineralogy, X-ray diffraction analysis was performed on an oriented sample mount, which was prepared by pipeting 4 ml of a 1% clay suspension on to a glass slide and allowing it to air dry. X-ray diffractogram is given in Fig. (App. 1).

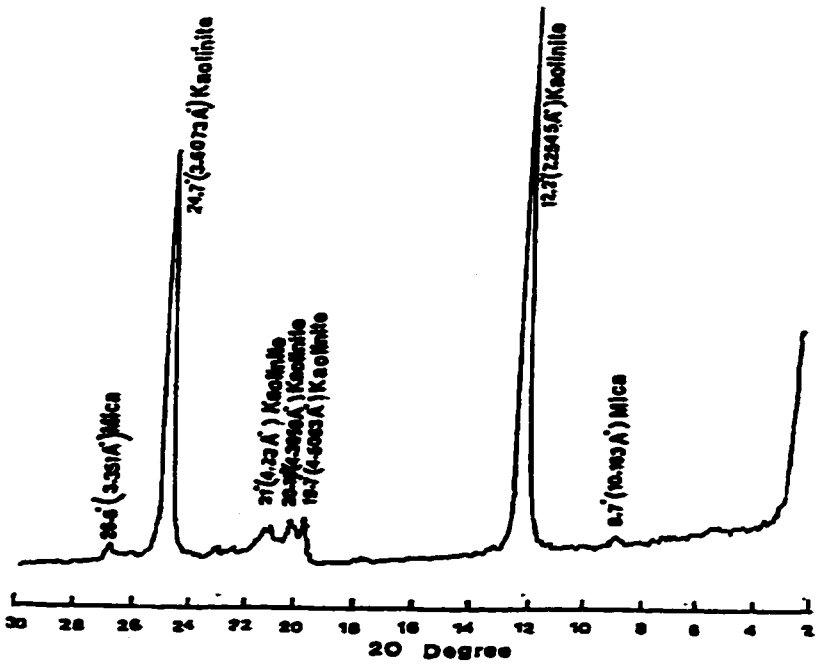

Figure App.1 X-Ray Diffraction Analysis for Kaolinite Soil (Hydrate PX)

Some physical properties of the soil under consideration is introduced in Table 1.

Table App. 1 Some Physical Properties of the Soil	
Soil Properties	Quantity
Medium Particle Size (Micron)	0.68
Surface Area ($m^{2/gr}$)	12
Specific Gravity	2.58
Cation Exchang Capacity (meq/100gr)	10

The result of chemical analysis of the soil is presented in Table App. 2.

Table App. 2 Soil Chemical Properties	
Material	Percentage
Aluminum Oxide (Al_{2O3}), combined	38.8
Silicon Dioxide (SiO_2), combined	45.2
Iron Oxide (Fe_{2O3})	0.3
Titanium Dioxide (TiO_2)	1.4
Calcium Oxide (CaO)	0.05
Magnesium Oxide (MgO)	0.3
Sodium Oxide (Na_{2O})	0.3
Potassium Oxide (K_{2O})	0.05
Loss on Ignition at 950^{oC}	13.6

APPENDIX 2. Analysis of Leachate Collected from A Disposal Site

The analysis of leachate collected from a disposal site in Lachena (35 Km east of Montreal) is presented in Table (App. 3). This analysis has been reported by the Environment Canada in 1979.

Table App. 3 Leachate Analysis of a Disposal Site

Parameter	ASTM Test no. (1984)	Ion Conct. (mg/l)	Drinking Water Standard (mg/l)
BOD	D 888	450	40
COD	D1252	860	100
TOC	D2579	190	---
TC	D2579	289	---
Oil & Grease	D4281	24	15
Phenol	D1783	0.04	0.02
Total Iron	D1068	5.0	17
Mg	D 511	35	150
Ca	D 511	180	200
K	D4192	16	---
Na	D4191	140	270
NH_3	D1426	20.0	0.5
Cl	D1253	190	250
CO_3	D 513	0.0	---
HCO_3	D 513	303	---
pH	D1293	6.8 (pH units)	---
Spec. Elec. Cond.	D1125	2.7×10^3 mho/cm	23.0 mho/cm
Zn	D1691	2.5	5.0
Pb	D3551	1.0	0.05
Cu	D1688	1.7	1.0

APPENDIX 3. Calibration Curves for the Utilized Thermocouple Psychrometers

Calibration curves for 5 utilized Thermocouple Psychrometers are presented in the following figures.

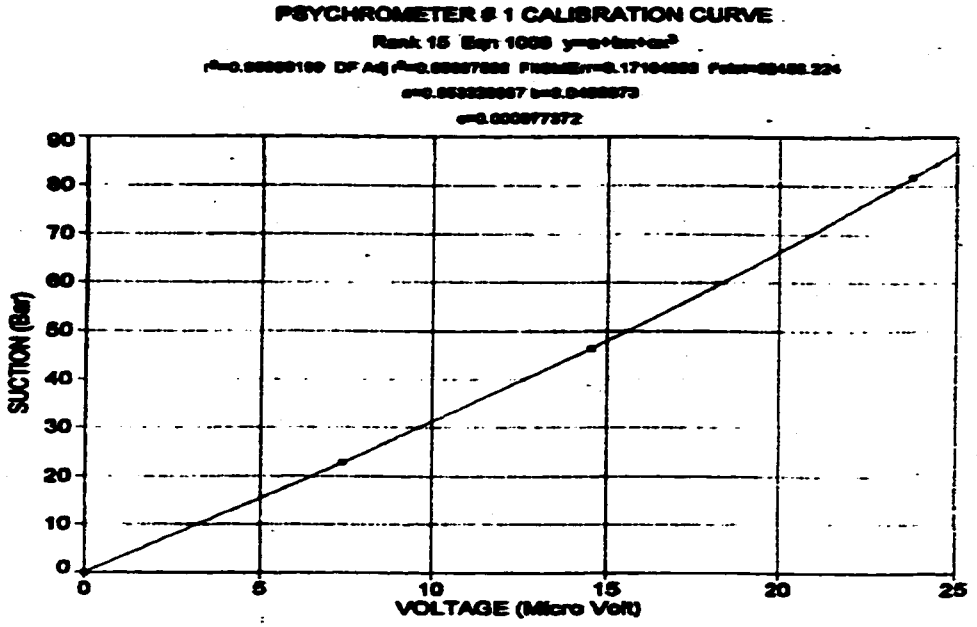

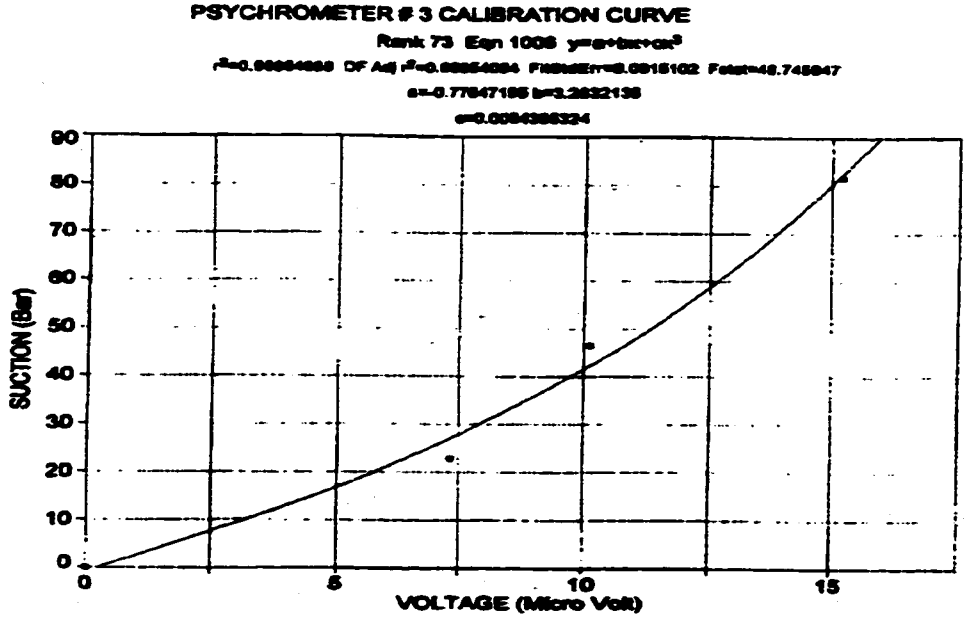

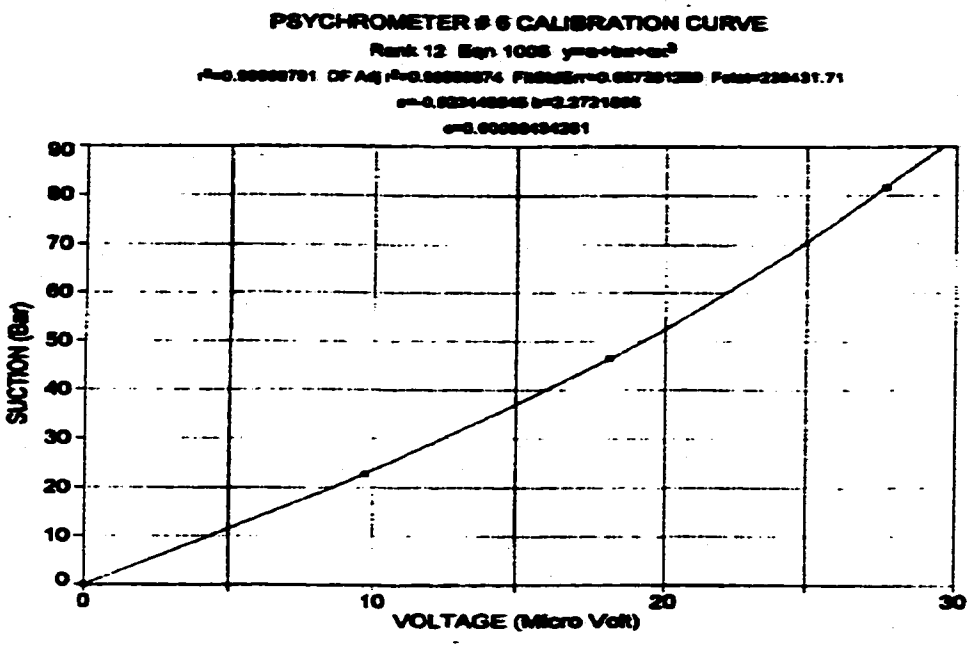
PSYCHROMETER # 6 CALIBRATION CURVE
SUCTION (Bar)
VOLTAGE (Micro Volt)
0
10
20
30
40
50
60
70
80
90

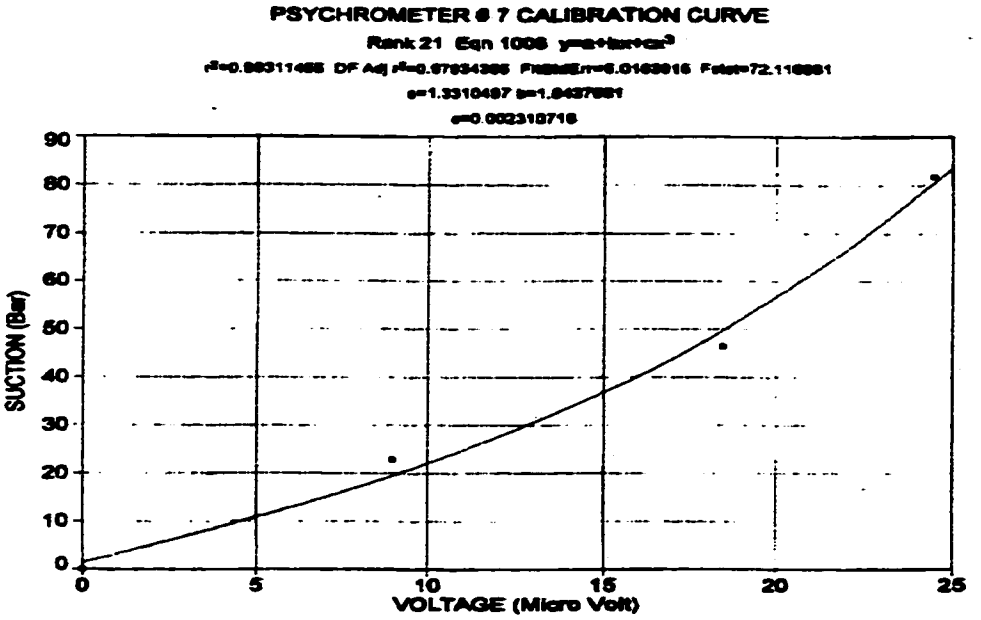
PSYCHROMETER # 7 CALIBRATION CURVE
SUCTION (Bar)
VOLTAGE (Micro Volt)
0
5
10
15
20
25
10
20
30
40
50
60
70
80
90

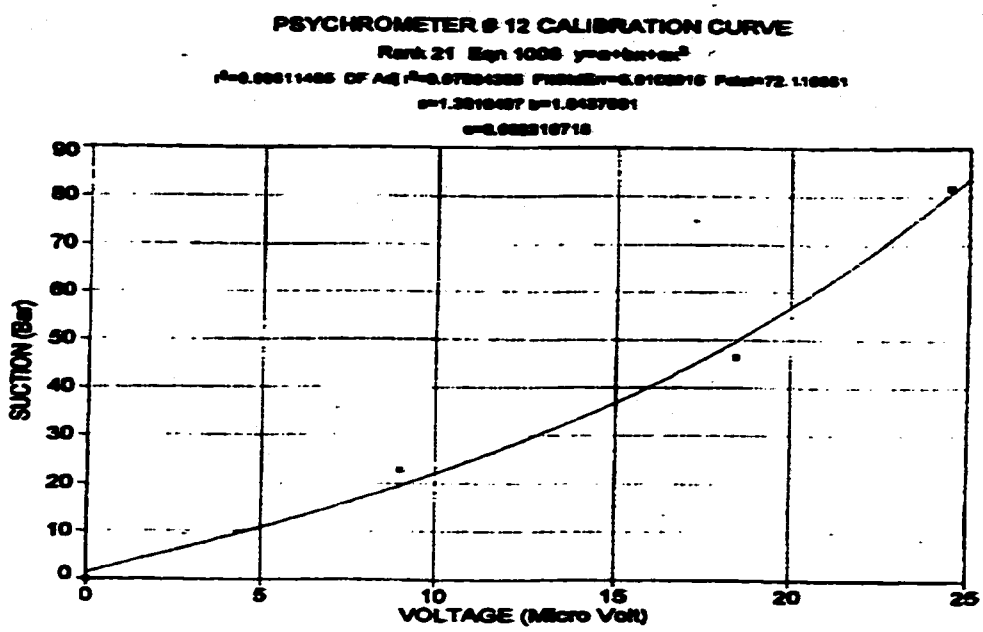
PSYCHROMETER @ 12 CALIBRATION CURVE
SUCTION (Bar)
VOLTAGE (Micro Volt)
0
10
20
30
40
50
60
70
80
90
0
5
10
15
20
25

APPENDIX 4. Adsorption and Desorption Concentrations 2-D and 3-D Graphs for $CuCl_2$ and $ZnCl_2$ Solutions

This appendix contains 6 figures concerning $CuCl_2$ and $ZnCl_2$ Solutions. These figures illustrate the variation of adsorption and desorption concentrations with respect to time (2-D graphs) and initial concentrations of the solution (3-D).

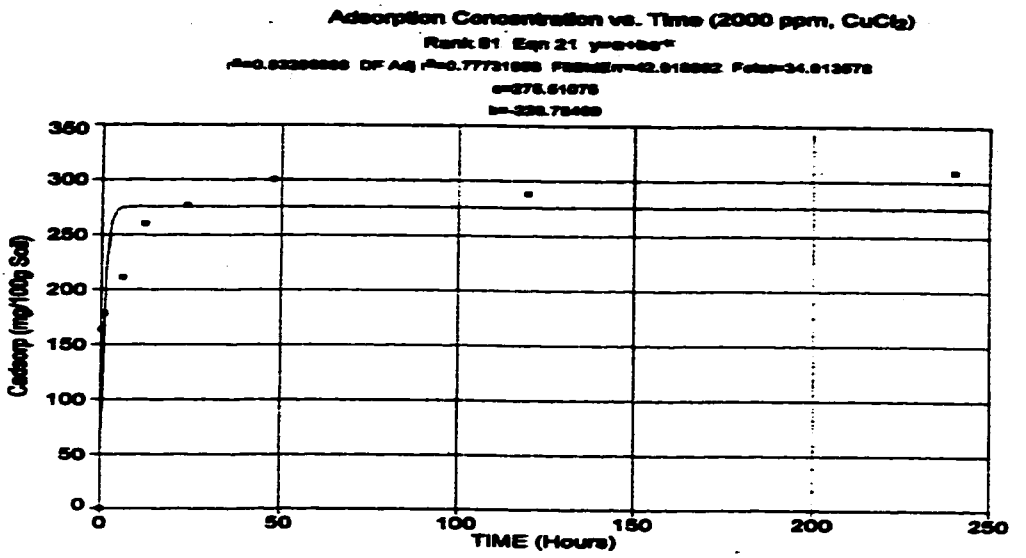

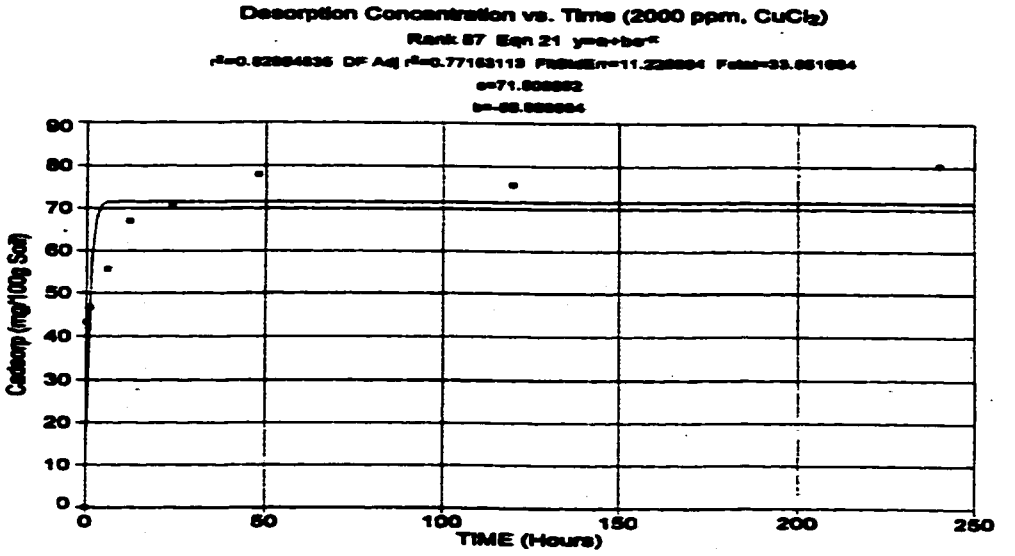

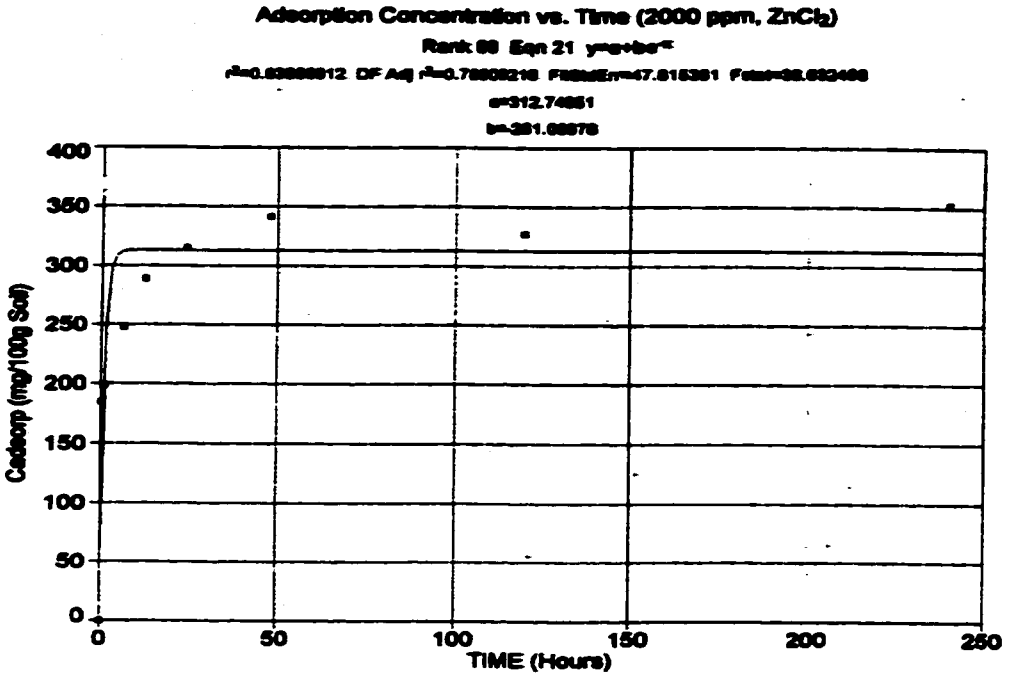
Adsorption Concentration vs. Time (2000 ppm, ZnCl2)
Rank: 88 Eqn 21 y=a+bx^c
r²=0.83888912 DF Adj r²=0.78800218 FitStdErr=47.815381 Fstat=38.632468
a=312.74881
b=-381.68878
Cadsorp (mg/100g Soil)
TIME (Hours)
0
50
100
150
200
250
300
350
400

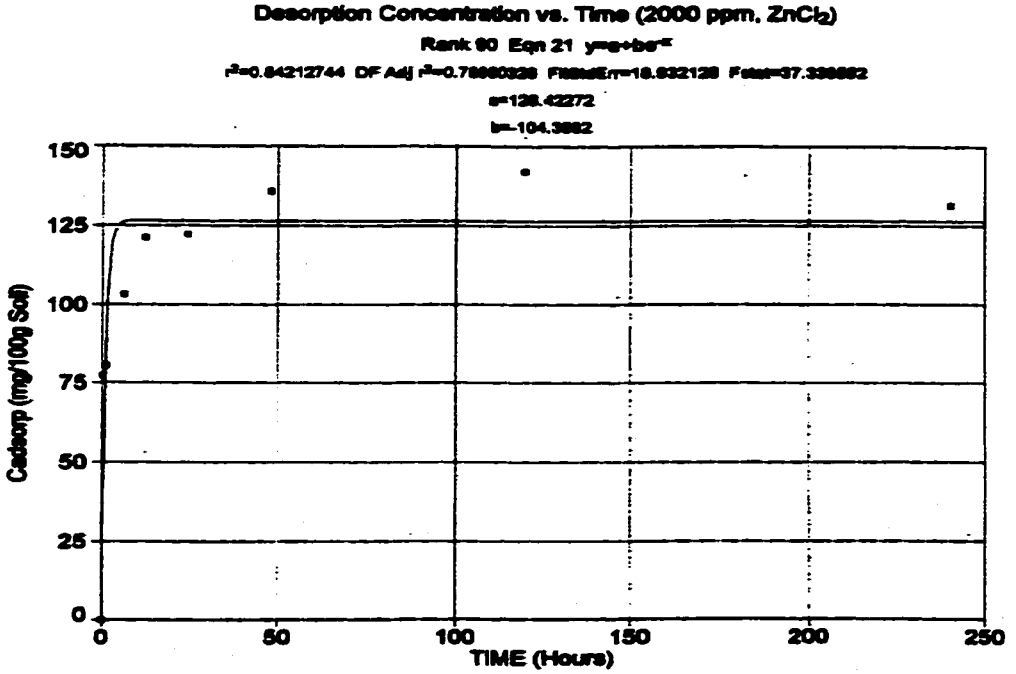
Desorption Concentration vs. Time (2000 ppm, ZnCl2)
Rank: 90 Eqn 21 y=a+bx^c
r²=0.84212744 DF Adj r²=0.78880928 FitStdErr=16.832128 Fstat=37.338882
a=128.42272
b=-104.3882
Cadsorp (mg/100g Soil)
TIME (Hours)
0
25
50
75
100
125
150

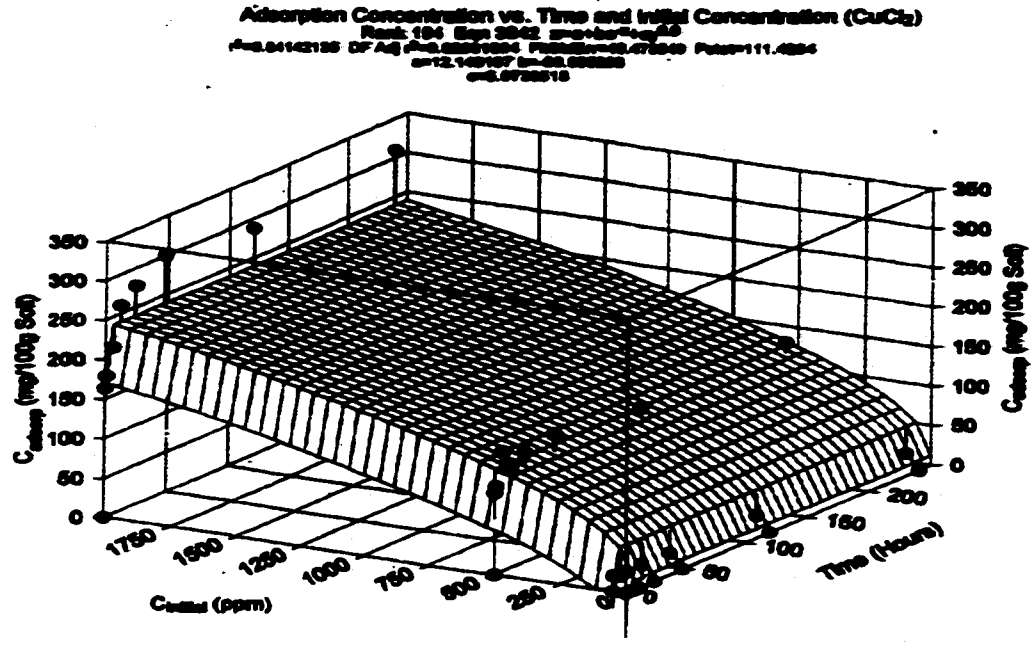
Adsorption Concentration vs. Time and Initial Concentration ($CuCl_2$)
Time (Hours)

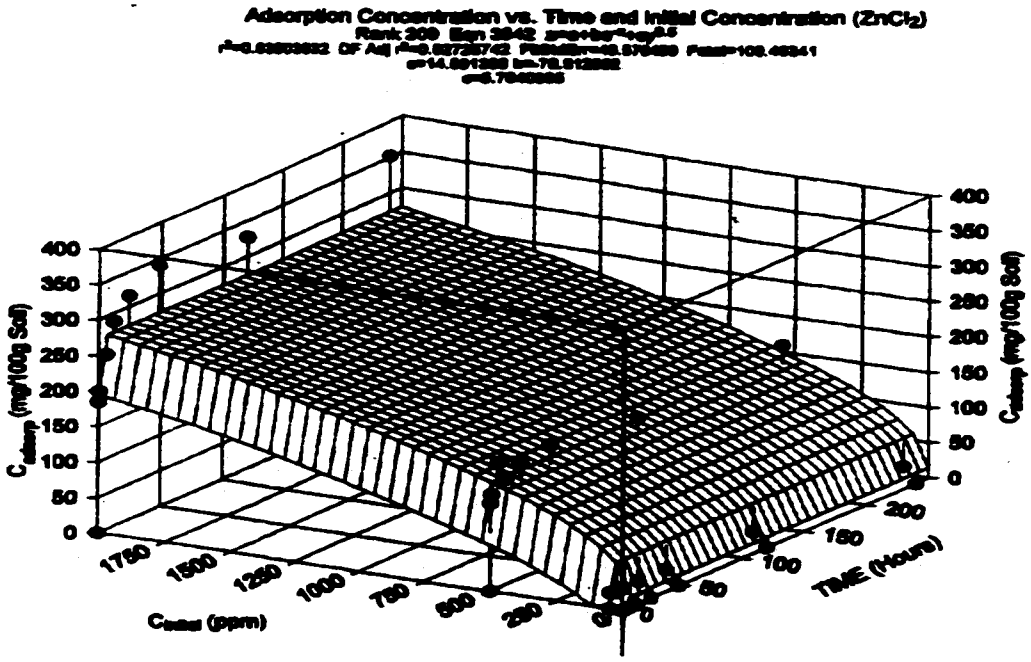
Adsorption Concentration vs. Time and Initial Concentration ($ZnCl_2$)
TIME (Hours)

APPENDIX 5. Experimental Results Data

The data concerning experimental results of this study are presented in this appendix, as follows. In these tables depth and soil water potential are in ***m***, solution concentration is in ***ppm***, adsorption concentration in ***mg/100 soil*** and time in ***day***, unless otherwise stated.

1. Variation of soil water potential and volumetric water content along the soil column are presented at various time intervals by the two following tables, respectively.

B	1	2	3	4	5	6	7
	Depth	T_05D	T_1D	T_3D	T_7D	T_15D	T_30D
1	0.25	0.08	0.14	0.33	0.41	0.42	0.42
2	0.23	0.09	0.16	0.35	0.41	0.42	0.42
3	0.21	0.09	0.17	0.37	0.42	0.42	0.42
4	0.19	0.12	0.21	0.38	0.42	0.42	0.42
5	0.17	0.13	0.23	0.39	0.42	0.42	0.42
6	0.15	0.15	0.28	0.41	0.42	0.42	0.42
7	0.13	0.17	0.32	0.42	0.42	0.42	0.42
8	0.11	0.21	0.35	0.42	0.42	0.42	0.42
9	0.09	0.28	0.37	0.42	0.42	0.42	0.42
10	0.07	0.30	0.41	0.42	0.42	0.42	0.42
11	0.05	0.38	0.42	0.42	0.42	0.42	0.42
12	0.03	0.42	0.42	0.42	0.42	0.42	0.42
13	0.01	0.42	0.42	0.42	0.42	0.42	0.42
14	0.00	0.42	0.42	0.42	0.42	0.42	0.42

A	1	2	3	4	5	6	7
	Depth	T_05D	T_1D	T_3D	T_7D	T_15D	T_30D
1	0.25	-386.23	-271.59	-120.38	-64.00	-53.24	-50.23
2	0.23	-348.32	-252.36	-90.04	-60.52	-46.75	-46.50
3	0.21	-328.12	-224.36	-93.12	-53.65	-47.33	-42.18
4	0.19	-324.35	-191.21	-87.42	-46.23	-34.24	-34.33
5	0.17	-288.65	-168.95	-73.58	-41.24	-34.56	-34.33
6	0.15	-252.69	-137.62	-55.24	-38.46	-34.00	-30.13
7	0.13	-210.36	-118.87	-58.35	-35.12	-22.25	-24.63
8	0.11	-179.38	-103.45	-52.64	-28.25	-16.17	-8.22
9	0.09	-159.63	-76.56	-44.62	-25.14	-15.03	-14.33
10	0.07	-130.22	-60.45	-29.33	-17.99	-14.23	-12.34
11	0.05	-93.34	-53.12	-12.35	-10.27	-14.21	-10.04
12	0.03	-43.86	-34.52	-7.68	-7.71	-8.56	-7.72
13	0.01	-14.02	-9.10	-4.20	-2.57	-4.79	-2.01
14	0.00	0.00	0.00	0.00	0.00	0.00	0.00

2. The Variation rate of Adsorption and desorption for $PbCl_2$ solution at a) 50, b) 200, c) 500, d) 1000, and e) 2000 ppm initial solution concentration are shown in the following tables. (Time in ***hours***)

A	1	2	3
	TIME	ADSORP	DESORP
1	0.00	0.00	0.00
2	0.25	41.80	5.65
3	1.00	39.20	5.77
4	6.00	35.10	7.23
5	12.00	38.00	5.17
6	24.00	36.60	4.96
7	48.00	38.90	5.36

B	1	2	3
	TIME	ADSORP	DESORP
1	0.00	0.00	0.00
2	0.25	108.07	15.21
3	1.00	117.54	16.16
4	6.00	155.61	19.37
5	12.00	132.58	22.49
6	24.00	148.43	19.58
7	48.00	138.40	19.77

C	1	2	3
	TIME	ADSORP	DESORP
1	0.00	0.00	0.00
2	0.25	185.60	35.29
3	1.00	197.60	43.60
4	6.00	238.50	58.91
5	12.00	291.70	46.71
6	24.00	264.00	51.31
7	48.00	277.20	51.85

D	1	2	3
	TIME	ADSORP	DESORP
1	0.00	0.00	0.00
2	0.25	386.25	101.88
3	1.00	408.38	107.23
4	6.00	483.63	127.02
5	12.00	549.13	142.41
6	24.00	587.25	151.35
7	48.00	641.25	169.38
8	120.00	668.50	176.16

E	1	2	3
	TIME	ADSORP	DESORP
1	0.00	0.00	0.00
2	0.25	280.47	69.90
3	1.00	294.36	72.57
4	6.00	323.63	82.58
5	12.00	384.09	93.16
6	24.00	461.72	112.22
7	48.00	454.26	99.53
8	120.00	472.11	96.02

3. The variation rate of Adsorption and desorption for a) $CuCl_2$ and b) $ZnCl_2$ solutions at i) 50, ii) 500, and iii) 2000 ppm initial solution concentration are shown in the following tables. (Time in ***hours***)

A1	1	2	3
	TIME	ADSORP	DESORP
1	0.00	0.00	0.00
2	0.25	20.30	3.02
3	1.00	19.70	3.06
4	6.00	16.00	3.15
5	12.00	18.40	2.74
6	24.00	19.20	2.87
7	48.00	17.60	2.62

B1	1	2	3
	TIME	ADSORP	DESORP
1	0.00	0.00	0.00
2	0.25	22.48	5.14
3	1.00	22.00	5.23
4	6.00	18.64	5.31
5	12.00	20.24	4.68
6	24.00	21.36	4.50
7	48.00	19.44	4.88

A2	1	2	3
	TIME	ADSORP	DESORP
1	0.00	0.00	0.00
2	0.25	104.31	22.19
3	1.00	112.05	23.09
4	6.00	152.01	25.62
5	12.00	129.42	31.66
6	24.00	139.77	29.32
7	48.00	146.79	28.14

B2	1	2	3
	TIME	ADSORP	DESORP
1	0.00	0.00	0.00
2	0.25	125.23	39.25
3	1.00	136.81	40.45
4	6.00	178.20	44.89
5	12.00	149.69	54.34
6	24.00	163.62	49.07
7	48.00	171.32	51.05

A3	1	2	3
	TIME	ADSORP	DESORP
1	0.00	0.00	0.00
2	0.25	163.60	43.29
3	1.00	178.50	46.65
4	6.00	211.40	55.62
5	12.00	260.20	66.92
6	24.00	277.10	70.83
7	48.00	300.00	77.81
8	120.00	288.10	75.49

B3	1	2	3
	TIME	ADSORP	DESORP
1	0.00	0.00	0.00
2	0.25	184.50	77.15
3	1.00	198.60	80.37
4	6.00	247.20	103.10
5	12.00	288.30	121.12
6	24.00	315.10	122.25
7	48.00	341.00	135.92
8	120.00	326.60	142.11

4. The variation rate of sequential extraction components for $PbCl_2$ solution at a) 50, b) 200, c) 500, d) 1000, and e) 2000 ppm initial solution concentration (ISC) are shown in the following tables. (Time is in ***hours*** for all sequential extraction tests)

A	1	2	3	4	5
	TIME	ADSORP	DESORP	EX_CAT	RESIDU
1	0.00	0.00	0.00	0.00	0.00
2	0.25	41.80	5.65	34.98	6.82
3	1.00	39.20	5.77	30.88	8.32
4	6.00	35.10	7.23	23.73	11.37
5	12.00	38.00	5.17	23.13	14.87
6	24.00	36.60	4.96	22.60	14.00
7	48.00	38.90	5.36	23.30	15.60
8	120.00	37.10	5.45	21.79	15.31
9	240.00	39.80	5.05	25.24	14.56

B	1	2	3	4	5
	TIME	ADSORP	DESORP	EX_CAT	RESIDU
1	0.00	0.00	0.00	0.00	0.00
2	0.25	108.07	15.21	76.09	31.98
3	1.00	117.54	16.16	79.10	38.44
4	6.00	155.61	19.37	98.02	57.59
5	12.00	132.58	22.49	83.00	49.58
6	24.00	148.43	19.58	92.97	55.46
7	48.00	138.40	19.77	87.20	51.19
8	120.00	149.91	21.67	94.45	55.46
9	240.00	140.11	19.37	88.39	51.72

C	1	2	3	4	5
	TIME	ADSORP	DESORP	EX_CAT	RESIDU
1	0.00	0.00	0.00	0.00	0.00
2	0.25	185.60	35.29	133.54	52.06
3	1.00	197.60	43.60	137.56	60.04
4	6.00	238.50	58.91	161.19	77.31
5	12.00	291.70	46.71	190.01	101.69
6	24.00	264.00	51.31	170.71	93.29
7	48.00	277.20	51.85	179.25	97.95
8	120.00	253.40	49.26	162.90	90.50
9	240.00	271.92	53.37	175.79	96.13

D	1	2	3	4	5
	TIME	ADSORP	DESORP	EX_CAT	RESIDU
1	0.00	0.00	0.00	0.00	0.00
2	0.25	280.47	69.90	194.22	86.25
3	1.00	294.36	72.57	202.58	91.78
4	6.00	323.63	82.58	220.13	103.50
5	12.00	384.09	93.16	264.78	119.30
6	24.00	461.72	112.22	310.78	150.93
7	48.00	454.26	99.53	316.26	138.00
8	120.00	472.11	96.02	329.97	142.14
9	240.00	440.59	102.50	308.11	132.48

E	1	2	3	4	5
	TIME	ADSORP	DESORP	EX_CAT	RESIDU
1	0.00	0.00	0.00	0.00	0.00
2	0.25	385.25	101.88	295.37	89.88
3	1.00	408.38	107.23	311.61	96.77
4	6.00	483.63	127.02	356.76	126.86
5	12.00	549.13	142.41	398.22	150.90
6	24.00	587.25	151.35	421.07	166.18
7	48.00	641.25	169.38	462.56	178.69
8	120.00	668.50	176.16	495.10	173.40
9	240.00	607.13	158.69	422.99	184.13

6. The variation rate of sequential extraction components for $CuCl_2$ solution at a) 50, b) 500, and c) 2000 ppm initial solution concentration are shown in the following tables.

A	1	2	3	4	5
	TIME	ADSORP	DESORP	EX_CAT	RESIDU
1	0.00	0.00	0.00	0.00	0.00
2	0.25	20.30	3.02	17.89	2.41
3	1.00	19.70	3.06	17.03	2.67
4	6.00	16.00	3.15	11.98	4.02
5	12.00	18.40	2.74	13.04	5.36
6	24.00	19.20	2.87	14.08	5.12
7	48.00	17.60	2.62	12.27	5.33
8	120.00	19.10	2.65	13.47	5.63
9	240.00	18.80	2.83	13.36	5.44

B	1	2	3	4	5
	TIME	ADSORP	DESORP	EX_CAT	RESIDU
1	0.00	0.00	0.00	0.00	0.00
2	0.25	104.31	22.19	80.49	23.82
3	1.00	112.05	23.09	85.69	26.36
4	6.00	152.01	25.62	119.74	32.27
5	12.00	129.42	31.66	89.66	39.76
6	24.00	139.77	29.32	104.27	35.50
7	48.00	146.79	28.14	109.87	36.92
8	120.00	134.10	30.49	98.24	35.86
9	240.00	136.98	29.68	102.84	34.14

C	1	2	3	4	5
	TIME	ADSORP	DESORP	EX_CAT	RESIDU
1	0.00	0.00	0.00	0.00	0.00
2	0.25	163.60	43.29	136.90	26.70
3	1.00	178.50	46.65	145.28	33.22
4	6.00	211.40	55.62	166.00	45.40
5	12.00	260.20	66.92	207.66	52.54
6	24.00	277.10	70.83	220.54	56.56
7	48.00	300.00	77.81	236.71	63.29
8	120.00	288.10	75.49	222.88	65.22
9	240.00	309.30	80.28	247.70	61.60

5. The variation rate of sequential extraction components for $ZnCl_2$ solution at a) 50, b) 500, and c) 2000 ppm ISC are shown in the following tables.

A	1	2	3	4	5
	TIME	ADSORP	DESORP	EX_CAT	RESIDU
1	0.00	0.00	0.00	0.00	0.00
2	0.25	22.48	5.14	22.15	0.33
3	1.00	22.00	5.23	21.58	0.42
4	6.00	18.64	5.31	18.03	0.61
5	12.00	20.24	4.68	19.41	0.83
6	24.00	21.36	4.50	20.50	0.86
7	48.00	19.44	4.88	18.65	0.79
8	120.00	19.68	4.78	18.93	0.75
9	240.00	21.12	4.53	20.26	0.86

B	1	2	3	4	5
	TIME	ADSORP	DESORP	EX_CAT	RESIDU
1	0.00	0.00	0.00	0.00	0.00
2	0.25	125.23	39.25	121.64	3.59
3	1.00	136.81	40.45	132.82	3.99
4	6.00	178.20	44.89	172.82	5.38
5	12.00	149.69	54.34	142.82	6.86
6	24.00	163.62	49.07	157.65	5.97
7	48.00	171.32	51.05	165.59	5.73
8	120.00	156.82	50.06	150.61	6.21
9	240.00	168.56	47.61	162.53	6.03

C	1	2	3	4	5
	TIME	ADSORP	DESORP	EX_CAT	RESIDU
1	0.00	0.00	0.00	0.00	0.00
2	0.25	184.50	77.15	179.74	4.76
3	1.00	198.60	80.37	193.18	5.42
4	6.00	247.20	103.10	239.76	7.44
5	12.00	288.30	121.12	279.72	8.58
6	24.00	315.10	122.25	305.46	9.64
7	48.00	341.00	135.92	330.47	10.53
8	120.00	326.60	142.11	316.49	10.11
9	240.00	352.30	131.48	341.36	10.94

7. Solution concentration variation along the soil column for a) $PbCl_2$, b) $ZnCl_2$, and c) $CuCl_2$ solutions at various time intervals are presented in the following tables.

A	1	2	3	4	5	6
	Depth	t1	t3	t7	t15	t30
1	0.25	0.00	0.00	0.00	0.00	0.00
2	0.23	0.00	0.00	0.00	0.00	0.00
3	0.21	0.00	0.00	0.00	0.00	0.00
4	0.19	0.00	0.00	0.00	0.00	20.00
5	0.17	0.00	0.00	0.00	0.00	70.00
6	0.15	0.00	0.00	0.00	10.00	150.00
7	0.13	6.00	10.00	15.00	150.00	400.00
8	0.11	10.00	20.00	20.00	300.00	610.00
9	0.09	15.00	40.00	150.00	520.00	800.00
10	0.07	30.00	80.00	500.00	700.00	1010.00
11	0.05	150.00	440.00	800.00	900.00	1400.00
12	0.03	520.00	985.00	1200.00	1400.00	1500.00
13	0.01	1560.00	1750.00	1800.00	1850.00	1900.00
14	0.00	2000.00	2000.00	2000.00	2000.00	2000.00

B	1	2	3	4	5	6
	Depth	t1	t3	t7	t15	t30
1	0.25	0.00	0.00	0.00	0.00	0.00
2	0.23	0.00	0.00	0.00	0.00	10.00
3	0.21	0.00	0.00	0.00	0.00	30.00
4	0.19	0.00	0.00	0.00	0.00	100.00
5	0.17	0.00	0.00	0.00	45.45	250.00
6	0.15	0.00	4.50	5.00	110.34	460.00
7	0.13	8.00	8.24	10.00	150.45	520.00
8	0.11	20.00	10.69	120.00	400.41	580.00
9	0.09	35.00	70.85	260.00	650.23	910.00
10	0.07	50.00	112.35	400.00	720.48	940.00
11	0.05	110.00	310.45	712.00	1006.54	1400.00
12	0.03	350.00	1150.42	1300.00	1634.00	1740.00
13	0.01	1000.00	1811.31	1800.00	1900.00	1900.00
14	0.00	2000.00	2000.00	2000.00	2000.00	2000.00

C	1	2	3	4	5	6
	Depth	t1e	t3e	t7e	t15e	t30e
1	0.25	0.00	0.00	0.00	0.00	10.00
2	0.23	0.00	0.00	0.00	0.00	35.00
3	0.21	0.00	0.00	0.00	0.00	87.00
4	0.19	0.00	0.00	0.00	5.00	187.00
5	0.17	0.00	0.00	0.00	41.00	354.00
6	0.15	0.00	0.00	5.00	100.00	512.00
7	0.13	4.00	6.00	50.00	244.00	624.00
8	0.11	6.00	20.00	91.00	566.00	750.00
9	0.09	10.00	40.00	212.00	695.00	1065.00
10	0.07	60.00	120.00	398.00	912.00	1200.00
11	0.05	200.00	600.00	880.00	1050.00	1300.00
12	0.03	410.00	1021.00	1380.00	1536.00	1690.00
13	0.01	1500.00	1400.00	1600.00	1725.00	1830.00
14	0.00	2000.00	2000.00	2000.00	2000.00	2000.00

8. Adsorption concentration variation along the soil column for a) $PbCl_2$, b) $ZnCl_2$, and c) $CuCl_2$ solutions at various time intervals are presented in the following tables.

A	1	2	3	4	5	6
	Depth	t1e	t3e	t7e	t15e	t30e
1	0.25	0.00	0.00	0.00	0.00	0.00
2	0.23	0.00	0.00	0.00	0.00	0.00
3	0.21	0.00	0.00	0.00	0.00	0.00
4	0.19	0.00	0.00	0.00	0.00	0.00
5	0.17	0.00	0.00	0.00	0.00	63.00
6	0.15	0.00	0.00	0.00	56.00	146.00
7	0.13	0.00	0.00	52.00	162.00	300.00
8	0.11	35.00	42.00	102.00	241.00	406.00
9	0.09	90.00	98.00	220.00	377.00	500.00
10	0.07	150.00	165.00	305.00	485.00	590.00
11	0.05	250.00	300.00	444.00	587.00	650.00
12	0.03	340.00	540.00	610.00	640.00	700.00
13	0.01	594.00	650.00	702.00	725.00	724.00
14	0.00	780.00	785.00	781.00	789.00	790.00

B	1	2	3	4	5	6
	Depth	t1e	t3e	t7e	t15e	t30e
1	0.25	0.00	0.00	0.00	0.00	0.00
2	0.23	0.00	0.00	0.00	0.00	15.00
3	0.21	0.00	0.00	0.00	0.00	35.00
4	0.19	0.00	0.00	0.00	0.00	87.00
5	0.17	0.00	0.00	0.00	36.00	120.00
6	0.15	0.00	0.00	22.00	97.00	185.00
7	0.13	0.00	23.00	65.00	160.00	250.00
8	0.11	32.00	50.00	88.00	200.00	270.00
9	0.09	57.00	86.00	139.00	232.00	320.00
10	0.07	70.00	150.00	200.00	310.00	340.00
11	0.05	122.00	200.00	300.00	370.00	370.00
12	0.03	250.00	345.00	400.00	410.00	410.00
13	0.01	330.00	400.00	430.00	440.00	450.00
14	0.00	515.00	520.00	520.00	510.00	515.00

C	1	2	3	4	5	6
	Depth	t1e	t3e	t7e	t15e	t30e
1	0.25	0.00	0.00	0.00	0.00	10.00
2	0.23	0.00	0.00	0.00	0.00	32.00
3	0.21	0.00	0.00	0.00	0.00	76.00
4	0.19	0.00	0.00	0.00	0.00	130.00
5	0.17	0.00	0.00	0.00	27.00	170.00
6	0.15	0.00	0.00	20.00	52.00	185.00
7	0.13	0.00	14.00	39.00	95.00	213.00
8	0.11	20.00	32.00	75.00	160.00	240.00
9	0.09	40.00	50.00	140.00	230.00	250.00
10	0.07	80.00	105.00	150.00	260.00	270.00
11	0.05	100.00	200.00	230.00	300.00	306.00
12	0.03	150.00	276.00	280.00	320.00	321.00
13	0.01	240.00	300.00	323.00	333.00	342.00
14	0.00	341.00	320.00	345.00	350.00	361.00